

The Effect of the Surfactant Hydrophilic groups and Concentration
of Electrolyte in an Internal Aqueous Phase on the Interfacial
Interactions and Rheology of Highly Concentrated Emulsions

by

KARINA KOVALCHUK

submitted in fulfilment of the requirements for the degree

MASTER OF TECHNOLOGY: CHEMICAL ENGINEERING

Faculty of Engineering

Cape Peninsula University of Technology

CAPE PENINSULA
UNIVERSITY OF TECHNOLOGY
Library and Information Services
Dewey No.

CAPE PENINSULA
UNIVERSITY OF TECHNOLOGY



20122127

CDT ARC. 660.294514 KOV
(NOT FOR LOAN)



Cape Peninsula
University of Technology

377268

**THE EFFECT OF THE SURFACTANT HYDROPHILIC GROUPS AND
CONCENTRATION OF ELECTROLYTE IN AN
INTERNAL AQUEOUS PHASE ON THE INTERFACIAL
INTERACTIONS AND RHEOLOGY OF HIGHLY CONCENTRATED
EMULSIONS**

by

KARINA KOVALCHUK

Dissertation submitted in fulfilment of the requirements for the degree

Master of Technology: Chemical Engineering

in the Faculty of Engineering

at the Cape Peninsula University of Technology

Supervisor: Prof. I. Masalova

Cape Town

DECLARATION

I, KARINA KOVALCHUK, declare that the contents of this dissertation represent my own unaided work, and that the dissertation has not previously been submitted for academic examination towards any qualification. Furthermore, it represents my own opinions and not necessarily those of the Cape Peninsula University of Technology.

Signed

Date

ABSTRACT

Emulsion explosives are classified as highly concentrated Water-in-Oil emulsions with an internal phase volume fraction of approximately 94%, i.e. far beyond the close packing limit of spherical droplets of 74%. These emulsions are thermodynamically unstable compounds and their instability is related to the crystallisation in the dispersed phase, which is a supersaturated solution of ammonium nitrate salt in water. This presents a problem, because the emulsion weakens or becomes unstable, which results in droplet crystallisation, so that the explosive generally loses at least some of its sensitivity to detonation. Considerable effort has been applied to the improvement of emulsion stability by explosive manufacturers, but important aspects such as the effect of salt and surfactant content/type in emulsions are not fully understood and described in the literature.

The purpose of this study was to investigate these shortcomings and to focus on the effect of surfactant nature and concentration and electrolyte concentration/type on the interfacial properties and interactions in emulsion explosives. Interfacial properties (interfacial tension and interfacial elasticity), thermal behaviour (freezing temperatures) of emulsions and rheological aspects (viscoelastic and flow properties) were investigated in terms of surfactant-electrolyte interactions.

It was demonstrated that different surfactant types (belonging to the class of polyisobutylene succinic anhydride (Pibsa) derivatives with a varying head group) yield different interfacial properties. The interfacial properties (interfacial tension and interfacial elasticity) are governed by the interaction of a surfactant with the matter of the droplet. In fact, both the interfacial tension and the interfacial elastic modulus were found to decrease according to the sequence MEA-UREA-MEA/SMO-IMIDE-SMO. It was established that the surfactant type and electrolyte concentration influence the stability (in terms of crystal initiation) of the emulsion and bulk rheological properties. Both the elastic modulus and the yield stress as functions of surfactant type decreased in the following order: MEA-IMIDE-UREA-MEA/SMO. The addition of salt produced an increase of viscoelastic and flow parameters and improved the emulsion stability.

The experimental part of the research work was carried out using the instrumental techniques of the Rotation Rheometer MCR-300", the PAT 1 Profile Analysis Tensiometer, the Perkin Elmer Spectrum 100 FT-IR Spectrometer and the Differential scanning calorimeter Q 2000.

ACKNOWLEDGEMENTS

I would like to thank the following persons and organisations for their contributions towards the completion of this thesis:

My supervisor, Prof. Irina Masalova, for her support and professional guidance throughout the whole research process, which was accompanied by much inspiration and motherly advice;

Prof. Alexander Yakovlevich Malkin, for his very professional and useful comments and suggestions addressed to my work;

African Explosives Limited, for providing the materials used to manufacture emulsions for the investigation and for their sponsorship;

The Cape Peninsula University of Technology, as well as the Flow Process Research Centre, for the opportunity to join this world-recognised research unit and for the support I received.

My sincere thanks go to my laboratory supervisor, Mr Nazeem George, for his assistance and help.

My thankful appreciation also goes to all my colleagues and all my friends, near or far from me, for their moral support, assistance and numerous moments of fun.

DEDICATION

The present thesis is dedicated to my family (my dear mother and brother).

TABLE OF CONTENTS

DECLARATION.....	3
ABSTRACT	4
ACKNOWLEDGEMENTS.....	5
DEDICATION	6
TABLE OF CONTENTS	7
LIST OF FIGURES	11
LIST OF TABLES.....	14
GLOSSARY	16
NOMENCLATURE	19
CHAPTER 1	22
INTRODUCTION	22
CHAPTER 2	28
THEORY AND LITERATURE REVIEW.....	28
2.1 Introduction.....	28
2.2 General definition of AN emulsion	28
2.3 Highly concentrated emulsions and their structure.....	30
2.4 Emulsion stability: basic concepts.....	32
2.4.1 Mechanism of emulsion instability.....	33
2.4.2 Emulsion stabilisation mechanisms.....	34
2.4.3 Factors determining emulsion stability	36
2.5 Formation, stability of interface and interfacial tension	37
2.5.1 Curvature and orientation at the interface	39
2.6 Interaction energies (forces) between emulsion droplets and their combinations	40
2.6.1 Van der Waals attraction.....	40
2.6.2 Electrostatic repulsion.....	41
2.6.3 Steric repulsion	42
2.7 Aqueous solution.....	42
2.7.1 Hydrogen bond formation at complex aqueous interfaces.....	45
2.7.1.1 Hydrogen bonds in water	45
2.7.1.2 Effect of pH and cation type on hydrogen bond formation	46
2.8 Surfactant, interfacial properties and their characterisation.....	48
2.8.1 Definition of surfactant	48
2.8.2 Surfactant classification	49
2.8.3 Polymeric surfactants.....	50

2.8.4	Molecular organisation of surfactants in solution.....	51
2.8.4.1	Critical micelle concentration	51
2.8.4.2	Factors affecting critical micelle concentration (CMC).....	52
2.8.4.2	Reversed micelles	53
2.8.5	Thermodynamic of adsorption.....	55
2.9	Emulsion explosives and their properties	58
2.9.1	Emulsion explosive composition	58
2.9.2	Structure of AN melt.....	59
2.9.3	Stability of explosive emulsions.....	60
2.9.3.1	Factors affecting the stability of emulsions	60
2.9.4	Role of emulsifiers in emulsion explosives	63
2.9.5	Emulsifiers used in stabilisation of explosive emulsions	64
2.9.5.1	Pibsa-based surfactants and their characterisation	66
2.10	Rheology of emulsions	70
2.10.1	Flow properties	71
2.10.1.1	Shear-rate dependent non-ideal liquids.....	71
2.10.1.2	Factors affecting rheological behaviour.....	73
2.10.1.3	Flow properties of explosive emulsions.....	75
2.10.1.4	Effect of surfactant type and concentration	75
2.10.1.5	Effect of electrolyte type and concentration on rheological properties	76
2.10.2	Viscoelastic properties	76
2.10.2.1	Viscoelasticity and microstructural parameters	77
2.11	Research issues identified.....	82
CHAPTER 3	83
MATERIALS AND METHODS	83
3.1	Introduction.....	83
3.2	Materials	83
3.2.1	Surfactants	84
3.2.2	Properties of fuel oil	89
3.3	Emulsion preparation	90
3.4	Matrix of samples.....	90
3.5	Methods	93
3.5.1	Droplet size analysis	93
3.5.2	Microscopy	93
3.5.3	Rheological analysis.	94
3.5.4	Interfacial properties investigation.....	95

3.5.5	FT-IR analysis.....	96
3.5.6	DSC analysis	98
3.5.7	ACD Laboratory software (version 6.0). Advanced Chem. Development Inc..	99
CHAPTER 4		101
RESULTS AND DISCUSSION		101
4.1	Interfacial properties and interactions in highly concentrated emulsions.....	101
4.1.1	<i>Effect of surfactant hydrophilic head group on the interfacial properties and interfacial interactions in highly concentrated emulsions</i>	<i>101</i>
4.1.1.1	Interfacial properties	101
4.1.1.2	FT-IR study	109
4.1.2	<i>Effect of AN concentration and electrolyte composition on interfacial properties and interfacial interactions in highly concentrated emulsions.</i>	<i>117</i>
4.1.2.1	Interfacial tension.....	117
4.1.2.1.1	Effect of AN concentration on interfacial tension	117
4.1.2.1.2	Effect of electrolyte type on interfacial tension	122
4.1.2.2	FT-IR study.....	124
4.1.3	<i>Effect of surfactant and electrolyte type/concentration and pH on emulsion stability.....</i>	<i>131</i>
4.1.3.1	Effect of surfactant type and concentration	131
4.1.3.2	Effect of the AN concentration on emulsion stability.....	135
4.1.3.3	Effect of NaNO ₃ and Ca(NO ₃) ₂ on emulsion stability	137
4.1.3.4	Effect of pH on emulsion stability with regard to coalescence	141
4.1.4	<i>General conclusion regarding the effect of surfactant hydrophilic groups and electrolyte nature and concentration on the interfacial properties, interactions and emulsion stability.....</i>	<i>145</i>
CHAPTER 5		147
5.1	Rheological properties of highly concentrated emulsions	147
5.1.1	<i>Effect of surfactant hydrophilic groups on rheological properties of highly concentrated emulsions</i>	<i>147</i>
5.1.1.1	Droplet size measurements	147
5.1.1.2	Viscoelastic and flow properties	150
5.1.2	<i>Effect of electrolyte concentration and composition on rheological properties of highly concentrated emulsions.....</i>	<i>156</i>
5.1.2.1	Effect of electrolyte concentration on rheological properties of highly concentrated emulsions.	156

5.1.2.2	Effect of electrolyte type on rheological properties	161
5.1.2.2.1	Viscoelastic and flow properties	164
5.1.2.2.1.1	Scaling by Laplace pressure	166
5.1.3	<i>General conclusion regarding the effect of surfactant type and the AN concentration/composition of the aqueous phase on the rheological properties of highly concentrated emulsions</i>	167
CHAPTER 6	169
SUMMARY	169
BIBLIOGRAPHY	173
APPENDICES	184

LIST OF FIGURES

Figure 3.1: 2-D view of the head group structure of Pibsa-MEA.....	84
Figure 3.2: 3-D view of possible conformation of Pibsa-MEA surfactant	85
Figure 3.3: 2-D view of Pibsa-IMIDE head group structure	85
Figure 3.4: 3-D view of the possible conformation of Pibsa-IMIDE surfactant.....	86
Figure 3.5: 2-D view of Pibsa-UREA head group structure	87
Figure 3.6: 3-D view of possible conformation of Pibsa-UREA surfactant	87
Figure 3.7: 2-D view of SMO structure	88
Figure 3.8: 3-D view of possible conformation of SMO surfactant	88
Figure 3.9: Mastersizer 2000 instrument.....	93
Figure 3.10: Leica microscope	94
Figure 3.11: Rotational Rheometer MCR 300 (Paar Physica)	95
Figure 3.12: Kruss K 100 Tensiometer.....	96
Figure 3.13: Basic components of an FT-IR spectrometer	97
Figure 3.14: Perkin Elmer Spectrum 100 FT-IR Spectrometer	97
Figure 3.15: A multiple reflection ATR system.....	98
Figure 3.16: Differential scanning calorimeter Q 2000.....	98
Figure 3.17: Screen with the Structure Mode enabled.....	99
Figure 4.1: Determination of CMC value of Pibsa-MEA surfactant.....	103
Figure 4.2: Experimental evaluation of interaction parameter β between Pibsa-MEA and SMO surfactants.....	106
Figure 4.3: Possible models of Pibsa-based surfactant conformations at the interface: (1) Pibsa-MEA, (2) Pibsa-UREA, (3) Pibsa-IMIDE.....	108
Figure 4.4: General spectrum of emulsion explosive, containing AN solution as an aqueous phase.....	109
Figure 4.5: FT-IR spectra of AN solution (40%) and aqueous phase after mixing.....	110
Figure 4.6: FT-IR spectra of oil phase with dissolved Pibsa-MEA surfactant in it before and after phase mixing.....	110
Figure 4.7: Possible variant of hydrogen bond formation between NH_4^+ and carboxylic group of surfactant.....	111
Figure 4.8: Possible variants of salt (complex) formation between AN ions and surfactant head group.....	112

Figure 4.9: Part of emulsion spectra stabilised by different surfactants (Pibsa-MEA -3, Pibsa-UREA -2 and Pibsa-IMIDE -1).....	112
Figure 4.10: Part of FT-IR spectra of emulsions.....	113
Figure 4.11: Chemical structures of Pibsa-based surfactant head groups.....	114
Figure 4.12: The delocalisation of the nitrogen electron pair in a succinimide molecule.....	115
Figure 4.13: Interfacial tension as a function of ammonium nitrate concentration.....	118
Figure 4.14: Determination of slope ($dy/d\ln c$) and CMC values for systems with 10% - (1) - and 60% - (2) - AN in the aqueous phase and Pibsa-MEA surfactant in the oil phase.....	120
Figure 4.15: Interfacial film growth without the presence of AN salt in aqueous phase, Pibsa-MEA.....	121
Figure 4.16: Water-oil interface in presence of AN salt (5%) in the water phase, Pibsa-MEA.....	122
Figure 4.17: Possible hydrogen bonding interaction between Pibsa-MEA head group and NH_4^+ ion.....	123
Figure 4.18: Possible ion attraction to the head group of Pibsa-MEA.....	124
Figure 4.19: FT-IR spectra of aqueous solutions with different AN concentrations.....	125
Figure 4.20: Comparison of Pibsa-MEA, water emulsion and AN emulsion spectra.....	128
Figure 4.21: Part of FT-IR spectra of emulsions with 30% and 40% AN.....	129
Figure 4.22: Possible hydrogen bond formation between two molecules of Pibsa-MEA head group and NH_4^+ ion (R: $\text{CH}_2\text{-CH}_2\text{-OH}$, R_1 : polyisobutylene).....	130
Figure 4.23: Possible manner of salt formation between the Pibsa-MEA head group and the NH_4^+ ion.....	131
Figure 4.24: Heat Flow as a function of temperature for emulsions with different AN concentrations.....	135
Figure 4.25: Freezing temperature of emulsions and solutions as a function of electrolyte concentration.....	136
Figure 4.26: Determination of slope ($dy/d\ln c$) and CMC values for systems with 10% and 60% AN in the aqueous phase and Pibsa-IMIDE surfactant in the oil phase.....	140
Figure 4.27: Evolution of droplet size distribution of water emulsion during the measurement ($\text{pH} = 7$).....	141
Figure 4.28: Evolution of droplet size distribution of emulsion with NaNO_3 during the measurement ($\text{pH} = 7$).....	142
Figure 4.29: Evolution of droplet size distribution of emulsion with NH_4NO_3 during the measurement ($\text{pH} = 7$).....	142
Figure 4.30: Coalescence of highly concentrated water emulsion prepared at $\text{pH} = 7$:.....	143

Figure 4.31: Coalescence of highly concentrated emulsion with NaNO_3 prepared at $\text{pH} = 7$	143
Figure 4.32: Effect of pH on the charge distribution in the Pibsa-MEA surfactant head group...	144
Figure 5.1: Droplet size distribution as a function of time for emulsion stabilised by Pibsa-MEA surfactant	147
Figure 5.2: Droplet size as a function of mixing time of emulsions stabilised by different emulsifiers (8% wt. in oil phase): Pibsa-MEA, Pibsa-IMIDE, Pibsa-UREA, Pibsa-MEA/SMO, SMO	148
Figure 5.3: Droplet size as a function of mixing time for the emulsion stabilised with Pibsa-MEA surfactant fitted by model	149
Figure 5.4: Storage Modulus as a function of surfactant type: $\text{DS}[3,2] = 12$ micron	150
Figure 5.5: Yield Stress as a function of surfactant type: $\text{DS}[3,2] = 12$ micron	152
Figure 5.6: Effect of surfactant type on the dimensionless elastic modulus	154
Figure 5.7: Histogram of drop size distribution of the emulsions containing 5% of AN at different mixing times	156
Figure 5.8: Droplet size as a function of mixing time for emulsions with 0, 2, 5, 10, 20, 30, 40, 50, 60 and 80% AN in the aqueous phase	157
Figure 5.9: Droplet size as a function of mixing time for the 5% AN emulsion fitted by model	158
Figure 5.10: Storage Modulus as a function of ammonium nitrate concentration: $\text{DS}[3,2] = 8$ micron	159
Figure 5.11: Yield Stress as a function of ammonium nitrate concentration: $\text{DS}[3,2] = 8$ micron	160
Figure 5.12: Histogram of drop size distribution of the water emulsion at different mixing times	162
Figure 5.13: Droplet size as a function of mixing time for emulsions with water, AN, SN and CN solutions as an aqueous phase	162
Figure 5.14: Droplet size as a function of mixing time for an emulsion with water as an aqueous phase	163
Figure 5.15: Storage modulus as a function of electrolyte type presence in the aqueous phase	164
Figure 5.16: Yield Stress as a function of electrolyte type presence in the aqueous phase	165
Figure 5.17: Storage modulus as a function of electrolyte type scaled by Laplace pressure	166

LIST OF TABLES

Table 3.1: Summary of surfactants' properties	89
Table 3.2: Summary of fuel oil properties	89
Table 3.3: AN and AN-NaNO ₃ emulsions stabilised by different surfactants	91
Table 3.4: Emulsions with different AN concentrations	91
Table 3.5: Emulsions with different additions of Ca(NO ₃) ₂	92
Table 3.6: Emulsions with different salts in the aqueous phase	92
Table 4.1: Summary of interfacial tension, interfacial elastic modulus and CMC values for Pibsa-based surfactants and SMO	104
Table 4.2: Area of Pibsa-MEA molecule occupied at the interface	108
Table 4.3: Variation of IR frequencies with surfactant type	113
Table 4.4: Variation of IR frequencies with surfactant concentration for emulsions stabilised by Pibsa-MEA and Pibsa-IMIDE emulsifiers	114
Table 4.5: Interfacial tension at different ammonium nitrate concentrations in the aqueous phase (8% of surfactant in oil phase)	118
Table 4.6: Interfacial tension as a function of surfactant concentration for 10% and 60% AN in the aqueous phase	119
Table 4.7: Surface tension of aqueous solution with different ammonium nitrate concentrations in the aqueous phase	120
Table 4.8: Interfacial tension of the oil-Pibsa-MEA/salt solution system as a function of different electrolytes	123
Table 4.9: IR spectral assignments for the H ₂ O and NH ₄ NO ₃ (Pavia <i>et al.</i> , 2001)	125
Table 4.10: The variation of IR frequencies with ammonium nitrate concentration	126
Table 4.11: The variation of IR frequencies with AN concentrations	130
Table 4.12: Effect of surfactant type on the crystallisation temperature of highly concentrated emulsion (8% surfactant in oil phase)	132
Table 4.13: Crystallisation temperature of emulsions stabilised with Pibsa-MEA and Pibsa- IMIDE as a function of surfactant concentration	134
Table 4.14: Crystallisation temperatures of emulsions and solutions with different concentrations of AN in the aqueous phase	136
Table 4.15: Crystallisation temperature of emulsions with AN and AN-NaNO ₃ as an aqueous phase	138
Table 4.16: Crystallisation temperatures of emulsions and solutions with addition of calcium nitrate salt to the AN	138

Table 4.17: Pibsa-IMIDE surfactant concentration at the interface with presence of AN in the aqueous phase	140
Table 5.1: Limiting diameter (D_{lim}) of emulsion droplets stabilised by different surfactants ..	149
Table 5.2: Storage modulus as a function of surfactant type for two surfactant concentrations (8% and 14%).....	151
Table 5.3: Yield stress of emulsions stabilised by different surfactant types for two surfactant concentrations (8% and 14%).....	153
Table 5.4: Critical diameter of emulsion droplets containing different AN concentrations	158
Table 5.5: Storage Modulus and Yield Stress of emulsions with different concentrations of ammonium nitrate: DS[3,2] = 8 micron.....	160
Table 5.6: Critical diameter of emulsions with different salts in the aqueous phase	163
Table 5.7: Storage Modulus and Yield Stress dependence on the type of salt added to the aqueous phase	165

	employed.
Rheology	The science of deformation and flow of matter.
Shear	The relative movement of parallel adjacent layers
Shear modulus	The ratio of shear stress to its corresponding shear strain.
Shear rate	The rate of change of shear strain with time. For liquids, the shear rate, rather than strain, is generally used in describing flow.
Shear stress	The component of stress that causes successive parallel layers of a material body to move in their own planes (i.e. the plane of shear), relative to each other.
Shear-thinning	A decrease in viscosity with increasing shear rate during steady shear flow.
Steady shear flow	Condition under which a fluid is sheared continuously in one direction for the duration of a rheometric experiment.
Storage modulus	The quotient of the part of the stress in phase with the strain divided by the strain under sinusoidal conditions.
Surfactant	An amphiphilic (amphipathic) molecule that has a hydrophilic head group (polar region), which has a high affinity for water, and a lipophilic tail group (non-polar region), which has a high affinity for oil
Viscoelastic	A time-dependent property in which a material under stress produces both a viscous and an elastic response.
Yield stress	A critical shear stress value below which an ideal plastic

GLOSSARY

This part of the dissertation provides definitions of terms and expressions used. Terms relating to the measurement of rheological properties in liquid-based systems (emulsion, suspension, etc.) are published by the National Institute of Standards and Technology in the "Guide to Rheological Nomenclature" by V.A. Hackley and C.F. Ferraris, 2001, Special Publication 949. Definitions are generally consistent with nomenclature published by the American Concrete Institute (ACI), the British Standards Institute (BSI), the International Union of Pure and Applied Chemistry (IUPAC) and the Society of Rheology (Hackley & Ferraris, 2001).

Terms	Definition
Coalescence	Spontaneous joining of smaller droplets in an emulsion system to form larger ones.
Elastic	A conservative property in which part of the mechanical energy used to produce deformation is stored in the material and recovered on release of stress.
Elastic modulus	A modulus of a body that obeys Hook's law.
Emulsion	Two immiscible liquids (usually oil and water), with one of the liquids dispersed as small spherical droplets in the other.
Flow	Continuous increasing deformation of a material body under the action of finite forces. When the forces are removed, and the strain does not eventually return to zero, then flow has occurred.
Flow curve	A graphical representation of the behaviour of flowing materials in which shear stress is related to shear rate.
Modulus	The quotient of stress and strain where the type of stress and strain is defined by the type of deformation

or viscoplastic material behaves like a solid (i.e. will not flow). Once the yield stress is exceeded, a plastic material yields (deforms plastically) while a viscoplastic material flows like liquid.

NOMENCLATURE

Symbol	Description	Unit
A	interfacial area	m ²
β	Interaction parameter for mixed surfactant monolayer at the interface	
C	concentration of solute	mol/l
C _{el}	electrolyte concentration	g/l
CMC	critical micelle concentration	mol/l
C _S	solubility	g/l
D or d	diameter of droplet (particle)	m
D _{crit}	critical droplet size	m
D ₀	initial droplet size	m
De	Debora number	-
dA	increase in contact area	J/m ²
dG	increase in free energy of the system	J/m ²
E ^s	total surface energy	J/m ²
F	free energy	J
F	force	N
f _a [*]	adhesion force between droplets	N
G _A	attractive energy between two drops	J
G _{el}	electrostatic energy between two drops	J
G _T	total energy between two drops	J
G'	storage modulus	Pa
G''	loss modulus	Pa
G ^s	surface free enthalpy	J/m ²
h	film thickness	nm
H ^s	surface enthalpy	J/m ²
K	equilibrium constant	-
L	length	m
M	molar mass of compound	g/mol
μ_i	chemical potential of the solute	J/mol
n _i	excess surfactant concentration at the surface	-
Pc	critical packing parameter of the surfactant	-
R ₃₂	surface-volume mean drop radius	m

R, r	droplet radii	m
R	universal gas constant	J/mole K
$S(\infty)$	solubility of the solute in the continuous phase for a droplet with infinite curvature (a planar interface)	g/l
S°	solubility of the solute when contained in spherical droplet of radius r	
S^s	surface entropy	J/m ²
T	absolute temperature	K
t	time	s
V_D	volume of emulsion droplets	m ³
V_E	total volume of the emulsion	m ³
V_m	molar volume of the solute	m ³ /mol
$\Delta_{ad} F$	free adhesion energy	J
Δp	drop in pressure	Pa
Γ	surface excess concentration	mol/m ²
Γ_{∞}	surface excess concentration when the surface is completely saturated with solute	mol/m ²
E	elasticity of the interface	N/m
ϕ	dispersed phase volume fraction	%
ϕ^*	volume fraction that corresponds to the hexagonal close packing of undistorted spheres	%
ϕ_c	volume fraction at which the modulus G' collapses to zero	%
ϕ_{eff}	effective volume fraction	%
ϕ_m	dispersed mass fraction	%
γ	shear strain	%
π	surface pressure	N/m ²
θ	characteristic time	min
θ, α	contact angle	grad
ρ_c	density of the continuous phase	Kg/m ³
ρ_{Dph}	density of the dispersed phase	Kg/m ³
γ, σ	interfacial tension	N/m
τ	shear stress	Pa
τ_y	yield stress	Pa
X_1	mole fraction	-

ω	angular frequency	Hz
W_A	adhesion work between two surfaces	N/m

Subscripts

Abbreviations

Abbreviation Expansion

AN	Ammonium nitrate
CMC	Critical micelle concentration
CN	Calcium nitrate
DSC	Differential scanning calorimetry
FT-IR	Fourier Transform Infrared
HIPE	High-internal-phase emulsion
HLB	Hydrophilic-lipophilic balance
Pibsa	Poly(isobutylene succinic) anhydride
SMO	Sorbitan monooleate
SN	Sodium nitrate
DSD	Droplet Size Distribution

CHAPTER 1

INTRODUCTION

The subject of this study is an investigation of the effect of surfactant nature (structure of the hydrophilic head group) and electrolyte concentration on interfacial interactions in highly concentrated water-in-oil (W/O) super-concentrated emulsions used as pumpable explosives. Such emulsions comprise a rather special class of colloids. In contrast to standard emulsions and suspensions, the concentration of the dispersed phase in highly concentrated explosive emulsions exceeds the limit of the closest packing of regular spheres (app. 74%). This is possible due to the "compressed" state of droplets which have a polyhedron shape. The aqueous phase is an oversaturated (overcooled) nitrate salt solution at room temperature, comprising less than 20% water by mass. Compounds of this kind are thermodynamically unstable and their instability is related to the coarsening of emulsions (droplet coalescence) and phase transition (crystallisation) in the dispersed phase.

Such emulsions have a variety of industrial applications as pharmaceuticals, food products, crude oil recovery, mining, polymer blends, biological liquids, explosives and so on. Considerable interest is currently concentrated on the investigation of physical properties of highly concentrated emulsions and their stability.

Emulsion explosives have become the preferred choice as blasting agents for numerous industries including mining, agriculture, and construction. Nowadays, emulsion explosives are in large-scale commercial use around the world. These emulsions, however, are subject to transport-induced structural decomposition caused by high speed pumping, as well as by ageing. Uncontrolled crystallisation can lead to emulsion breakdown and/or reduction in flow ability and detonation sensitivity (McKenzie & Lawrence, 1990; Hales, Cranney, Hurley & Preston, 2004). One of the most important components in such an emulsion is an emulsifier, which influences the emulsification, the interfacial, rheological properties and the stability of the explosive. Therefore a lot of research work has been devoted to the synthesis of new emulsifier molecules which can provide desirable rheological properties and better stability of emulsions. Two main directions can be found in the published work regarding emulsifier developing: development of surfactant structure (new head groups and new tail groups) (Sudweeks & Harvey, 1979; Binet, Cloutier, Edmonds, Holden & McNicol, 1982; Yates & Dack., 1987; Cooper & Baker, 1989; Forsberg, 1989; McKenzie, 1991; Venter & Kruger, 1995; Chattopadhyay, 1996; Boer, 2003; Hales, Cranney, Hurley, & Preston, 2004) and development of new surfactant blends (Binet *et al.*, 1982; Chattopadhyay, 1996; Hales *et al.*, 2004).

PIBSA (polyisobutenyl succinic anhydride) derivatives were used as superior polymeric emulsifiers for emulsion explosives (Boer, 2003). The increased stability of PIBSA-stabilised emulsions was ascribed to the highly ordered and stable film formed in the presence of the polymeric surfactant (McKenzie & Lawrence, 1990; Chattopadhyay, 1996; Boer, 2003; Hales *et al.*, 2004). One of the interesting mechanisms of explosive emulsion stabilisation discussed in a few publications is the interaction between the electrolyte and the PIBSA-based surfactant. Some studies investigated the influence of ammonium nitrate on adsorbed surfactant monolayers and surfactant-electrolyte interactions (Ganguly, Mohan, Bhasu, Mathews, Adisheshaiah & Kumar, 1992; Chattopadhyay, Ghaicha, Oh & Shah, 1992). The work by Ganguly *et al.* (1992) is one of a few exceptions. They showed that an electrolyte strongly interacts with a PIBSA surfactant and can affect the packing of hydrophobic tail groups at the interface. Improvement of emulsion stability with the addition of electrolytes to the aqueous phase was observed by some authors (Ganguly *et al.*, 1992; Aronson & Petko 1993; Park *et al.*, 2003). The improvement of stability was attributed in some cases to the interaction of the surfactant hydrophilic part with the electrolyte (Ganguly *et al.*, 1992; Chattopadhyay *et al.*, 1992; Aronson & Petko, 1993).

Only a few investigations concerning the effect of electrolytes and surfactants on the interfacial structure and interactions in highly concentrated explosive emulsions could be found. This presented a problem, because knowledge of factors affecting interfacial structure and interfacial properties of emulsions can provide a clear understanding of emulsion stability.

Because of this lack of knowledge, the present study was undertaken to investigate the factors that affect the interfacial structure and properties of such emulsions. The emulsion consisted of aqueous droplets which was covered by an oil phase. The concentration of the dispersed phase in the emulsion was 90-96 wt%, the rest comprised the oil phase. The concentration of AN (ammonium nitrate) in the dispersed phase was 80 wt% and this phase was a super-cooled (over-saturated) aqueous solution of AN.

In following the above theme, the study was designed to search for answers to the following questions:

- How does the content of the emulsion (surfactant type; concentration of ammonium nitrate; different nitrate salts) affect the structural properties (strength and structure) at the interface and interfacial interaction between surfactant head group and electrolyte?

- How does the emulsion content (surfactant type/concentration and electrolyte concentration) affect the stability (crystal initiation) of explosive emulsions and rheological properties (storage modulus and yield stress)?

The main purpose of the study was to determine how the emulsion content (electrolyte and surfactant type/concentration) affects the structure at the water-oil interface of fresh, highly-concentrated emulsions and the emulsion stability in terms of surfactant-electrolyte interactions.

The specific objectives for investigations were:

- The effect of surfactant type (with varied hydrophilic parts of surfactant molecules) and electrolyte concentration on interfacial properties (determination of interfacial tension and interfacial elasticity as a function of electrolyte and surfactant type/concentration)
- The effect of surfactant and electrolyte type/concentration on structure at the water-oil interface (determination of hydrogen bond formation between electrolyte and surfactant in emulsions)
- The effect of surfactant and electrolyte concentration on an emulsion's thermal behaviour (determination of emulsion freezing temperatures as a function of electrolyte and surfactant type/concentration)

As an application of the above-mentioned points, the following objective consequently had to be studied in this work:

- The rheological bulk properties (storage modulus and yield stress) of fresh explosive emulsions as a function of surfactant type and electrolyte type/concentration.

The following methodologies were adopted to answer these questions and achieve the overall aim of the study:

1. Investigation of interfacial properties:

The PAT 1 Profile Analysis Tensiometer, supplied by Sinterface Technologies (Berlin, Germany), was used to perform the experiment. This instrument is designed to measure the interfacial tension and interfacial complex modulus at the liquid/gas or liquid/liquid interface. The tensiometer operates on the principle that the shape of a liquid droplet emerging from a capillary can be described by the Young-Laplace equation. The Young-Laplace equation is then fitted to the digitised image of the droplet edge. The instrument software reports time, t , interfacial tension, γ , droplet surface area, A , droplet volume, V , droplet diameter, D , and the contact angle, α .

Investigations included:

- Interfacial tension and interfacial elasticity as a function of surfactant type and electrolyte type/concentration.
- Explanation of the obtained interfacial properties in terms of emulsion content (surfactant and electrolyte type/concentrations).

2. Spectroscopic investigation

FT-IR analysis was carried out to detect structural changes in terms of surfactant-electrolyte interactions. The FT-IR spectra were conducted with the use of a PerkinElmer Spectrum 100 FT-IR Spectrometer. In infrared spectroscopy, IR radiation is passed through a sample. Some of the infrared radiation is absorbed by the sample and some of it is passed through (transmitted). The resulting spectrum represents the molecular absorption and transmission, creating a molecular fingerprint of the sample. FT-IR enables identification of materials, and determining the quality of a sample and amount of components in a mixture. The spectra of the emulsions that were investigated were recorded at room temperature using an Attenuated Total Reflectance accessory. The Germanium (Ge) is a crystalline material. The range of measurements could be between 8500 cm^{-1} to 350 cm^{-1} . Investigations included:

- Determination of spectra of pure emulsion components for identification purposes of all peaks in the emulsion spectrum (to give a full description of emulsion spectrum).
- Detection of hydrogen bond formation (from NH peak occurring at lower frequency) between the surfactant and electrolyte in emulsion as a function of electrolyte and surfactant type/concentration.

- Comparison of the strength of hydrogen bond between surfactant and electrolyte by analysing the modification in NH peak for emulsions with different electrolyte and surfactant contents.

3. Thermal analysis

DSC analysis was performed to follow the freezing temperature changes in the emulsion. DSC studies were carried out with use of a DSC Q 2000 instrument coupled with a computer for data analysis for determining the emulsion freezing temperature. The temperature range studied was from 30°C to -70°C with the cooling rate being 2°C/min.

Investigations included:

- Determination of emulsion freezing temperatures as a function of electrolyte and surfactant type/concentration.
- Determination of emulsion freezing temperatures as a function of salt content of different nitrates in the ammonium nitrate.
- Correlation of emulsion formulation content with emulsion stability (initiation of crystals).

4. Optical methods

The optical analysis was conducted to use visual observations for the analysis of the structural changes of materials with differing emulsion content. The analysis was carried out with a Leica optical microscope equipped with a digital camera, at a magnification of 500.

Optical methods were also used to obtain the particle size distribution of the dispersed phase. This was done by using the Malvern Mastersizer 2000 technique. This method is based on measuring the angle distribution of the He-Ne laser light scattered by particles.

The expectation is that the results of this study will benefit a wide range of industries, such as the explosives, food, cosmetics and pharmaceutical industry, etc., which deal with highly concentrated emulsions, their formation, transportation and storage.

5. Rheological investigations

Rheological experimental methods are based on measuring the rheological properties of emulsions. These results were obtained by using the modified sophisticated modern instrumental technique of the Rotation Rheometer MCR-300 ("Paar-Physica", Germany). The wide range of shear rates (from app. 10^{-4} to 10^3 s⁻¹) and shear stresses available for

investigation allows one to obtain characteristics of rheological properties in a very wide range. This instrument can also operate in a wide range of frequencies, from 10^{-3} to 10^2 Hz. In this oscillating mode of deformations, dynamic modules are measured as a function of frequency. In addition, the amplitude of deformation can be varied between 0.01% to several hundred per cent. Instrument measurement facilities are supported with modern software, which includes many applied programs. Rheological investigations included:

- Flow curve and amplitude sweep of fresh explosive emulsions as a function of surfactant and electrolyte type/concentration.
- Correlation of the rheological properties (storage modulus and yield stress) with different emulsion contents (different surfactant and electrolyte type/concentrations).

In this study, a systematic investigation of the effect of surfactant and electrolyte type/concentrations on the emulsion's rheological properties and emulsion stability (crystal initiation) was performed, which has not been investigated before. The experimental results have allowed a deeper understanding of the factors governing the stability of multi-component systems such as highly concentrated emulsions. This study was expected to ensure an appropriate method for the determination of emulsion stability in terms of crystal initiation.

The thesis is subdivided into the following chapters:

- Chapter 1 serves as an introduction to this thesis.
- Chapter 2 comprises a presentation of the relevant literature pertaining to the study. It covers relevant literature on theoretical fundamentals of high internal phase ratio emulsions, as well as the relevant experimental work.
- Chapter 3 provides a comprehensive description of the methods of experimentation and the procedures used in the analysis of the results.
- Chapters 4 and 5 present the analysis of the results and the inherent discussions pertaining to the experimental findings.
- Chapter 6 presents a summary of the thesis. It offers an overview of the research and conclusions drawn from the experimental results are presented.

CHAPTER 2

THEORY AND LITERATURE REVIEW

2.1 INTRODUCTION

This chapter presents the literature pertaining to the theory of emulsions in general and of high internal phase ratio emulsion explosives in particular. The relevant fundamentals of emulsion stability are discussed with greater emphasis on the stability of high internal phase ratio emulsions, particularly high internal phase ratio emulsion explosives. The theory of the basic rheological properties of viscoelastic materials is also presented. This includes the applicable flow models for pseudo-plastics fluids. The dependence of electrolyte type and concentration as well as surfactant type and surfactant concentration, and the effect on the rheological properties and stability of such emulsions is also discussed.

This chapter covers relevant theoretical aspects associated with the stability of emulsions and the flow of non-Newtonian fluids, and the following topics are presented:

- definition of emulsions
- general consideration of emulsion stability
- factors determining emulsion stability
- surfactant and interfacial properties
- stability of high internal phase emulsion explosives
- definition of rheology
- general classifications of flow behaviour
- general description of viscoelastic behaviour
- rheology of emulsions, with emphasis on high internal phase emulsions, particularly high-internal phase emulsion explosives
- dependence of electrolyte and surfactant type and electrolyte and surfactant concentration on the rheology and stability of high internal phase emulsions, particularly high-internal phase emulsion explosives.

2.2 GENERAL DEFINITION OF AN EMULSION

An emulsion is a suspension of particles of a liquid of a certain size within a second, immiscible liquid. Macro emulsions are of two types, based on the nature of the dispersed phase: oil-in-water (O/W) and water-in-oil (W/O). The O/W type is a dispersion of a water-

immiscible liquid or solution, always called the oil (O), regardless of its nature, in an aqueous phase (W). The oil, in this case, is the “discontinuous” (inner) phase; the aqueous phase is the “continuous” (outer) phase. The W/O type is a dispersion of water or an aqueous solution (W) in a water-immiscible liquid (O) (Myers, 1999; Rosen, 2004).

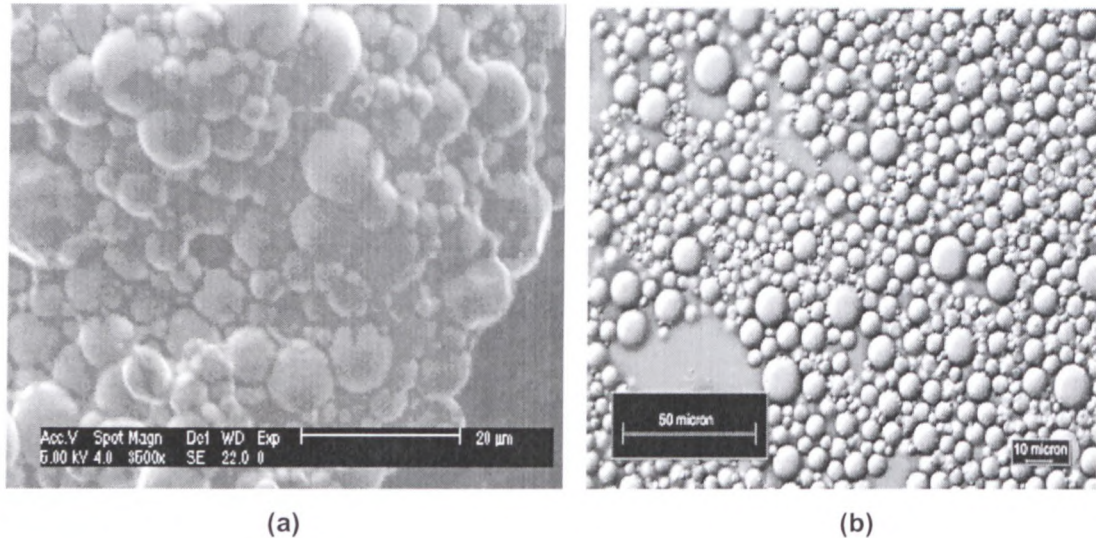
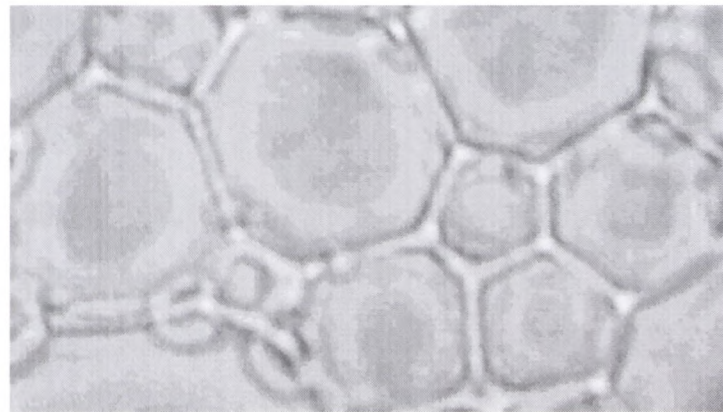


Figure 2.1: Microscopic images of a concentrated emulsion – (a) general case where the droplet deformation at compression is clearly seen in an image made in the Research Rheology laboratory of the Cape Peninsula University of Technology (South Africa); (b) dilute emulsion, image adapted from: McClements, 2005:3

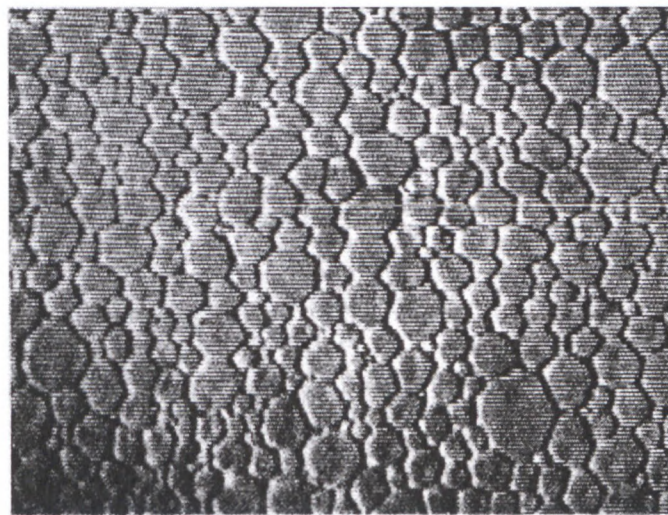
The presence of emulsifier is usually required for emulsion formation. Normally, an emulsifier (stabiliser) is required to facilitate the formation of drops of the desired size and stability. Stabilisers may perform two primary functions: (1) lower the energy requirements of drop formation (i.e., lower the interfacial tension) and (2) retard the process of drop reversion to separate bulk phases. In order to function properly, it must adsorb at the liquid-liquid interface (Myers, 1999). In its second function, the additive must form some type of film or barrier (monomolecular, electrostatic, steric, or liquid crystalline) at the new liquid-liquid interface that will prevent or retard droplet flocculation and coalescence. The process of barrier formation or adsorption must be rapid relative to the rate of drop coalescence or a rather coarse emulsion will result (Myers, 1999).

The type of emulsion formed by the water and the oil depends primarily on the nature of the emulsifying agent and, to some extent, on the process used in preparing the emulsion and the relative proportions of oil and water present. In general, O/W emulsions are produced by emulsifying agents that are more soluble in the water than in the oil phase, whereas W/O emulsions are produced by emulsifying agents that are more soluble in the oil than in the water phase. This is known as the Bancroft rule (Binks, 1998; Rosen, 2004).

remaining separated by thin stable films of the continuous phase (Sjöblom, 2001), as shown in Figure 2.2



(a)

10 μ m

(b)

Figure 2.2: Image of highly concentrated emulsion – (a) image made in Research Rheology laboratory of Cape Peninsula University of Technology (South Africa) – (b) Adapted from Binks, 1998:368

At sufficiently high Φ , the drops become distinctly polyhedral, albeit with rounded edges and corners. At this stage, the continuous phase is confined to two structural elements: linear Plateau borders with essentially constant cross-section over some finite length, and tetrahedral Plateau borders where four linear borders converge (Sjöblom, 2001). This is shown in Figure 2.3 (a).

Most emulsions are much more complex than the simple three-component (oil, water and emulsifier) systems. The aqueous phase may contain a variety of water-soluble ingredients. The oil phase usually consists of a complex mixture of oil-soluble components. The interfacial region may contain a mixture of various surface-active components. In addition, these components may form various types of structural entities in the oil, water, or interfacial region (McClements, 1999).

Knowledge of the concentration of droplets is important because the droplet concentration influences the appearance, texture, stability and cost (in terms of concentration of the dispersed phase and, therefore, surfactant) of emulsion-based products. The concentration of droplets in an emulsion is usually described in terms of the dispersed phase volume fraction (ϕ), which is equal to the total volume of the emulsion droplets (V_{DPh}) divided by the total volume of the emulsion (V_E):

$$\phi = \frac{V_{DPh}}{V_E} \quad \text{Equation 2.1}$$

In some situations, it is more convenient to express the composition of an emulsion in terms of the dispersed phase mass fraction (C), which is related to the volume fraction by the following equation:

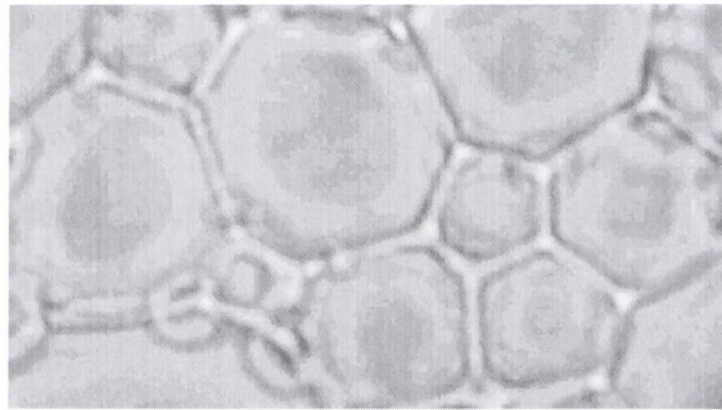
$$C = \frac{\phi \rho_{DPh}}{\phi \rho_{DPh} + (1 - \phi) \rho_c}, \quad \text{Equation 2.2}$$

where ρ_c and ρ_{DPh} are the densities of the continuous and dispersed phases, respectively. When the densities of the two phases are equal, the mass fraction is equivalent to the volume fraction. The dispersed-phase volume fraction of an emulsion is often known because the concentrations of the ingredients used to prepare it are carefully controlled (McClements, 1999).

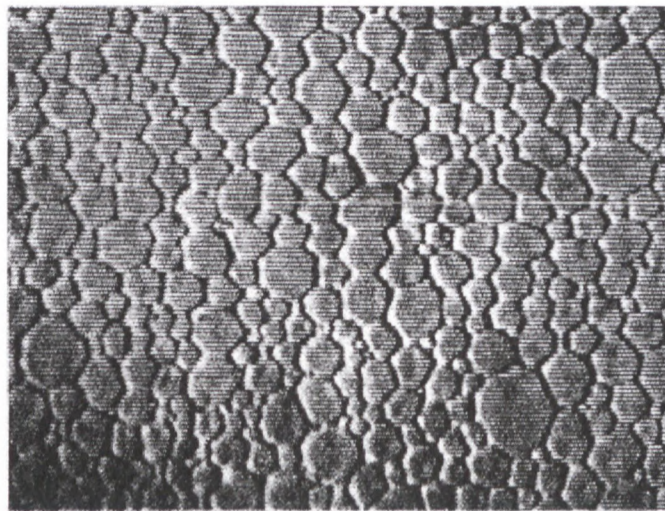
2.3 HIGHLY CONCENTRATED EMULSIONS AND THEIR STRUCTURE.

The highly concentrated emulsions are characterised by their large internal phase volume fraction (as large as 0.99), low surfactant content (as low as 0.5 wt%) and gel-like consistency (Aronson & Petko, 1993; Binks, 1998; Kizling & Kronberg, 2001). The internal phase volume fraction in a gel emulsion is larger than the critical value of the most compact arrangement of uniform, undeformed spherical droplets. When the volume fraction is raised beyond $\phi_c = 0.74$, the drops lose their sphericity and are increasingly deformed while

remaining separated by thin stable films of the continuous phase (Sjöblom, 2001), as shown in Figure 2.2



(a)

10 μ m

(b)

Figure 2.2: Image of highly concentrated emulsion – (a) image made in Research Rheology laboratory of Cape Peninsula University of Technology (South Africa) – (b) Adapted from Binks, 1998:368

At sufficiently high Φ , the drops become distinctly polyhedral, albeit with rounded edges and corners. At this stage, the continuous phase is confined to two structural elements: linear Plateau borders with essentially constant cross-section over some finite length, and tetrahedral Plateau borders where four linear borders converge (Sjöblom, 2001). This is shown in Figure 2.3 (a).

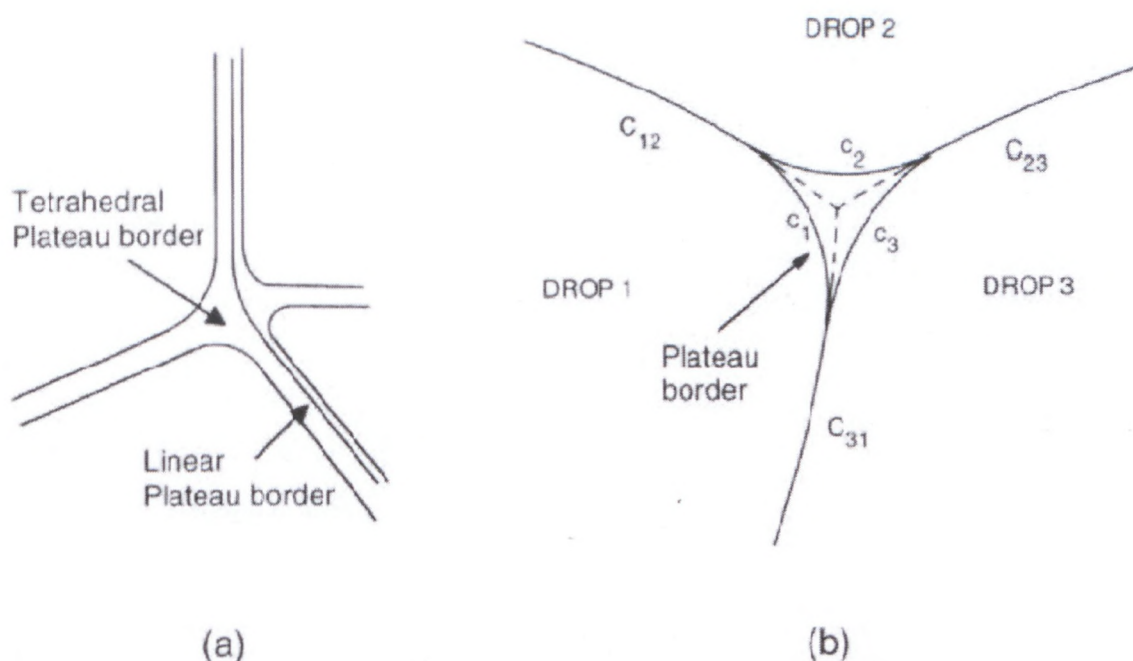


Figure 2.3: (a) Four linear Plateau borders meeting in a tetrahedral Plateau border; (b) cross-section through a linear Plateau border and its three associated films and drops

(Adapted from Sjöblom, 2001: 245)

Each linear border is generally curvilinear and fills the gap between the rounded edges of three adjoining polyhedral drops. In cross-section, its sides are formed by three arcs, each pair of which meets tangentially to form the thin film separating the corresponding droplet pair (Figure 2.3b).

Depending on the emulsion forming system the droplet size and polydispersity can be sufficiently low. Highly concentrated emulsions can be classified as W/O and O/W. The surfactant in W/O emulsion is distributed between the interface and reversed micelles (Binks, 1998; Reynolds, Gilbert & White, 2000; 2001).

2.4 EMULSION STABILITY: BASIC CONCEPTS

Emulsions are often required to possess excellent storage stability. Their shelf life needs to exceed several months or possibly years. In other applications, the goal is to produce emulsions with limited but controlled stability.

2.4.1 Mechanism of emulsion instability

According to Binks (1998) the four main ways in which an emulsion can become unstable are creaming (or sedimentation), flocculation, coalescence and Ostwald ripening. Creaming (in O/W emulsions) arises from the action of gravity on drops of lower density than that of the continuous phase and is reversible in that gentle agitation can re-establish the original uniform distribution of drops. In W/O emulsions the equivalent phenomenon is called sedimentation (Binks, 1998; McClements, 1999; 2005). Flocculation is the process by which emulsion drops aggregate without rupture of the stabilising layer at the interface. It may be weak (reversible) and strong (not easily reversible) depending on the strength of the inter-drop forces (Binks, 1998). Coalescence is referred to as the process in which two or more emulsion drops fuse together to form a single large drop and it is irreversible (Binks, 1998). Extensive droplet coalescence can eventually lead to the formation of a separate layer of oil on top of the sample (McClements, 1999). Ostwald ripening is a molecular diffusion from smaller to larger droplets which leads to an increase in the droplet size of emulsion (Binks, 1998; Park, 2003). The driving force for Ostwald ripening is the difference in solubility of the substance in small and large droplets (the smaller droplets have higher Laplace pressure and higher solubility than the larger ones). Theoretically, Ostwald ripening should lead to condensation of all droplets into a single drop. This does not occur in practice, since the rate of growth decreases with increasing droplet size (Binks, 1998; Tadros, 2005).

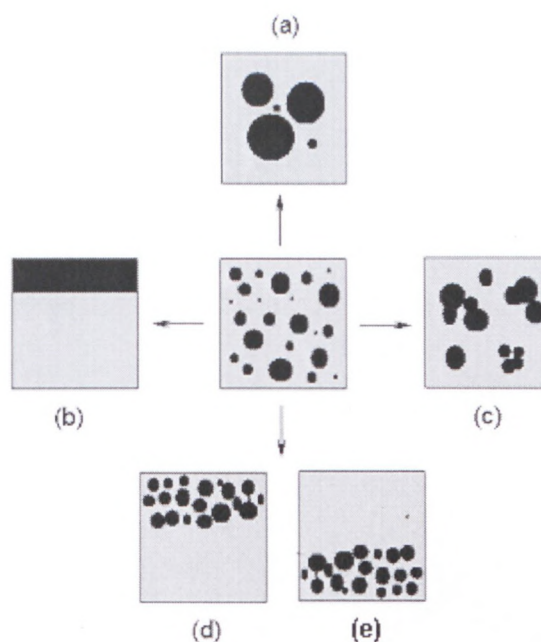


Figure 2.4: The ultimate fates of emulsions related to colloidal stability: (a) coalescence; (b) breaking; (c) flocculation; (d) creaming; (e) sedimentation
(Adapted from Myers, 1992: 213)

As a general rule, creaming/sedimentation, flocculation, Ostwald ripening, and coalescence are simultaneous processes. However, since coalescence can only occur if the droplets are close enough, flocculation and creaming/sedimentation are considered to be precursor mechanisms to coalescence (Radeva, 2001).

2.4.2 Emulsion stabilisation mechanisms

There are four general classes of materials that can, under the proper circumstances, act as emulsifiers or stabilisers for emulsions. The list includes common ionic materials, colloidal solids, polymers, and surfactants. Each class varies greatly in its effectiveness in a given role, and in its mode of action (Myers, 1999).

Adsorbed nonsurfactant ions (Fig.2.5a) usually do little to affect interfacial tension (except to raise it in some cases) and therefore do little to facilitate emulsification. However, some may aid in stabilising the system by imposing a slight electrostatic barrier between approaching drops. Alternatively, they may affect the stability of the system by their action in orienting solvent molecules in the neighbourhood of the interface, altering some local physical properties such as dielectric constant, viscosity, and density, thereby producing a small stabilising effect (solvation effects) (Myers, 1999).

Small colloidal materials (sols), while not directly affecting interfacial tensions, can stabilise an emulsion by forming a physical barrier between drops, thereby retarding or preventing drop coalescence (Fig.2.5b).

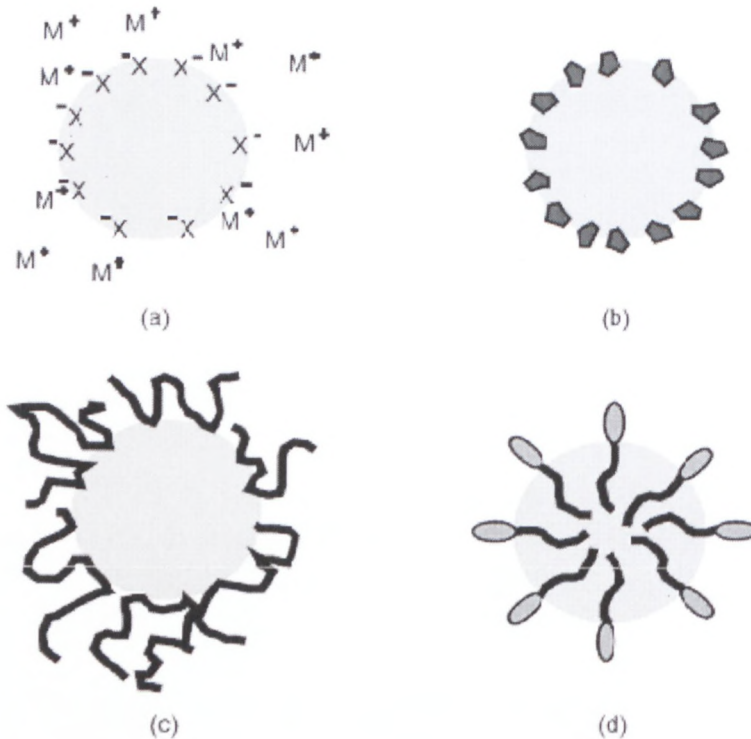


Figure 2.5: Emulsion stabilisation by the presence of adsorbed ions and non surface-active salts (a), by presence of colloidal sols (b), by adsorbed polymer molecules (c), by adsorbed surfactant molecules (the most common stabilisation mechanism) (d)

(Adapted from Myers, 1999: 11)

The action of such materials will depend on several factors, the most important of which are the particle size and the specific interfacial interactions between the solid surface and the two liquid phases making up the system. In general, a particle should be partially wetted by both liquid phases, but with a slight preference for the external phase (Myers, 1999).

Polymeric additives may aid in emulsion formation as a result of surface-active properties, but are usually more important as stabilisers. Their action may result from steric or electrostatic interactions, from changes in the interfacial viscosity or elasticity, or from changes in the bulk viscosity of the system. In many if not most cases, the function of polymeric stabilisers is a combination of several actions (Fig.2.5c) (Myers, 1999).

Surfactants are effective at significantly lowering the interfacial tension between the two liquid phases (Myers, 1999).

2.4.3 Factors determining emulsion stability

According to Rosen (2004), emulsion stability has been found to depend on a number of factors:

- the physical nature of the interfacial film
 - the existence of an electrical or steric barrier on the droplets
 - the viscosity of the continuous phase
 - the size distribution of the droplets
 - the phase volume ratio
 - the temperature
-
- *Physical nature of the interfacial film.*

Mechanical strength of the interfacial film is one of the prime factors determining emulsion stability (Rosen, 2004). For maximum mechanical stability, the interfacial film resulting from the adsorbed surfactants should be condensed, with strong lateral intermolecular forces, and should exhibit high film elasticity. According to Myers (1999), condensed film is composed of densely packed, highly oriented molecules with little mobility and low compressibility. This type of film is especially important in stabilisation of W/O emulsions, since the water droplets are mostly stabilising by a steric barrier (Rosen, 2004).

- *Existence of an electrical or steric barrier on the droplets*

The presence of a charge on the dispersed droplets constitutes an electrical barrier to the close approach of two particles to each other (Rosen, 2004). Such electrical stabilisation may occur when droplets are covered by electrically charged emulsifier and by creating an electrical double layer (McClements, 1999; 2005). Steric barriers also play an important role in emulsion stabilisation. The most important of these is polymeric steric stabilisation due to the presence of polymeric emulsifiers at the oil-water interface, which prevents droplet contact due to steric repulsion forces. Macromolecules (polymer, proteins) provide strong steric stabilization due to their conformational rearrangement at the interface (McClements, 1999; 2005). Many polymeric emulsifiers are charged and therefore they stabilise emulsion droplets against aggregation through a combination of electrostatic and steric repulsion (McClements, 1999).

- *Viscosity of the continuous phase*

An increase in the viscosity η of the continuous phase reduces the diffusion coefficient D of the droplets, since, for spherical droplets:

$$D = \frac{kT}{6\pi\eta a}, \quad \text{Equation 2.3}$$

where k – Boltzmann constant, T – absolute temperature and a – radius of the droplet.

As the diffusion constant is reduced, the frequency of collision of the droplets and their rate of coalescence are reduced. The viscosity of the external phase is increased as the number of suspended particles increases, and this is one of the reasons that many emulsions are more stable in concentrated form than when diluted. The viscosity of the external emulsion phase is usually increased by addition of thickening agents (Rosen, 2004).

- *Droplet size distribution.*

The smaller the range of sizes, the more stable the emulsion. Since larger particles have less interfacial surface per unit volume than smaller droplets in emulsions, they are thermodynamically less stable than the smaller droplets and tend to grow at the expense of the smaller ones. If this process continues, the emulsion eventually breaks. An emulsion with a fairly uniform size distribution is therefore more stable than one with the same average particle size having a wider distribution of sizes (Rosen, 2004).

- *Temperature.*

Temperature affects the interfacial tension between two phases, viscosity of interfacial film, relative solubility of the emulsifying agent in the both phases, vapour pressures and thermal agitation of the dispersed particles and thereby influence the emulsion stability. It may invert the emulsion or cause it to break (Rosen, 2004).

2.5 FORMATION, STABILITY OF INTERFACE AND INTERFACIAL TENSION

The change in free energy when a molecule is brought from the interior of the phase to the interface is determined by changes in the interaction energies of the molecules involved, as well as by various entropy effects.

$$G^S = \sigma = H^S - TS^S \quad \text{Equation 2.4}$$

Often, and as a good approximation, H^S and the surface energy E^S are not distinguished, so Equation 2.6 can be seen in the form (Adamson, 1997):

$$G^S = \sigma = E^S - TS^S \quad \text{Equation 2.5}$$

E^S : The total surface energy; It is generally larger than the interfacial tension and is frequently the more informative of the two quantities, or, at least, is more easily related to molecular models (Adamson, 1997). It characterises the interaction energy between the molecules present at the interface.

S^S : The surface entropy per unit area of surface. The thermal energy associated with the entropy has a disorganising influence, inducing a continual motion of molecules (translation, rotation and vibration) that opposes molecular interaction energy. The entropy effect associated with the interface is mainly due to the fact that a molecule, when located at an interface, is confined to a region which is considerably smaller than the volume it would occupy in a bulk liquid and its molecular rotation is restricted. Both of these effects are entropically unfavourable.

Because of the thermal energy, fluctuations at the interface tend to take place to cause the latter to be in a very turbulent state; wave-like behaviour of the interface may occur, which will tend to merge the two phases (Adamson, 1997; McClements, 1999).

$$\left(\frac{\delta G^S}{\delta T} \right)_p = \frac{d\sigma}{dT} = -S^S \quad \text{Equation 2.6}$$

- If $\sigma > 0$ ($E^S > TS^S$), a thin, stable interface will form because the strong repulsions between the molecules present at the interface is greater than the dispersive forces. The interactions between the different types of molecules are highly unfavourable and the interfacial region is relatively thin because the protrusion of a molecule from one phase into another involves a large expenditure of energy (Adamson, 1997).
- If $\sigma < 0$ ($E^S < TS^S$), the two liquids are miscible and the interfacial region disappears altogether: the fluctuations will lead to a complete dispersion of one phase into another.
- If $\sigma = 0$ ($E^S = TS^S$), an unstable interface is formed; the liquids are partially miscible. The fluctuation forces will lead to a partial dispersion of one phase into another and the interfacial region will increase in thickness. In this case, the interface tends to exhibit undulations and molecules will be twisting and turning continually, as well as moving in and out of the interfacial region (Adamson, 1997).

2.5.1 Curvature and orientation at the interface

A general prerequisite for the existence of a stable interface between two phases is that the free energy of the formation of the interface be positive. Where the interfacial tension is negative or zero, fluctuations would lead to partial or complete dispersion of one phase into another system (the thickness and mobility of the interfacial region are therefore governed by a balance between the interaction energies and the thermal energy of the system (Adamson, 1997; Israelachvili, 1992; McClements, 1999).

The majority of surfaces and interfaces found in emulsions are curved rather than planar. The curvature of an interface alters its characteristics in a number of ways (McClements, 2005).

Droplets tend to be spherical because this shape minimises the energetically unfavourable contact area between oil and water molecules (this shape gives the smaller surface for a given volume). At equilibrium, the pressure within the droplet is larger than that outside and can be related to the interfacial tension and radius of the droplets, using the Laplace-equation:

$$\Delta p = \frac{2\sigma}{r} \quad \text{Equation 2.7}$$

Where Δp is the drop in pressure across a curved interface and r is the radius of the droplet.

This equation indicates that the pressure difference across the interface of an emulsion droplet increases as the interfacial tension increases or the size of the droplet decreases.

Droplets become non-spherical when they experience an external force that is large enough to overcome the Laplace pressure (e.g. gravity, centrifugal forces or mechanical agitation). The Laplace equation emphasises that the magnitude of the force needed to deform a droplet decreases as the interfacial tension decreases or the radius increases. This accounts for the ease with which the relatively large droplets in highly concentrated emulsions are deformed into polygons (McClements, 1999; 2005).

For any curvature, the general form of the Young-Laplace equation is given by:

$$\Delta p = \sigma \left(\frac{1}{r_1} + \frac{1}{r_2} \right) \quad \text{Equation 2.8}$$

r_1 and r_2 are the principal radii of curvature.

An important characteristic of an interface is that it is directional. Properties vary differently, both along and perpendicular to the interface. To be incorporated at an interface, some molecules must be in a specific orientation (McClements, 1999). Unsymmetrical molecules will be oriented at an interface so that their mutual interaction energy will be at maximum. A somewhat more quantitative development along this subject was given by Langmuir in what he termed the principle of independent surface action. He proposed that, qualitatively, one could suppose each part of a molecule to possess local surface free energy. One can employ this principle to decide how surface-active molecules should be oriented (Adamson, 1997).

2.6 INTERACTION ENERGIES (FORCES) BETWEEN EMULSION DROPLETS AND THEIR COMBINATIONS

Emulsions are generally stabilised by repulsive charges on the surface of the dispersed phase and by adsorbed layers of surfactants that act as an interfacial barrier to prevent the close contact or coalescence of the dispersed droplets (Chen, Lu, Chang, Yang & Maa, 2000). Generally, there are three main interaction energies (forces) between emulsion droplets: Van der Waals attraction, electrostatic repulsion and steric repulsion (Tadros, 2005). The attractive Van der Waals forces in the film are counteracted by repulsive forces that provide separation of emulsion droplets (Tadros, 2005; Kizling & Kronberg, 2001).

2.6.1 Van der Waals attraction

There are three types of Van der Waals attraction between atoms or molecules: dipole-dipole (Keesom), dipole-induced dipole (Debye) and dispersion (London) interactions. London dispersion interactions, which arise from charge fluctuations, are the most important contribution to the total Van der Waals interaction because of their universal nature, as contrasted with the dipolar and induced dipolar forces, which vary with the exact chemical natures of the species involved and may or may not make a significant contribution to the total energy (Myers, 1999; Tadros, 2005).

Hamaker suggested that the London dispersion interactions between atoms or molecules in macroscopic bodies (such as emulsion droplets) can be added, resulting in a strong Van der Waals attraction, particularly at short separations between the droplets. For two droplets with equal radii R , at a separation distance h , the Van der Waals attraction G_A is given by the following equation (Tadros, 2005):

$$G_A = -\frac{AR}{12h}, \quad \text{Equation 2.9}$$

where A is the effective Hamaker constant. From the above equation it can be seen that G_A rapidly increases with decreasing h .

According to McClements (1999; 2005), some general features of Van der Waals interactions can be defined:

- The interaction between two oil droplets (or between two water droplets) is always attractive.
- The strength of the interaction decreases with droplet separation, and the interaction is fairly long-range.
- The interaction becomes stronger as the droplet size increases.
- The strength of the interaction depends on the physical properties of the droplets and the surrounding liquid (through the Hamaker function).
- The strength of the interaction depends on the thickness and composition of the adsorbed emulsifier layer.
- The strength of the interaction decreases as the concentration of electrolytes in an oil-in-water emulsion increases because of electrostatic screening.

To balance the Van der Waals attraction, it is necessary to create repulsive forces. The two main types of repulsion that can be distinguished, depending on the nature of the emulsifier used, are electrostatic (due to the creation of double layers) and steric (due to the presence of adsorbed surfactant or polymer layers) (Tadros, 2005).

2.6.2 Electrostatic repulsion

The droplets in many emulsions have electrically charged surfaces because of the adsorption of emulsifiers which are either ionic or capable of being ionized. The magnitude and sign of the electrical charge on an emulsion droplet therefore depend on the type of emulsifier used to stabilise it, the concentration of the emulsifier at the interface, and the prevailing environmental conditions, such as pH, temperature, ionic strength. All the droplets in an emulsion are usually stabilised by the same type of emulsifier and therefore have the same electrical charge. The electrostatic interaction between similarly charged droplets is repulsive, and so electrostatic interactions play a major role in preventing droplets from coming close enough together to aggregate (McClements, 1999; 2005).

There are three types of ions which can influence surface charge into three categories (McClements, 1999):

- Potential-determining ions. This type of ion is responsible for the association-dissociation of charged groups.

- Indifferent electrolyte ions. This type of ion accumulates around charged groups because of electrostatic interactions. The influence of indifferent electrolyte ions on surface charges is determined principally by the ionic strength of the surrounding solution.
- Adsorbed ions. The surface charge can also be altered by the adsorption of surface-active ions.

When two droplets approach to a distance h that is smaller than the double layer extension, double layer overlap occurs and this leads to repulsion (the double layers cannot be fully developed). The double layer extension depends on electrolyte concentration and valency (the lower the electrolyte concentration and the lower the valency, the more extended the double layer is) (Tadros, 2005). The double layer extension decreases with increasing electrolyte concentration, meaning that the repulsion decreases with decreasing electrolyte concentration (Tadros, 2005). The combination of Van der Waals attraction and double layer repulsion results in the well-known theory of colloid stability that is due to Deryaguin, Landau, Verwey and Overbeek (DLVO theory):

$$G_T = G_A + G_{el} \quad , \quad \text{Equation 2.10}$$

where, G_T – total energy, G_A – attractive energy and G_{el} – electrostatic repulsive energy between two drops.

2.6.3 Steric repulsion

Steric repulsion is the term used to describe the repulsion between surfaces covered by layers of polymer or non-ionic surfactant. The concept is that as the coated surfaces approach each other a large local osmotic pressure develops as the layers interact. Initially the interaction is a mixing one as the outer layers start to interpenetrate but, as the surfaces approach closer, the interaction includes changes due to restriction of chain conformation as the space is reduced (Goodwin & Hughes, 2000). The interaction is governed by:

- the number of chains per unit area on the surface
- the thickness of the layer
- the solvent quality
- the strength of the 'anchor' of the chains.

2.7 AQUEOUS SOLUTION

The aqueous phase of most emulsions contains a variety of water-soluble constituents (minerals, surfactants, acids). Many of the solutes present in an emulsion are capable of

being ionized. Most ionic solutes have high water solubility because the formation of many ion-dipole bonds (ion-water) in an aqueous solution helps to compensate for the strong ion-ion bonds in the crystal (McClements, 1999; 2005). When an ionic solute is added to the water, it disrupts the existing tetrahedral arrangement of the water molecules and imposes a new order on the water molecules. The influence of ionic solutes on the overall properties of water depends on their concentration (Israelachvili, 1992; Robinson *et al.*, 1996; McClements, 1999; 2005). At low solute concentrations, the majority of the water molecules is not influenced by the presence of the ions and therefore has properties similar to that of bulk water. At intermediate solute concentrations some of the water molecules have properties similar to those of bulk water, whereas the rest have properties that are dominated by the presence of the ions. At high solute concentrations, all the water molecules are influenced by the presence of the solute molecules and therefore have properties that are appreciably different from those of bulk water (McClements, 1999; 2005).

In studies on the surface tension of a number of solutions it was found that, when a solute is put into the water, the surface tension will change with the solute concentration.

The surface tension depends only on the surface excess of the ions, which is a measure of the magnitude of the intermolecular attractive forces. This means that the surface tension critically depends on where the ions are located with respect to the water surface, as defined by the Gibbs dividing surface (Petersen & Saykally, 2006).

The decrease/increase in surface tension of aqueous solutions with respect to pure water is related to a surface excess/deficit (negative surface excess) by the Gibbs equation, a macroscopic thermodynamic relation (Petersen & Saykally, 2006):

$$d\gamma = \sum \Gamma_i d\mu_i, \quad \text{Equation 2. 11}$$

wherein γ is the surface tension (units: $\text{dyn cm}^{-1} = \text{mN m}^{-1}$), Γ_i is the surface excess (moles cm^{-2}) relative to the Gibbs dividing surface of the solvent, μ_i is the chemical potential (J mole^{-1}), and the summation is taken over all solute species (Petersen & Saykally, 2006).

The following groups of compounds affecting surface tension can be detected:

- Inorganic salts (NaCl, Na_2SO_4 , KOH, NH_4Cl , KNO_3 and other inorganic salts and organic substances such as sucrose and mannite) increase the surface tension of water (Xuguang, 1994; Petersen & Saykally, 2006). At concentrations above 0.01 M, the surface tension increases approximately linearly with concentration, with the magnitude of the increase following the charge density of the anions. The changes in

the surface tension with addition of salt depend on the ion distribution in water, which was currently proposed in literature. The cations are drawn toward the interface by the electrostatic interactions with the anions and are enhanced just below the outermost liquid layer, where the anions are then depleted. Accordingly, there will be a minimum in the Gibbs free energy for the anions at the outermost liquid layer but a maximum just below it, while, for the cations, there will be a minimum just below the outermost layer (Petersen & Saykally, 2006).

- Most organic compounds such as alcohols, aldehydes, acids and esters decrease the surface tension of water (Xuguang, 1994). It has recently been proposed that hydronium is actually enhanced at the water surface, as opposed to the behaviour of ordinary cations. The proposed mechanism that brings hydronium to the surface is quite different to that operating for anions. Due to the reduced negative charge on the oxygen atom, hydronium is only capable of forming three hydrogen bonds (all donor), as opposed to the two acceptor and two donor hydrogen bonds formed among solvent molecules. Hydronium thus perturbs the bulk hydrogen bonding network and is expelled to the surface, where it is more easily accommodated (Petersen & Saykally, 2006).
- Soap, organic acids and alkalis of a straight chain above C₈, metallic soaps, high carbon and straight chain alkyl sulphate or sulfonate, benzene sulfonate, etc. sharply decrease the water surface tension (Xuguang, 1994)

Surface tension is the excess Gibbs free energy per unit area needed to create a surface between liquid and air and results from the difference in the forces/pressures acting parallel and perpendicular to the surface in the interfacial region (Xuguang, 1994; Petersen & Saykally, 2006). If two phases are immiscible liquids, the surface tension is replaced by interfacial tension. The interfacial tension is a physical characteristic of a system which is determined by the imbalance of molecular forces across an interface: the greater the interfacial tension, the greater the imbalance of forces (Israelachvili, 1992).

The following relationships exist between surface and interfacial tension:

- $W_A = \gamma_1 + \gamma_2 - \gamma_{12}$, where W_A – adhesion works between two surfaces, γ_1 and γ_2 – the surface tensions of individual liquids, γ_{12} – interfacial tension between two liquids.
- Antonoff's rule: $\gamma_{12} = \gamma_1 - \gamma_2$, where γ_{12} – interfacial tension between two immiscible liquids, γ_1 , γ_2 – surface tension of liquids saturated by another one (Xuguang, 1994).

2.7.1 Hydrogen bond formation at complex aqueous interfaces

2.7.1.1 Hydrogen bonds in water

The process of breaking and making hydrogen bonds play a crucial role in the dynamic behaviour of liquid water. The study of hydrogen-bond formation (H-bond) dynamics in aqueous interfaces has therefore become a subject of intense current interest (Senapati, 2007).

Hydrogen bonds are relatively weak bonds and involve interaction of covalent bound hydrogen with an electronegative atom or group. They can be considered to be present when a group AH, which is capable of serving as a donor, and an atom or group B, which is capable of serving as an acceptor, are present in a system (Baker, 1971). Two common hydrogen bond acceptors are the carbonyl group and water.

In most cases the existence of strong hydrogen bonds results in the donor and acceptor groups (AH and B) being closer together than the sum of the Van der Waals radii for A-H and B. The distance between A and along the line of the bond is usually decreased by about 0.2 Å. This does not mean that there is no hydrogen bonding when this condition is not met; it simply implies that longer bonds will be weaker (Baker, 1971).

Polar compounds such as alcohols, unionized amines, silylhydriyls, carboxylic acids, ethers, esters, and phenols interact with the water by the formation of hydrogen bonds and by dipole interactions. If they fit into water structures with relatively little distortion and can form stable hydrogen bonds with it, they will be soluble. If they disrupt the water structure and hydrogen bond poorly, they will be relatively insoluble. The strength of water-solute hydrogen bonds is similar to the strength of solute-solute hydrogen bonds and there is competition between solvent and solute for hydrogen-bonding sites in those solutes having donor and acceptor groups for hydrogen-bond formation. Depending on the specific substance and the conditions used, solvation of polar molecules by water can strongly influence their physical, chemical, and biochemical properties (Baker, 1971).

The hydrogen bonding interaction between head groups can be important in ordering of surfactant tails at the water-oil interface. The X-ray reflectivity measurements were used to show that triacontanoic acid ($\text{CH}_3(\text{CH}_2)_{28}\text{COOH}$) forms rigid-rod monolayers at the water-hexane interface, even though it differs from triacontanol ($\text{CH}_3(\text{CH}_2)_{29}\text{OH}$), which forms disordered-tail monolayers, by essentially just one oxygen atom in the head group.

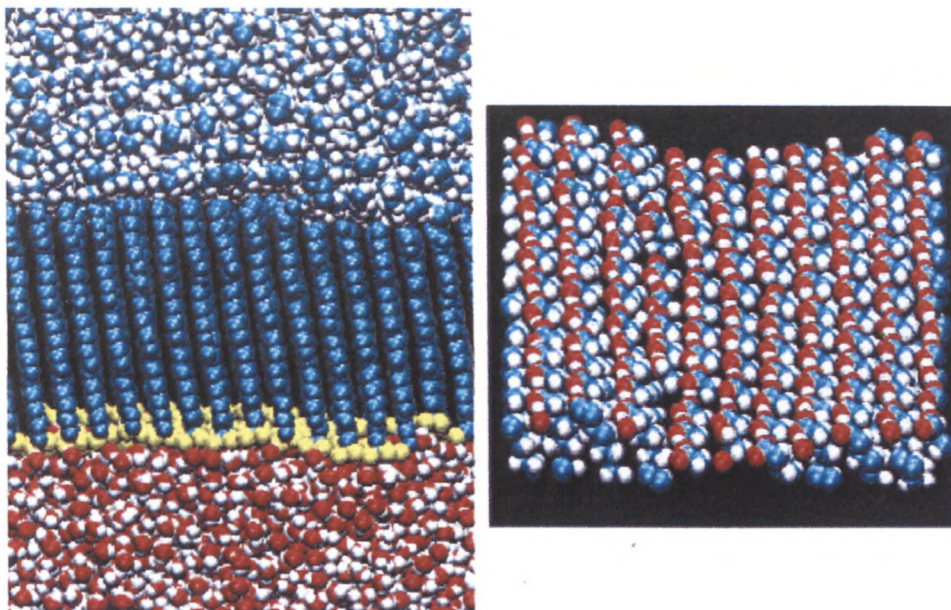


Figure 2.6: Molecular dynamics simulation of a triacontanoic acid monolayer at the water-hexane interface.

(Adapted from Tikhonov, Patel, Garde & Schlossman, 2006)

Colour scheme: H - white, C - blue, O - red, except that head groups of triacontanoic acid in the left view are yellow. View on the left illustrates the ordered all-trans alkyl tails (from bottom to top: water/triacontanoic acid/hexane). The view on the right, with hexane, water molecules, and most of the surfactant tail removed, illustrates nearly parallel rows of hydrogen bonds between adjacent -COOH head groups.

Molecular dynamics simulations of these surfactants at the water-hexane interface reveal extensive hydrogen bonding along rows of -COOH head groups, but much less hydrogen bonding between the -CH₂OH groups. Hydrogen bonding is a strong attractive interaction between the head groups that tips the balance toward surfactant tail ordering in the triacontanoic acid monolayers (see Figure 2.6) (Tikhonov *et al.*, 2006).

2.7.1.2 Effect of pH and cation type on hydrogen bond formation

The degree of ionization of many of the solutes present in the aqueous solution is governed by the pH, and so their interactions are particularly sensitive to pH (McClements, 1999; 2005).

Drying studies of latexes containing carboxylic groups showed that drying rate decreased as the carboxyl group content increased. In the presence of water, carboxylic groups are partially ionized and undissociated carboxylic acid molecules participate in hydrogen bonding with water molecules more readily than the dissociated strong acids (Khutoryanskiy, Mun, Nurkeeva & Dubolazov, 2004; Pedraza & Soucek, 2008).

The effect of pH on the functional groups of bacterial cells was studied by Infrared Spectroscopy (Dittrich & Sibling, 2006). The presence of the $-\text{COOH}$ group of bacterial cells was detected at pH range over 3.03 and the signal was absent at $\text{pH} > 5.82$. These results suggest that protons can rapidly protonate carboxylic groups at low pH that prevent it from dissociation. The progressive H^+ dissociation of carboxylic groups was found present in 0.1M NaNO_3 over the pH range 3.03-8.24, indicating that salt promotes dissociation of the COOH group. Because of sensitivity of the carboxylic group in the acidic pH range, it can act as a metal binding site below pH 5 (Dittrich & Sibling, 2006). The different cation type effects on COOH group dissociation were discussed by Singh and co-workers (2007). The COOH group in a hard base preferred to bind with a hard acid such as Li^+ (or Ca^{2+}), which has a small radius: the smaller the radius of the cation ionized from the salts containing various mono-or divalent cations, the stronger the binding ability on $-\text{COOH}$. This action makes the $-\text{COOH}$ group transform into a $-\text{COO}^-$ group. This H^+ abstraction effect is observed in the order $\text{Li}^+ > \text{Na}^+ > \text{K}^+$ and $\text{Ca}^{2+} > \text{Sr}^{2+} > \text{Ba}^{2+}$.

Specific types of interaction of the Ca^{2+} ion with the peptide chain was proposed by Moses, Inayathullah, Murugesan, Andrews, Balasubramanian and Jayakumar (2003). It was found that the presence of calcium ions lowers the CMC of peptide surfactants and changes the polarity. The observations made in this work support the possibility that Ca^{2+} ion complexation induces enhanced hydrophobicity. The authors pointed out the functional groups which can participate in interactions with the Ca^{2+} ion (see Figure 2.7).

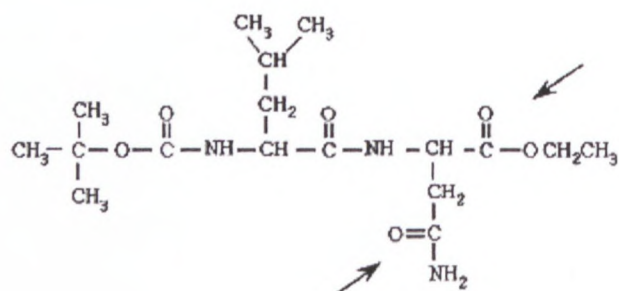


Figure 2.7: Structure of deipeptide

The hydrogen-bond dynamics at complex aqueous interfaces were studied by Senapati (2007). The author performed three independent molecular dynamics computer simulations to examine the effect of counterion identity on hydrogen-bond dynamics in the enclosed water pool of anionic surfactant-based reverse micelles. The water-water hydrogen-bond lifetime in the reverse micelle (RM) with calcium ions was found to be longer than that in the RM with sodium or ammonium ions. The lifetime of the hydrogen bond between a water

molecule and a surfactant head group is always found to be longer than that between two water molecules. It was shown that all three types of cations have a tendency to form contact-ion pairs, and that calcium ions stay closest to the head group surface, followed by Na^+ and NH_4^+ . Ca^{2+} ions with a high charge density (charge density order $\text{Ca}^{2+} > \text{Na}^+ > \text{NH}_4^+$) can strongly interact with the polar head group, and this may bring them closest to the head groups. The closely residing Ca^{2+} ions at the surface can then destabilise the water-head group hydrogen bonds relatively quickly to accomplish a shorter water-head group H-bond lifetime. It was found that the average number of water-head group hydrogen bonds per head group is reduced from 1.01 to 0.66 to 0.5 by going from the reversed micelles with NH_4^+ to Na^+ to Ca^{2+} ions. The hydrogen bonds break but reform most rapidly in the calcium ion contained reversed micelles (Senapati, 2007).

2.8 SURFACTANT, INTERFACIAL PROPERTIES AND THEIR CHARACTERISATION

2.8.1 Definition of surfactant

Surfactants are usually used for the stabilisation of emulsions. The molecules of a surfactant consist of a hydrophilic “head” group which has a high affinity for water and lipophilic “tail” group which has a high affinity for oil.



Figure 2.8: Schematic structure of surfactant molecule

The surfactant molecule organisation is based on the orientation of a polar group to the polar surface and nonpolar group to the nonpolar surface. It leads to decreasing the interface tension between water and oil. The head group may be anionic, cationic, zwitterionic or nonionic. The tail group usually contains one or more hydrocarbon chains, having between 8 and 20 carbon atoms per chain. Surfactant chains can be saturated or unsaturated and linear or branched, aliphatic or aromatic. The degree of branching, position of the polar group in the chain and length of the chain are the main characteristics defining the physicochemical properties of surfactants (Pashley & Karaman, 2004; McClements, 2005).

2.8.2 Surfactant classification

Several classifications of surfactants exist. The most useful chemical classification of surface-active agents is based on the nature of the hydrophile; subgroups are defined by the nature of the hydrophobe (Myers, 1999).

The four general groups of surfactants are defined as follows:

1. Anionic, with the hydrophilic group carrying a negative charge
2. Cationic, with the hydrophile bearing a positive charge
3. Nonionic, where the hydrophile has no charge but derives its water solubility from highly polar groups
4. Amphoteric (and zwitterionic), in which the molecule has, or can have, a negative and a positive charge on the principal chain (Myers, 1999). Such surfactants can be pH-sensitive and pH-insensitive and can be adsorbed onto both negatively and positively charged surfaces without changing the charge of the surface significantly (Yoshimura, Nyuta & Esumi, 2005).
 - pH-sensitive zwitterionics may show the properties of anionics at high pH and those cationics at low pHs (Rosen, 2004; Singh *et al.*, 2007). Zwitterionic surfactants with two nonidentical head groups containing both ammonium and carboxylate exhibit pH-dependent behaviour (Yoshimura *et al.*, 2005). This property arises from the ability of the molecule to carry both positive and negative charges. For example, proteins are made up of peptide chains, that is, of amino acid residues joined by amide linkage. Some of these chains contain basic groups: -NH_2 , and some of them contain acidic groups: -COOH . Because of these acidic and basic side chains, there are positively and negatively charged groups along the peptide chain. The behaviour of proteins in an electric field is determined by the relative numbers of these positive and negative charges, which in turn are affected by the acidity of the solution. At the isoelectric point (Ip), the positive and negative charges are exactly balanced and the protein shows no net migration; as with amino acids, solubility is usually at a minimum here (Morrison & Boyd, 1987; Rosen, 2004; Tadros, 2005).
 - pH-insensitive surfactants are zwitterionics at all pHs (Rosen, 2004; Tadros, 2005).

2.8.3 Polymeric surfactants

The different conformations of polymer chains can be found at the interface, depending on the quality of solvent, affinity of monomer chains to the surface and crowding conditions at the interface. Figure 2.9 shows schematically possible conformational regimes for polymers at interfaces. If the distance between the chains is larger than their size, one can look at the conformation of a single chain since there are no *interchain* interactions (between neighbouring chains). If there is a strong interaction between the surface and the chain monomers, the chain will lie flat on the surface, a situation referred to as a “pancake” conformation (Figure 2.9). If the chain monomers do not have an affinity to the surface, the polymer chain will adopt a “mushroom” conformation (Figure 2.9), where only one chain end is attached to the surface and the rest roughly forms a random coil. When the surface becomes more crowded, the chains will start to interact mutually, eventually resulting in a stretching of the individual chains away from the surface, leading to a so-called “brush” formation (Figure 2.9). This state is the result of a balance between excluded volume interaction, free energy of the segments and the loss of conformational entropy upon stretching (the latter being associated with the elastic free energy of the chain) (Feuz, 2006).

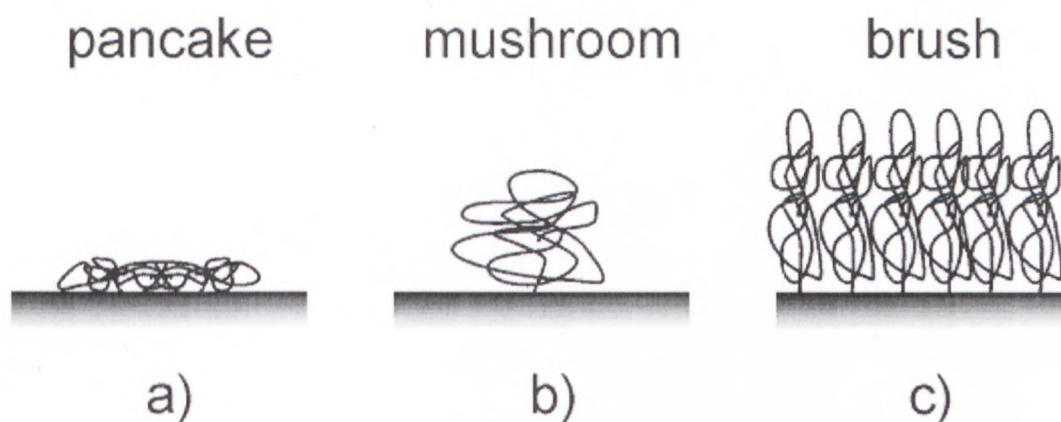


Figure 2.9: Different conformations of polymers at surfaces:

- a) pancake conformation of a single adsorbed chain, occurring when there is strong attraction between the surface and the chain monomers,
- b) mushroom conformation of a single chain under good solvent conditions, and
- c) brush conformation for high grafting densities, leading to extension of the chains away from the surface (Adapted from Feuz, 2006)

2.8.4 Molecular organisation of surfactants in solution

2.8.4.1 Critical micelle concentration

Surfactants exist in solution as monomers at their low concentration. As their concentration is increased they can spontaneously aggregate into association colloids (micelles), which are thermodynamically stable. The colloid structure depends on the kind of surfactant from which it is formed. The driving force for the forming of these structures is the hydrophobic effect: the molecules' organisation tries to minimise the contact between polar parts of molecules and oil. The surfactant concentration at which micelles start to form is called the critical micelle concentration (CMC). This concentration is the most important characteristic of surfactant properties.

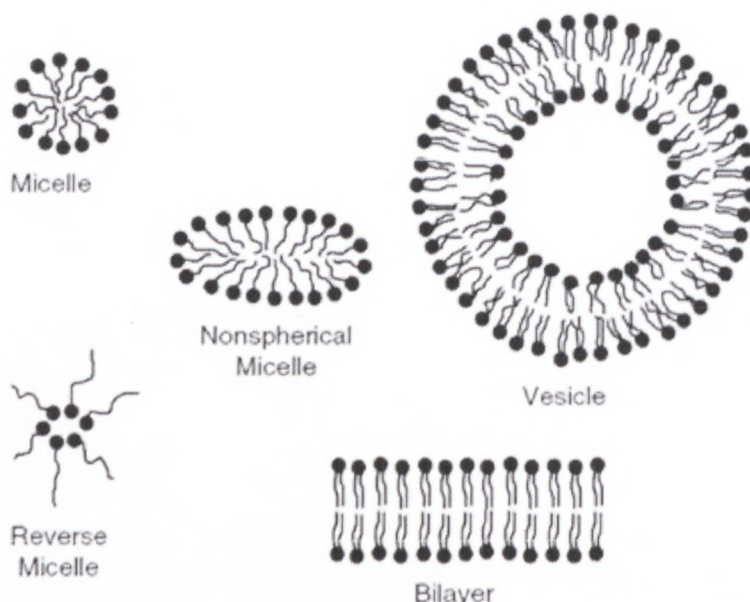


Figure 2.10: Some typical structures formed due to the self-association of surfactant molecules at relatively low surfactant concentrations. At higher surfactant concentrations, many different kinds of liquid crystalline phases may form. (Adapted from McClements, 2005:31)

There are two extended methods of measurement of CMC: from changing of surface tension and from solubilisation. In the case of ionic surfactants, the conductance-measuring method can be used. There also are a lot of recourses for CMC observation, such as self-diffusion, nuclear magnetic resonance (NMR) or fluorescence (McClements, 2005; Holmberg, Jönsson, Kronberg & Lindman, 2002).

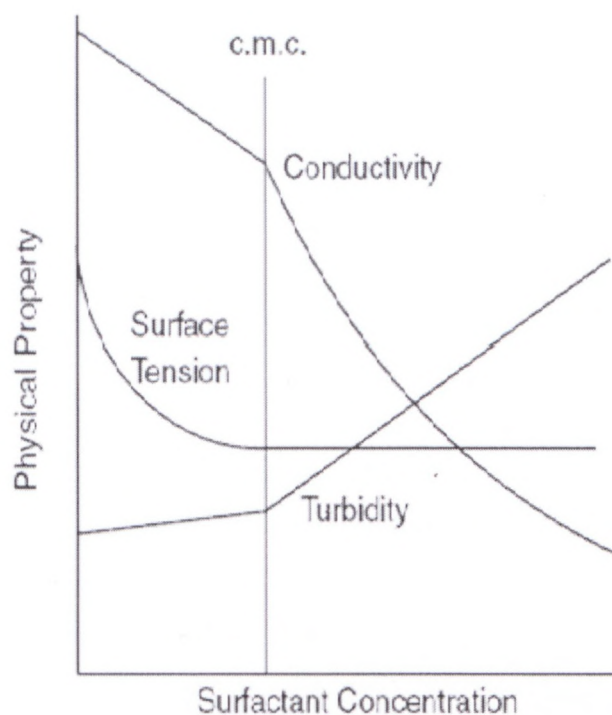


Figure 2.11: A number of important and accessible physical manifestations of micelle formation (Adapted from Myers, 1999)

Micelles are not static species. They are very dynamic in that there is a constant, rapid interchange of molecules between the aggregates and the solution phase. It is also reasonable to assume that surfactant molecules do not pack into a micelle in such an orderly manner as to produce a smooth, uniform surface structure (Myers, 1999).

2.8.4.2 Factors affecting critical micelle concentration (CMC)

- *The CMC dependence on the chemical structure of surfactants* (Holmberg, 2002; Myers, 1999):
 - i. The CMC tends to decrease at increasing surfactant lengths. The CMC of ionic surfactants decrease by two times and by three times for nonionic surfactants at an increase of the alkyl chain on one $-CH_2-$ group.
 - ii. The CMC of nonionic surfactants is lower than the CMC of ionic surfactants.
 - iii. The CMC of cationic surfactants is always not much more than the CMC of anionic surfactants.

- iv The value of the CMC greatly depends on the nature of the compensating ion. Single inorganic compensating ions do not influence CMC. Doubly-charged compensating ions reduce the CMC.

- *CMC dependence on the temperature and additional agents (electrolytes):*

The CMC has a weak dependence on temperature at first. The effect of addition agents on the CMC is extensive and important. The most important question concerns the effect of electrolytes on the CMC of ionic surfactants (Holmberg, 2002 Myers, 1999).

At this point there are the following regularities:

- i. The addition of salt leads to a decrease of CMC.
- ii. It has a great effect on long-chain surfactants and a weak effect on short-chain surfactants.
- iii The influence of a salt additive on CMC depends on the amount of ionic charge.

- *CMC dependence on the pH*

A number of amphoteric surfactants have pH sensitivity related to the pKs of their substituent groups. The possibilities can be grouped in the following way (Myers, 1999):

- i. Quaternary ammonium-strong acid salts will show little or no significant pH sensitivity.
- ii. Quaternary ammonium-weak acid combinations will be zwitterionic at high pH and cationic below the pK_a of the acid.
- iii. Amine-weak acid combinations will be anionic at high pH, cationic at low pH, and zwitterionic at some pH between the respective pK values.
- iv. Amine-strong acid combinations will be anionic at high pH and zwitterionic below the pK_b of the amine.

2.8.4.2 *Reversed micelles*

Some amphiphilic molecules self-assemble in apolar solvents, forming globular aggregates called reversed micelles which are structurally characterised by an internal polar core constituted by opportunely arranged hydrophilic head groups surrounded by the alkyl chains of the amphiphile (Garti, 2000).

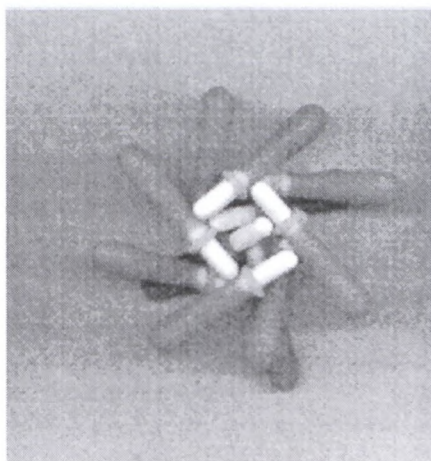


Figure 2.12: Micellar aggregate of “amphiphilic molecules” (Adapted from Garti, 2000)

A significant energetic consequence of nonaqueous micelle formation is the reduction of unfavourable interactions between the ionic head group of the surfactant and the nonpolar solvent molecules (Myers, 1999). Interactions between the hydrophobic tails contribute little to the overall free energy of micelle formation; ionic, dipolar, or hydrogen bonding interactions between head groups in reversed micelles are one of the primary driving forces favouring aggregation (Myers, 1999).

With extensive aggregation, a number of translational and rotational degrees of freedom of surfactant molecules are converted into translational, rotational, and internal degrees of freedom of the entire aggregate. In the case of a reversed micelle, its dynamics are characterised by a wide variety of processes such as diffusion of a surfactant molecule within the aggregate; conformational dynamics of the polar and apolar molecular moieties; micellar shape fluctuation; exchange of surfactant molecules between bulk solvent and micelle; structural collapse of the aggregate leading to its dissolution and vice versa; diffusion and rotation of the entire aggregate; and intermicellar collisions (Garti, 2000).

The evolution of the size and shape of reversed micelles as a function of the water and surfactant concentrations is system-specific. The micellar size is mainly controlled by the strong tendency of the surfactant to be located at the interface between water and apolar solvent, which involves an enormous value of the interfacial surface and micelles of nanometric size. Spherical micelles result from a minimisation of the micellar surface-to-volume ratio, i.e. a minimisation of water-surfactant interactions less favourable than water-water and/or surfactant-surfactant interactions (Garti, 2000).

Water solubilisation involves hydration of the surfactant head group, accompanied by an increase in the head group area; a micellar swelling; a marked increase in the surfactant

aggregation number; and, at constant surfactant concentration, a decrease in the number density of reversed micelles (Garti, 2000).

Solubilisation of water within the micellar core transforms reversed micelles from small and labile aggregates to more stable aggregates with greater persistence in the size and shape of the entire aggregate (even if each molecular component is continuously exchanged with the surroundings); influences the intermicellar interactions; and widens the spectrum of their dynamics (Garti, 2000).

2.8.5 Thermodynamic of adsorption

The accumulation of surfactant molecules at an interface is characterised by the surface excess concentration

$$\Gamma = \frac{n_i}{A} \quad , \quad \text{Equation 2.12}$$

where A is the surface area and n_i is the excess surfactant concentration at the surface. It corresponds to the total amount of surfactant present in the system, minus that which would be present if the surfactant was not surface-active (McClements, 1999; 2005).

The surface excess concentration is often identified with an experimentally measurable parameter called the surface load, which is the amount of surfactant adsorbed to the surface of emulsion droplets per unit area of interface (McClements, 1999; 2005).

The ability of surfactant molecules to shield direct interactions between two immiscible liquids is governed by their optimum packing at the interface, which depends on their molecular geometry. When the curvature of an interface is equal to the optimum curvature of a surfactant monolayer, i.e., optimum packing is possible, the interfacial tension is extra low because the direct interactions between the oil and water molecules are effectively eliminated. On the other hand, when the curvature of an interface is not at its optimum, the interfacial tension increases because some of the oil molecules are exposed to the polar regions of the surfactant or some water molecules come into contact with the hydrophobic part of the surfactant (McClements, 1999; 2005).

A quantitative prediction of the surface or interfacial tension produced by a given concentration of surfactant can most conveniently be made using an equation of the state of the monolayer (McClements, 2005). In such equations, surface tension lowering is expressed in terms of the surface pressure, π , defined as

$$\pi = \sigma^0 - \sigma \quad \text{Equation 2.13}$$

σ^0 : the interfacial tension of the pure oil-water interface

σ : the interfacial tension in the presence of the surfactant (Hiemenz, 1986; McClements, 1999).

Two different thermodynamic approaches have been developed to describe this relationship: the Langmuir adsorption isotherm and the Gibbs adsorption isotherm (Hunter, 1993; Hiemenz & Rajagopalan, 1997). These approaches are based on a thermodynamic analysis of the adsorption process, assuming that the adsorption-desorption of solutes at the surface is reversible, and that solute-solute interactions do not occur in the bulk solution or at the surface.

The Langmuir adsorption isotherm is useful for relating the amount of solute present at a surface to the concentration and surface activity of the solute in the bulk solution:

$$\theta = \frac{\Gamma}{\Gamma_{\infty}} = \frac{c/c_{1/2}}{1 + c/c_{1/2}}, \quad \text{Equation 2.14}$$

where θ is the fraction of adsorption sites that are occupied, Γ_{∞} is the surface excess concentration when the surface is completely saturated with solute, and $c_{1/2}$ is the solute concentration in the bulk solution where $\theta = 1/2$. The equilibrium constant for adsorption ($K = 1/c_{1/2}$) provides a good measure for the surface activity or binding affinity of an emulsifier: the greater $1/c_{1/2}$ the higher the binding affinity. The surface activity of a molecule is related to the free energy of adsorption by the following equation:

$$K = \frac{1}{c_{1/2}} = \exp\left(-\frac{\Delta G_{\text{ads}}}{RT}\right), \quad \text{Equation 2.15}$$

where ΔG_{ads} corresponds to the free energy change associated with exchanging a solvent molecule with a solute molecule at the surface.

There is equilibrium between surfactant molecules at the interface and those in the bulk liquid. As the concentration in the bulk liquid is increased, so does the concentration at the interface. The presence of the surfactant molecules at the interface shields the unfavourable contact within oil and water molecules and therefore reduces the tension. The relationship between the decrease in interfacial tension with surfactant concentration and the amount of surfactant present at the surface is known as the Gibbs isotherm equation.

For a dilute solution (McClements, 1999):

$$\Gamma = -\frac{1}{RT} \left[\frac{d\sigma}{d \ln c} \right] = \frac{1}{RT} \left[\frac{d\pi}{d \ln c} \right] \quad \text{for non-ionic surfactants} \quad \text{Equation 2.16}$$

$$\Gamma = -\frac{1}{2RT} \left[\frac{d\sigma}{d \ln c} \right] = \frac{1}{RT} \left[\frac{d\pi}{d \ln c} \right] \quad \text{for ionic surfactants} \quad \text{Equation 2.17}$$

c : the concentration of surfactant in the bulk solution

Γ : the surface excess concentration; the slope of the curve of the interfacial tension versus the logarithm of concentration

σ : the interfacial tension

π : surface pressure

The Gibbs adsorption isotherm can also be presented in the following form:

$$\pi = pRT \int_0^c \Gamma(c) d \ln c \quad \text{Equation 2.18}$$

$p = -1$ for non ionic surfactant; $p = -1/2$ for ionic surfactant.

Insertion of the Langmuir adsorption isotherm into the above Equation 2.20 and expressing the surface excess concentration in units of mass per unit area rather than moles per unit area gives

$$\pi = \left(\frac{pRT}{M} \right) \Gamma_{\infty} \ln \left(1 + \frac{c}{c_{1/2}} \right) \quad \text{Equation 2.19}$$

A typical plot of surface tension against the logarithm of concentration is shown in Figure 2.13.

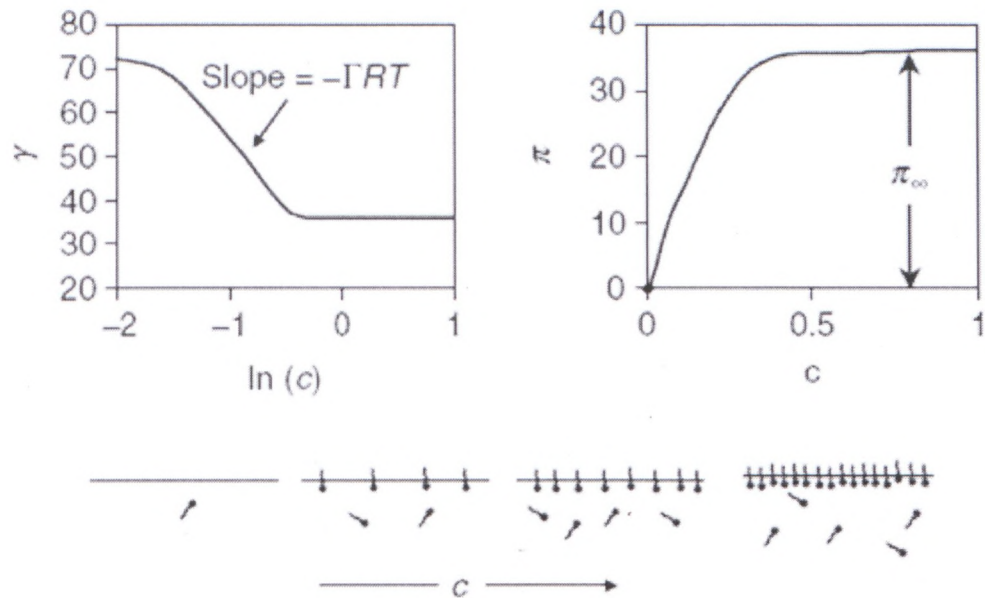


Figure 2.13: Interfacial tension as a function of surfactant concentration in the bulk solution (Adapted from McClements, 2005: 7)

2.9 EMULSION EXPLOSIVES AND THEIR PROPERTIES

2.9.1 Emulsion explosive composition

Emulsion explosives, as described by Bluhm (1969), typically consist of a dispersed aqueous phase of inorganic oxidiser salt solution droplets in a continuous fuel phase in the presence of an emulsifier. The inorganic oxidiser salt solution droplets typically are in the super-cooled state and generally comprises salt in amounts from 45% to 95% by weight of the total composition (Hales *et al.*, 2004). Suitable oxidiser salt components are oxygen containing salts such as, for example, nitrates, chlorates, and perchlorates, in which oxygen is used in the explosive reaction. These oxidizer salts include ammonium nitrate, sodium nitrate, calcium nitrate, potassium nitrate, or mixtures thereof (Nguyen, 1990; Hales *et al.*, 2004). The organic liquid fuel forming the continuous phase of the emulsion phase is immiscible with water. It can be aliphatic, alicyclic or aromatic and can be saturated and unsaturated, as long as it is liquid at the formulation temperature (Cooper & Baker, 1989; Nguyen, 1990; McKenzie, 1991; Hales *et al.*, 2004).

2.9.2 Structure of AN melt

The aqueous phase of the emulsion explosive typically contains 80% AN by mass (molar concentration 50 mol kg^{-3}). The quantity of water in such concentrated systems is not enough to form a proper hydration shell of ammonium nitrate ions. Therefore there is a suggestion that highly concentrated solutions should be correctly referred to as melts.

Ammonium nitrate holds a unique position with regard to the properties of salts in very concentrated aqueous solutions. The classical works of Vollmar (1963) and Narten (1970) emphasise the striking similarity of the NH_4^+ ion to the water molecule concerning mass, partial molar volume, bond angles and inter-atomic distances. NH_4^+ and H_2O form hydrogen bonds of about the same strength and the electrostatic forces exerted on their neighbours are likely to be the same (Bengtsson, Frostemark & Holmberg, 1994).

A few studies were performed on the concentrated AN solutions for the investigation of the ionic structure of solutions.

Two trends were found with increasing AN concentration in water:

- There is a decrease in the coordination number forming a weakly defined hydration shell around the ammonium ion (Walker, Lawrence, Neilson & Cooper, 1989; Adya & Neilson, 1991). It has been established that, in a solution with a molality of 5 mol kg^{-3} , the hydration number of the ammonium ion, NH_4^+ , is about 11, i.e. about 11 water molecules are associated with each ammonium ion (Walker *et al.*, 1989; Nielson & Tromp, 1991). At a molality of 50 mol kg^{-3} the hydration number is 5, suggesting that water molecules favour the neighbourhood of the ammonium ion (Adya & Nielson, 1991; Nielson & Tromp, 1991).
- The hydration shell moves closer to the ammonium ion at higher AN concentrations (Adya & Nielson, 1991).

The above findings showed that there is direct cation-anion contact between the ammonium nitrate ions at the highest concentration (Walker *et al.*, 1989). Stabilisation of ammonium nitrate melts often involves the addition of other ions. The mechanism by which such stabilisation can take place depends on the structure of the solution and how it can be altered.

The results of the study performed on the AN concentrated solution with the addition of calcium nitrate indicated that there is an overall relaxation of the solution structure. In particular the nearest – neighbour N1-N2 – distance (distance between nitrogen atoms in nearest NH_4^+ and NO_3^-) was found to be 5.5 \AA in the mixed molten salts, compared to 4.5 \AA in pure AN (Adya & Neilson, 1996). This provided clear evidence that the presence of doubly

charged Ca^{2+} brings a significant difference in coordination and separation of the ammonium nitrate ions (Adya & Neilson, 1991; 1996).

2.9.3 Stability of explosive emulsions

An inherent problem with emulsion explosives is their relative instability due to the fact that they comprise a thermodynamically unstable dispersion of supercooled solution or melt droplets in a continuous oil phase. If the emulsion remains stable, these supercooled droplets are prevented from crystallising or solidifying into a lower energy state. If the emulsion weakens or becomes unstable, then crystallisation of the droplets results and the explosive generally loses at least some of its sensitivity to detonation (Cooper & Baker, 1989; McKenzie *et al.*, 1989; 1990). Indeed, the investigation of aging of highly concentrated explosive emulsions showed that their instability was related to the crystallisation process and that mechanisms such as aggregation and flocculation do not take place due to tight droplet packing (Malkin, Masalova, Slatter & Wilson, 2004a, Masalova, Malkin, Ferg, Taylor, Kharatiyan & Haldenwang, 2006; Masalova & Malkin, 2007b).

The instability mechanism can be considered as:

- Crystal initiation in the dispersed phase affected by the presence of impurities (Becher, 1988), which could be influenced by interactions of matter of droplets with the surfactant head group (Ganguly *et al.*, 1992; Ashok & Neilson, 1991).
- Crystal penetration (growth) through the bulk of the emulsion could be affected by the concentration of micelles (White, Henderson & Perriman, 2004) and interface strength (Kharatiyan, 2005; White, Reynolds, Hawley & Perriman, 2005).

2.9.3.1 Factors affecting the stability of emulsions

The following factors described in the literature can affect emulsion crystallisation:

- Droplet size distribution and dispersed volume fraction (Kharatiyan, 2005; Masalova *et al.*, 2006; Masalova & Malkin, 2007b)
- Electrolyte concentration (Ganguly *et al.*, 1992) and impurities inside the electrolyte solution: dust (Becher, 1988), other ions (Ashok & Neilson, 1991)
- Surfactant concentration and surfactant characteristics which are related to the surfactant type (Ganguly *et al.*, 1992; White *et al.*, 2004)
- Oil type (White *et al.*, 2005)

Crystallisation can occur when conditions change through cooling or super saturation, so that the free energy of a solid phase is lower than the free energy of liquid. In almost all bulk liquids some impurities in the melt will act as the starting point for nucleation before this

degree of supercooling can be reached and crystallisation will occur more rapidly (i.e. heterogeneous nucleation). However, when the liquid is finely divided into emulsion droplets, the number of droplets may significantly exceed the number of impurities and the bulk of the mass of the droplets will be impurity free and hence crystallise by an apparently homogeneous mechanism (Coupland, 2002).

An investigation of crystal growth in explosive emulsions showed that the crystal penetration is quicker in emulsions characterised by bigger droplets and an increased volume fraction of the dispersed phase (Kharatiyan, 2005; Masalova *et al.*, 2006; Masalova & Malkin, 2007b).

Recently, freeze/thaw treatment has been developed to demulsify W/O emulsions, which has been widely used to measure the stability of inverted emulsions. In 1993 Aronson & Petko reported the freeze/thaw-induced breakage of highly concentrated W/O emulsions. In addition, a demulsification mechanism for emulsions with exceedingly dense packing droplets was developed, which was described as the direct rupture of oil film following the formation of ice domains in adjacent droplets, and inversion of emulsions occurred in the frozen state (Clausee, Gomez, Pezron, Komunjer & Dalmazzone, 2005).

The effect of different ions on the emulsion stability was studied by thermal analysis. It was stated that salts of weak acids, owing to their basicity, stabilised ammonium nitrate formulations. AN formulations were spiked with a variety of sodium or ammonium salts (SO_4^{2-} , BF_4^- , $\text{B}_4\text{O}_7^{2-}$, HCO_3^-) and sodium-salt-containing AN formulations were slightly more stable than ammonium-salt-containing AN formulations. It was concluded that added ammonium cations accelerate the decomposition of AN formulations, although this destabilisation may not always be evident if the anion is stabilising. Although this conclusion is based on only slight differences in the effect of sodium and ammonium salts, it is concurrent with the fact that the ammonium ion is a weak base, and the salt of weak bases acidify aqueous solutions. In acidifying the solution, added NH_4^+ destabilises AN formulations. It was also found that a number of sodium salts of weak acids (carbonic, acetic, formic, oxalic and hydrofluoric), when added to the AN, retarded the decomposition. Cobalt and copper nitrate exhibited no strong destabilising effects on AN thermal stability, even though both commonly use two oxidation states ($\text{Co}^{2+}/\text{Co}^{3+}$ and $\text{Cu}^+/\text{Cu}^{2+}$). However, aluminium, which has only one state, Al^{3+} , as well as Cr^{3+} and Fe^{3+} , had a strong destabilising effect. The effect was attributed to the common property of these ions in producing acidic aqueous solutions (Oxley, Kaushik & Gilson, 1992). The presence of Ca^{2+} ions stabilises concentrated AN solutions by separating the ammonium nitrate ions from each other. This brings the solution to the relaxation state and prevents it from crystallisation (Adya & Neilson, 1991; 1996).

Ganguly and co-workers (1992) compared the stability behaviour of concentrated water-in-oil (white mineral oil or a mixture of mineral oil and waxes) emulsions at various salt (ammonium

nitrate or mixture of ammonium and sodium nitrate) concentrations for two types of surfactant. One was sorbitan mono-oleate (SMO), a nonionic surfactant, while the other one was a polymeric emulsifier, whose code name is LZX. The chemical structure of LZX is unclear because information on it is proprietary. However, according to the authors, LZX must be considered as a zwitterionic surfactant as a result of the reaction of poly(butenyl succinic anhydride) with alkanolamine. It is also important to mention that the weight average molecular weight of LZX is 2500 g/mol; LZX thus is a small polymer. The study revealed that the presence of salt is required to prepare stable emulsions using the nonionic surfactant. Due to the addition of salt, the stability enhancement of emulsions formulated with LZX is much more important than for SMO. The authors showed that the interactions between the surface-active agent and the added electrolyte are held responsible for stability improvement. The uncharged emulsifier and electrolyte can only interact through hydrogen bonding, while the zwitterionic character of the polymer chains would enable the macro surfactant to develop more intense interactions, therefore explaining the greater stability enhancement observed for the polymer (Radeva, 2001). The authors also found that surfactant concentration has an effect on the freezing behaviour of emulsions.

The crystallisation of AN under organised monolayers of various amphiphiles was studied by Yubai, Munger, Leblanc, Ghaicha & Chattopadhyay (1996). The results obtained from four different amphiphilic monolayer systems indicated that the crystallisation of AN is affected by the nature of molecules present in the monolayer. The changes in the functionalities of the polar head group led to significant differences in nucleation and growth of the pattern of AN crystals. The authors suggested that crystallisation of AN can be induced under conditions where there is a structural and stereo chemical matching between the attached crystal phase and the polar head groups constituting the organic surfaces (Yubai *et al.*, 1996).

Stability of water-in-oil emulsions was studied by low temperature DSC to relate the crystallisation and solidification aspects of the surfactant films to the emulsion instability. It was found that not only the nature of the head group can affect the crystallisation, but also the ordering of surfactant tails at the interface and their nature. It is known that n-alkyl chains in the emulsifiers undergo rapid structural ordering and crystallise more readily, compared to the unsaturated hydrocarbon chains (Villamagna, Whitehead, Chattopadhyay, 1995). The stability of emulsions stabilised by SMO and Alkaterge-T were investigated. The results showed that terminal methyl groups of an SMO surfactant has a higher degree of freedom in comparison with Alkaterge-T. The emulsion stabilised by SMO was found to be more stable, and was then stabilized by Alkaterge-T. The emulsion stability results were consistent with mobility of surfactant at the interface. It was also mentioned by Coupland (2002) that, if the hydrophobic portion of the interfacial surfactant has a similar molecular structure to the oil, it

can increase the nucleation rate. In this case, the nucleation rate was proportional to the interfacial area (i.e. surface heterogeneous nucleation) and not volume. Secondly, solid droplets can induce nucleation in liquid droplets that they are physically mixed with; presumably through a collision mechanism (i.e. interdroplet nucleation) (Coupland, 2002).

2.9.4 Role of emulsifiers in emulsion explosives

All of the emulsion explosive compositions contain an emulsifier ingredient. Selection of the emulsifier used to prepare an emulsion explosive is of major importance in providing an emulsion.

An inherent problem with emulsion explosives is their relative instability due to the fact that they comprise a thermodynamically unstable dispersion of supercooled solution or melt droplets in an oil continuous phase. If the emulsion remains stable, these supercooled droplets are prevented from crystallising or solidifying into a lower energy state. If the emulsion weakens or becomes unstable, then crystallisation of the droplets results and the explosive generally loses at least some of its sensitivity to detonation (Cooper *et al.*, 1989; McKenzie *et al.*, 1990; 1991; Boer, 2003).

The formation of an explosive emulsion and the stabilisation of an emulsion explosive, once formed, make a number of demands on an emulsifier system (Binet *et al.*, 1982; Cooper *et al.*, 1989; Chattopadhyay, 1996):

- An ability to stabilise new surfaces as the emulsion is formed by lowering the interfacial tension, i.e. an emulsifying capacity
- An ability to form a structured bilayer (since an emulsion explosive is mainly composed of densely packed droplets of supersaturated dispersed phase in a fuel phase) so that the tendency, in an emulsion at rest, for droplets to coalesce and for crystallisation of salts to spread from nucleated droplets to their dormant neighbours is suppressed.
- A third desired feature, related to the first, but seemingly at odds with the second would be an ability to preserve bilayer integrity dynamically when an emulsion explosive is sheared, e.g. when being pumped.

Thus emulsifiers in emulsion explosives not only facilitate the emulsification process of the electrolyte phase, but prevent crystallisation growth and organise a strong barrier against droplet coalescence. The performance of an emulsion explosive therefore strongly depends on the properties of the emulsifier agent.

2.9.5 Emulsifiers used in stabilisation of explosive emulsions

Water-in-oil explosive emulsions comprising a large volume of nitrate salt solutions dispersed in a small volume of hydrocarbon oil require surfactants of low HLB (hydrophilic-lipophilic balance) values such as sorbitan monooleate or various polymeric surfactants (Ghaicha, Leblanc, Villamagna & Chattopadhyay, 1995). Sorbitan monooleate surfactant was one of the first used in stabilisation of explosive emulsions, but it did not provide the desirable long-term emulsion stability. Various attempts to improve the storage characteristics of emulsion explosive compositions continued to be concentrated on the emulsifier component of the compositions and particularly on the selection of suitable emulsifiers, or blends thereof, which are designed to suppress coalescence of the supersaturated droplets of the oxidiser salts present in the discontinuous phase (Cooper *et al.*, 1989).

Therefore a lot of research was devoted to the synthesis of new emulsifier molecules that could provide better stability of emulsions. Two main directions can be found in the published research work regarding emulsifier development: development of surfactant structure (new head and new tail groups) and development of new surfactant blends:

- Development of new surfactant structures.

Structure of head group:

- Presence of amine group in surfactant structure is claimed (Sudweeks & Harvey, 1979; Binet *et al.*, 1982; Cooper & Baker, 1989; Forsberg, 1989; McKenzie, 1991; Chattopadhyay, 1996; Boer, 2003; Hales *et al.*, 2004). The surfactant acts as a crystal habit modifier in the oxidiser salt solution to control and limit the growth and size of any salts that may precipitate. Secondly, such an emulsifier may enhance adsorption of hydrocarbon fuel on the small salt crystals that may form (Sudweeks & Harvey, 1979).
- Presence of carboxylic and hydroxyl groups in surfactant structure is claimed (Yates & Dack., 1987; Chattopadhyay, 1989; Cooper & Baker, 1989; Forsberg, 1989; McKenzie, 1991; Venter & Kruger, 1995). Carboxylic groups or groups capable of being hydrolysed to a carboxylic acid provide minimum deterioration during storage (Yates & Dack, 1987).

Structure of tail group:

- Branched polyalkyl hydrocarbons are claimed to be present in the emulsifier structure. A preferred type of lipophilic moiety is a saturated or unsaturated hydrocarbon chain derived, for example, from polymers of a mono-olefin of polymer chain containing from 40 to 500 carbon atoms. Suitable polyolefins

- include those derived from olefins containing from 2 to 6 carbon atoms, in particular ethylene propylene butane-1 and isoprene, but especially isobutene (Cooper & Baker, 1989). Special attention was concentrated on the PIB (polyisobutylene) lipophilic group with a molecular weight in a range of 400 to 5000. (Binet *et al.*, 1982; Cooper & Baker, 1989; McKenzie, 1989; Venter & Kruger, 1995; Hales *et al.*, 2004). Polymeric emulsifiers are known to give excellent shelf life to emulsion explosives, due to enhanced steric stabilisation effected by the hydrophobic portion of the molecules (Hales *et al.*, 2004).
- A bis derivative (with additional polymer chain) is claimed for the improved emulsion stability and detonation properties (McKenzie & Lawrence, 1990).
 - Copolymers which contain oxygen and nitrogen atoms in the chain are claimed as an emulsifier tail group such as a polyoxyethylene chain and a polyethylene-imine chain (replacing the oxygen atom by N-H) (Binet *et al.*, 1982). Branched polyalkylene polyamines were proposed by Forsberg (1989).
- Development of surfactants blends:
 - The addition of conventional emulsifier is claimed to obtain stable emulsion (Binet *et al.*, 1982; Chattopadhyay, 1996; Hales *et al.*, 2004). The addition of nonpolymeric emulsifier to the polymeric surfactant provides homogenisability of the emulsion. Homogenisation additives are effective in that they are more mobile (they diffuse or migrate easily) than more bulky polymeric emulsifiers. Thus, when new interfaces are created by the high shearing action, the more mobile molecules (animal oil, fatty acid additive, common emulsifier) migrate to the interface to stabilise it, thereby promoting the formation of smaller droplet sizes and also preventing crystallisation of the internal phase. Furthermore, the additives are replaced by the more tightly bound polymeric emulsifier (Hales *et al.*, 2004).
 - The ratio of polymeric emulsifier to conventional water-in-oil emulsifier is claimed to be in the range of 1:25 to 3:1, but preferably in the range of 1:5 to 1:1 (Binet *et al.*, 1982; Hales *et al.*, 2004). A ratio of 4:1 for the mixture was used by Chattopadhyay (1996).

A variety of emulsifier types and blends of emulsifiers have been tried in attempts to reduce deterioration during storage. Some of the emulsifiers were designed to suppress the coalescence of droplets while others functioned as crystal habit modifiers to limit the

development of crystals. The recent investigations are trying to produce an emulsifier which can provide both types of emulsion stability (against coalescence and against crystallisation).

2.9.5.1 Pibsa-based surfactants and their characterisation

Pibsa (polyisobutenyl succinic anhydride) derivatives were used as superior emulsifiers for emulsion explosives (Boer, 2003). Current research still concentrates on developing new Pibsa derivative surfactants and the preparation of surfactant blends for the stabilisation of emulsions. Pibsa-derivative emulsifiers are usually produced in two steps: synthesis of Pibsa and addition of alkanol amine derivatives to the Pibsa. The first step is shown in Figure 2.14.

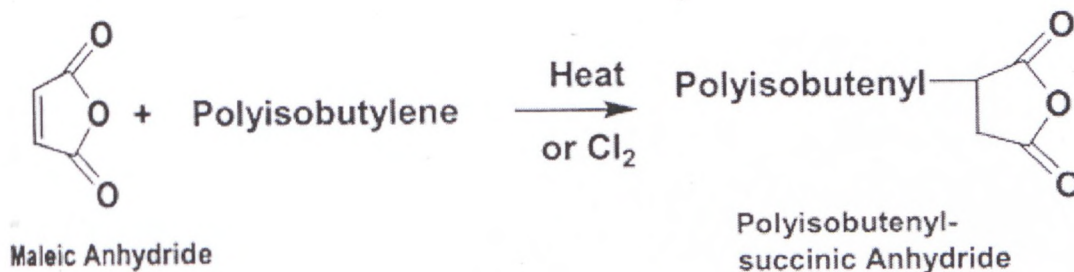
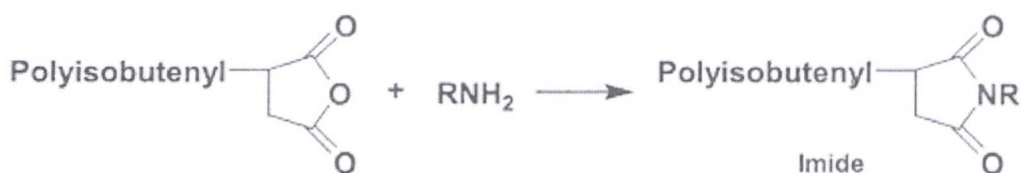


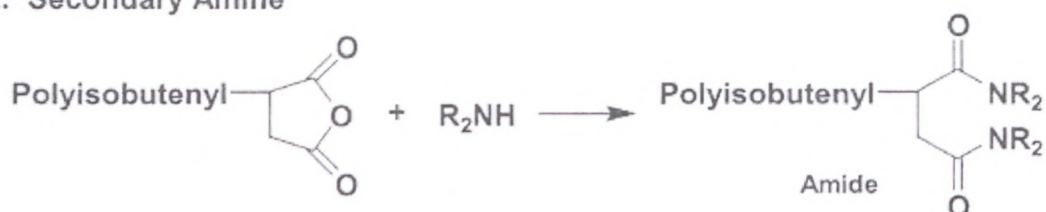
Figure 2.14: Alkenylsuccinic anhydride formation (Adapted from Rudnick, 2003)

Polyisobutylene is the most commonly used olefin. One of the reasons for its preference is its extensive branching. This causes the derived emulsifier to possess excellent oil solubility, in both the non-associated and associated forms. However, if the hydrocarbon chain in the emulsifier is too small, its solubility suffers greatly (Rudnick, 2003). The second step of emulsifier production is shown in Figure 2.15.

1. Primary Amine



2. Secondary Amine



3. Tertiary Amine

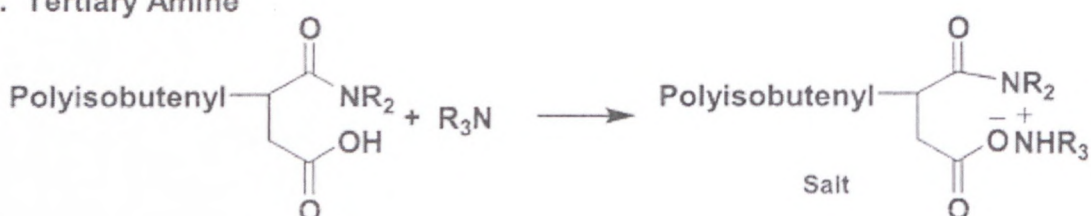


Figure 2.15: Amine-anhydride reaction products (Adapted from Rudnick, 2003)

The polar group is usually nitrogen- or oxygen-derived. Nitrogen-based groups are derived from amines and are usually basic in character. Oxygen-based groups are alcohol-derived and are neutral. The head group of such emulsifiers (succinimide derivatives) is polar. Both amide- and alcohol-derived functional groups contribute to the polarity of the head group. The polarity is a consequence of the electro-negativity difference between carbon, oxygen and nitrogen. The greater the electro-negativity difference, the stronger the polarity. This implies that groups that contain carbon-oxygen bonds are more polar than those containing carbon-nitrogen bonds. However, since head groups have many bonds with various combinations of atoms, the overall polarity in a molecule and its ability to associate with polar materials are not easy to predict (Rudnick, 2003). The polarity of the head group of these PIB derivatives can significantly influence their adsorption at the interface: the increasing polarity demonstrates increased adsorption and if the polarity decreases the adsorption of surfactant is reduced (Papke & Robinson, 1994).

A few research studies have also been carried out to examine the surface chemistry of the succinimide surfactants and their micelle structure:

- *Interfacial properties of Pibsa-based surfactants.* Small-angle neutron scattering (SANS) study was undertaken to investigate the surfactant behaviour in highly concentrated water-in-oil emulsions. It was found that the aqueous-oil interface is

stabilised by a monolayer of surfactant and the rest of surfactant forms reversed spherical micelles in the oil phase (Reynolds *et al.*, 2000; 2001). The Pibsa MEA surfactant is tightly bound to the interface compared to that in the micelles (Reynolds *et al.*, 2000; 2001). The adsorption occurs through the polar head group of the succinimide surfactant that results in very strong adsorption of succinimide surfactants on the calcium sulfonate colloids (Papke & Robinson, 1994). The study of PIBSA, PIB-DETA, PIB-TERA and PIB-PERA dispersants showed that their binding ability is controlled by the presence of secondary amines in the head group: the more secondary amines present in the core the stronger the adsorption, due to the ability of such amines to organise hydrogen bonds (Shen & Duhamel, 2008). Pibsa-IMIDE was found to lose more material from the interface under compression, compared to Pibsa-MEA (Reynolds *et al.*, 2001). The investigation of interfacial properties of mono-, bis-, tris- succinimide surfactants (see Figure 2.16) revealed that C₈ alkyl chains are more rigid and pack together closer than the C₁₂ and C₁₈ chains, which are able to tilt over a greater extent (the higher molecular weight molecules begin to coil) (Tomlinson, Danks, Heyes, Taylor & Moreton, 1997; Reynolds *et al.*, 2002). Moreover, compressibility of the mono compounds increased at lower coverage in the order C₈ < C₁₂ < C₁₈ (Tomlinson *et al.*, 1997).

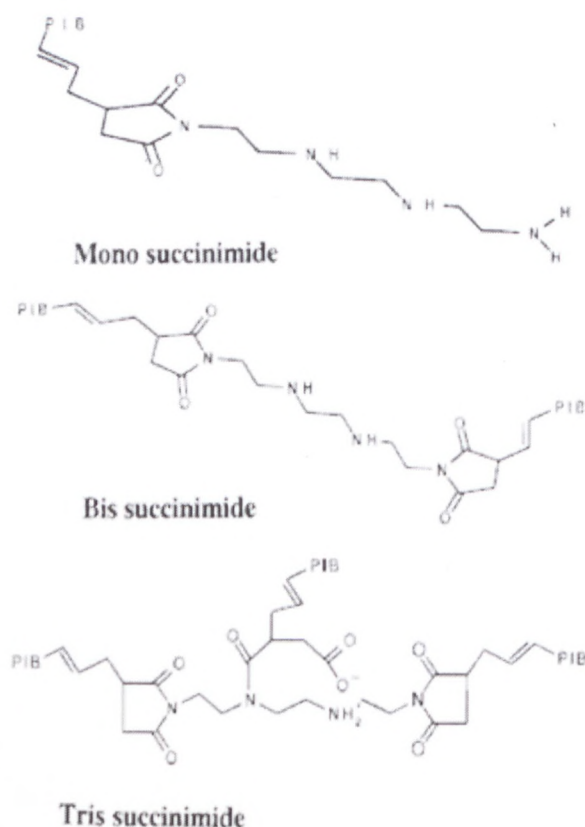


Figure 2.16: Range of PIBSA molecules using tetraethylene tetraamine (TETA) as an example amine head group (Adapted from Tomlinson *et al.*, 1997)

The areas per molecule of the bis and tris compounds are insensitive to the chain length, indicating that, for these molecules, the surface area per molecule is dominated by the head group region rather than the length of the tails (as in the mono case). This suggests that the hydrocarbon tails in the bis and tris molecules interact to a lesser extent than the mono molecules (Tomlinson *et al.*, 1997).

- *Effect of AN on monolayer of Pibsa-based surfactants.* The effects can be divided into two major classes, due to:
 - *direct interactions.* The polar head groups of Pibsa-based surfactants strongly interact with an NH_4NO_3 solution by direct hydrogen bond formation (Chattopadhyay *et al.*, 1992; Ganguly *et al.*, 1992; Ghaicha *et al.*, 1993) and another type of interaction due to the zwitterionic nature of the surfactant (Ganguly *et al.*, 1992). OH^- and $\text{C}=\text{O}$ groups in the polar head participate in the hydrogen bond formation (Ganguly *et al.*, 1992; Ghaicha *et al.*, 1993) and ammonium nitrate. The ions (NH_4^+ and NO_3^-) participate as the bridging component between the head groups (Ghaicha *et al.*, 1993). Ammonium nitrate

affects the molecular conformation owing to the structural modifications of the head groups and their environment and increased association of the salt ions or ion pairs with the head groups and subsequent replacement of the water molecules from the solvation sheath (Ghaicha *et al.*, 1993). The influence of AN on the large structural changes of the polar head group suggested that the electrostatic interactions between the head groups affect the packing of acyl chains by increasing the spacing and corresponding Van der Waals interactions between the chains. More adsorption at the water-oil interface was also found with AN presence in the aqueous phase (Reynolds *et al.*, 2001).

- *indirect interactions*. Ions of ammonium nitrate affect the orientation to the polar head groups through their modification of the solvent environment (Chattopadhyay *et al.*, 1992; Ghaicha *et al.*, 1993).

- *Bulk properties of Pibsa-based surfactants*. The radius of spherical reversed micelles was found to be unchanged at 30 – 37 Å over the entire range of concentrations used (from 4.5% to 0.36% of surfactant). The micellar core region of radius a little less than 15 Å was surrounded by a shell of ca. 20 Å thickness. There was no oil in the core and no water in the shell. In addition to this, an increase in micellar concentration was found with an increasing surfactant concentration in the emulsion (Reynolds *et al.*, 2000; 2001). It was found that increasing the number of secondary amines in the polyamine core led to an increase of the association strength of the dispersant as the CMC took place at a smaller dispersant concentration (Shen & Duhamel, 2008).

The micelles became smaller in the presence of AN and contained less water in the core (Reynolds *et al.*, 2001).

2.10 RHEOLOGY OF EMULSIONS

Rheology has been properly defined as the study of the flow and deformation of materials (Mezger, 2002; Barnes, 2000). The first goal of rheology is a search for stress versus deformation relationships in various technological and engineering materials in order to solve macroscopic problems related to continuum mechanics of these materials. The second goal of rheology consists of establishing relationships between rheological properties of a material and its molecular composition (Malkin, 1994). Rheological measurements can be used as a tool to provide fundamental insights about the structural organisation and interactions of the components within emulsions (McClements, 1999; 2005).

2.10.1 Flow properties

The liquid is often referred to as a Newtonian liquid, after Isaac Newton, the scientist who first described its behaviour (Macosko, 1994; Rao, 1995). When a shear stress is applied to an ideal liquid it continues to flow as long as the stress is applied. Once the applied stress is removed, the liquid will continue to flow until the kinetic energy stored within it is dissipated as heat due to friction (McClements, 1999; 2005).

Dilute colloidal dispersions are fluid systems and if the concentration is increased, the mean interparticle separation will eventually approach the range of the interactions between the particles. When this point is reached, a structure is formed which extends throughout the dispersion. Particle motion becomes restricted and viscoelasticity is observed, which is a manifestation of non-ideal liquid (Goodwin & Hughes, 2000; McClements, 2005).

2.10.1.1 Shear-rate dependent non-ideal liquids

For Newtonian liquids the viscosity displays constant behaviour, but this is not the case for the non-Newtonian liquids. The viscosity does not remain constant and can decrease or increase with increasing the shear rate (McClements, 1999; 2005).

According to Hackley and Ferraris (2001), the flow behaviour can be classified into the six most frequently encountered flow types shown in Figure 2.17:

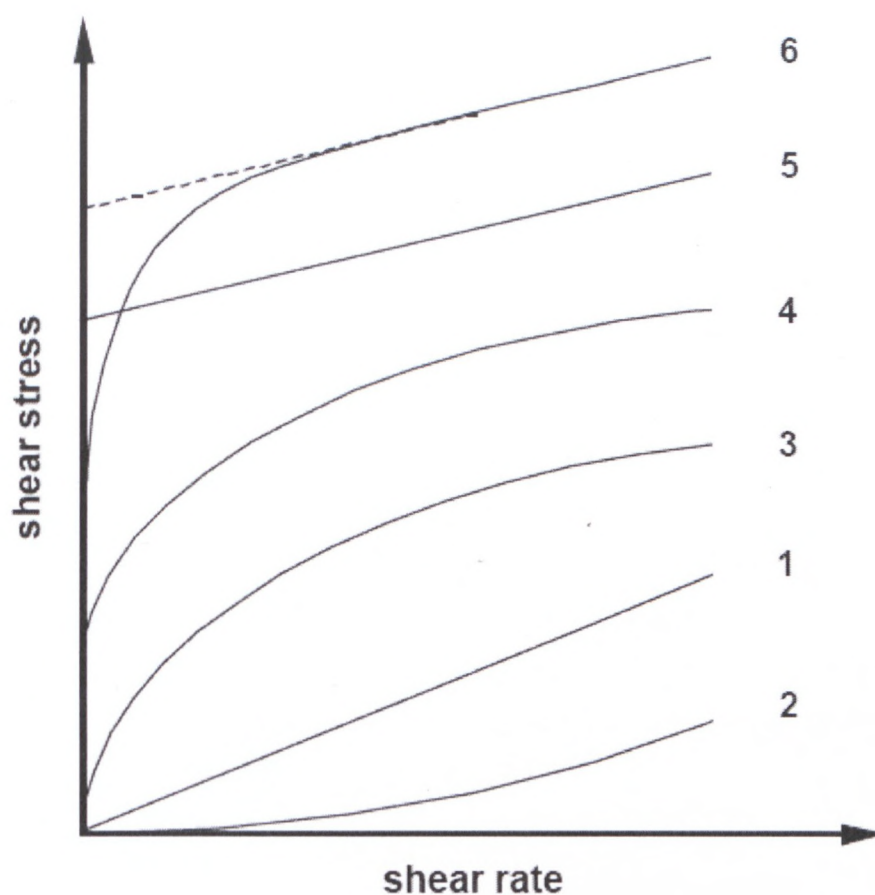


Figure 2.17: Comparison of the flow behaviour of ideal and non-ideal liquids – Shear stress versus shear rate (Adapted from Becher, 1988)

1. *Newtonian*. The differential viscosity and coefficient of viscosity are constant with the shear rate (Figure 2.17).
2. *Shear thickening*. Differential viscosity and the coefficient of viscosity increase continuously with shear rate (Figure 2.17).
3. *Shear thinning (pseudoplastic)*. Differential viscosity and the coefficient of viscosity decrease continuously with shear rate. No yield value (Figure 2.17).
4. *Shear thinning (pseudoplastic) with yield response*. Differential viscosity and coefficient of viscosity decrease continuously with shear rate once the yield stress has been exceeded (Figure 2.17).
5. *Bingham plastic (ideal)*. Obeys the Bingham relation ideally. Above the Bingham yield stress, the differential viscosity is constant, while the coefficient of viscosity decreases continuously to some limiting value at infinite shear rate (Figure 2.17).

6. *Bingham plastic (non-ideal)*. Above the apparent yield stress, the coefficient of viscosity decreases continuously, while the differential viscosity approaches a constant value with shear rate (Figure 2.17).

Emulsions can show a rheological behaviour known as plasticity (Sherman, 1968). Below the yield stress the material exhibits elastic properties, but behaves as a liquid when stress is exceeded. Non-ideal plastic materials exhibit non-ideal behaviour above yield stress, as well as below it (McClements, 1999).

2.10.1.2 Factors affecting rheological behaviour

When interpreting rheological data for emulsions, it should be appreciated that many factors other than the phenomenological effects may exert some effect. All the factors involved are influenced by the chemical nature, and other properties, of the ingredients used in preparing the emulsions (Sherman, 1968). Some of the most important factors associated with emulsion ingredients which influence rheological behaviour are the following (Sherman, 1968):

1. Internal phase
 - a. Volume concentration;
 - b. Viscosity; deformation of droplets in shear;
 - c. Droplet size, and droplet size distribution, technique used to prepare emulsions; interfacial tension between the two liquid phases;
 - d. Chemical constitution.
2. Continuous phase
 - a. Viscosity and other rheological properties;
 - b. Chemical constitution;
 - c. Electrolyte concentration in the polar medium.
3. Emulsifying agent
 - a. Chemical constitution;
 - b. Concentration and solubility in internal and continuous phases;
 - c. Thickness of film adsorbed around droplets.
4. Additional stabilising agents

Highly concentrated emulsions are classified as high internal phase ratio emulsions (or simply HIPRE) and the dispersed phase droplets are arranged in a closely packed hexagonal configuration (i.e. far beyond the close packing limit of spherical ordered monodispersed droplets of 74%). This closely packed configuration and the profound hydrodynamic

interaction between neighbouring droplets induce mechanical interference between the droplets, thus prohibiting their free movement. In such systems, extensive aggregation or flocculation of the dispersed phase droplets occurs, which results in a stable, weak, gel-like, particulate network (Jager-Lézer, Tranchant, Alard, Vu, Tchoreloff & Grossiord, 1998; Partal, Guerrero, Berjano & Gallegos, 1997).

High internal phase ratio emulsion systems exhibit a plastic-like response to shear deformations: for small deformations, they resist the shear elastically, with the stress being linearly proportional to the strain; however, for large enough deformations, they flow, offering comparatively much less additional resistance (Webber, 1999; Masalova, Malkin, Slatter & Wilson, 2003a). Grassi, Lapasin and Prici (1996) mentioned that the plastic behaviour is generally ascribed to the existence of a three-dimensional network under limiting shear conditions (i.e. $\dot{\gamma} \rightarrow 0$). The shear-dependent behaviour just described is typical of weak gel systems (many polymer solutions and dispersed systems), for which the application of large or continuously increasing deformations leads to the progressive breakdown of their networks into smaller clusters (Grassi *et al.*, 1996) leading to a strong decrease in viscosity and permitting the flow of the system (Manca, Lapasin, Partal & Gallegos, 2001). Since nearly all practical applications of emulsions require their transport, it is important to understand how their flow behaviour is influenced by the surfactant type and concentration and the properties of the constituent droplets, such as their packing, their degree of deformation, their radius and their volume fraction.

As was pointed out by Mason, Bibette and Weitz (1996), the flow properties of compressed, elastic emulsions can be broadly divided into two categories: yielding and steady shear flow. The change from a linear to non-linear stress-strain relationship can be crudely characterised by yield stress, which marks the significant departure of the microscopic droplet structure from its initial, unsheared configuration. For shear stresses higher than the yield stress, the emulsion flows irreversibly, creating a residual deformation, after the stress has been removed, which cannot be attributed to the equilibrium dissipation of fluctuations. During steady shear flow, the strain rate dependence of the additional viscous stress above the yield stress reflects the interplay of dissipative mechanisms like fluid flow and droplet rearrangements, with storage mechanisms like deformation. Thus the flow properties of the compressed emulsions depend sensitively on the packing and the deformation of the droplets, and on their intrinsic elasticity.

The flow properties of polydispersed emulsions have been extensively investigated in a comprehensive set of experiments using well-controlled samples (Princen & Kiss, 1986b; 1989; Khan & Armstrong, 1987). The flow properties of emulsions have also been

investigated theoretically (Princen, 1983) and through simulation (Reinelt & Kraynik, 1989; 1990). Models predicting rheological properties of emulsions were also proposed by Paliarne (1990); Madiedo and Gallegos (1997); and Pal (1997; 2001). However, this work was focused on idealised emulsions that were perfectly monodispersed and/or perfectly ordered.

At the limit of the very high volume fraction, the emulsion is composed of a network of thin films, and its stability under shear is determined entirely by the mechanical stability of the intersection of these films at the plateau borders; three continuous phase films which meet at an edge must be separated by 120° angles, and four films which meet at a corner must meet at tetrahedral angles (Thomson, 1887).

2.10.1.3 Flow properties of explosive emulsions

In recent times, Masalova and Malkin (2005; 2007c), Malkin and Masalova (2007) and Kharatiyan (2005) have emphasised the presence of an inflection point on the flow curve of explosive emulsions suggesting two competing processes taking place in the shearing of an emulsion. One of them dominates at low shear rates and leads to an increase in viscosity, while the other prevails at high shear rates, resulting in typical shear thinning behaviour. According to some direct optical observations, the model that follows was proposed. In the low shear rate domain, drops maintain their shape and flow proceeds as larger particles rolling over smaller ones until a critical shear stress ("second yield stress") is reached. When $\tau \geq$ "second yield stress", the drops will deform more strongly and become arranged in "trains", thus causing more uniform "inner shear layers" of the oil phase, which triggers the shear thinning behaviour. The plastic deformation of droplets occurs and then results in a catastrophic suppression of the Reynolds mechanism of dilatancy. In addition, the yield stress was found to be proportional to D^{-2} , while Newtonian viscosity was proportional to D^{-1} . In the low shear rate domain, emulsion explosives are rheopectic materials (a slow increase of viscosity at constant shear rate was observed).

2.10.1.4 Effect of surfactant type and concentration

There are no published data on the behaviour of the surfactant film in high-internal-phase systems such as emulsion explosives. It may be speculated that, since both distortion of droplet shape and shearing of the inter-droplet layer must be involved for the systems to flow, there would be an effect due to surfactant changes. Indeed, this can be observed in a quantitative way, e.g., oxazoline and amine surfactants tend to give lower viscosity emulsions than do sorbitan derivatives, but little systematic work has been done on this (Becher, 1988).

There is a further mechanism by which a surfactant in this system can affect the rheology. Bampffield and Cooper (1988) have shown that certain polymeric surfactants dramatically increase the viscosity of emulsion explosives, while at the same time making them rubbery. It is possible that such materials operate through bridging between the droplets, giving some structure to the emulsion.

2.10.1.5 Effect of electrolyte type and concentration on rheological properties

In general, a considerable increase in the viscosity, yield stress, is produced with the addition of inorganic salts (Aronson & Petko, 1993; Solans, Pons, Zhu, Davis, Evans, Nakamura & Kunieda, 1993; Binks, 1998; Martinez *et al.*, 2007). The increase in rheological properties was associated with more surfactant adsorption at the interface (Aronson & Petko, 1993) changing the configuration of surfactant at the interface (Solans *et al.*, 1993; Binks, 1998; Martinez *et al.*, 2007).

According to Binks (1998), the packing of surfactant molecules at the interface changed significantly with the addition of salt. Thus the enhanced rheological properties produced by electrolyte might be due to dehydration of the hydrophilic part of the surfactant. The surfactant-surfactant interactions would increase and consequently the interfacial film would become more rigid.

Some authors have mentioned that the influence is strongly dependent on the type of electrolyte (Aronson & Petko, 1993; Solans *et al.*, 1993; Binks, 1998; Martinez *et al.*, 2006). The stability of an emulsion as a function of Na₂SO₄, CaCl₂, NaCl and KI concentration showed that the first three stabilised the emulsion significantly while KI did not improve the emulsion stability (Binks, 1998). Different degrees of influence on the yield stress by different types of electrolyte was observed by Aronson & Petko (1993). Electrolytes with a large salting out effect decreased the clouding point in water/non-ionic surfactants. Consequently, the HLB temperature in the water/non-ionic surfactant/oil system was the most effective stabilisers (Solans *et al.*, 1993; Binks, 1998).

2.10.2 Viscoelastic properties

Malkin (1994) noted that rheological behaviour related to viscoelasticity is the most relevant for the description of a majority of real materials. In general, viscoelasticity is a combination (or superposition) of characteristic properties for liquids (viscous dissipative losses) and solids (storage of elastic energy). Therefore, a general definition of viscoelastic materials includes two components – elastic potential and intensity of dissipative losses. Viscoelastic behaviour can be considered as a delayed development of stresses and deformations in

time, and this delay must not be confused with inertial effects also characterised by a specific lag time.

The time of observation of the viscoelastic processes is very important. The dimensionless criterion called the Deborah Number, De , was introduced as a measure of a ratio between characteristic time of observation, t_{obs} , and the time scale of inherent processes in the material, t_{inh} . The Deborah Number is especially important for viscoelastic phenomena because they always proceed in time. Since the time interval is very wide, it must encounter a situation when the Deborah Number is of the order of 1 (Malkin, 1994).

There are three fundamental experiments, which are treated as reflections of viscoelastic behaviour of any matter:

- Creep – delayed development of deformations under the action of constant force (or stress)
- Relaxation – slow delay of stresses while preserving constant deformation
- Periodic oscillations – harmonic changing of stresses or deformations with relative shift of deformation in relation to stress.

In oscillatory shear, the evolution of the linear viscoelastic functions in the frequency range between 10^{-2} and 10^2 rad/s, for highly concentrated emulsions, is characterised by the appearance of a minimum in the loss modulus at intermediate frequencies and a “plateau region” in the storage modulus ($G' \gg G''$) (Franco, Guerrero & Gallegos, 1995; Franco, Berjano & Gallegos, 1997; Tadros, 1994; Kharatiyan, 2005).

2.10.2.1 Viscoelasticity and microstructural parameters

Some attempts at correlating rheology and microstructural parameters may be found in the literature. An early study based on a model of a foam-like structure valid for monodispersed foams and highly concentrated emulsions was carried out by Princen (1983), who derived an expression that related the elastic shear modulus, G' , to the interfacial tension, σ , the volume fraction of the dispersed phase, ϕ , and a characteristic size of the unit cell, represented by the surface-volume mean radius of undistorted spheres, $R_{3,2}$. Princen and Kiss (1986a) extended this treatment to obtain, experimentally, an equation for the small-strain elastic shear modulus for real polydispersed emulsions:

$$G = a \frac{\sigma}{R_{3,2}} \phi^{1/3} (\phi - \phi^*) , \quad \text{Equation 2.20}$$

where a and ϕ^* are dimensionless constants, although their values may depend slightly on the thickness of the aqueous films located between the oil droplets and droplet size distribution (DSD). The latter constant is thought to be related to the volume fraction of close-packed undistorted droplets (Bengoechea, Cordobés & Guerrero, 2006). Thus, it has been shown that the elastic modulus of a concentrated emulsion is proportional to the interfacial tension, σ , and inversely proportional to the droplet radius, R .

As the thickness of the films separating individual droplets was negligible in the case of the emulsions investigated by Princen and Kiss (1986a; 1989), the above equations are valid for emulsions with negligible interdroplet film thickness. According to Princen (1983), the effect of a finite film thickness can be taken into account by using the effective volume fraction (ϕ_{eff}) of the dispersed phase (instead of the true volume fraction ϕ) in the above equations. The relationship between (ϕ_{eff}) and ϕ is given by (Princen & Kiss, 1986a):

$$\phi_{\text{eff}}^{-1/3} = \phi^{-1/3} - 1.105 \frac{h}{D}, \quad \text{Equation 2.21}$$

where h is the film thickness and D is the average droplet diameter.

According to this model, the considerable elasticity of the concentrated emulsions exists only because the repulsive droplets have been compressed by an external osmotic pressure Π , and thus concentrated to a sufficiently large droplet volume fraction $\phi > \phi^*$, which permits the storage of interfacial elastic shear energy (Dimitrova & Leal-Calderon, 2004). Indeed, two droplets forced together will begin to deform before their interfaces actually touch, due to the intrinsic repulsive interactions between them. Thus, emulsions minimise their total free energy by reducing the repulsion (which may have a different origin) at the expense of creating some additional surface area by deforming the droplet interfaces. The necessary work to deform the droplets is done through the application (by any means) of an external osmotic pressure, π , and the excess surface area of the droplets determines the equilibrium of elastic energy stored at a given osmotic pressure. Provided the droplets are compressed by osmotic pressure, the additional excess surface area created by a perturbative shear deformation determines the elastic shear modulus, $G'(\phi)$ (Dimitrova & Leal-Calderon, 2004). Some authors have successfully used this equation to correlate structural and rheological parameters for emulsions stabilised by low molecular weight surfactants (Princen & Kiss, 1986b; Pons, Solans & Tadros, 1995; Sánchez, Berjano, Brito, Guerrero & Gallegos, 1998) or polymeric surfactants (Perrin, 2000). Working on monodispersed concentrated emulsions of dodecane stabilised by sodium dodecyl sulphate (SDS), Mason, Lacasse, Grest, Levine, Bibette & Weitz (1997) observed a sharp increase of the elasticity at ϕ^* and showed that the

elastic modulus of the concentrated emulsion could be rescaled by σ/R , in agreement with Princen's model. Nevertheless, they obtained a universal master curve for the evolution of G' versus ϕ that obeyed the following relationship:

$$G' \propto \phi(\phi - \phi^*), \quad \text{Equation 2.22}$$

where ϕ^* is the close-packing volume fraction that has a value of 0.64 for randomly packed monodispersed spheres. Therefore, the elasticity is governed by the Laplace pressure, $2\sigma/R_{32}$ of the droplets, in agreement with Princen's model. Their work has provided incontestable proof for the original work by Princen, who first predicted the scaling of the G' with the capillary pressure, σ/R (σ being the interfacial tension and R being the drop radius). Moreover, the scaling with σ/R confirms that the elasticity of compressed monodispersed emulsions depends only on the packing geometry of the droplets (Dimitrova & Leal-Calderon, 2004). However, the increase of the G' elastic modulus was slower than originally predicted by Princen. By means of numerical simulations of shearing of soft spheres, Lacasse, Grest and Levine (1996) showed that this quasi-linear rise of G' with ϕ was due to the positional disorder of the droplets. Indeed, due to disorder, under an affine deformation, droplets depart randomly from affine motion and thus relax some of the imposed deformation, leading to a smaller elasticity than that predicted for ordered systems and in good agreement with Mason's experimental results.

Some authors have recently tried to use the scaling procedure reported by Mason *et al.* (1997) for protein-stabilised oil-in-water emulsions (Dimitrova & Leal-Calderon 2001; 2004; Bressy, Hebraud, Schmitt & Bibette, 2003), water-in-oil emulsions stabilised by non-ionic polymeric and non-ionic low molecular weight surfactants (Malkin *et al.*, 2004a; Masalova & Malkin, 2007a; 2007c; Alvarez, Mougel, Baravian, Caton, Marchal, Stébé & Choplin, 2006; Lee, 2006). However, the elastic modulus was much higher than that predicted by Princen's model or Mason's law. Thus, an additional source of elasticity should be considered.

In all studies cited above, it was implicitly supposed that the interfacial tension does not change with the application of the perturbative strain, due to the rapid relaxation of the surfactant layers. This corresponds to the case of deformation/strain applied at zero frequency. In fact, at non-zero frequency, the local variation of the interfacial tension (interfacial elasticity) will also contribute to the overall elasticity, and the stored elastic energy can be higher than at rest (zero frequency) (Dimitrova & Leal-Calderon, 2004).

Lacasse *et al.* (1996) performed Monte Carlo simulations aimed at predicting the dependence of the elastic shear modulus on the volume fraction. Their simulations provide a physical insight into the origin of the behaviour of the shear modulus of emulsions: The energy of deformation per facet (film) formed between two neighbouring droplets is not Hookean; i.e., the droplets do not relax instantaneously.

Hemar, Hocquart and Lequeux (1995) also considered the viscoelasticity of emulsions and showed that both dilatational and shear elasticity of the stabilising amphiphilic layer contribute to the emulsion's overall elasticity. The contribution is pronounced differently for the dilatational and shear case, being, as expected, a function of the frequency of the deformation. Evidently, interfacial layers will produce an experimentally observable effect only if their relaxation time is comparable to (or higher than) the inverse frequency applied in the conventional mechanical rheometers. Generally, the frequencies at which the elastic shear modulus of an emulsion is determined are of the order of 1 Hz. The relaxation time of surfactant monolayers is of the order of milliseconds (or even less), therefore no surface elasticity effects are detectable for a low molecular weight surfactant under typical experimental conditions. The elasticity of the polymeric layers is generally much higher than the elasticity of the low molecular weight surfactants and, since the polymeric layers can store energy themselves, it is reasonable to expect this effect to influence the bulk (3D) rheology of emulsions (Dimitrova & Leal-Calderon, 2004).

Buzza and Cates (1994) have shown that the free energy change, δF , of a piece of interface whose area, A , is increased by δA , obeys:

$$\frac{\delta F}{A} = \sigma \left(\frac{\delta A}{A} \right) + \frac{1}{2} \varepsilon \left(\frac{\delta A}{A} \right)^2, \quad \text{Equation 2.23}$$

where ε is the elasticity of the layer, which can be formally defined in different ways.

For a static strain (zero frequency) one has $F \propto G\alpha^2$, where $G = G' (\omega = 0) \propto \sigma/R$. This arises purely from the first term on the right-hand side in Equation (2.28). At non-zero frequency, the local variation of the interfacial tension will also contribute, and the stored elastic energy can be higher than in equilibrium (zero frequency). Note that the term 'non-zero frequency' should always be considered in conjunction with the characteristic relaxation time of the surfactant layer stabilising the emulsion. A different approach was adopted by Hemar *et al.* (1995). They suggested scaling rules for G' in the case of concentrated emulsions stabilised by layers with dilatational viscosity or shear elasticity. The scaling with the capillary pressure on the non-deformed droplets is preserved, but the viscoelastic nature of the interfacial layers leads in both cases to an increase in G' , i.e. $G' (\omega > 0) > G' (\omega = 0)$.

Dimitrova and Leal-Calderon (2004) studied the oscillatory shear behaviour of protein-stabilised HIPREs of small droplet size (mean radius about 0.25 μm). Their data did not support the shear modulus equation of Princen and Kiss. The values of $G'/(\sigma/R)$ exhibited by their protein-stabilised emulsions were substantially larger than the ones obtained for equivalent emulsions stabilised by low molecular weight surfactants. They found that the protein layer adsorbed at the surface of the droplets contributed to the emulsion's overall elasticity.

Hemar and Horne (2000) measured the dynamic rheological properties (storage and loss moduli) of protein-stabilised HIPREs over a ϕ range of 0.68-0.89. The Sauter mean radius of the droplets was approximately 10 μm . Their data supported the shear modulus equation of Princen and Kiss (1983; 1986a).

The rheological behaviour of soya bean oil emulsions stabilised by sodium caseinate (0.1 and 0.7% sodium caseinate) was studied by Bressy *et al.* (2003). While having a very low interfacial tension ($\sigma = 0.1$ mN/m and 0.3 mN/m; $D = 1$ μm and 6 μm), these emulsions, when concentrated up to an oil volume fraction of 64%, have very high elasticity. It is 30 times higher than those usually observed for surfactant-stabilised emulsions. This high elasticity originates from the interfacial shear elasticity of the bilayer interface. The elastic shear modulus can be rescaled by $1/R$ but not by σ/R , as predicted by Mason *et al.* (1997). So, sodium caseinate-stabilised droplets can be regarded as droplets coated with a solid shell (Bressy *et al.*, 2003). An opposite result was observed on hexadecane-in-water emulsions stabilised by casein (Dimitrova & Leal-Calderon, 2004). This is probably due to the high value of the interfacial tension (14.5 mN/m), which might hide the other possible origins of the elasticity, or individual pure casein used by Dimitrova and Leal-Calderon (2004), which does not have the same interfacial characteristics as the caseinate aggregates used in Bressy's work (Bressy *et al.*, 2003).

Highly concentrated oil-in-water (OW) emulsions stabilised by means of gluten and soya protein isolate (SPI) at low pH have been characterised by means of linear dynamic viscoelasticity (Bengoechea *et al.*, 2006). It should be noted that, in general, the values obtained for SPI-based emulsions were much higher than those shown for gluten-based emulsions. This effect should be attributed to a difference in the values of the interfacial tension (Bengoechea *et al.*, 2006). The Mason model of elasticity of compressed emulsions has been used to correlate viscoelastic and microstructural parameters, giving adequate fitting but underestimating the elastic properties obtained for the highest concentration of gluten. According to the authors, these deviations can be explained in terms of an

enhancement of the elastic network formed in the aqueous phase in which the glutenin fraction must play an important role.

2.11 RESEARCH ISSUES IDENTIFIED

The interest in such highly concentrated emulsions is great because they have numerous potential technological applications in cosmetics, mining, oil recovery and explosives. In all these applications, two principal characteristics of highly concentrated emulsions determine their properties, namely their rheological properties in a newly prepared state ("fresh" materials) and the stability of these properties.

It must also be mentioned that, among the numerous published works devoted to emulsions, only a limited number touch on emulsions of this type, which is the subject of this project, i.e. emulsions in which the dispersed phase is formed by supercooled water solutions of inorganic salts. Meanwhile, the metastable nature of this phase creates new and very promising features for these types of systems.

In the current state of knowledge concerning the rheological properties of highly concentrated inverse phase emulsions, there is a lack of systematic experimental data, especially concerning the effect of electrolyte (type and concentration) and surfactant (type and concentration) as the main two parameters present in the system and affecting the rheological properties of emulsions and emulsion stability.

Therefore the main objective of this thesis was to investigate how the emulsion formulation concentration of electrolyte and surfactant as well as surfactant and electrolyte type affects the rheological properties and stability (crystal initiation) of highly concentrated water-in-oil emulsion explosives in the context of surfactant-electrolyte interactions.

CHAPTER 3

MATERIALS AND METHODS

3.1 INTRODUCTION

This chapter provides the description of materials and methods used in the present investigation. The main goal of this research was to determine how the emulsion formulation (surfactant type – surfactant molecules with varied hydrophilic parts and concentration, electrolyte concentration and type) affects the structure at the water-oil interface of fresh highly concentrated emulsions and the emulsion stability in terms of surfactant interactions with the matter in droplets.

The investigation included measuring the interfacial properties, the first interest of this research project. The rheological investigation consequent to this is also presented. The research covered the following:

1. Interfacial properties:
 - Interfacial tension
 - Interfacial elasticity
2. FT-IR analysis
3. Differential scanning calorimeter (DSC) analysis
4. Rheological properties:
 - Viscoelastic properties
 - Flow properties
5. Microscopic observation

3.2 MATERIALS

The materials for the project were provided by African Explosives Limited and Lake International Technologies. Four emulsifiers were used for this study; they are identified here as Pibsa-MEA, Pibsa-IMIDE, Pibsa-UREA, and SMO. The first three are derivatives of Polyisobutylene succinic anhydride (Pibsa) and belong to the same type of chemical compounds, though with different end groups. These surfactants can be treated as oligomers, while SMO (a sorbitan ester) is a monomeric product. A mixture of Pibsa-MEA and SMO was also used in the present study in the ratio 10:1. When originally synthesised, the surfactants were dissolved in paraffinic petroleum oil with no additives. Further dilution with

other hydrocarbon-based oils was used to achieve the desired concentration and viscosity. The Mosspar-H oil was used in this study.

3.2.1 Surfactants

Surfactants used in the present study have a low HLB number and are therefore soluble in hydrocarbon oil. All structures were drawn with the use of Advanced Chemistry Development Labs software. The description of the software is given in section 3.5.7.

3.2.1.1 Pibsa-MEA

This emulsifier, described by *Lake International Technologies, Republic of South Africa*, as Pibsa (i.e. polyisobutylene succinic anhydride) of molecular weight 1048, reacted approx 1:1 with monoethanolamine to an uncondensed amide/acid head group, as shown in Figure 3.1.

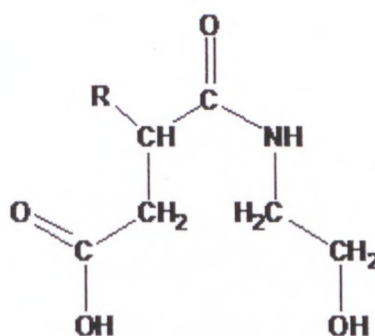


Figure 3.1: 2-D view of the head group structure of Pibsa-MEA

The R indicates polyisobutylene, the repeat unit of which is $-\text{C}(\text{CH}_3)_2\text{-CH}_2-$ i.e. a chain of carbon atoms with two methyl side groups attached to every second one. To give a molecular weight of 1048, there would have to be about 19 repeat units in the chain. If these were contained in a single chain, the length would be 38 carbon atoms with an additional 38 in the methyl side groups (the chain might be attached to the carbon atom adjacent to the carboxylic acid group, rather than the one adjacent to the amide group as shown). The overall molecular weight would be about 1109. The HLB number is not known precisely, but would be low (< 4). One of the possible conformations of Pibsa-MEA surfactant is shown in Figure 3.2.

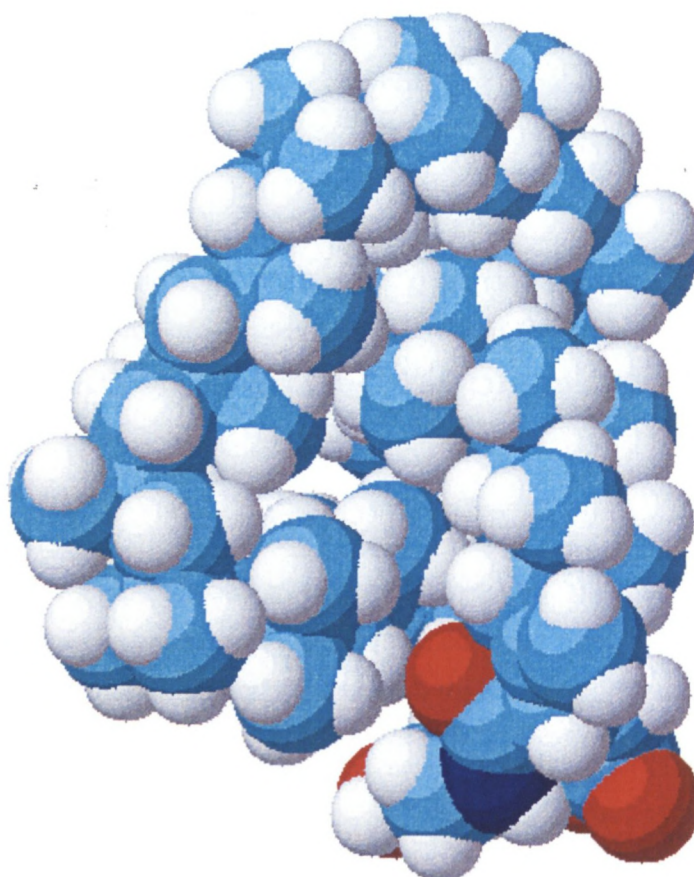


Figure 3.2: 3-D view of possible conformation of Pibsa-MEA surfactant (Oxygen – red, Nitrogen – blue, Carbon – light blue, Hydrogen – white)

3.2.1.2 Pibsa-IMIDE

Pibsa-IMIDE is described by Lake as Pibsa-MEA condensed to an N-substituted pyrrolidinedione (succinimide) structure, as shown below in Figure 3.3.

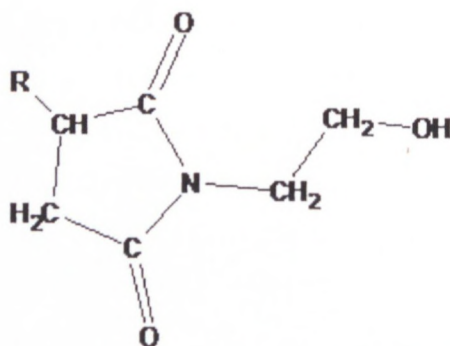


Figure 3.3: 2-D view of Pibsa-IMIDE head group structure

The overall molecular weight will be 1091, the HLB number will be low (< 4). One of the possible conformations of the Pibsa-IMIDE surfactant is shown in Figure 3.4.

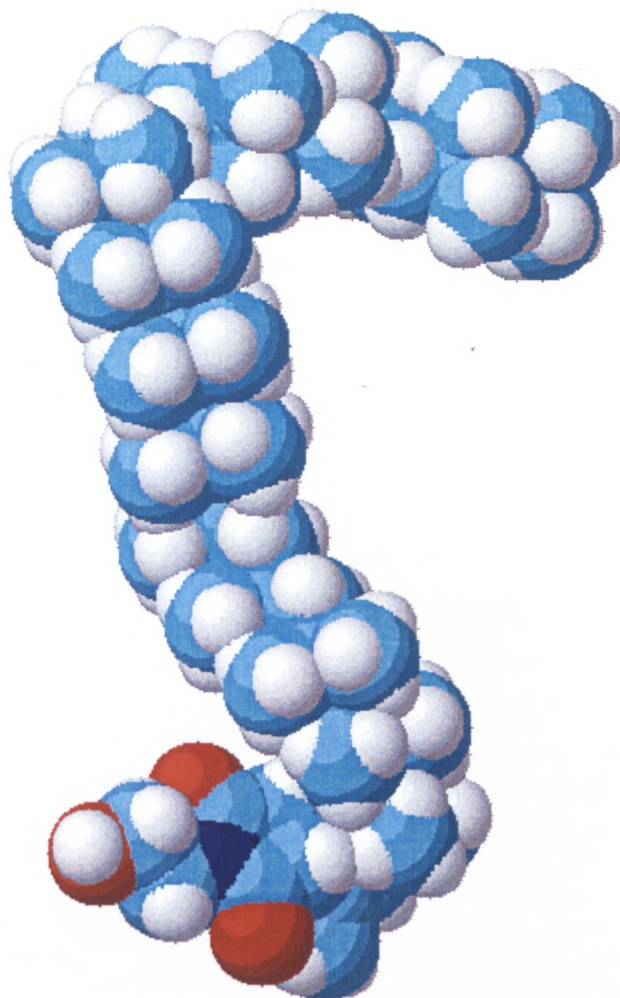


Figure 3.4: 3-D view of the possible conformation of Pibsa-IMIDE surfactant
(Oxygen – red, Nitrogen – blue, Carbon – light blue, Hydrogen – white)

3.2.1.3 Pibsa-UREA

Pibsa-UREA is an adduct of Pibsa and urea, with a head group structure as shown in Figure 3.5

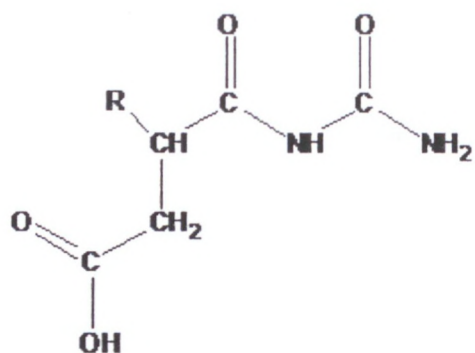


Figure 3.5: 2-D view of Pibsa-UREA head group structure

The overall molecular weight is about 1109, and the HLB number will be low (< 4). One of the possible conformations of Pibsa-UREA surfactant is shown in Figure 3.6.

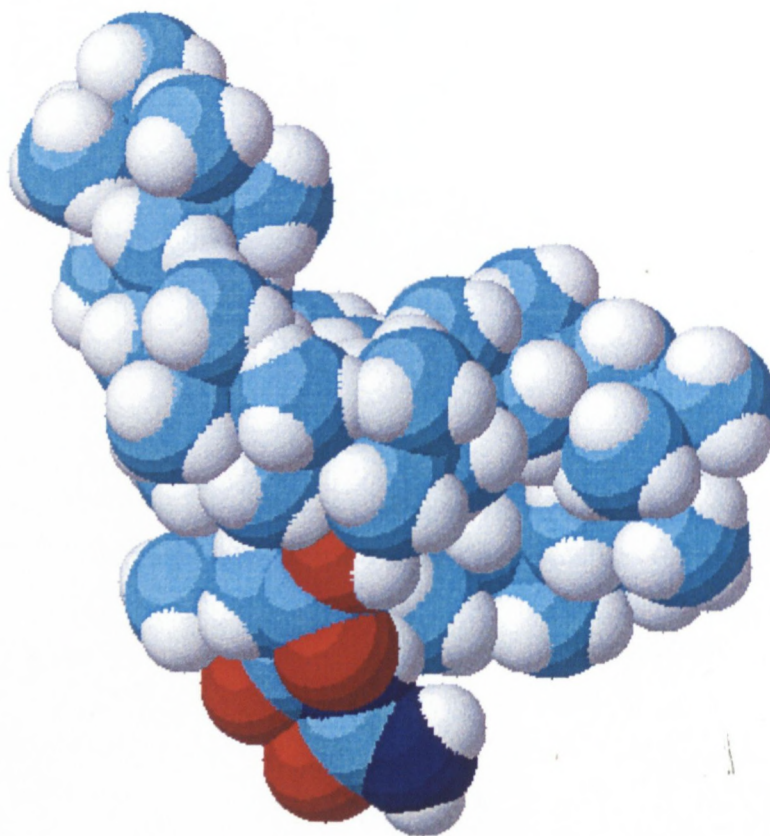


Figure 3.6: 3-D view of possible conformation of Pibsa-UREA surfactant
(Oxygen – red, Nitrogen – blue, Carbon – light blue, Hydrogen – white)

3.2.1.4 Sorbitan monooleate (SMO)

SMO is an ester formed between sorbitan and oleic acid (oleic acid is a C18 fatty acid with a single *cis* double bond, written as C18:1). The structure of SMO is given below in Figure 3.7.

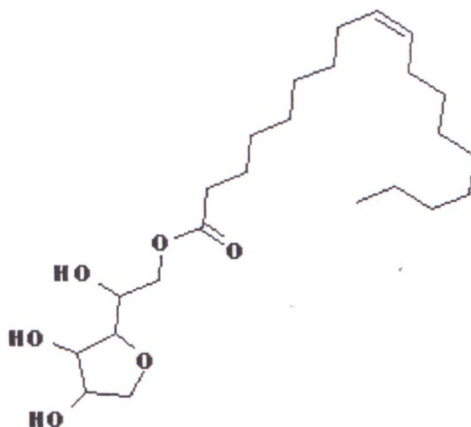


Figure 3.7: 2-D view of SMO structure

The molecular weight of sorbitan monooleate is 428, with the HLB number about 4.3. Commercial SMO is often known by its trade name Span[®]80. One of the possible conformations of SMO is shown in Figure 3.8 below.

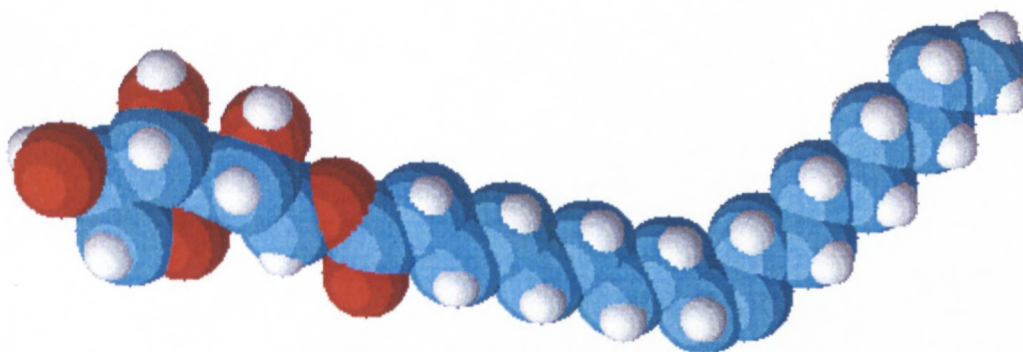


Figure 3.8: 3-D view of possible conformation of SMO surfactant
(Oxygen – red, Carbon – light blue, Hydrogen – white)

3.2.1.5 Summary of surfactant properties

The summary of the surfactants' properties is given in Table 3.1.

Table 3.1: Summary of surfactants' properties

<i>Surfactant type</i>	<i>Approximate relative molecular mass</i>	<i>Head group relative molecular mass</i>	<i>HLB number</i>
<i>Pibsa-MEA</i>	1210	161	low (< 4)
<i>Pibsa-IMIDE</i>	1190	148	low (< 4)
<i>Pibsa-UREA</i>	1210	160	low (< 4)
<i>SMO</i>	429	133	4.3

3.2.2 Properties of fuel oil

The surfactants used for this study were originally dissolved at high concentrations in Parprol 32. The fuel oil used for dilution to the required concentration was Mosspar-H. The properties of these materials are given in Table 3.2.

Table 3.2: Summary of fuel oil properties

<i>Properties</i>	<i>Parprol 32</i>	<i>Mosspar H</i>
<i>Manufacturer</i>	Engen Chemicals	PetroSA
<i>Manufacturers description</i>	Solvent dewaxed light paraffinic distillate	Isoparaffinic solvent
<i>Boiling range, °C</i>		290 - 300
<i>iso-paraffins, %</i>	70	80-90
<i>n-paraffins, %</i>		1-10
<i>Cycloparaffins, %</i>	26	10-15
<i>Aromatics, %</i>	4	<0.1 (< 0.05 typical)
<i>Density 20 °C, kg m⁻³</i>	866 or 874	790 – 820 (792 typical)
<i>Density 22 °C, kg m⁻³ (measured)</i>	863	794

3.3 EMULSION PREPARATION

The internal phase was formed by an oversaturated aqueous solution of ammonium nitrate (AN). For the preparation of emulsions, the granulated AN was added to the distilled water at 80° C. The concentration of AN in the aqueous solution was kept at 80-wt %. The equilibrium crystallisation temperature (fudge point) of the solution with the chosen concentration of AN was approximately 60 °C. The density of the solution was about 1.4 to 1.5 g/l. For all emulsion formulations, the concentration of the aqueous phase in the emulsion was kept at 90% by volume. Trace amounts (< 0.5%) of pH-buffering additives and acids were also present.

The Hobart mixer was used to manufacture emulsion samples. All the samples were prepared using the continuous sampling procedure. The following instructions were applied:

- Transfer the fuel phase into the preheated bowl. Allow 5 minutes for the fuel phase to heat up.
- Cover the mixing bowl with plastic or the aluminium cover to stop the emulsion from splashing.
- Switch “on” the mixer at speed 1.
- Slowly transfer the oxidiser solution into the bowl by running the solution into the bowl with the help of a spatula.
- Ensure that an emulsion is formed.
- Continue adding the entire oxidiser solution. Stop the mixer and switch to speed 2. Then run the mixer at speed 2 for a further minute (60 seconds).
- Stop the mixer and switch to speed 3.
- Take small samples of the fuel phase from speed 3 every 2.5 mins till 60 mins. Repeat this procedure for all formulations.
- Then take samples for measurement of droplet size distributions, using the Malvern Mastersizer.

3.4 MATRIX OF SAMPLES

The samples could be divided into following groups:

- Emulsions stabilised by different surfactants
- Emulsions stabilised by the same surfactant at different surfactant concentration
- Emulsions prepared with different AN content and addition of other nitrate salts
- Emulsions prepared with different nitrate salts as an aqueous phase

All the samples are given below, in Tables 3.3 to 3.6:

Table 3.3: AN and AN-NaNO₃ emulsions stabilised by different surfactants

Type of surfactant	AN emulsions		AN-NaNO₃ emulsions (7:1)	
	C_{AN}, %	C_{SURF}, %	C_{SALT}, %	C_{SURF}, %
<i>MEA</i>	80	4,8, 14 and 20	80	8 and 14
<i>UREA</i>	80	8 and 14	80	8 and 14
<i>IMIDE</i>	80	4,8, 14 and 20	80	8 and 14
<i>MEA/SMO (10:1)</i>	80	8 and 14	80	8 and 14
<i>SMO</i>	80	8	80	8

Table 3.4: Emulsions with different AN concentrations

Type of surfactant	AN emulsions	
	C_{AN}, %	C_{SURF}, %
<i>Pibsa-MEA</i>	0	8
	2	8
	5	8
	10	8
	20	8
	30	8
	40	8
	50	8
	60	8

Table 3.5: Emulsions with different additions of $\text{Ca}(\text{NO}_3)_2$

Type of surfactant	AN-$\text{Ca}(\text{NO}_3)_2$ emulsions	
	$C_{\text{Ca}(\text{NO}_3)_2}$, %	C_{SURF}, %
<i>Pibsa- IMIDE</i>	0	8
	15	8
	35	8

Table 3.6: Emulsions with different salts in the aqueous phase

Surfactant type	Aqueous phase of emulsion	pH
<i>Pibsa-MEA</i>	Water	4 and 7
	NH_4NO_3	4 and 7
	NaNO_3	4 and 7
	$\text{Ca}(\text{NO}_3)_2$	4 and 7

3.5 METHODS

Droplet size analysis, rheological and optical analysis, FT-IR and DSC studies were performed to characterise prepared samples. Interfacial properties measurements were also carried out.

3.5.1 Droplet size analysis

Measuring the size of dispersed particles was carried out with the Mastersizer 2000 device (Malvern Instruments Co.) (Figure 3.9). The procedure for measuring is based on sample dispersion under software control and the measurement of angle dependence of the intensity of scattering of a collimated He-Ne laser beam. Particle size in a range from 0.26 to 1500 μm can be measured; this range is much wider than the sizes of the real samples used in this investigation. The size distribution calculations were based on the rigorous Mie theory and the standard software applied to the instrument was used. Each emulsion sample (a small amount of sample was taken) was dispersed in the large volume of oil to reach a very dilute concentration of water droplets in oil and to avoid the formation of agglomerates. The average value D_{32} was used as a measure of droplet size in the investigation. Accuracy of measurement was 99 %.

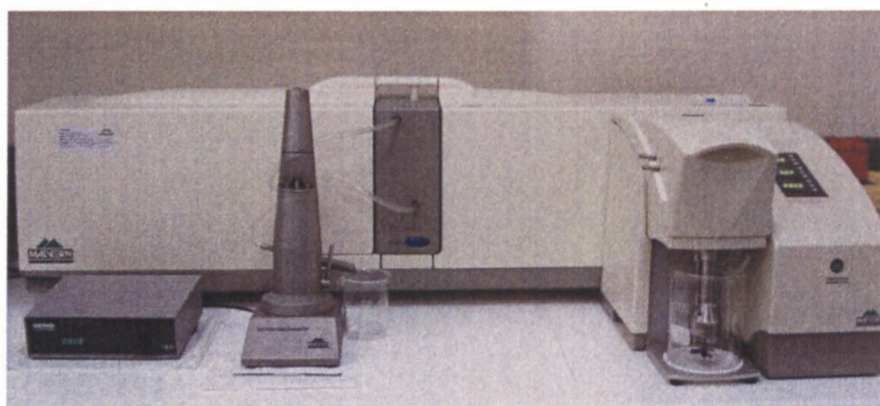


Figure 3.9: Mastersizer 2000 instrument

3.5.2 Microscopy

The observations were carried out on the samples under investigation with an optical microscope (Leica) equipped with a digital camera, at a magnification of x 500. The microscope is shown in Figure 3.10.

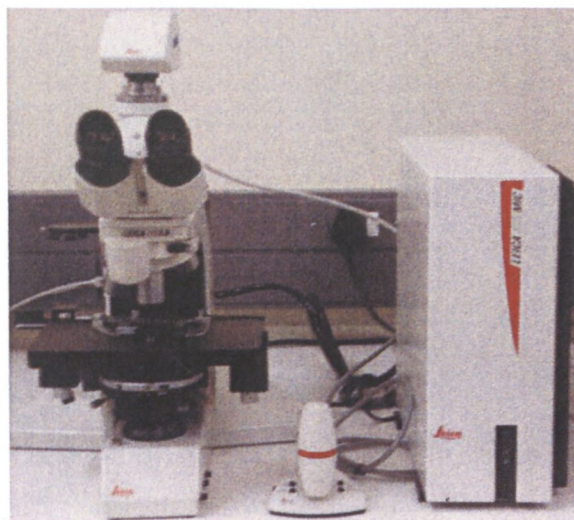


Figure 3.10: Leica microscope

3.5.3 Rheological analysis

All rheological studies were conducted with a rotational stress rheometer MCR 300 (Paar Physica) (shown in Figure 3.11). The geometry of the measuring unit was plate-and-plate with a sandblasted surface (the plate diameter was 50 mm). The experiments were made in the following regimes of deformation:

- Oscillatory measurements for measuring strain amplitude dependencies of the (storage and loss) components of dynamic modules; the frequency (1Hz) was kept constant in the amplitude sweep test. Strain was controlled between 0.01 and 200%.
- Steady state flow measuring flow curves (shear stress versus shear rate).

Torque resolution was 0.1 nNm. Angular resolution was 0.01 μ rad.

All the rheological measurements were conducted at 30°C.

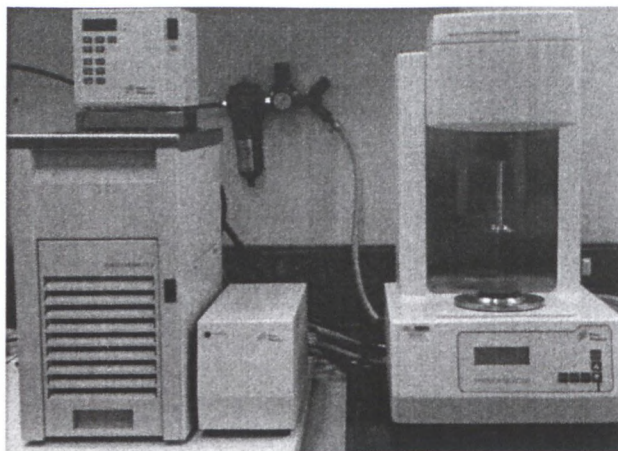


Figure 3.11: Rotational Rheometer MCR 300 (Paar Physica)

3.5.4 Interfacial properties investigation

The interfacial tension was determined using the Krüss K100 tensiometer (Figure 3.12), supplied by Krüss GmbH, Germany. The principle of operation of the K100 is straightforward. About 15 cm³ ammonium nitrate solution is placed in a clean 70 mm diameter glass dish. A hydrophilic platinum (Wilhelmy) plate is suspended vertically from a sensitive force transducer with its lower edge penetrating the surface of the ammonium nitrate solution. About 50 cm³ of the oil phase are added, so that the plate is wholly submerged.

The interfacial tension is given by following equation:

$$\gamma = F / L \cos\theta \quad \text{Equation 3.1}$$

where F , [mN], is the vertical force acting on the plate, after a correction has been made for the plate buoyancy; L , [m], is the wetted plate length; θ is the contact angle. Since the plate is hydrophilic, the contact angle is taken as zero.

The resolution is 0.01, accuracy of measurement is 0.1.

All the experiments were conducted at 30°C.

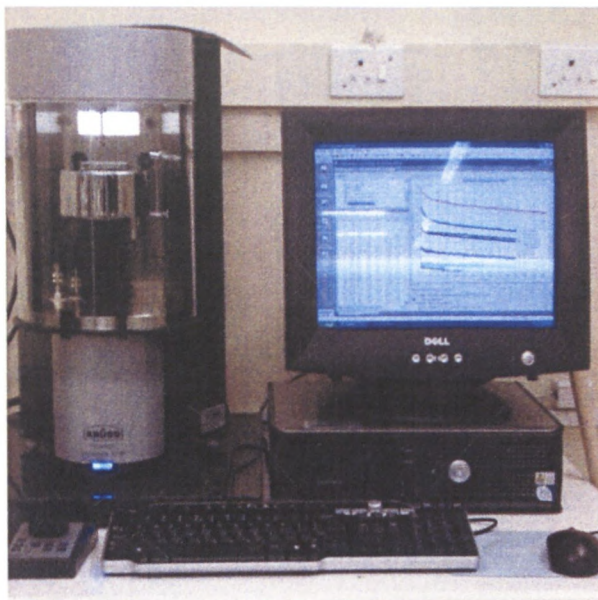


Figure 3.12: Kruss K 100 Tensiometer

3.5.5 FT-IR analysis

Infrared spectroscopy detects the vibration characteristics of chemical functional groups in a sample. When an infrared light interacts with the matter, chemical bonds will stretch, contract and bend. As a result, a chemical functional group tends to absorb infrared radiation in a specific wave number range, regardless of the structure of the rest of the molecule. The correlation of the band wave number position with the chemical structure is used to identify a functional group in a sample.

A Fourier Transform spectrometer simply is a technical variant of a common infrared spectrometer which yields an intensity signal as a function of wavelength or 'spectral colour'. The setup differs from a classical grating or prism spectrometer in that it does not record the spectral intensity directly as a function of the wavelength, but an interferogram is taken instead. The central component of an FT-IR spectrometer is a Michelson interferometer and the signal is recorded as a function of the optical path difference between the fixed and the movable mirror. From this interferogram the spectrum as a function of wavelength is calculated by applying a Fourier Transform (FT), which gives the instrument its name. The basic components of an FT-IR spectrometer are shown schematically in Figure 3.13.

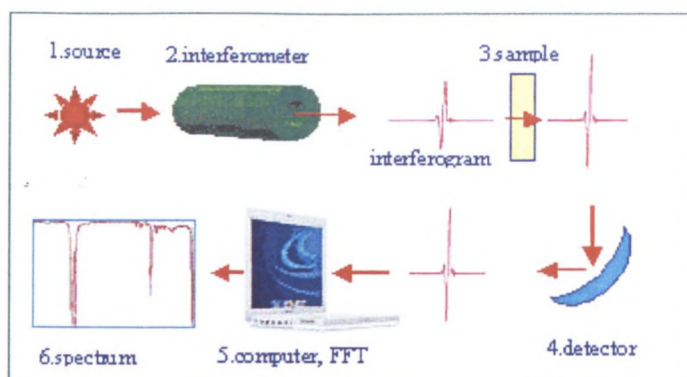


Figure 3.13: Basic components of an FT-IR spectrometer

The FT-IR studies were conducted with the use of a Perkin Elmer Spectrum 100 FT-IR Spectrometer (Figure 3.14). The resolution used was 4 cm^{-1} . The spectra of the emulsions were recorded at room temperature using an Attenuated Total Reflectance accessory (which does not require any sample preparation). The Germanium (Ge) was a crystalline material. The range of measurements was 4000 cm^{-1} to 500 cm^{-1} . The wavelength accuracy is equal 0.1 cm^{-1} at resolution 4 cm^{-1} .



Figure 3.14: Perkin Elmer Spectrum 100 FT-IR Spectrometer

Attenuated total reflectance (ATR) is a sampling technique used in conjunction with infrared spectroscopy which enables samples to be examined directly in the solid or liquid state without further preparation. ATR uses a property of total internal reflection called the evanescent wave. A beam of infrared light is passed through the ATR crystal in such a way that it reflects at least once off the internal surface in contact with the sample. This reflection forms the evanescent wave which extends into the sample, typically by a few micrometres. The beam is then collected by a detector as it exits the crystal (Figure 3.15).

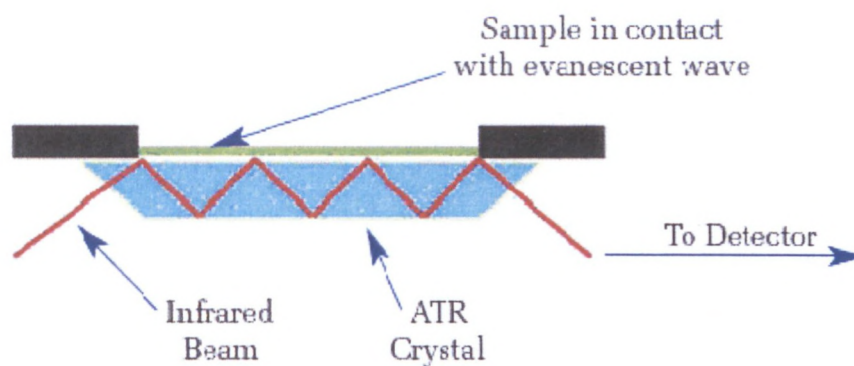


Figure 3.15: A multiple reflection ATR system

3.5.6 DSC analysis

DSC studies were carried out with use of a DSC Q 2000 instrument (Figure 3.16) coupled to a computer for data analysis. Liquid nitrogen was the coolant. About 5 mg of sample was taken for each run. The temperature range studied was from 30°C to -70°C, with the cooling rate being 2°C/min. The temperature accuracy is 0.1°C and sensitivity is 0.2μW.



Figure 3.16: Differential scanning calorimeter Q 2000

3.5.7 ACD Laboratory software (version 6.0). Advanced Chemical Development Inc.

ACD/ChemSketch is a chemical drawing software package from Advanced Chemistry Development Inc., designed to be used alone or integrated with other applications. ChemSketch is used to draw chemical structures, reactions, and schematic diagrams. The screen with the open software is shown in Figure 3.17.

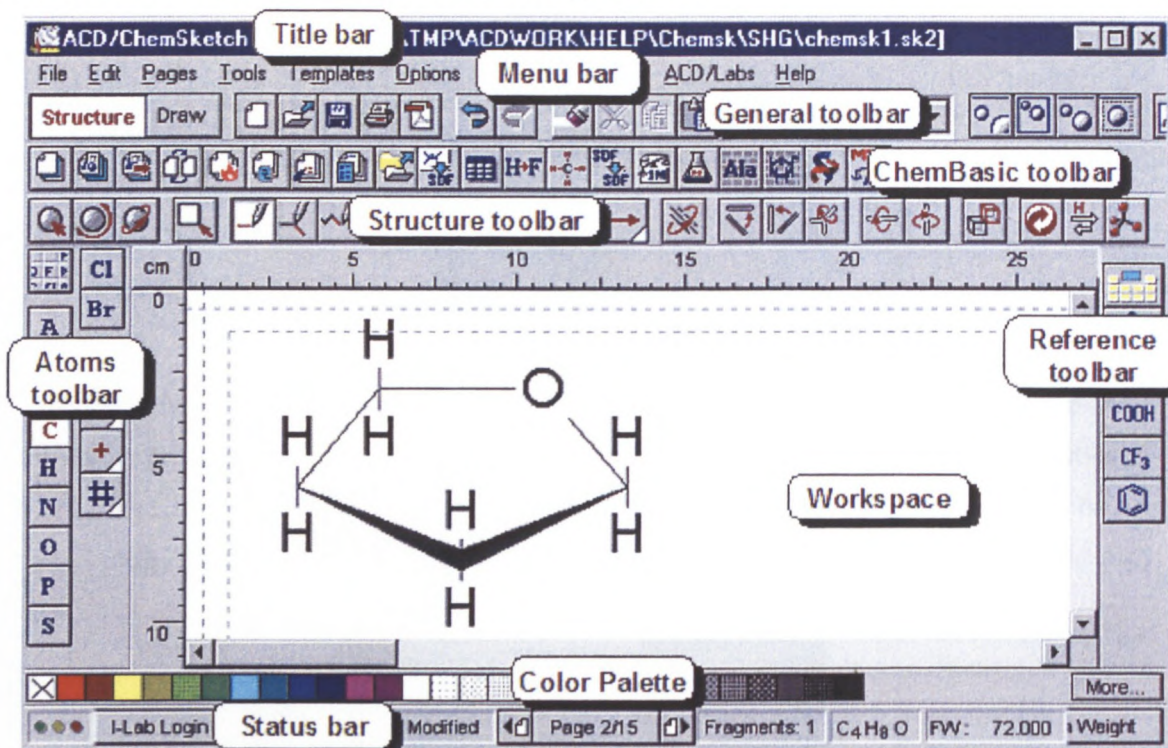


Figure 3.17: Screen with the Structure Mode enabled

2-D Optimisation

Two-dimensional optimisation involves redrawing and resizing the drawn structure to standardise all the bond lengths and angles.

3-D Optimisation

The 3-D optimisation algorithm transforms the planar (2-D) structure into a realistic three-dimensional structure. It is based on modified molecular mechanics which take into account bond stretching, angle bending, internal rotation, and Van der Waals non-bonded interactions. Modifications include minor simplification of potential functions and enforcement of the minimisation scheme by additional heuristic algorithms for dealing with "bad" starting conformations. The 3-D optimisation algorithm is a proprietary version of molecular mechanics with the force field initially based on CHARMM parameterisation (CHARMM: A

program for macromolecular energy, minimisation and dynamics calculations). The modifications involve some simplification and were intended to increase the stability and speed of computation. The 3-D optimiser is not a full-scale molecular mechanics engine. Its design aims to reliably reproduce reasonable conformations from 2-D drawings, rather than to precisely optimise 3-D structures. 3-D optimisation shows one of the suitable molecular conformations. The simple structural parameters such as distance and angle between two atoms can be calculated.

CHAPTER 4

RESULTS AND DISCUSSION

4.1 INTERFACIAL PROPERTIES AND INTERACTIONS IN HIGHLY CONCENTRATED EMULSIONS

This chapter presents the interpretation of experimental results from an investigation of interfacial properties of highly concentrated water-in-oil emulsions and emulsion stability from crystal initiation in the aqueous phase.

4.1.1 Effect of surfactant hydrophilic head group on the interfacial properties and interfacial interactions in highly concentrated emulsions

The main interest in this part of the present study was to look closely at the nature (in terms of surfactant head groups) of the interfacial region separating the two immiscible phases. Special attention is given to the chemical and physical nature of the adsorbed film, the role of mixed films and hydrogen bonds (complex) formation, and interfacial rheology. To understand how these factors influence emulsion stability of an emulsion is shown. The emulsions under investigation were stabilised with Pibsa-based surfactants, which had the same polymeric tail group but contained different head groups.

4.1.1.1 *Interfacial properties*

The dynamic interfacial tension and interfacial elastic modulus were determined using a PAT 1 tensiometer supplied by Sinterface Technologies, Berlin, Germany. The basic principle in the operation of this instrument is that the Young-Laplace equation is fitted to the profile of an image of a droplet in the more dense phase suspended in the less dense phase from a capillary. The Young-Laplace equation balances the interfacial tension against gravity, with the interfacial tension tending to reduce the interfacial area and gravity tending to increase it by extending the droplet. This balance leads to certain practical considerations concerning the capillary diameter and the droplet volume. For example, if the droplet volume is too low, the interfacial tension dominates and the droplet assumes a spherical shape from which the interfacial tension cannot be extracted. If the droplet volume is too high, gravity dominates and the droplet detaches from the capillary. A droplet volume of 3 mm³ with a capillary outer diameter of 1.97 mm was used for the samples considered here.

Except for SMO, the interfacial tension quoted was measured after 15,000 seconds, by which time a reasonably constant value had been reached. For SMO, the droplet tended to detach from the capillary, and the experiment could only be sustained for one hour.

For the Fourier algorithm to be applicable, and for measurements made at different frequencies to be comparable, the interfacial tension should be constant. In practice this criterion should not change appreciably for the duration of the oscillation experiment.

The range of frequencies used was also a matter of judgment and trial and error. The Fourier software requires at least two cycles, preferably more, so the low frequency limit depends in part on the rate at which the material properties change over time, and in part on how long the operator is prepared to wait for a data point. But the magnitude of the complex interfacial modulus, and therefore the amplitude of the oscillating interfacial tension, must increase with increasing frequency. This means that the lower the frequency, the lower the oscillation amplitude, and the less easily the oscillating interfacial tension can be distinguished from the mean interfacial tension. Thus the low frequency limit also depends on the material properties and the resolution of the instrument. The high frequency limit depends on the response time of the mechanical components of the instrument, and on the sampling rate, since the Fourier algorithm requires a minimum number of points per cycle.

It was experimentally found that a frequency range of 0.01 Hz to 1 Hz could be used for most samples (because the droplet fell down at higher frequencies). Indeed, if the interfacial moduli are low, the results of measurements at the higher and lower frequencies can have large uncertainties. The frequencies used were 0.01 Hz, 0.02 Hz, 0.05 Hz, 0.1 Hz, 0.2 Hz, 0.5 Hz and 1.0 Hz for a given strain of 7.5%. The table of moduli at 0.1 Hz is given in the following section of this study, as data at this frequency were the most reliable.

4.1.1.1.1 Determination of CMC

The critical micelle concentration (CMC) is determined by an abrupt change in the slope of the curve when interfacial tension versus \ln (surfactant concentration) is plotted. Below the critical micelle concentration, the Γ is given by Equation 2.16 (see section 2.7.5), which is derived from the Gibbs adsorption isotherm (McClements, 1999; 2005). Γ determines the minimum concentration of surfactant which is needed to cover the interface. If the condition of

saturation adsorption is achieved, the plot of concentration against the natural logarithm of the interfacial tension will be linear.

The interfacial tension was determined using the Krüss K100 tensiometer, supplied by Krüss GmbH, Germany. This was used in preference to the PAT1 because Equation 3.1 requires the equilibrium interfacial tension, which is arrived at more rapidly with the K100.

Surfactant solutions were made up by successive dilution. After each dilution, the solution was split and the interfacial tension measurement was taken using one part of the dilution, the other part being used for the next dilution. All experiments were conducted at 30°C.

The plot of interfacial tension against the ln of surfactant concentration for Pibsa-MEA emulsifier is shown below in Figure 4.1.

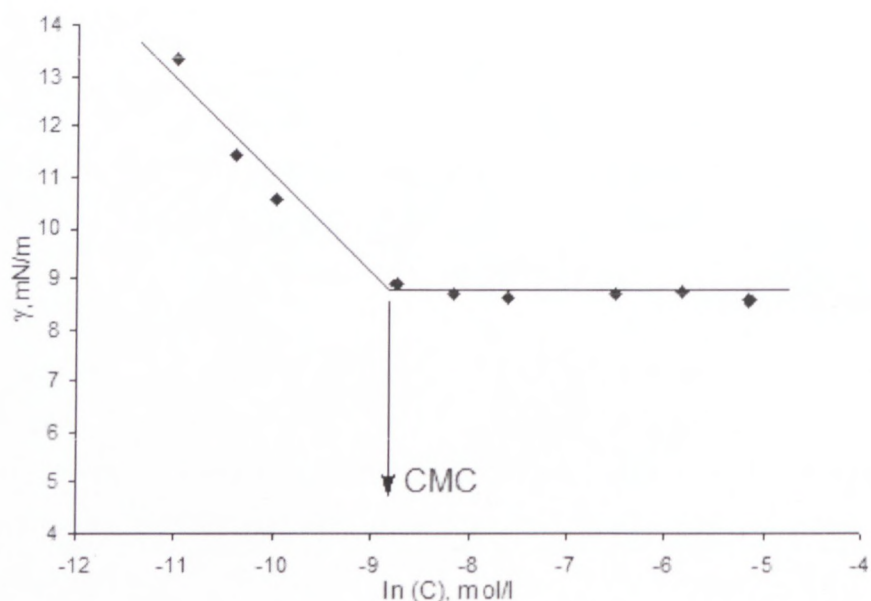


Figure 4.1: Determination of CMC value of Pibsa-MEA surfactant

Determination of CMC values for others surfactants (Pibsa-IMIDE, Pibsa-UREA, SMO) is given in Appendix A. A summary of interfacial properties is presented in Table 4.1.

Table 4.1: Summary of interfacial tension, interfacial elastic modulus and CMC values for Pibsa-based surfactants and SMO

<i>Surfactant type</i>	<i>% Surfactant</i>	$\gamma, \text{mN/m}$	$E', \text{mN/m}$	$\text{CMC} \times 10^4 \text{ mol/l}$	<i>Area per molecule, \AA^2</i>
<i>Pibsa-MEA</i>	8	8.7	2.9	0.9	150
	14	8.6	3		
<i>Pibsa-IMIDE</i>	8	1.0	1.1	2.2	100
	14	1.1	1.2		
<i>Pibsa-UREA</i>	8	5.9	2.9	1.2	150
	14	5.5	2.7		
<i>Pibsa-MEA/SMO</i>	8	5.1	2.1	-	-
	14	4.9	2		
<i>SMO</i>	8	0.6	0.3	0.6	80
	14	0.7	0.3		

From the above it is clear that the trend in interfacial tension is as follows: Pibsa-MEA > Pibsa-UREA > Pibsa-MEA/SMO > Pibsa-IMIDE > SMO. The differences between the three simple Pibsa-based surfactants are in the hydrophilic head groups only, and the observed trend can therefore be attributed to these differences.

Among the three Pibsa-based surfactants, the Pibsa-IMIDE possesses lower polarity (which depends on the functional group present in the head group and its structure (Rudnick, 2003)). It can be assumed that, due to this, Pibsa-IMIDE has less a interactive head group, which should lead to a higher free energy state at the interface (higher interfacial tension) compared with more the polar head groups of Pibsa-MEA and Pisa-UREA. However, Pibsa-IMIDE has lower interfacial tension compared to the two others surfactants. This effect could be due to the increased concentration of Pibsa-IMIDE at the interface, since the area per molecule for this surfactant is less than for Pibsa-MEA and Pibsa-UREA. This was confirmed by experiment and ACD/Labs calculations (described further in this section).

The addition of SMO (low molecular weight (LMW) surfactant) to the Pibsa-MEA polymeric surfactant lowers the interfacial tension relative to the interfacial tension of Pibsa-MEA and the value of the interfacial tension drops significantly when it is measured using only SMO surfactant. It is a smaller molecule in comparison with the bulky polymeric Pibsa-MEA molecule and therefore it rapidly diffuses through the bulk, covers the interface and reduces the interfacial tension, but eventually is partly displaced by Pibsa-MEA, which results in the rising of interfacial tension. It is possible to determine the molar fraction of both surfactants at

the interface and their degree of compatibility in the system. The methodology that was used was that which is described by Chattopadhyay (1996). The average molecular surface area of the surfactant blend is measured and compared with the arithmetic mean of the molecular surface areas of the independent surfactants. A reduction in average area can be attributed to the intermolecular attraction between the surfactant molecule, and an increase in area can be attributed to repulsion or increased disorder at the interface. These interactions can be quantified by a parameter, β , which is known as an interaction parameter, and determined as described below.

The interaction parameter, β , for mixed surfactant monolayer formation at the liquid-liquid interface can be determined from plots of interfacial tension of an aqueous AN solution/oil phase interface versus log surfactant concentration for each of the two surfactants (Pibsa-MEA and SMO) in the system and a mixture of them at a fixed mole fraction. The interaction parameter can be calculated from the following equations (Chattopadhyay, 1996; Rosen, 2004):

$$\frac{X_1^2 \ln(\alpha C_{12} / X_1 C_1)}{(1 - X_1)^2 \ln[(1 - \alpha) C_{12} / (1 - X_1) C_2]} = 1, \quad \text{Equation 4.2}$$

$$\beta = \frac{\ln(\alpha C_{12} / X_1 C_1)}{(1 - X_1)^2}, \quad \text{Equation 4.3}$$

where C_1 , C_2 , C_{12} are the critical concentrations of the pure Pibsa-MEA, pure SMO and mixture of Pibsa-MEA/SMO respectively required to produce a given interfacial tension value; α is the mole fraction of the Pibsa-MEA surfactant and $(1 - \alpha)$ is the mole fraction of the SMO in the surfactant/oil mixture; X_1 is the mole fraction of Pibsa-MEA in the total surfactant in the mixed monolayer.

For attractive interactions between surfactants, β becomes negative, which can be interpreted as positive synergism. For repulsive interactions, β becomes positive, which can be interpreted as negative synergism or antagonism. The larger the numerical value of β , the stronger the interaction (Chattopadhyay, 1996). The experimental evaluation of the interaction parameter is shown in Figure 4.2.

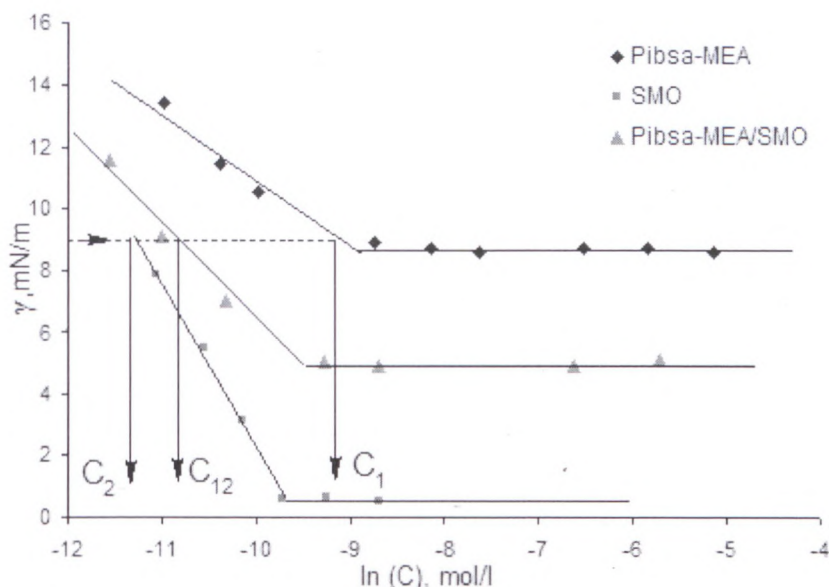


Figure 4.2: Experimental evaluation of interaction parameter β between Pibsa-MEA and SMO surfactants

As shown in Figure 4.2, the values $C_1 = 1.60 \cdot 10^{-4}$ mol/l, $C_2 = 1.37 \cdot 10^{-5}$ mol/l, $C_{12} = 1.92 \cdot 10^{-5}$ (for the interfacial tension $\gamma = 8.8$ mN/m) were taken at the linear region of slope and lower than CMC values. The portion of maximum slope for the SMO was extrapolated linearly to reach the value of the given interfacial tension. The weight ratio of a mixture of Pibsa-MEA and SMO was taken at 10:1 and was converted into a mole fraction of each surfactant: α (Pibsa-MEA) = 0.78; $(1 - \alpha) = 0.22$ for SMO. The $X_1 = 0.403$ was obtained, solving Equation 4.2, and the interaction parameter ($\beta = -4.1$) was derived from Equation 4.3.

From the above calculations it can be seen that the Pibsa-MEA mole fraction in the monolayer was equal to 0.403 and therefore both surfactants (Pibsa-MEA and SMO) were present at the interface. This implies that the SMO surfactant was not fully replaced from the interface by the polymeric surfactant and competed with Pibsa-MEA in the monolayer. The negative value of interaction factor β shows that there was an attraction between surfactants (positive synergism) in the mixed monolayer that allowed them to pack close to each other and provide lower interfacial tension in comparison with Pibsa-MEA (Chattopadhyay, 1996; Rosen, 2004).

As can be seen from Table 4.1, the interfacial elastic modulus was following the same trend as the interfacial tension: Pibsa-MEA > Pibsa-UREA > Pibsa-MEA/SMO > Pibsa-IMIDE > SMO. It has been documented in the literature that a difference in the packing features of surfactants at the interface leads to different degrees of oil molecule penetration into the

surfactant films and changes the cohesive interactions in the aliphatic layers of the surfactant films (Ghaicha *et al.*, 1995). The increased penetration of oil molecules increases the cohesive interactions in the aliphatic layer, leading to a long-range ordered and more rigid interface (Ghaicha *et al.*, 1995). The packing of polymeric surfactants (Pibsa-MEA, Pibsa-UREA, Pibsa-IMIDE) provides a more rigid interface due to increased cohesive interactions between tails (more oil penetration) in comparison with the conventional emulsifier (SMO) and this results in a larger value of the interfacial elastic modulus. It has been shown that SMO is present at the interface when added to Pibsa-MEA and therefore reduces the interactions between the polymeric tails, leading to lower elasticity of the interfacial film. The difference in interfacial elastic modulus for Pibsa-based surfactants (polymeric molecules) can be accounted for in terms of the orientation of the molecules at the interface due to a different chemical structure of their head groups and therefore different strength of interaction with the AN solution (see section 4.1.2.1.1).

It also appears, from Table 4.1, that the surfactant concentration in the studied samples was far above the CMC value and this provides evidence of reverse micelles present in the system (Reynolds *et al.*, 2000; 2001; Shen & Duhamel, 2008). The results show that Pibsa-based surfactants aggregate at a low surfactant concentration. Moreover, the associative strength of surfactants depends on the chemical structure of the surfactant head group and their ability to create hydrogen bonds. Among the three Pibsa-based surfactants, Pibsa-IMIDE, which has no secondary amine and carboxylic group in the polar head core, exhibited the highest CMC value. This result suggests that the micellisation of a Pibsa-based surfactant is favoured by the presence of secondary amines and carboxylic groups in the polar core of the surfactant, as was observed earlier with other succinimide dispersants (Shen & Duhamel, 2008).

The areas per molecule of Pibsa-based surfactants were calculated from their molar concentration (Γ , mol/m²) at the interface, which were obtained from the Gibbs equation using the slope value of curve, and is shown in Figure 4.1. The values of the molecular areas are given in Table 4.1. Besides this, values of molecular surfactant areas were estimated using ACD/Labs free software, which allows drawing the chemical structures of molecules according to the lengths of bonds, and the sizes and angles of atoms in 2-D and 3-D views. The molecular models of surfactants are shown below, in Figure 4.3.

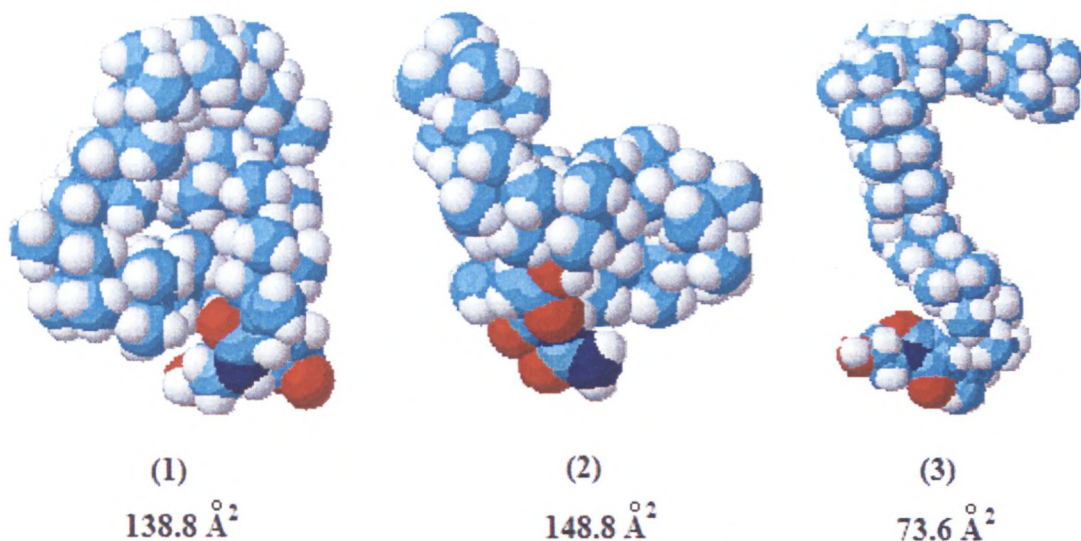


Figure 4.3: Possible models of Pibsa-based surfactant conformations at the interface:

(1) Pibsa-MEA, (2) Pibsa-UREA, (3) Pibsa-IMIDE

The calculated results correspond with the values obtained practically. Moreover, the area per molecule of Pibsa-MEA surfactant is available in the literature and supports the found value. A comparison of values from the literature, values obtained experimentally and values from software is presented in Table 4.2.

Table 4.2: Area of Pibsa-MEA molecule occupied at the interface

	<i>Experimental value</i>	<i>ACD/Labs software value</i>	<i>Literature value</i>
<i>Area per molecule, Å^2</i>	150.0	138.8	140.0* ~150**

* - result reported by Reynolds *et al.*, 2001

** - result reported by Ghaicha, *et al.*, 1993

From Table 4.2 it is clearly seen that all the values are very close. This indicates that the drawn structures could be considered as possible conformations of studied surfactants at the interface. Moreover, the similarity of the experimental and calculated (by using software) values suggests that surfactant molecules pack close to each other at the interface.

Since the chemical nature of the surfactant head group affects the interfacial properties (which is obvious from the above experimental results and existing literature), it was regarded as reasonable to investigate the interaction of the surfactant with the matter of the droplet. This was expected to allow deeper understanding of why different chemical structures can influence the surfactant packing and orientation at the interface. This investigation is reported in following section.

4.1.1.2 FT-IR study

All the samples were studied using the FT-IR Spectrometer 100 instrument supplied by Perkin Elmer. The resolution was 4 cm^{-1} . The spectra of the samples were recorded at room temperature using the Attenuated Total Reflectance accessory. This accessory does not require any sample preparation. The background scan performed before each test, was the baseline correction. An emulsion is a complex system containing several components such as oil, AN solution and surfactant. Spectra of each component were conducted by placing a sample of pure components on the Germanium disk. A spectral range of $500\text{-}4000\text{ cm}^{-1}$ was chosen. Spectra of each component of the sample are shown in Appendix A. The general spectrum of the emulsion is shown in Figure 4.4.

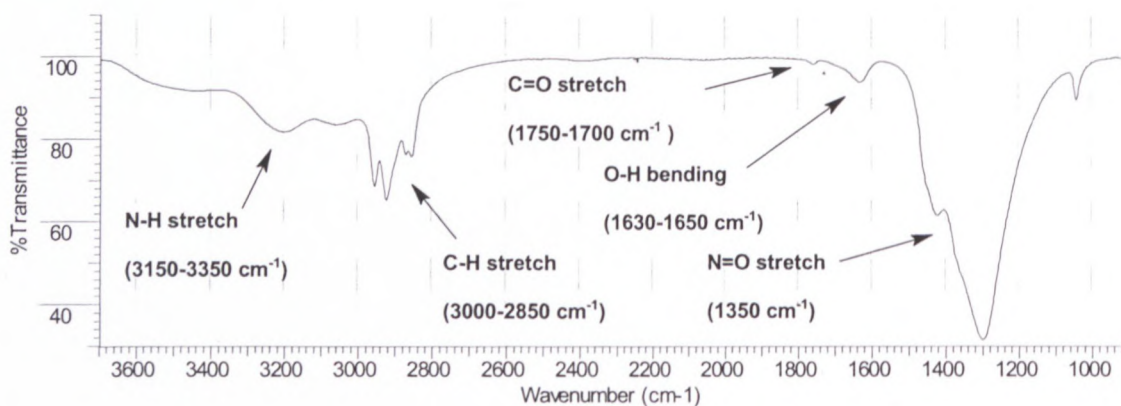


Figure 4.4: General spectrum of emulsion explosive, containing AN solution as an aqueous phase

As can be seen from Figure 4.4, an emulsion, as expected, contains compounds: all of the oil components, the surfactant, and AN components. The spectrum contained the expected strong C-H stretching band at $3000\text{-}2850\text{ cm}^{-1}$, which was assigned to the presence of isoparaffins and paraffin molecules (Pavia *et al.*, 2001); N-H stretching at $3150\text{-}3350\text{ cm}^{-1}$ (Ganguly *et al.*, 1992; Pavia *et al.*, 2001) and N = O stretching at 1350 cm^{-1} , which implied the presence of AN molecules; C = O stretching at $1750\text{-}1700\text{ cm}^{-1}$ (Ganguly *et al.*, 1992;

Pavia *et al.*, 2001) corresponded with the amide or carboxylic group of the surfactant; O-H bending at $1630\text{-}1650\text{ cm}^{-1}$ was a fundamental mode of water (Pavia *et al.*, 2001).

At the beginning of this study it was of interest to understand where the interactions took place. In order to understand whether the surfactant penetrated inside the ammonium nitrate droplets or not and whether AN was present in the oil phase, the following experiment was carried out. The FT-IR spectra of two phases (the water phase containing AN and the oil phase with dissolved surfactant in it) were obtained and after that mixed and left for two hours for phase separation to occur. After that, each of the phases was tested and spectra of the phases were compared with the results obtained before mixing. No changes were found between spectra before and after mixing. The results are presented in Figures 4.5 and 4.6.

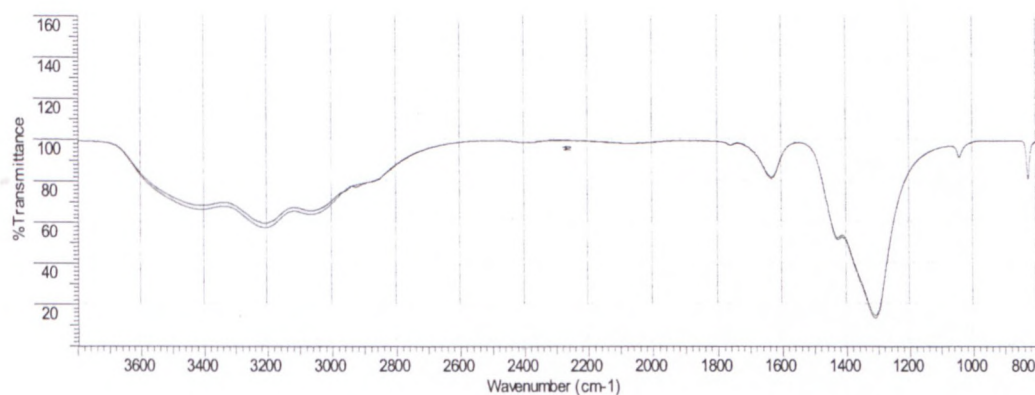


Figure 4.5: FT-IR spectra of AN solution (40%) and aqueous phase after mixing

It can be seen that the spectra merge. This reports the absence of surfactant in the aqueous phase.

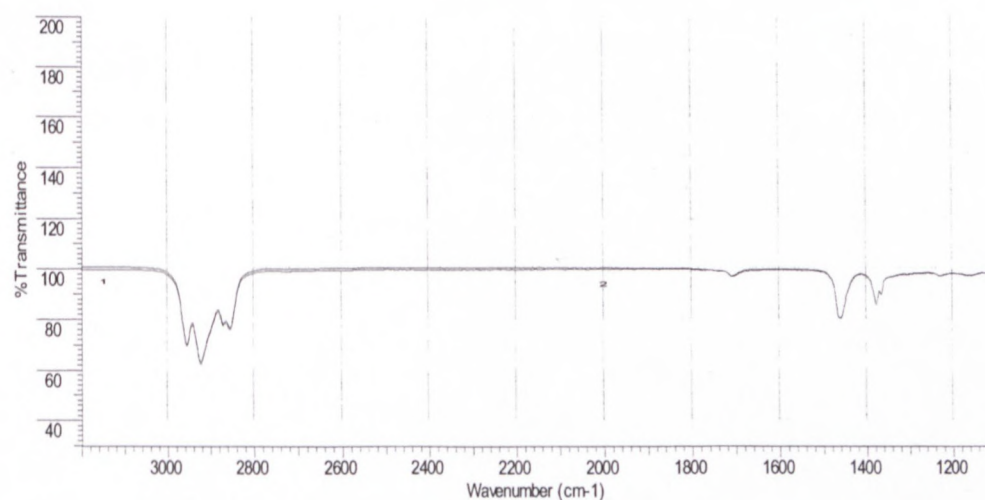


Figure 4.6: FT-IR spectra of oil phase with dissolved Pibsa-MEA surfactant in it before and after phase mixing

No changes are seen in the behaviour of spectra. It shows that ammonium nitrate was not present in the oil phase. This means that ammonium nitrate and surfactant meet at the interface and therefore surfactant- electrolyte interactions occur at the interface.

According to the literature that was studied, the following interactions can take place between the Pibsa-based surfactant head group and AN solution:

- Hydrogen bonding between NH_4^+ and head group (Ganguly *et al.*, 1992; Ghaicha *et al.*, 1993; Yubai *et al.*, 1996; Maheshwari & Dhathathreyan, 2004). The H-bond is a bond between an electron-deficient hydrogen and a region of high electron density such as $\text{C}=\text{O}$ and $\text{O}-\text{H}$ groups which are present in a surfactant. Formation of the $\text{N}-\text{H}\cdots\text{O}$ H-bond results in weakening of the $\text{N}-\text{H}$ covalent bond. This weakening is accompanied by bond elongation and a concomitant decrease of the $\text{N}-\text{H}$ stretch vibration frequency compared to the noninteracting species (Domenicano & Hargittai, 2002). The hydrogen bond formation is shown in Figure 4.7.
- The salt (complex) formation between the AN ions (NH_4^+ ; NO_3^-) and head group (Venter & Kruger, 1996; Boer, 2003) and electrostatic type of interactions was suggested by Ganguly *et al.* (1992). Any of these interactions can also result in weakening the $\text{N}-\text{H}$ covalent bond in NH_4^+ . This is illustrated in Figure 4.8. The weakening of the covalent bond can be detected by spectrometer and correlated with the strength of interactions.

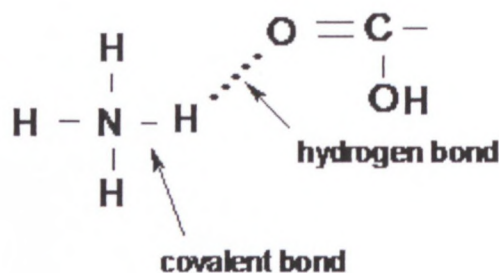
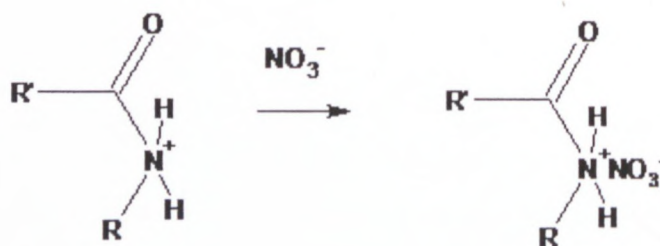
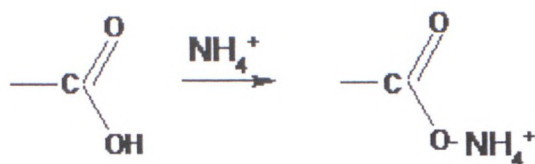


Figure 4.7: Possible variant of hydrogen bond formation between NH_4^+ and carboxylic group of surfactant



(a)



(b)

Figure 4.8: Possible variants of salt (complex) formation between AN ions and surfactant head group

- (a) complex formation between NO_3^- and amide group
 (b) salt formation between NH_4^+ and carboxylic group

In the present study, it was found that the NH covalent bond is sensitive to the surfactant type and surfactant concentration. The variation in the NH group was mostly attributed to the changes in ammonium ions, since the same group was not detected in surfactant molecules. The results are shown in Figure 4.9 and Figure 4.10.

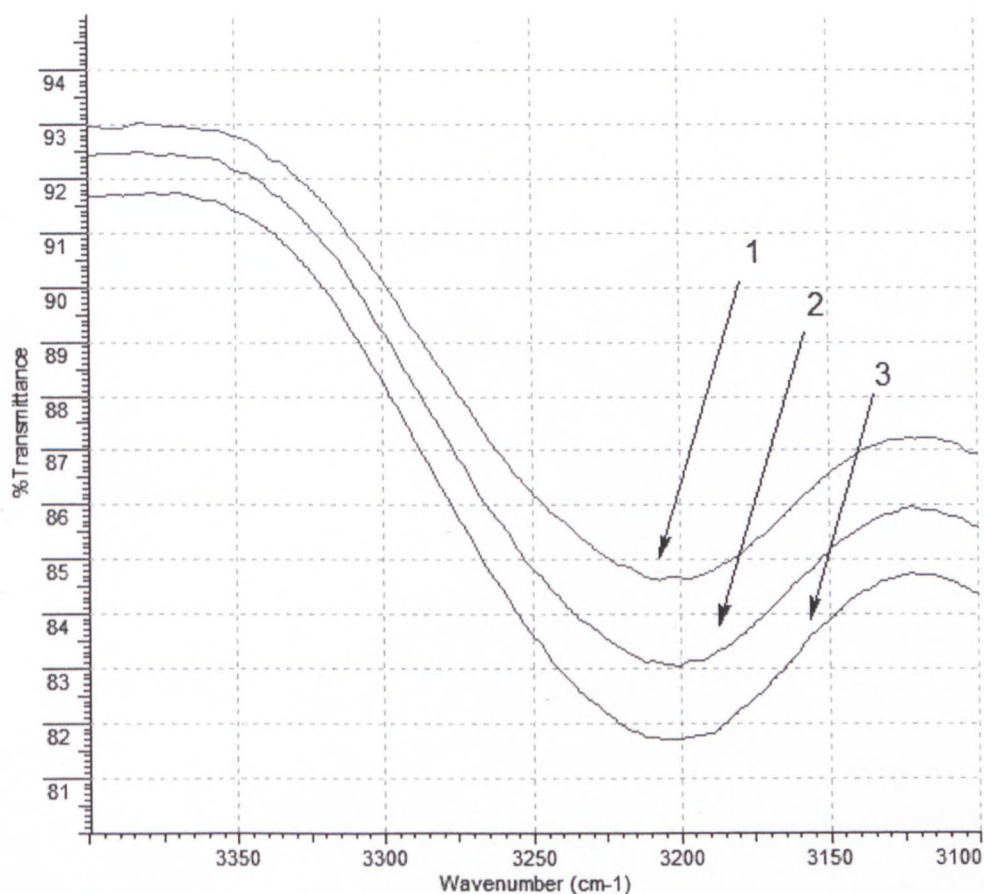


Figure 4.9: Part of emulsion spectra stabilised by different surfactants (Pibsa-MEA -3, Pibsa-UREA -2 and Pibsa-IMIDE -1)

The frequency variations are summarised in Table 4.3.

Table 4.3: Variation of IR frequencies with surfactant type

Type of surfactant	Frequency, $\nu(NH)$, cm^{-1}
Pure AN solution (60%)	3208*
Pibsa-MEA	3204
Pibsa-UREA	3204
Pibsa-IMIDE	3207

* - wave number accuracy is 0.1 cm^{-1} at used resolution 4 cm^{-1}

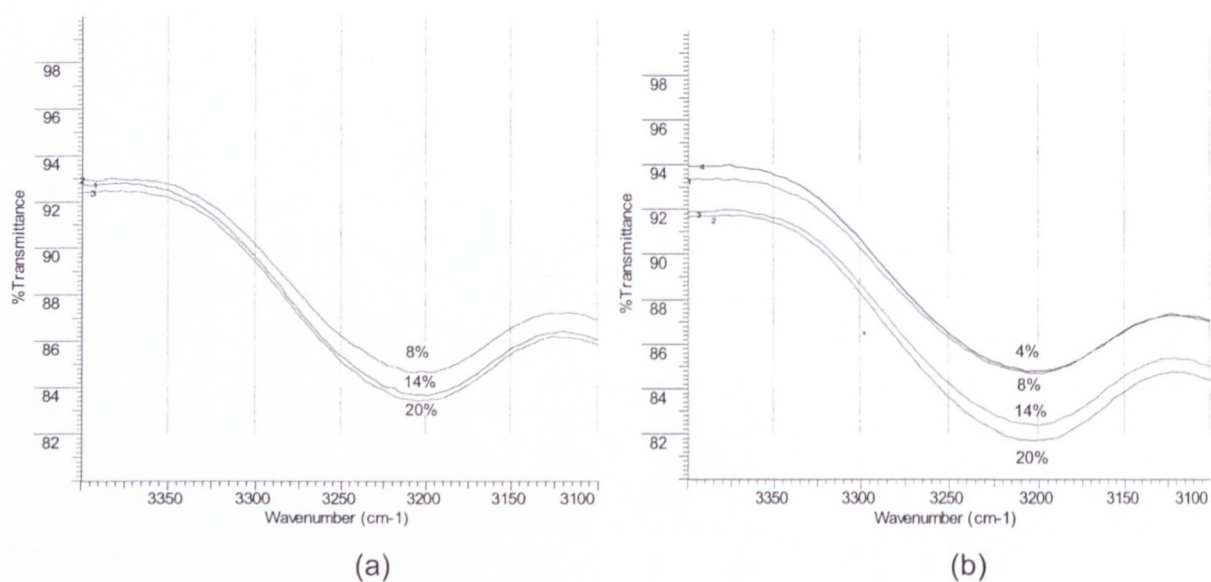


Figure 4.10: Part of FT-IR spectra of emulsions

(a) Pibsa-IMIDE surfactant concentrations (8%, 14%, 20%)

(b) Pibsa-MEA surfactant concentrations (4%, 8%, 14%, 20%)

The frequency variations are given in Table 4.4.

Table 4.4: Variation of IR frequencies with surfactant concentration for emulsions stabilised by Pibsa-MEA and Pibsa-IMIDE emulsifiers

C_{SUF} , %	Frequency $\nu(NH)$, cm^{-1}	
	Pibsa-MEA	Pibsa-IMIDE
4	3208*	-
8	3204	3207
14	3200	3205
20	3199	3199

* wave number accuracy is 0.1 cm^{-1} at a resolution of 4 cm^{-1}

It appears from Table 4.3 that the NH peak shifts to the lower frequency in the case of Pibsa-MEA and Pibsa-UREA surfactants and almost no changes can be found in the spectrum of the emulsion stabilised by Pibsa-IMIDE in comparison with the frequency of the peak in pure AN solution. This difference primarily can be attributed to the different strength of interaction between the surfactant head group and ammonium ions. The lower the frequency bond vibration the weaker the bond. This means that Pibsa-MEA and Pibsa-UREA provide a stronger interaction with AN ion (this results in greater weakening of the NH covalent bond) than Pibsa-IMIDE. The difference in chemical structure of surfactant head groups (Figure 4.11) can explain the above observation.

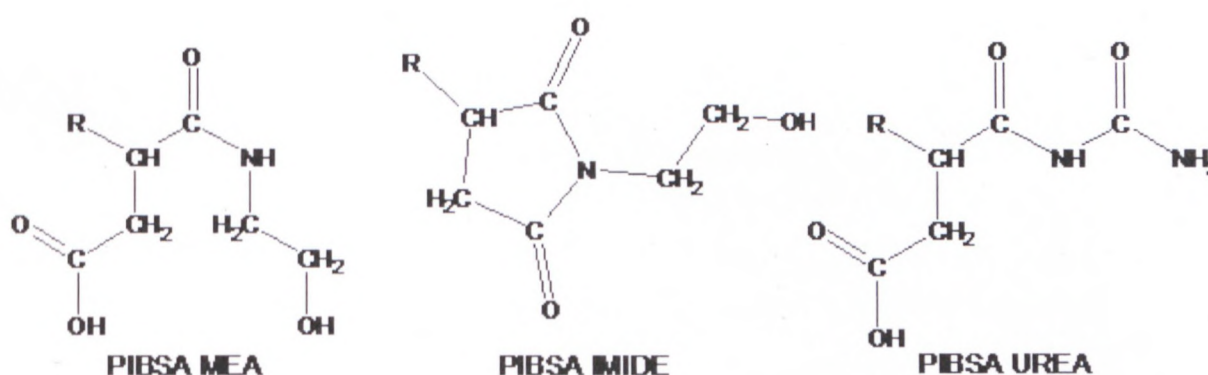


Figure 4.11: Chemical structures of Pibsa-based surfactant head groups (R – polyisobutylene)

It can be seen, from Figure 4.11, that head groups of studied emulsifiers are nitrogen- or oxygen-derived and are therefore polar. Both amide- and alcohol-derived functional groups contribute to the polarity of head groups. The polarity is a consequence of the

electronegativity difference between carbon, oxygen and nitrogen. The greater the electronegativity difference, the stronger the polarity (Rudnick, 2003). This implies that groups that contain carbon-oxygen bonds are more polar than those containing carbon-nitrogen bonds. Since head groups have many bonds with various combinations of atoms, the overall polarity in a molecule is not easy to predict. However, it is possible to assume that the head group of Pibsa-IMIDE surfactant is less polar, in comparison with Pibsa-MEA and Pibsa-UREA, due to the symmetry of polar bonds in the ring-closed Pibsa-IMIDE structure. However, it can be mentioned here that the Pibsa-IMIDE head group contains an –OH group (see Figure 4.11) which brings some polarity to the molecule. Pibsa-MEA and Pibsa-UREA molecules have asymmetric open structures of the head groups (Figure 4.11) that obviously result in greater polarity and thereby better solubility in the aqueous phase in comparison with the Pibsa-IMIDE head group (Reynolds *et al.*, 2002). All of this leads to the stronger adsorption of Pibsa-MEA and Pibsa-UREA at the interface (Papke & Robinson, 1994). Moreover, the chemical structure of Pibsa-IMIDE suggests only hydrogen bond formation with the AN and no electrostatic interaction because there is little possibility of the presence of head group charge exists. Indeed, the succinimide is actually neutral because the electron pair of nitrogen is delocalised over two carbonyl groups (Figure 4.12):

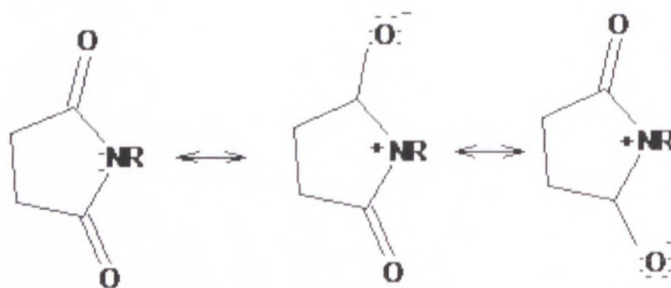


Figure 4.12: The delocalisation of the nitrogen electron pair in a succinimide molecule

Inversely, the Pibsa-MEA and Pibsa-UREA can probably participate in electrostatic interactions with the AN ions, as this type of interaction was suggested by Ganguly *et al.* (1992) and Ghaicha *et al.* (1993). The salt formation for Pibsa-MEA and Pibsa-UREA head groups is also possible due to the presence of COOH and NH functional groups in their chemical structure. These interactions (shown in Figure 4.8) possibly improve the ability of the head group anchoring at the interface and affecting the monolayer expansion.

The effect of surfactant concentration on the IR spectra is also observed (see Figure 4.10) in the case of both surfactants studied (Pibsa-MEA and Pibsa-IMIDE). It can be seen from Table 4.4 that $\nu(\text{NH})$ shifts to the lower value that reflects greater weakening of the NH bond in AN, and therefore stronger interactions between the surfactant head group and AN, with

more surfactant added to the oil phase of the emulsion. For Pibsa-MEA there is no significant change after 14% of surfactant, which probably shows a fully covered interface, while, in case of Pibsa-IMIDE, the frequency value of the NH bond is still decreasing with increasing surfactant concentration. These results correspond to the sequence of area per molecule for these surfactants: Pibsa-MEA > Pibsa-IMIDE. Therefore the full coverage of the interface for Pibsa-IMIDE can be expected at a higher surfactant concentration.

From the above discussion it appears that:

- Interaction (hydrogen bonding/salt (complex) formation) between the Pibsa-surfactant head group and the aqueous phase improves the ability of the surfactant to anchor at the interface (Chattopadhyay *et al.*, 1992; Ganguly *et al.*, 1992; Ghaicha *et al.*, 1993).
- Greater polarity induces the stronger interaction between the head group and the matter of droplets and results in more efficient weakening of the NH bond of ammonium nitrate ion.
- Pibsa-IMIDE interacts with the AN to a lesser extent in comparison with Pibsa-MEA or Pibsa-UREA. Besides this, it was found that IMIDE amphiphile, when spread on the water surface, loses more material than Pibsa-MEA on compression (Reynolds *et al.*, 2002). This fact can be used as a proof of a weak interaction of Pibsa-IMIDE with the matter of droplets.
- Presence of COOH and OH functional groups in the Pibsa-surfactant head group is necessary for intensive hydrogen bond formation and is strongly linked with the polarity of molecules.
- It seems that the presence of COOH and NH₂ groups is required for salt formation.
- An increase in surfactant concentration leads to a higher degree of interaction with the AN.

The addition of SMO to the Pibsa-MEA reduces the extent of AN-Pibsa-MEA surfactant interactions because SMO molecules are present at the interface and they are hardly replaced by polymeric surfactant. For the SMO surfactant, only one type of interaction, hydrogen bonding, with the matter of droplets is possible (Ganguly *et al.*, 1992; Opawale & Burgess, 1997). This means that the overall intensity of interactions with the AN for the mixture Pibsa-MEA/SMO is lower in comparison with pure Pibsa-MEA surfactant.

It is necessary to mention that the efficiency of SMO in forming hydrogen bonds is higher than that of Pibsa-IMIDE due to the abundant presence of –OH groups in the SMO head group structure (see Figure 3.8).

From the above, it seems reasonable to assume that the AN-surfactant interaction follows the trend Pibsa-MEA = Pibsa-UREA > Pibsa-MEA/SMO > SMO > Pibsa-IMIDE. The similarity of the trend found for AN-surfactant interaction among Pibsa-based surfactants under study (Pibsa-MEA = Pibsa-UREA > Pibsa-MEA/SMO > Pibsa-IMIDE) and the interfacial properties (Pibsa-MEA > Pibsa-UREA > Pibsa-MEA/SMO > Pibsa-IMIDE) is observed. This similarity of trend is an indication that any effect of Pibsa-based surfactants on interfacial tension values or on the interfacial dilatational elastic modulus primarily can be attributable to the intensity of surfactant interaction with the aqueous phase of emulsion. The interaction (hydrogen bonding, salt/complex formation) of the polar surfactant head group with the aqueous phase results in molecular reorganisation at the interface (Opawale & Burgess, 1997; Dickinson, 2002; McClements 2005; Claesson *et al.*, 2006). The interaction (hydrogen bonding) is highly directional and thus requires highly specific orientations to reach the optimal strength (Claesson *et al.*, 2006). It can therefore have an effect on the polymeric chain conformation at the interface (Tikhonov *et al.*, 2006) and enhance the lateral interactions between the chains, which could result in the increase of monolayer rigidity (Babak & Stebe, 2002) and lead to high interfacial elasticity (strength of the interface).

4.1.2 Effect of AN concentration and electrolyte composition on interfacial properties and interfacial interactions in highly concentrated emulsions.

In this section, the effect of salt content and salt composition on the interfacial properties and interactions will be discussed. The main aim of this part of the study was to understand the role of electrolytes in surfactant-electrolyte interactions and how it can influence rheological properties of emulsions and emulsion stability.

4.1.2.1 *Interfacial tension.*

4.1.2.1.1 Effect of AN concentration on interfacial tension

Interfacial tension was measured with varied salt concentrations in the aqueous phase in order to see the impact of interfacial tension on the elastic shear modulus and yield stress. The interfacial tension was determined using the Krüss K100 tensiometer, supplied by Krüss GmbH, Germany. The Wilhelmy plate method was used for the measurements. Equilibrium values for the interfacial tension were found by plotting the dynamic interfacial tension against the reciprocal of square root time and extrapolating the linear part of the curve to infinity time

value. The dynamic interfacial tension curves and extrapolation curves for the equilibrium values of interfacial tension are presented in Appendix B.

The variation of interfacial tension for the oil-PIBSA surfactant-water-salt system is shown in Figure 4.13. Accuracy of measurements is given in section 3.5.4.

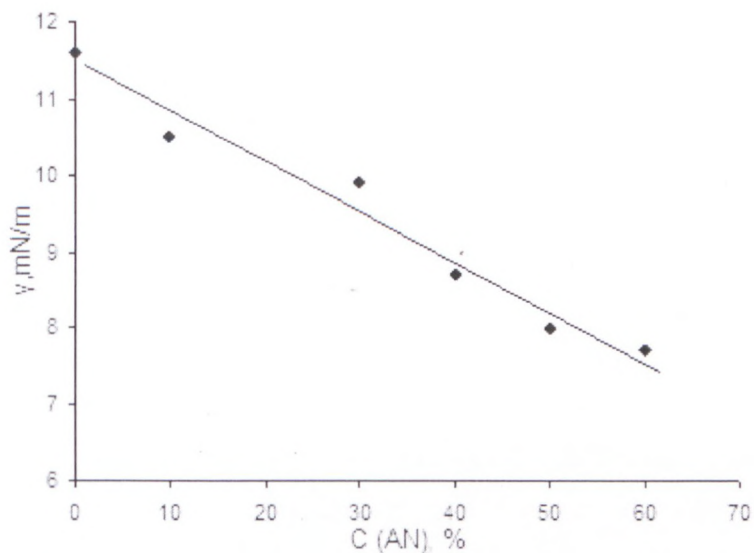


Figure 4.13: Interfacial tension as a function of ammonium nitrate concentration

Figure 4.13 indicates that interfacial tension is sensitive to the salt concentration. A linear decrease in interfacial tension with increasing salt concentration was observed. The values are listed in Table 4.5.

Table 4.5: Interfacial tension at different ammonium nitrate concentrations in the aqueous phase (8% of surfactant in oil phase)

$C(AN)$, %	γ , mN/m
0	11.6
10	10.5
30	9.9
40	8.7
50	8
60	7.7

From Table 4.5 it is clear that interfacial tension decreased with increasing AN concentration. This behavior primarily can be attributed to the progressive adsorption of surfactant at the interface (electrolytes attract more surfactant) (Aronson & Petko, 1993; Kent & Saunders,

2001). Secondly, the surface tension of the AN solution can have an impact on the interfacial tension which is described by the following equation – Antonoff’s rule (Xuguang, 1994):

$$\gamma_{12} = \gamma_1 - \gamma_2, \quad \text{Equation 4.4}$$

where γ_{12} – interfacial tension between two immiscible liquids, γ_1 , γ_2 – surface tension of liquids saturated by another one (Xuguang, 1994). In the present case, the γ_1 – surface tension of AN solution (variable parameter due to different concentrations of salt in the aqueous phase) and γ_2 – surface tension of oil phase with surfactant dissolved in it (constant parameter was a surfactant concentration and was kept the same). From this relationship one can see that, if the surface tension of the AN solution (γ_1) is changed, the interfacial tension (γ_{12}) will be changed automatically. The surface tension of AN solutions and excess of surfactant concentration at the interface at 10% and 60% AN were measured to determine the factors that affected the interfacial tension. For these experiments the Krüss K100 tensiometer was used. All the data was obtained using the Wilhelmy plate method. Each surface tension experiment was run for 200 s. Results are given in Table 4.7. For the determination of the Pibsa-MEA surfactant excess concentration (slope $dy/d\ln c$), the dynamic interfacial tension was obtained by standard procedure. Equilibrium values for the interfacial tension were found by plotting the dynamic interfacial tension against the reciprocal of square root time and extrapolating the linear part of the curve to infinity time value (these curves are presented in Appendix B). The results are summarised in Table 4.6 and shown in Figure 4.14.

Table 4.6: Interfacial tension as a function of surfactant concentration for 10% and 60% AN in the aqueous phase

$C_{SURF}, \%mass$	$C_{SURF}, mol/l$	$\gamma, mN/m, 10\% AN$	$\gamma, mN/m, 60\% AN$
5.00E-03	3.31E-03	10.6	7.7
2.00E-03	1.32E-03	10.2	7.7
2.50E-04	1.65E-04	10.5	8.1
1.40E-04	9.26E-05	10.7	8.5
5.00E-05	3.31E-05	11.8	10.4
2.50E-05	1.65E-05	14.6	12.4
1.45E-05	9.59E-06	17.9	15.6

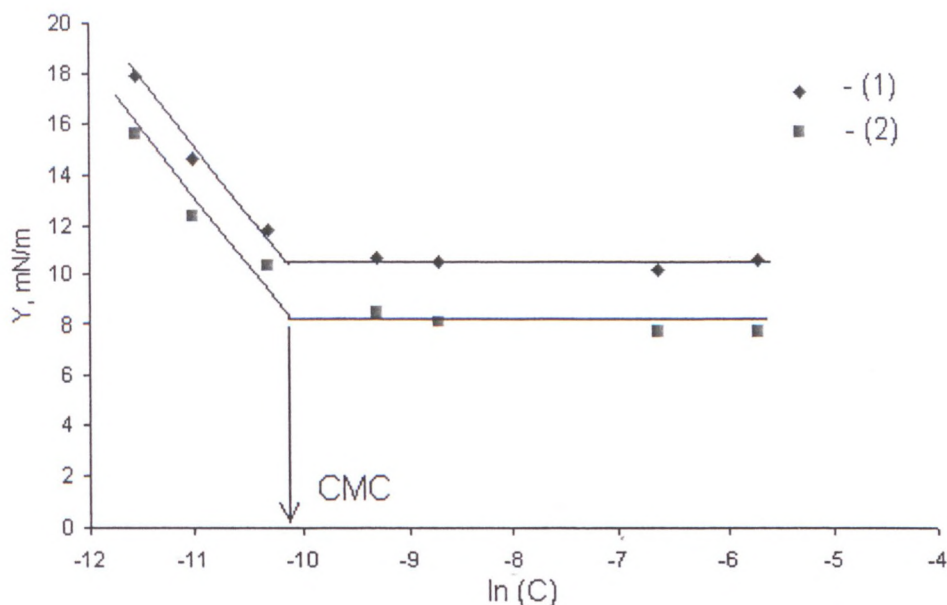


Figure 4.14: Determination of slope ($dy/d\ln c$) and CMC values for systems with 10% - (1) - and 60% - (2) - AN in the aqueous phase and Pibsa-MEA surfactant in the oil phase

The best linear fit to the decreasing part of the curve gives a slope of $-4.8 \times 10^{-3} \text{ N m}^{-1}$.

Molar concentration at the interface \square , $\Gamma = - (d \gamma / d \ln c) / RT = 4.8 \times 10^{-3} / (8.314 \times 300) = 1.9 \times 10^{-6} \text{ mol m}^{-2}$; CMC (molar) = $\exp(-10.1) = 4.1 \times 10^{-5} \text{ mol/l}$.

Table 4.7: Surface tension of aqueous solution with different ammonium nitrate concentrations in the aqueous phase

[AN], %	σ , mN/m
0	71
10	68
30	58
40	56
50	53
60	50

The following can be noted from the above experimental results:

- The AN concentration did not affect the Pibsa-MEA surfactant concentration at the interface. The Pibsa-MEA surfactant concentration at the water-oil interface at 10% and at 60% of salt in water was the same. This was provided by the same values of slopes for the systems with 10% and 60% of AN in the aqueous phase. The CMC values for 10% and 60% also coincided. This behaviour provides evidence of the strong ability of a surfactant head

group to interact with the matter of droplets at a relatively low concentration of salt (Ganguly *et al.*, 1992; Ghaicha *et al.*, 1993; Maheshwari & Dhathathreyan, 2004) that provides strong adsorption and better anchoring of the molecules at the interface. These results also demonstrate the fact that surfactant molecules are relatively widely spaced because of the mutual repulsion of oriented head groups induced by the presence of salt ions (Ghaicha *et al.*, 1993; Rosen, 2004).

○ The surface tension of the aqueous solution decreases with a raising AN concentration. This implies an impact on interfacial tension from the changes in the surface tension as a function of AN concentration. The change in surface tension with the change in concentration is primarily dependent on the electrolyte type and ion distribution in the solution (Petersen & Saykally, 2006; Matubayasi *et al.*, 2009). The last investigations in this regard suggest that preferential accumulation of anions is at the surface and cations are attracted by this layer of anions (Petersen & Saykally, 2006; Matubayasi *et al.*, 2009).

The changes in interfacial tension as a function of AN concentration are mainly due to the changing surface properties in the aqueous phase.

Visual observation has revealed that the presence of ammonium nitrate in the water phase led to the formation of a stable interface between water and oil in comparison with droplets containing pure water. The images are presented in Figures 4.15 to 4.16.

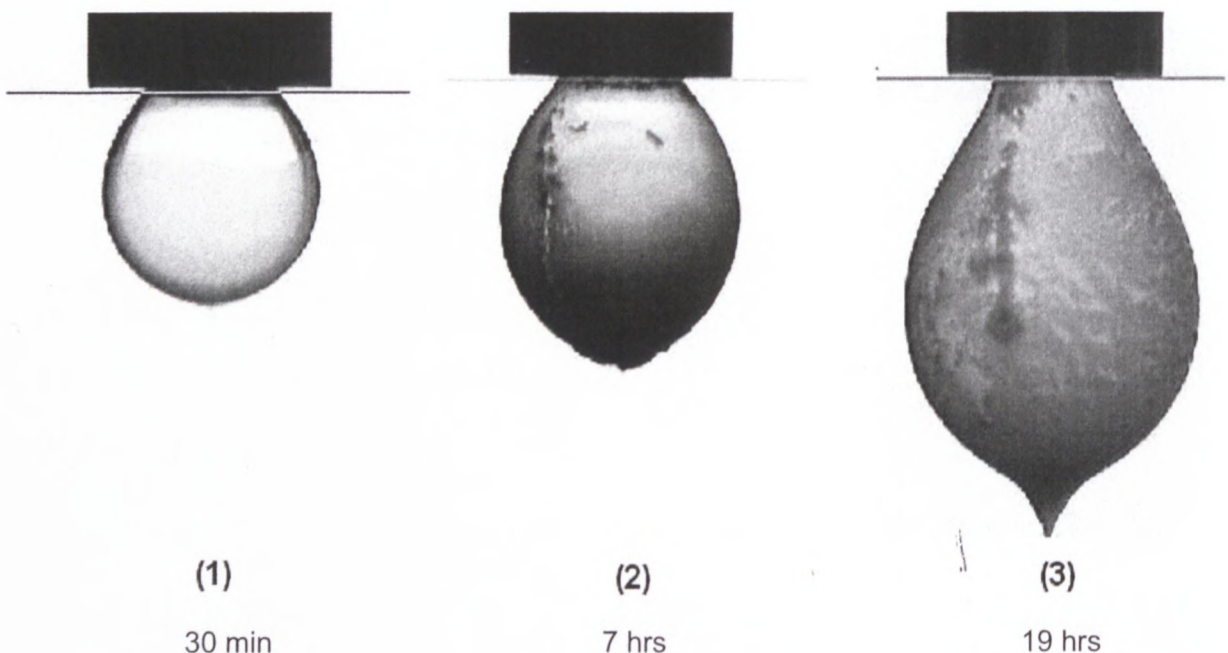


Figure 4.15: Interfacial film growth without the presence of AN salt in aqueous phase, Pibsa-MEA

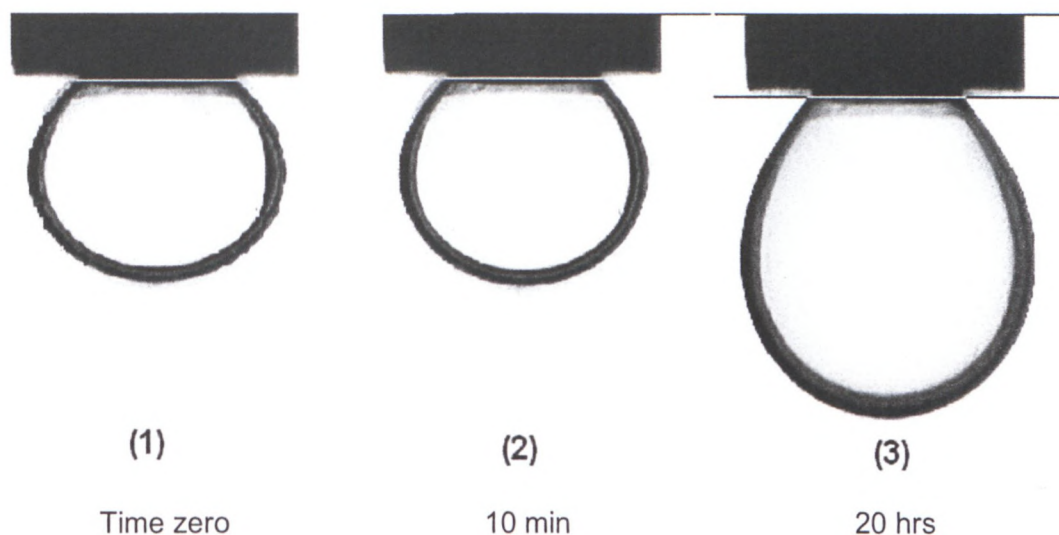


Figure 4.16: Water-oil interface in presence of AN salt (5%) in the water phase, Pibsa-MEA.

As the images show, the film is visible towards the bottom of the droplet after 30 min (Figure 4.15) and continues to develop for at least 19 hours. The origin of this film probably is the surfactant coming out of the solution or spontaneous emulsification (Aronson & Petko, 1993). The similar film appears when the interface is formed away from the tensiometer in a small vial. The forming of a bright and shiny interface was also observed by Aronson and Petko (1993) when an electrolyte was incorporated in the aqueous phase. This observation makes it possible to assume that AN salt stabilises the W/O interface due to interactions with the surfactant (Ganguly *et al.*, 1992; Chattopadhyay *et al.*, 1992; Ghaicha *et al.*, 1993; Maheshwari & Dhathathreyan, 2004). This will be discussed in following part of the present study.

4.1.2.1.2 Effect of electrolyte type on interfacial tension

Interfacial tension of the oil-Pibsa-MEA surfactant/salt solution was obtained by using the Kruss technique and the Wilhelmy plate method. The salt solution was freshly prepared with an adjustment of pH = 4. The molar concentration of the salt solutions was kept at a constant ($C_M = 4.14 \text{ mol/l}$). The concentration of Pibsa-MEA in the oil phase was 8% wt. The interfacial tension of the systems with different cations in the aqueous phase is summarised in Table 4.8.

Table 4.8: Interfacial tension of the oil-Pibsa-MEA/salt solution system as a function of different electrolytes

Salt type	γ, mN/m
Water	11.6
NH_4NO_3	9.9
$NaNO_3$	7.1
$Ca(NO_3)_2$	5.5

As can be seen from Table 4.8, different salts induced different interfacial tensions and interfacial tension decreased in the following order: $H_2O > NH_4NO_3 > NaNO_3 > Ca(NO_3)_2$. These results were probably achieved by an increased adsorption density of emulsifier at the W/O interface (Aronson & Petko, 1993). Based on references in the literature (Para, Jarek & Warszynski, 2006; Zhang & Cremer, 2006; Senapati, 2007; Singh *et al.*, 2007), we can suppose that cations probably affect the surface activity of the surfactant due to interactions with the head group. It has to be mentioned here that the cation charge, size and polarisability increase in the order $NH_4^+ < Na^+ < Ca^{2+}$. In other words, the presence of smaller, less hydrated cations (and therefore less restricted from closer penetration to the surfactant head group) could generate stronger interactions with the emulsifier and result in more efficient lowering of interfacial tension.

- The following proposed interactions between Pibsa-MEA and NH_4^+ , Na^+ , Ca^{2+} ions can take place (Figures 4.17 and 4.18):

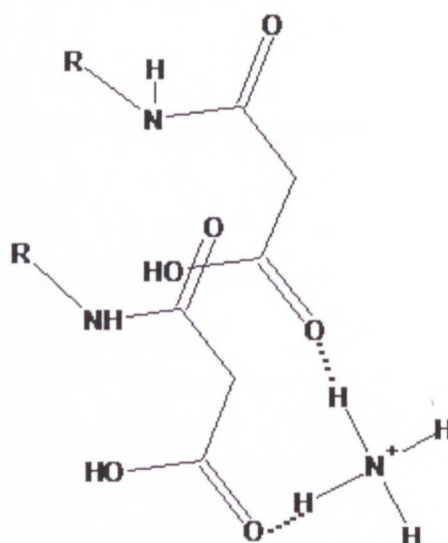


Figure 4.17: Possible hydrogen bonding interaction between Pibsa-MEA head group and NH_4^+ ion

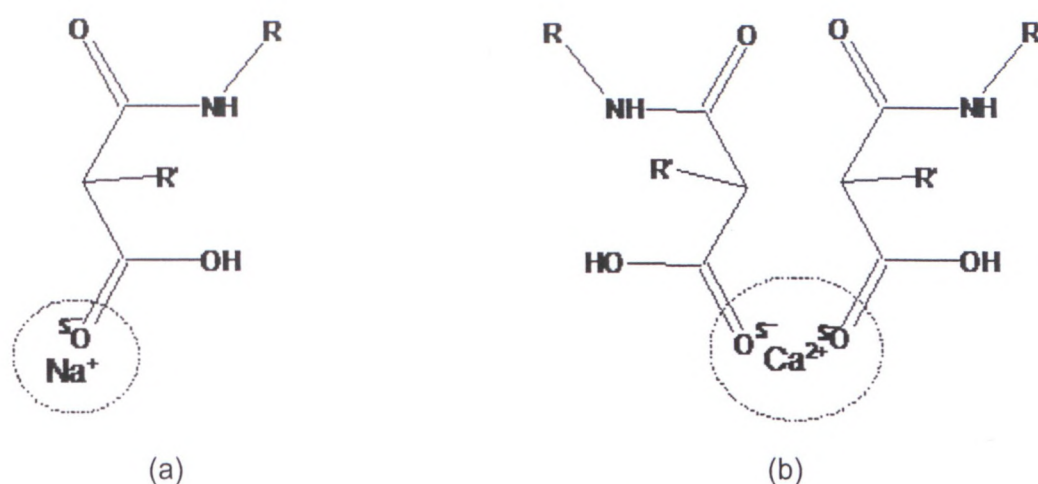


Figure 4.18: Possible ion attraction to the head group of Pibsa-MEA

(a) sodium ion attraction to the head group

(b) calcium ion attraction to the head group

The above possible surfactant-electrolyte interactions were drawn on the basis of the literature study which suggested the hydrogen bonding formation between surfactant head group and NH_4^+ ions (Ganguly *et al.*, 1992; Ghaicha *et al.*, 1993; Maheshwari & Dhathathreyan, 2004). The ion's attraction to the carbonyl group was suggested by Moses *et al.*, (2003), Senapati (2007), Singh *et al.* (2007).

Ca^{2+} ions with a high charge density (charge density order $\text{Ca}^{++} > \text{Na}^+ > \text{NH}_4^+$) can strongly interact with the polar head group, and this may bring them closest to the head groups (Moses *et al.*, 2003; Senapati, 2007; Singh *et al.*, 2007). The closely residing Ca^{++} ions at the surface could then modify the aqueous surrounding of the surfactant molecule (Guerrero *et al.*, 2004; Clare, Lillard, Ramsey, Amato & Daubert, 2007) and accomplish a shorter water-head group H-bond lifetime (Senapati, 2007).

4.1.2.2 FT-IR study.

The FT-IR analysis was carried out with the Perkin Elmer Spectrum 100 FT-IR Spectrometer using methodology which was described earlier (see 3.5.5). The effect of the AN concentration on the IR spectra of aqueous solutions and emulsions was investigated.

4.1.2.2.1 Effect of AN concentration on the IR spectra of aqueous phase

The spectra for the aqueous solutions of AN were obtained. They are shown in Figure 4.19.

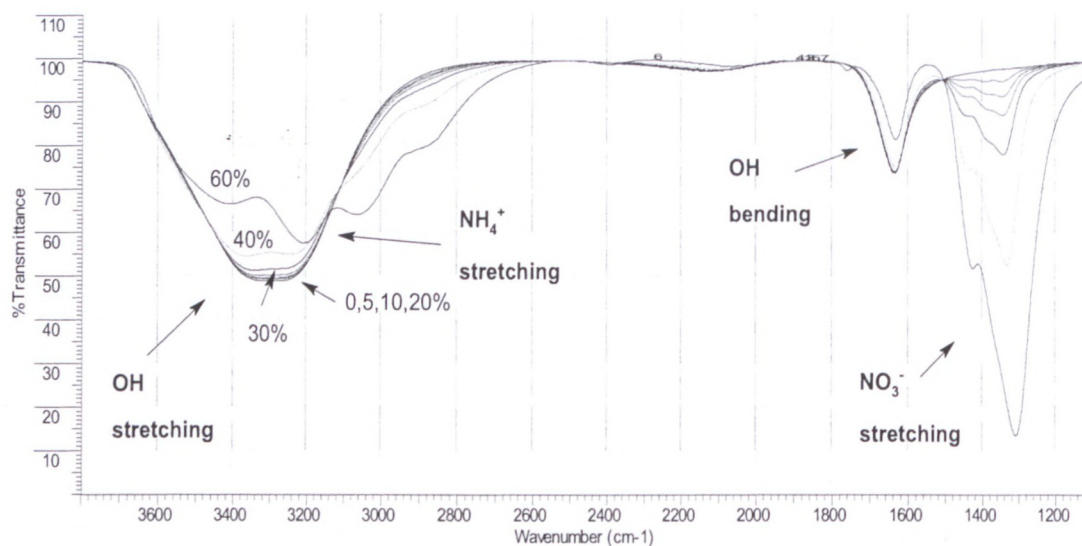


Figure 4.19: FT-IR spectra of aqueous solutions with different AN concentrations

The peak assignments to the functional groups of compounds (H_2O , NH_4NO_3) which were present in the AN solution are given in Table 4.9.

Table 4.9: IR spectral assignments for the H_2O and NH_4NO_3 (Pavia *et al.*, 2001)

Frequency (cm^{-1})	Functional group	Type of vibration
3335-3030	NH_4^+ , (ammonium)	stretching
1520-1280	NO_3^- , (nitrate)	stretching
1600-1650	O-H	bending
3500-3200	O-H	stretching

The variations of AN solution spectra as a function of AN concentration are given in Table 4.10.

Table 4.10: The variation of IR frequencies with ammonium nitrate concentration

Salt concentration, %	$\nu(N-H), \text{cm}^{-1}$	$\nu(N-O), \text{cm}^{-1}$
0	-	-
5	-	1348
10	-	1347
20	-	1347
30	3273	1344
40	3241	1335
60	3207	1311

From the above results, the following can be seen:

- The Intensity of nitrate ion peak increase with increasing AN concentration that reports an increasing concentration of electrolytes in water. The peak in range 3400 cm^{-1} to 3200 cm^{-1} which was assigned to the OH^- group in water shows the intensity decrease as the water content in the solution is decreasing.
- The peak in range 3300 cm^{-1} to 3200 cm^{-1} which was assigned to the NH covalent bond in ammonium ion begins to appear at a salt concentration equal to 30% and shifts to the lower frequency value as well as NO stretching vibration (the values are given in Table 4.10). The shift becomes more significant at 30% AN concentration, followed by 40% and 60%. This effect can probably arise from more intensive interactions between NH_4^+ and NO_3^- ions on increasing their concentration in water. The strong evidence for direct cation-anion contact at high AN concentrations in the aqueous phase was reported in the literature:
 - There is a decrease in the coordination number forming a weakly defined hydration shell around the ammonium ion (Walker *et al.*, 1989; Adya & Neilson, 1991). It has been established that the hydration number of the ammonium ion, NH_4^+ , in a solution with a molality of 5 mol kg^{-3} , is about 11, i.e. there are about 11 water molecules associated with each ammonium ion (Walker *et al.*, 1989; Neilson & Tromp, 1991). At a molality of 50 mol kg^{-3} (80% AN in water by weight), the hydration number is 5, suggesting that water molecules favour the neighbourhood of the ammonium ion (Adya & Nielson, 1991; Neilson & Tromp, 1991).

- The hydration shell moves closer to the ammonium ion at a higher AN concentration (Adya & Neilson, 1991).

The literature that was studied and the present investigation suggest that with an increasing AN concentration in the aqueous phase, the amount of water may be insufficient to form a complete hydration shell around the ions and that ion-ion interactions dominate under the ion-solvent interactions, which result in structural changes in the AN solution.

The results obtained in this experiment correspond well with the emulsion's emulsification data (see section 5.1.2.1.ii), where it has been shown that the emulsification process is more difficult at a higher AN concentration in the aqueous phase and increasing AN content leads to a larger critical droplet size of emulsion. This effect is also more pronounced at 30% of AN, followed by 40%, 50% and 60%.

4.1.2.2.2 Effect of AN on the IR spectra of emulsions

Before emulsion spectra were obtained, all the pure materials such as the AN solutions, water, the solution of Pibsa-MEA surfactant in oil and pure oil were tested. Emulsion spectra were compared with pure materials for peak identification and determination of peak modification. All the spectra are presented in Appendix 3A. The general spectrum of the emulsions was described earlier (4.1.1.2).

As was shown before in the present study (see Figure 4.16), incorporation of AN to the aqueous phase stabilises the W/O interface. For better understanding of this stabilisation mechanism, the spectra of Pibsa-MEA surfactant dissolved in oil, water emulsion and 5% AN emulsion stabilised by the same surfactant were obtained and compared. The results are shown in Figure 4.20.

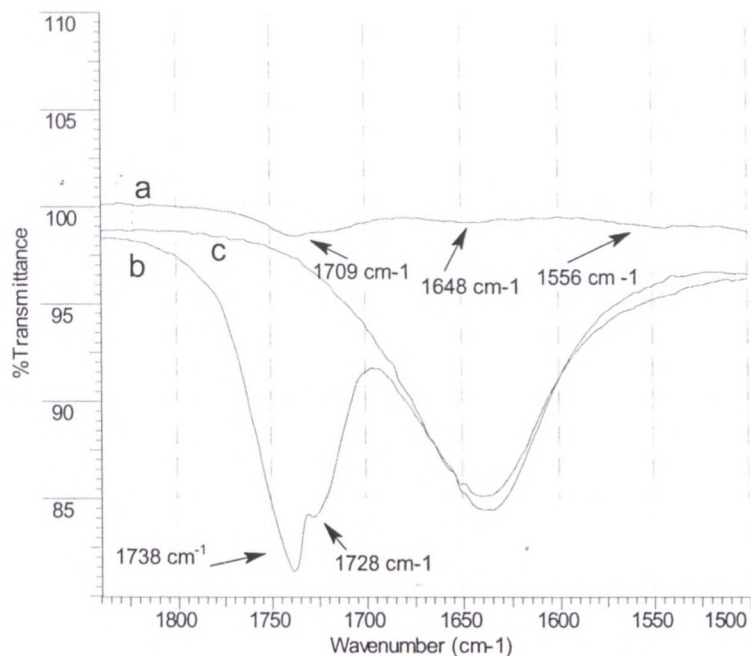


Figure 4.20: Comparison of Pibsa-MEA, water emulsion and AN emulsion spectra.

(a) Pibsa-MEA (dissolved in Mosspar-H oil) spectrum

(b) water emulsion spectrum

(c) AN (5 wt%) emulsion spectrum

As can be seen from Figure 4.20, the three peaks at approximately 1709 cm^{-1} , 1648 cm^{-1} and 1556 cm^{-1} are present in the spectrum of the Pibsa-MEA surfactant:

- The 1709 cm^{-1} is assigned to the C=O bond, which is a characteristic feature of normal esters and usually appears in the range $1750\text{ to }1735\text{ cm}^{-1}$ (Pavia *et al.*, 2001). Given that there is a peak in the spectra within this range, the peak at 1740 cm^{-1} can be attributed to the ester derivative emulsifier. However, there is a possibility that the peak is assigned with the carboxylic acid group in the amide derivative emulsifier where C=O bond stretching of the acid group is expected to produce a peak at $1730\text{--}1700\text{ cm}^{-1}$ (Pavia *et al.*, 2001).
- Primary and secondary amides have broad C=O adsorption in the range from 1680 cm^{-1} to 1630 cm^{-1} . The C=O band partially overlaps the N-H bending band which appears in the range $1640\text{--}1620\text{ cm}^{-1}$, making the C=O appear as a doublet (Pavia *et al.*, 2001). Thus it is reasonable to assume that the peak that appears at 1648 cm^{-1} in the spectra is attributed to the amide derivative emulsifier.
- The peak at 1556 cm^{-1} can be associated with the acid/salt (amino acid existing as zwitterion internal salt) group in the ester derivative emulsifier. Acid/salt groups exhibit spectra combinations of carboxylate and primary amine where N-H of amine salt bending adsorption occurs at a range from 1610 cm^{-1} and 1550 cm^{-1} , whilst the

carboxylate salt C=O asymmetric stretching mode occurs near 1600 cm^{-1} (Pavia *et al.*, 2001).

These peaks are characterisation peaks of the surfactant head group and two of them (1648 cm^{-1} and 1556 cm^{-1}) cannot be seen in the emulsion spectrum due to overlapping with the fundamental mode of water.

Two peaks at 1738 cm^{-1} and 1728 cm^{-1} can be detected in the water emulsion (without the presence of AN in the aqueous phase). They are assigned to the C=O bond of the normal ester group and the C=O bond in the carboxylic group of the emulsifier respectively (Ghaicha *et al.*, 1993; Pavia *et al.*, 2001). These two peaks fully disappear in the presence of AN. From this, the formation of COO^- species (Ganguly *et al.*, 1992) or a shift of the peaks to the lower frequency due to hydrogen bond formation with the NH_4^+ and NO_3^- ions (Ganguly *et al.*, 1992; Ghaicha *et al.*, 1993) can be suggested.

Moreover, the NH bond in AN was found to be sensitive to the AN concentration. The results obtained are shown in Figure 4.21.

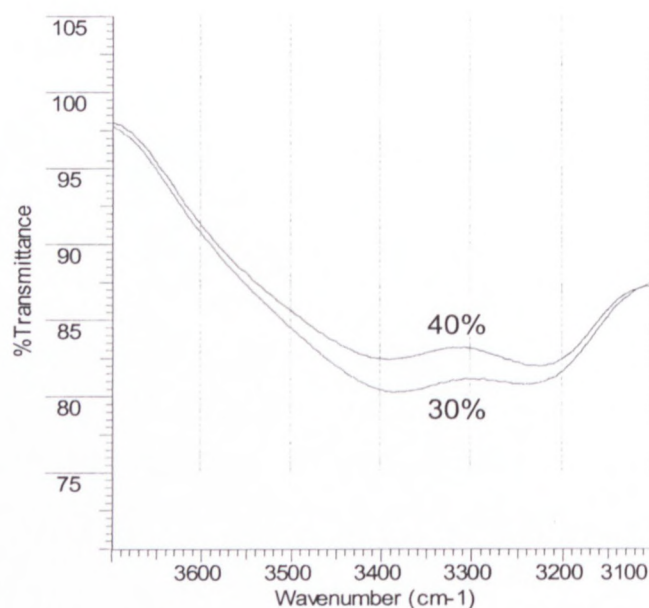


Figure 4.21: Part of FT-IR spectra of emulsions with 30% and 40% AN

The values are given in Table 4.11.

The NH stretch values in AN solution peaks were subtracted from NH stretch values in emulsion in order to determine the effect of the AN concentration on the surfactant-electrolyte interactions.

Table 4.11: The variation of IR frequencies with AN concentrations

$C_{AN}, \%$	$\nu(NH)$ in emulsion, cm^{-1}	$\nu(NH)$ in solution, cm^{-1}	$\nu(NH)$ shift difference, cm^{-1}
30	3264	3273	9
40	3226	3241	15

From the above experimental data it is clear that increasing the AN concentration results in the NH peak shifting to the lower frequency value in the emulsion state, as well as in the solution state, but a much stronger effect is observed in the case of the emulsion. The effect in the solution state is related to the increased ion-ion interactions (as discussed above). But in the emulsion state the bigger shift can be attributed to the stronger surfactant-electrolyte interactions with increasing AN content. This implies increasing hydrogen-bonding or salt formation between Pibsa-MEA head group and NH_4^+ ions. The following types of interactions can be suggested:

- Hydrogen bond formation between the Pibsa-MEA head group and NH_4^+ ion. Based on the suggestion that NH_4^+ and NO_3^- can participate as a bridging component between surfactant head groups (Ghaicha *et al.*, 1993) the following picture can be drawn:

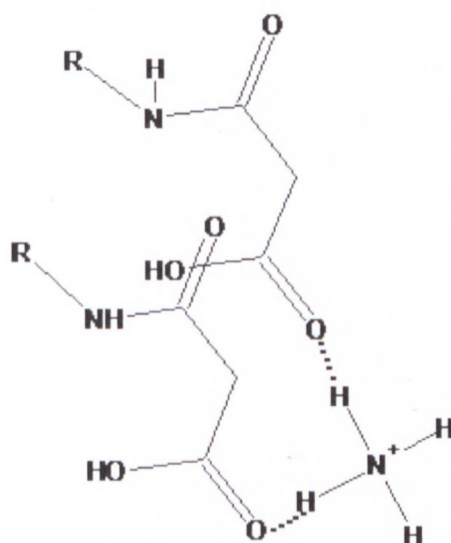


Figure 4.22: Possible hydrogen bond formation between two molecules of Pibsa-MEA head group and NH_4^+ ion (R: CH_2-CH_2-OH , R_1 : polyisobutylene)

- The salt formation between the surfactant head group and the NH_4^+ ion ($-COOH$ is a part of Pibsa-MEA head group):

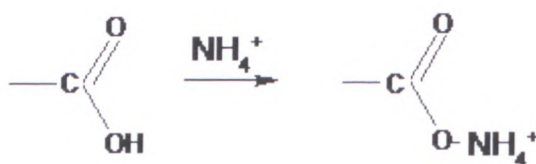


Figure 4.23: Possible manner of salt formation between the Pibsa-MEA head group and the NH_4^+ ion

It is obvious that incorporation of AN into the aqueous phase of the emulsion affects the chemical structure of the Pibsa-MEA polar head group due to hydrogen bonds and possible salt formation with the ammonium nitrate ions. Moreover, the changes in molecular conformation owing to the structural modification of the head groups and their environment, and increased association of the salt ions or ion pairs with the head groups, can affect the packing of acyl chains at the interface due to electrostatic interactions between the head groups (Chattopadhyay *et al.*, 1992; Ghaicha *et al.*, 1993; Claesson *et al.*, 2006) and due to the hydrogen bonding network (Tikhonov *et al.*, 2006; Claesson *et al.*, 2006). Furthermore, the increasing of ion association around the head groups lead to their dehydration and increased lateral interactions between the surfactant chains (Solans *et al.*, 1993). This means that orientation of adsorbed surfactant molecules at the interface depends on the strength of surfactant-electrolyte interactions and therefore on a concentration of electrolytes in the aqueous phase. It is reasonable to assume that an increase in AN concentration leads to the more stable and structured interface due to the hydrogen bonding network and electrostatic interactions between the head groups.

4.1.3 Effect of surfactant and electrolyte type/concentration and pH on emulsion stability

4.1.3.1 Effect of surfactant type and concentration

In previous studies (Ganguly *et al.*, 1992, Clausen, 1998; Coupland, 2002; Clause *et al.*, 2005) it has been shown that differential scanning calorimetry appeared to be a very suitable technique for studying the behaviour of emulsions submitted to a temperature gradient and to correlate data to the stability of emulsions. Furthermore it has been shown that freezing temperatures are composition-dependent and several factors have to be borne in mind while interpreting data pertaining to low-temperature DSC studies on emulsions. The freezing temperatures of emulsions generally depend on droplet size, surfactant type and

concentration, and dissolved salts in the aqueous phase (Ganguly *et al.*, 1992, Clauses, 1998; Coupland, 2002; Clause *et al.*, 2005; McClements, 2005; Spicer & Hartel, 2005).

In this part of the study, the DSC was used to determine the freezing point as a function of surfactant type and concentration. The crystallization of emulsions was accelerated by decreasing the temperature. Previous studies showed that a lower crystallisation temperature of an emulsion is followed by higher emulsion stability. DSC studies were carried out with the use of a DSC Q 2000 instrument coupled with a computer for data analysis. Liquid nitrogen was used as coolant. About 5 mg of sample was taken for each run; the temperature range studied was from 30°C to -70°C, with a cooling rate of 2°C/min. All emulsions studied had the same droplet size (equal to 13 µm) and the surfactant type was a variable parameter. The results are summarised in Table 4.12.

Table 4.12: Effect of surfactant type on the crystallisation temperature of highly concentrated emulsion (8% surfactant in oil phase)

Surfactant type	Pibsa-MEA	Pibsa-UREA	Pibsa-MEA/SMO	Pibsa-IMIDE	SMO
Crystallization temperature, °C	-41	-41	-23	-18	12

Analysis of the results in Table 4.12 reveals the following:

- The nature of the surfactant has an effect on emulsion crystallisation temperature and thereby on emulsion stability. The results correspond with the following sequence: Pibsa-MEA = Pibsa-UREA > Pibsa-MEA/SMO > Pibsa-IMIDE > SMO. It is reasonable to suggest that the difference in chemical structure, type and strength of interaction between the surfactant and AN melt plays an important role in crystal initiation.
- Among the three Pibsa-based surfactants, the effect of surfactant type on crystallisation temperature was observed to follow the same trend as the expected sequence of surfactant-ammonium nitrate interaction, namely Pibsa-MEA – Pibsa-UREA – Pibsa-IMIDE.

The above observations might support the fact that the initiation of crystallisation could depend mostly on surfactant-electrolyte interaction and might play a major role in the overall process of crystallisation in the case of emulsions with dissolved electrolytes in the aqueous phase (Adya & Neilson, 1991; Ganguly *et al.*, 1992). Indeed, the initiation of crystallisation depends mostly on the ability of additives (ions, molecules, or surfactant head group) to increase the separation distance between NH_4^+ and NO_3^- ions (Adya & Neilson, 1991; Ganguly *et al.*, 1992; Oxley *et al.*, 1992). The separation of charges inside the droplet is expected to keep the emulsion in a super-cooled state by reducing the chemical kinetics of oversaturated ammonium nitrate (in the case of Pibsa-MEA, Pibsa-UREA). Moreover, this separation could generate repulsive forces in the thin film between droplets, which could reduce the Van der Waals attraction and consequently improve the stability. On a qualitative level, a strong surfactant-ammonium nitrate interaction is expected to give rise to a more stable emulsion (Ganguly *et al.*, 1992).

It was pointed out that the nucleation of the AN crystals in droplets can be induced by changes in the functionalities of the surfactant head group (Yubai *et al.*, 1996) and thereby the ability of the head group interaction with AN ions and water molecules. As a hypothesis it can be assumed that nonionic surfactant (with no charge present in the head group – SMO, Pibsa-IMIDE) preferably interacts with water molecules while the charged head group of the surfactant (Pibsa-MEA, Pibsa-UREA) is more attractive to the salt ions. The dispersed aqueous droplets in emulsions consisted of a supersaturated aqueous solution of ammonium nitrate salt (at room temperature). The ammonium nitrate concentration was 80% by mass, while water comprised less than 20% by mass. It is worth noting that this concentration of AN corresponded to the ca. 1:1 molecular ratio of $\text{H}_2\text{O}:\text{NH}_4\text{NO}_3$ (Adya & Neilson, 1991). This implies strong sensitivity of such a concentrated solution to the water content, and in this case, crystallisation could be induced by reduction of water molecules in the AN melt network. This is more possible in the case of SMO and Pibsa-IMIDE surfactants.

Another point to stress is that molecular packing geometry and mobility of the surfactant lipophilic portion at the interface can affect the crystallisation temperature of the emulsion (Villamagna *et al.*, 1995) and dewetting of the droplet (Spicer & Hartel, 2005). While comparing the mobilities of different portions of a surfactant molecule present in an emulsion, it is evident that the mobility increases along the hydrocarbon chain, from zero in the head group region to a maximum at the chain end. The polymer chain is generally random (Myers, 1999; Tadros, 2005), therefore it can be assumed that tail groups of Pibsa-based polymeric surfactants have a higher degree of freedom in comparison with SMO. This could also be one of the reasons why more efficient packing of SMO at the interface is observed. This suggestion can be supported by the fact that SMO has the lowest interfacial tension (see

Table 4.1). The more efficient packing at the interface (in the case of SMO) could lead to the rapid crystallisation of the liquid interfacial film (Villamagna *et al.*, 1995) and to emulsion breaking.

The above suggestions imply that the low stability of an emulsion stabilised by a mixture of Pibsa-MEA/SMO and relative stability of an emulsion stabilised with only Pibsa-MEA could be the result of reduction interaction of Pibsa-MEA with the electrolyte and, possibly, dehydration of the AN melt due to the greater attraction of SMO to the water molecules. Moreover, the closer packing of surfactant molecules in the monolayer due to the SMO presence at the interface may also induce the crystallisation.

The effect of surfactant concentration on the emulsion stability with regard to crystal initiation was also studied. Results are shown in Table 4.13.

Table 4.13: Crystallisation temperature of emulsions stabilised with Pibsa-MEA and Pibsa-IMIDE as a function of surfactant concentration

<i>Crystallisation temperature, °C</i>				
<i>C_{SURF}, %</i>	4	8	14	20
<i>Pibsa- MEA</i>	4	-41	-46	-43
<i>Pibsa- IMIDE</i>	Cryst. at 20 °C	-18	-21	-41

From the above, Table 4.13, it is seen that:

- The surfactant concentration has an effect on the emulsion's freezing temperature and therefore on the emulsion stability (this is shown for two surfactant types: Pibsa-MEA, Pibsa-IMIDE). The improvement of emulsion stability with regard to crystallisation is observed with an increased surfactant concentration. It seems that the interaction between the surfactant head group and the matter of the droplet plays a role in crystal initiation.
- For the Pibsa-MEA surfactant, no improvement in emulsion stability was observed after 14%, which can be regarded as an optimal surfactant concentration for emulsion stabilisation.

The results correspond with the FT-IR analysis results and imply that more surfactant at the interface generates stronger interactions and results in a more stable emulsion up to a certain extent.

4.1.3.2 Effect of the AN concentration on emulsion stability

In this part of study, the DSC was used to determine the freezing point as a function of electrolyte concentration and as a function of salt additives to the AN. The crystallisation of emulsions was accelerated by decreasing the temperature. Figure 4.24 is a representation of DSC data for emulsions with various concentrations of electrolytes in the aqueous phase.

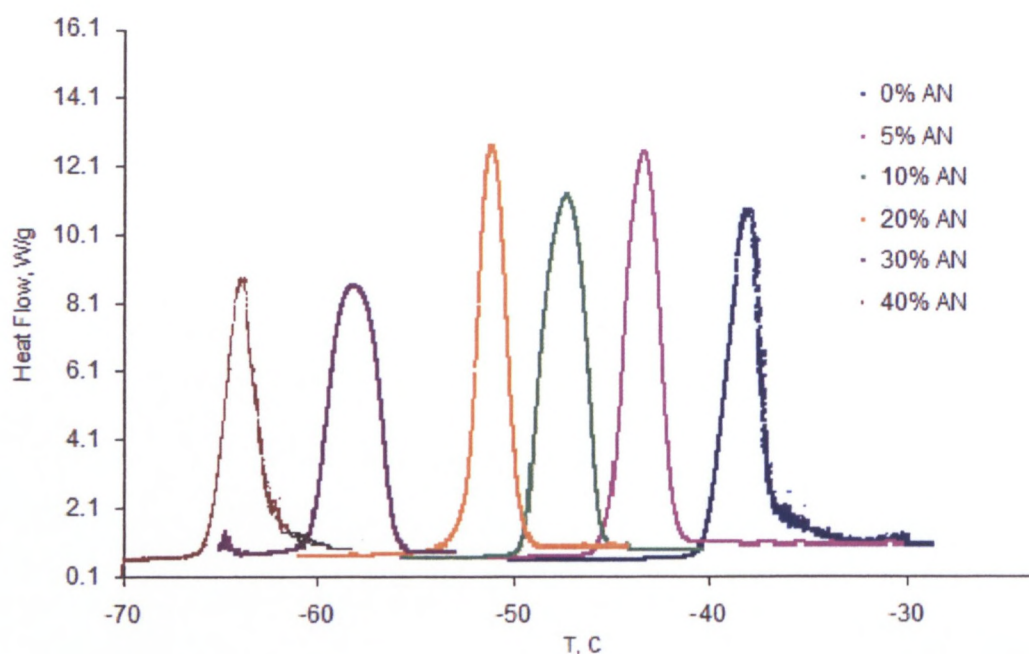


Figure 4.24: Heat Flow as a function of temperature for emulsions with different AN concentrations

Crystallisation temperatures for all emulsions are summarised in Table 4.14.

Table 4.14: Crystallisation temperatures of emulsions and solutions with different concentrations of AN in the aqueous phase

Concentration of AN in aqueous phase, %	Crystallisation temperature of emulsion, °C	Crystallisation temperature of solution, °C
0	-38	0
5	-43	-2
10	-47	-5
20	-51	-12
30	-58	-20
40	-63	-31

The results presented in Table 4.14 first of all show that crystallisation temperatures of solutions are much higher than they are with emulsions. This has implications for the stabilisation of solution in micro scaled drops. Similar results were reported by Ganguly et al., (1992) and by Aronson and Petko (1993). Just this physical peculiarity of the two-phase system in micro-sized droplets provides a possibility of creating highly concentrated solutions in the aqueous phase in highly concentrated emulsions.

The graphical representation of results is shown in Figure 4. 25.

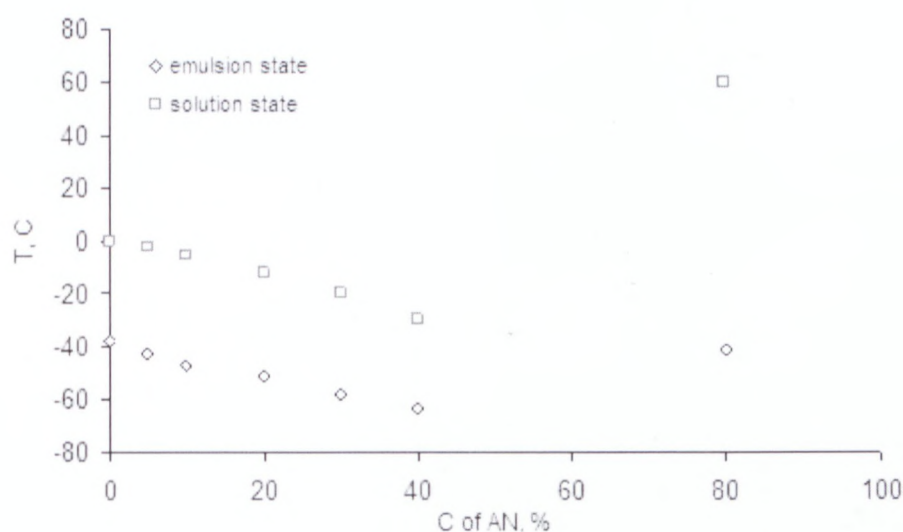


Figure 4.25: Freezing temperature of emulsions and solutions as a function of electrolyte concentration

From above results it can be seen that:

- The more salt added to the water, the lower the freezing point of the solution and emulsion. This behaviour can be explained from different properties of AN solutions with different salt content. For most of the solutes the relationship $\Delta T_h = 1.96\Delta T_m$ (where ΔT_h is a depression of the homogeneous freezing temperature and ΔT_m is the depression in the melting point of the system) is obeyed well, indicating that dissolved salts affect the freezing temperature of the emulsified aqueous phase. The initial steady decrease in freezing temperature with increasing salt concentration could be due primarily to solute effects as was established earlier. Thus the dissolved salt can reduce freezing point by reduction in the water activity and from changes in the activation energy of diffusion, changes in the ice-solution interfacial free energy, and possibly from other effects of ice network breakdown or formation at constant water activity (Ganguly *et al.*, 1992).
- In the emulsion state, the freezing temperatures are much lower than in the solution state. The property of emulsion droplets to remain liquid at low temperatures can be attributed to the large degree of subdivision (Becher, 1988). This physical behaviour of the two-phase solution in micro-sized droplets provides a possibility of creating stable highly concentrated emulsions.

4.1.3.3 Effect of NaNO_3 and $\text{Ca}(\text{NO}_3)_2$ on emulsion stability

The sodium and calcium nitrate were added to the AN solution for the emulsion stability investigation. The total concentration of salt in the aqueous phase was kept at 80%. The results are summarised in Tables 4.15 and 4.16.

Table 4.15: Crystallisation temperature of emulsions with AN and AN-NaNO₃ as an aqueous phase

Surfactant type	Crystallisation temperature, °C	
	AN salt	AN-NaNO ₃ salt (1:7)
<i>Fudge point of solution, °C</i>	60	47
<i>Pibsa MEA</i>		
8%	-41	-42
14%	-46	-42.5
<i>Pibsa UREA</i>		
8%	-41	-42.4
14%	-45	-42.6
<i>Pibsa IMIDE</i>		
8%	-18	-42
14%	-20	-45
<i>Pibsa MEA/SMO</i>		
8%	-23	-25.3
14%	-34	-42.2
<i>SMO</i>		
8%	12	-15.9

Table 4.16: Crystallisation temperatures of emulsions and solutions with addition of calcium nitrate salt to the AN

Surfactant type	Concentration of Ca(NO ₃) ₂ to the AN, %	Fudge point of solution, °C	T _{CRYST} of emulsion, °C
<i>Pibsa IMIDE</i>	0	60°	-18°
	15	47°	-45°
	35	below 20°	Below -70°

From Tables 4.15 and 4.16 the following can be noticed:

- The fudge point of the AN solution and crystallisation temperature of emulsions are lowered by the presence of an additive of SN and CN. This reflects about the stabilisation of the aqueous phase (solution) which contains AN by including an admixture of sodium and calcium ions, which results in structural changing of the solution. Indeed, an overall relaxation of the structure of the AN solution was found in the presence of Ca^{2+} ions. In particular the nearest – neighbour N1-N2 – distance (distance between nitrogen atoms in nearest NH_4^+ and NO_3^-) was found to be 5.5 Å in the mixed molten salts as compared to 4.5 Å in pure AN (Adya & Neilson, 1996). It provides clear evidence that the presence of doubly charged Ca^{2+} brings a significant difference to the coordination and separation of the ammonium nitrate ions (Adya & Neilson, 1991; 1996). The same effect can probably be ascribed to the addition of Na^+ ions.
- Emulsions stabilised with Pibsa-MEA and Pibsa-UREA surfactants did not show any improvement of their stability with the addition of SN to the AN, while considerable reduction in crystallisation temperature was observed for the emulsions stabilised with Pibsa-IMIDE, Pibsa-MEA/SMO and SMO. It is reasonable to assume that the enhanced stability of these emulsions can be explained in terms of extra adsorption of surfactant at the interface (Aronson & Petko, 1993) due to an increase of the droplet charge with the addition of Na^+ .

To support the above suggestion, the concentration of Pibsa-IMIDE surfactant at the interface was obtained for two concentrations of AN (10% and 60%) from the slope of CMC measurements. The measurements were carried out by following the methodology described earlier (see section 3.5.4). The results are shown in Figure 4.26.

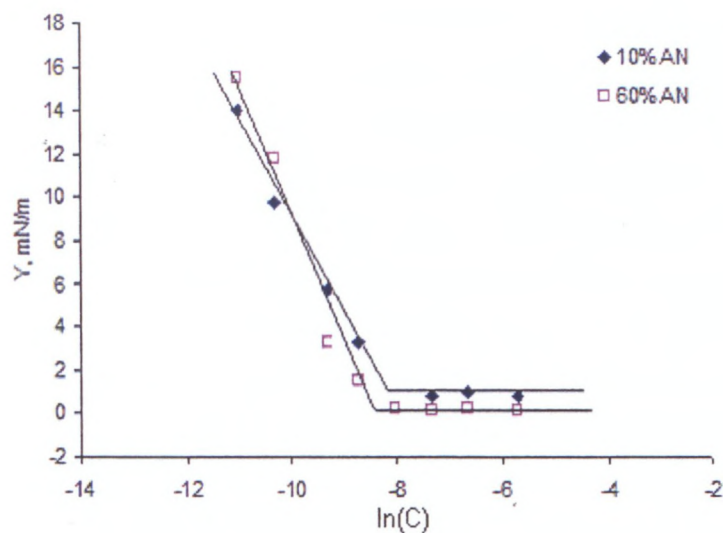


Figure 4.26: Determination of slope ($dy/d\ln c$) and CMC values for systems with 10% and 60% AN in the aqueous phase and Pibsa-IMIDE surfactant in the oil phase

The best linear fit to the decreasing part of the curve for 10% AN gave a slope of $-3.98 \times 10^{-3} \text{ N m}^{-1}$.

Molar concentration at the interface, $\Gamma = - (d \gamma / d \ln c) / RT = 3.98 \times 10^{-3} / (8.314 \times 298) = 1.6 \times 10^{-6} \text{ mol m}^{-2}$.

The fit to the decreasing part of the curve for the 60% AN gave a slope of $-6.55 \times 10^{-3} \text{ N m}^{-1}$. Molar concentration at the interface, $\Gamma = - (d \gamma / d \ln c) / RT = 6.55 \times 10^{-3} / (8.314 \times 298) = 2.64 \times 10^{-6} \text{ mol m}^{-2}$. The results are summarised in Table 4.17.

Table 4.17: Pibsa-IMIDE surfactant concentration at the interface with presence of AN in the aqueous phase

[AN, %]	$\Gamma \times 10^6, \text{ mol m}^{-2}$
10%	1.60
60%	2.64

From Table 4.17 it can be seen that the value Γ for the 10% concentration is lower compared to 60% of AN in the aqueous phase. It implies that more Pibsa-IMIDE surfactant was absorbed at the interface with 60% AN compared to 10% AN present in the aqueous phase. However, no extra adsorption of Pibsa-MEA surfactant at the interface was found with increasing AN concentration in the aqueous phase, which confirms monolayer expansion due to the strong interaction with the AN salt and electrostatic repulsion between the head

groups. The results obtained also prove that the head group of Pibsa-IMIDE surfactant does not undergo such strong structural changes due to interactions with the salt and therefore can be more mobile at the interface and less restricted to the greater adsorption with an increase of the droplet charge (concentration of electrolytes in the aqueous phase). Obviously, the Pibsa-IMIDE surfactant is more densely packed at the interface with an increased AN content (this is evidence from experimental results). This can lead to the “brush” formation (the chains in the brush are stretched out) and therefore increase the steric repulsive forces between the surfactant layers that will result in a more stable emulsion. The interaction of the head group with the matter of droplets can probably affect the distribution of ions, which will also give a rise to electrostatic repulsive forces between the droplets.

It is probable that similar behaviour can be found for the mixture of Pibsa-MEA/SMO and SMO surfactant.

4.1.3.4 Effect of pH on emulsion stability with regard to coalescence

Two sets of emulsions were prepared, at pH = 4 and pH = 7. Emulsions prepared at pH = 7 were unstable and showed coalescence while performing the droplet size measurements. Results for the measured droplet size of emulsions prepared at pH = 7 are shown in Figures 4.27 to 4.29.

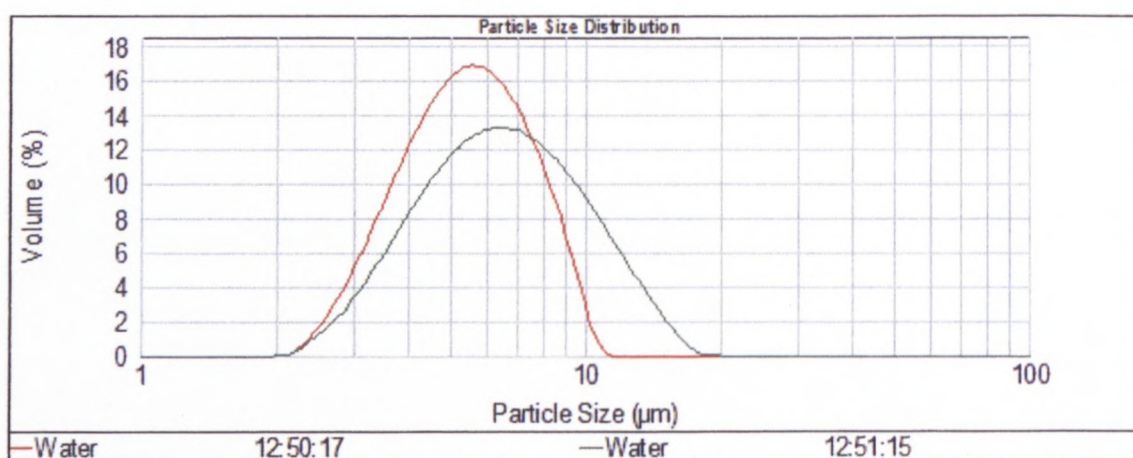


Figure 4.27: Evolution of droplet size distribution of water emulsion during the measurement (pH = 7)

Figure 4.27 shows that the droplet size of the sample increased over time during the droplet size measurement.

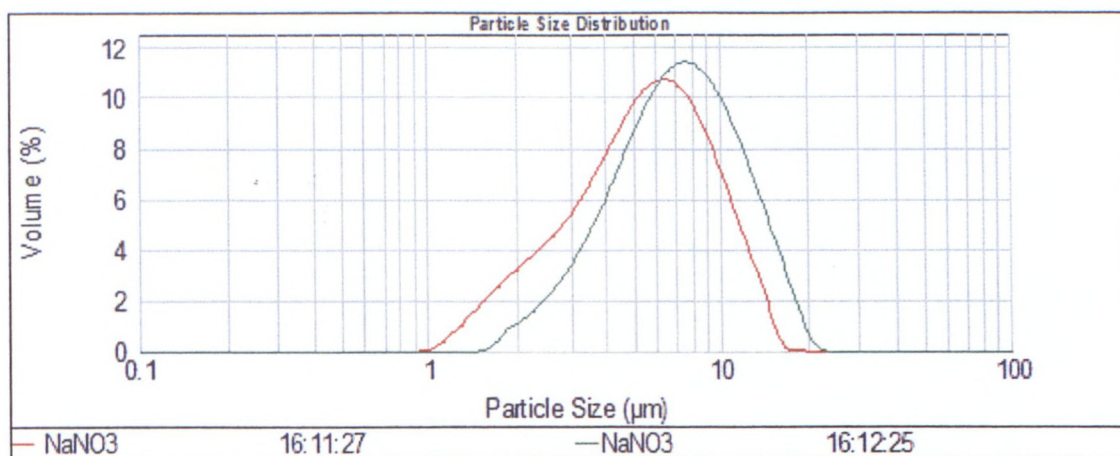


Figure 4.28: Evolution of droplet size distribution of emulsion with NaNO_3 during the measurement (pH = 7)

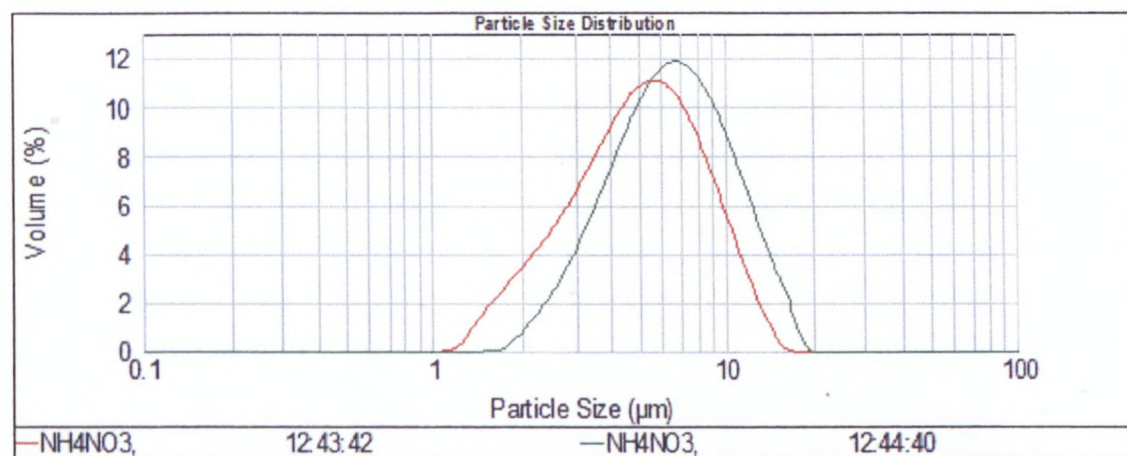


Figure 4.29: Evolution of droplet size distribution of emulsion with NH_4NO_3 during the measurement (pH = 7)

From the above, it can be seen that the droplet size in emulsions prepared at pH = 7 was changing during the droplet size measurements, therefore the rheological properties of these emulsions could not be investigated.

A qualitative microscopic study was undertaken to support the above suggestion. All the results revealed droplet coalescence (increase in droplet size) (Figures 4.30 and 4.31).

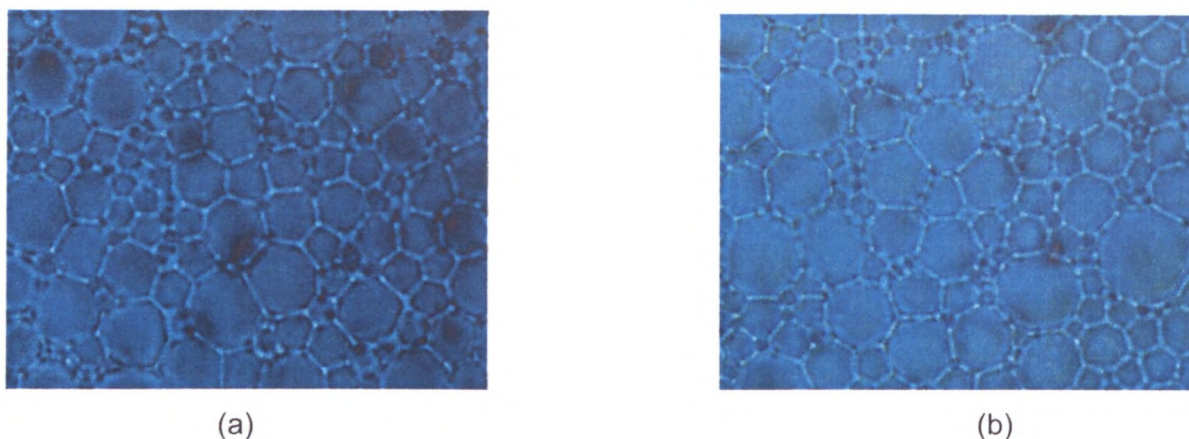


Figure 4.30: Coalescence of highly concentrated water emulsion prepared at pH = 7:

(a) fresh emulsion sample spread on the glass surface

(b) the same emulsion sample after two minutes

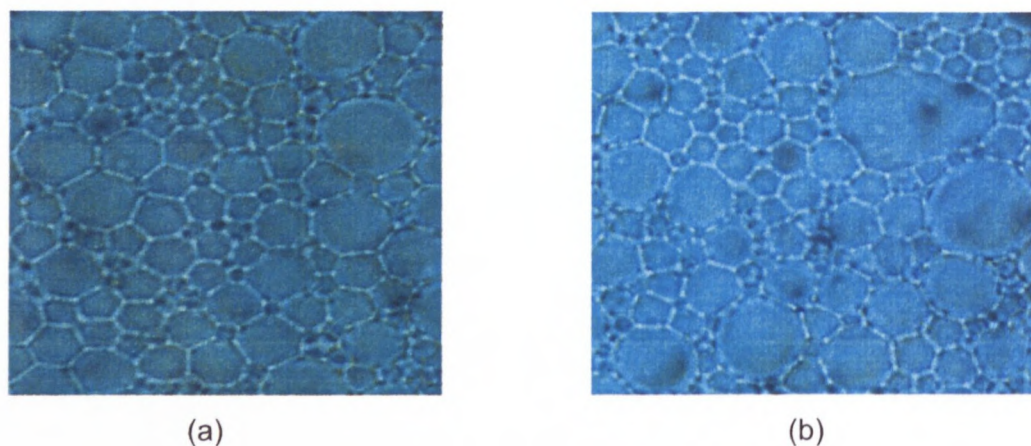


Figure 4.31: Coalescence of highly concentrated emulsion with NaNO_3 prepared at pH = 7:

(a) fresh emulsion sample after spread on the glass surface

(b) the same sample after two minutes

Rapid coalescence of samples after spreading the sample on the glass surface was observed during the microscopic investigation. From the above results it was clearly seen that the effect of pH is crucial to emulsion stability against coalescence. It is reasonable to assume that pH influences solubility, attractive forces and repulsive forces involved with the polar head group of the Pibsa-MEA surfactant and thereby influences the emulsifying activity of surfactant. In this case the Pibsa-MEA surfactant can be referred to the pH-sensitive zwitterionic class of surfactants (Ganguly *et al.*, 1992; Ghaicha *et al.*, 1993) which contains two nonidentical functional groups (amide and carboxylic group). Such surfactants based on

the ammonium group as cationic and carboxylate group as anionic may show the properties of anionics at high pHs and cationics at low pHs (Rosen, 2004; Singh *et al.*, 2007). The possible charge distribution in the head group of Pibsa-MEA surfactant at different pHs is displayed in Figure 4.32.

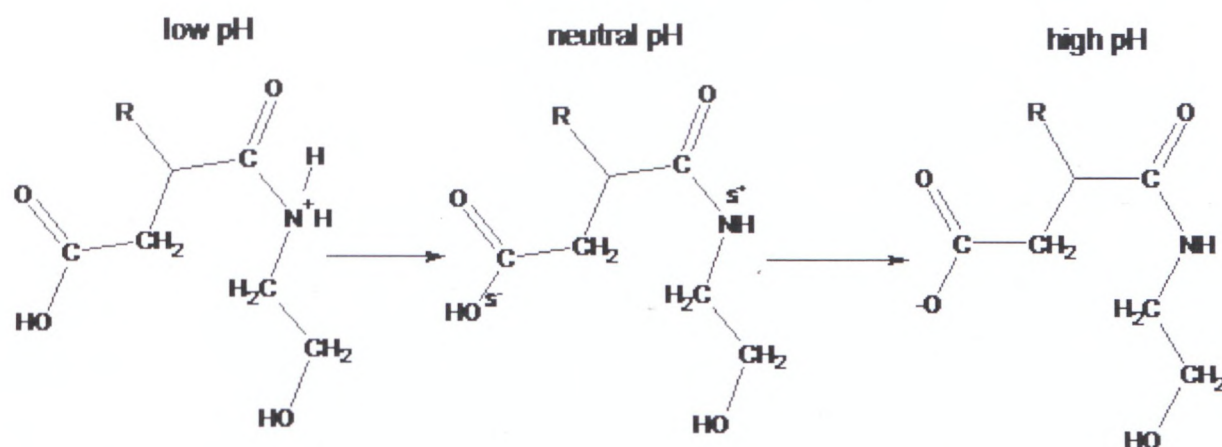


Figure 4.32: Effect of pH on the charge distribution in the Pibsa-MEA surfactant head group

In analysing Figure 4.32, the following can be mentioned:

- At low pH the secondary amine becomes protonated (Morrison & Boyd, 1987; Ghaicha *et al.*, 1993), while the carboxylic group is suppressed from dissociation (Morrison & Boyd, 1987; Khytoryanskiy *et al.*, 2004; Dittrich & Sibler, 2006). This leads to the positive charge of the head group.
- At neutral pH, both groups (amine and carboxylic) will be charged (Morrison & Boyd, 1987). Neutral pH is probably close to the isoelectric point (Ip). Ip is the pH at which a molecule carries no net electrical charge and can be found around 6 for amino acids (Morrison & Boyd, 1987) which have structures similar to the Pibsa-MEA head group. In the vicinity of the Ip they show minimum solubility in water (Morrison & Boyd, 1987; Rosen, 2004).
- In the region of high pH the carboxylic group is ionized (Ghaicha *et al.*, 1993), while the secondary amine cannot be protonated due to lack of protons in the base media. This leads to the negative charge of the head group.

The lower stability of an emulsion at pH = 7 in comparison with pH = 4 can be explained on the basis of the suggestion that neutral pH is close to the Ip and the surfactant has a lower solubility in water. Moreover, it is known that an ionized COOH group is not able to form

hydrogen bonds (Khytoryanskiy *et al.*, 2004; Pedraza & Soucek, 2008) and therefore the lack of a hydrogen bond network can probably decrease the stability of the interface at pH = 7.

All the samples prepared at pH = 4 showed remarkable stability against coalescence in contrast with samples prepared at pH = 7. The droplet size of emulsions was measured and rheological properties were investigated (see section 5.1.2.2).

4.1.4 General conclusion regarding the effect of surfactant hydrophilic groups and electrolyte nature and concentration on the interfacial properties, interactions and emulsion stability

The sensitivity of the interfacial properties (interfacial tension, interfacial elasticity) and stability to crystal initiation of high-internal phase water-in-oil explosive emulsions to the type and concentration of the surfactant and electrolyte were investigated in this part of the present study.

It was confirmed that changing the surfactant type gives rise to modification of both interfacial properties (interfacial tension and interfacial elasticity). In the present research, the differences in interfacial properties as a function of surfactant type were attributed to the strength and type of interactions between the surfactant head group and the matter of the droplet. The interaction between surfactant head group and oxidizer, as well as between head groups at the interface, was strongly linked to the conformation of polymeric tails. The tail ordering and tail interactions were seen to influence the interfacial elasticity, steric repulsion between droplets and to have an effect on the stability of an emulsion.

It was shown that Pibsa-MEA and Pibsa-UREA develop more stable interfaces compared to the Pibsa-IMIDE surfactant due to the stronger interactions with the aqueous phase. The interaction between surfactant head group and oxidizer solution allows for better anchoring at the interface and depends on the following factors:

- Polarity of the head group, which depends on the functional groups present in the structure and structural geometry of the head group,
- Ability to form hydrogen bonds (the presence of COOH and OH groups seems to be necessary),
- Ability to form salt with oxidizer ions (the presence of COOH and NH group seems to be important).

It was shown that SMO, when added to the Pibsa-MEA, partially remains at the interface and reduces the interaction of a polymeric surfactant with the aqueous phase and between the head groups, leading to lower interfacial tension and interfacial elasticity.

The investigation of interfacial properties demonstrated that the interaction between the AN and surfactant head group exists and provides stable and elastic interface. It was shown that the strength of interactions depends on the salt concentration and increases with the addition of salt. We suggest that interactions are also dependent on the nature of the salt (cation charge). In the present study we suggested that the strength of interactions for the calcium, sodium and ammonium ions follow the row in their density charge.

The DSC study revealed the following row of emulsion stability to crystal initiation: Pibsa-MEA = Pibsa-UREA > Pibsa-MEA/SMO > Pibsa-IMIDE > SMO. These results were in good agreement with the strength of interactions between the surfactant head group and the matter of droplets. These observations might support the fact that the initiation of crystallisation could depend mostly on surfactant-electrolyte interaction and possibly play a major role in the overall process of crystallisation in the case of emulsions with dissolved electrolytes in the aqueous phase. Moreover, the differing ability of surfactants to interact with water molecules, as well as differing packing behaviour of surfactants at the interface, can probably result in differences in emulsion stability.

The present study has showed that not only the surfactant, but also an electrolyte influences emulsion properties (due to interaction with the surfactant) and therefore can play an important role in controlling emulsion stability.

In the present study it has been shown that the structure of the aqueous phase has a great influence on the emulsion stability. Emulsions with the presence of $\text{Ca}(\text{NO}_3)_2$ and NaNO_3 in the AN melt displayed enhanced stability in comparison with the AN emulsions. The improvement in stability was attributed to the molecular reorganisation of AN ions due to the presence of Ca^{2+} and Na^+ ions and to increased separation distance between the NH_4^+ and NO_3^- ions, which resulted in the delaying of crystallisation in an emulsion. Besides this, enhanced adsorption of surfactant can also have an impact on the stability to freezing.

Emulsion stability to coalescence is significantly influenced by pH due to the effect on the surface activity of the surfactant (Pibsa-MEA). Emulsions prepared at low pH (pH = 4) were much more stable in comparison with those prepared at pH = 7.

CHAPTER 5

5.1 RHEOLOGICAL PROPERTIES OF HIGHLY CONCENTRATED EMULSIONS

This chapter continues the discussion of the results obtained in the present investigation, focusing on the effect of surfactant hydrophilic groups and electrolyte concentration and composition on the rheological properties of highly concentrated emulsions.

5.1.1 Effect of surfactant hydrophilic groups on rheological properties of highly concentrated emulsions

The discussion of the effect of surfactant hydrophilic groups on the rheological properties of highly concentrated emulsions is provided in terms of surfactant-electrolyte interactions.

5.1.1.1 Droplet size measurements

The evolution of droplet burst during the emulsification process was followed by taking samples from the evolving emulsion at different processing times, and analysing their DSD.

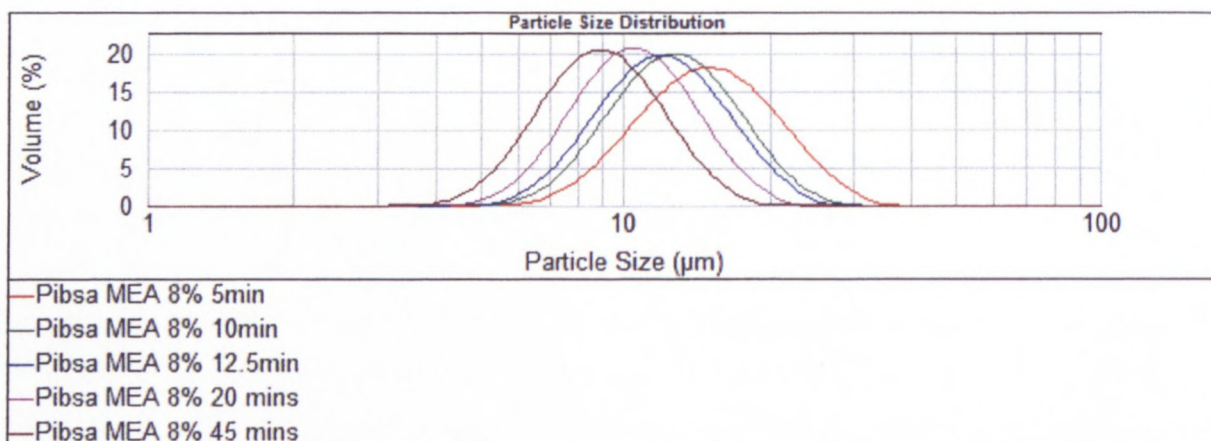


Figure 5.1: Droplet size distribution as a function of time for emulsion stabilised by Pibsa-MEA surfactant

It can be seen from Figure 5.1 that the droplet size distribution was unimodal and its width became narrower with a longer mixing time. Histograms of DSD for emulsions stabilised by other surfactants are very similar to this and can be found in Appendix A.

All the emulsions were mixed for a long time to reach the critical (limiting) diameter value (D_{lim}). Typical experimental results for droplet size evolution for emulsions with different surfactants present in the aqueous phase are shown in Figure 5.2.

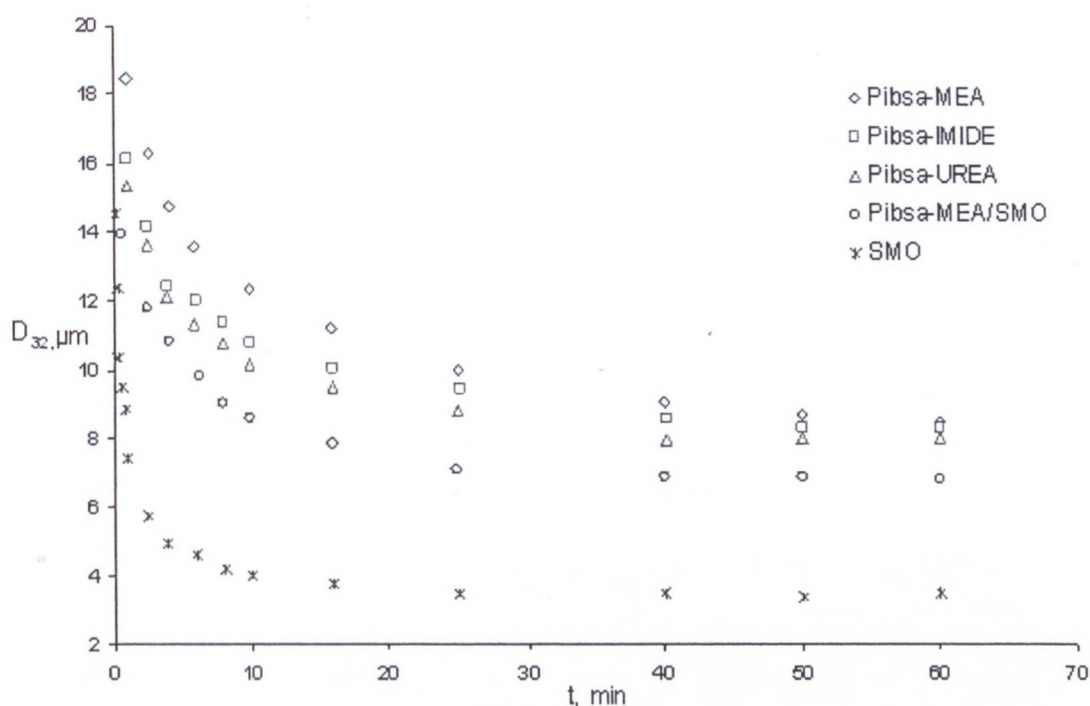


Figure 5.2: Droplet size as a function of mixing time of emulsions stabilised by different emulsifiers (8% wt. in oil phase): Pibsa-MEA, Pibsa-IMIDE, Pibsa-UREA, Pibsa-MEA/SMO, SMO

As illustrated in Figure 5.2, the droplet break-up was fast during the first 15 min. The droplet size reached the limiting constant value D_{lim} after app. 50 min. of mixing. The evolution of the average size in time is well fitted by the following equation:

$$D(t) = D_{lim} + e^{-(t/\theta)}(D_0 - D_{lim}), \quad \text{Equation: 5.1}$$

where $D(t)$ represents experimental values of D_{32} ; D_0 is the initial droplet size; D_{lim} is the limiting D value; θ is the characteristic time of the emulsification process. The fit of data for an emulsion stabilised by Pibsa-MEA surfactant is presented in Figure 5.3.

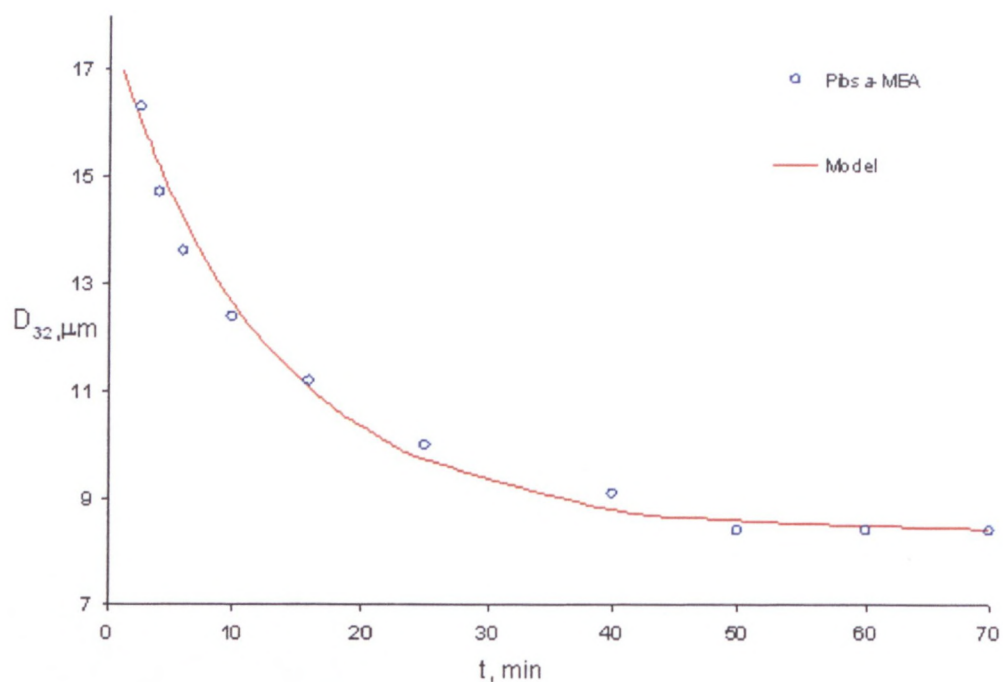


Figure 5.3: Droplet size as a function of mixing time for the emulsion stabilised with Pibsa-MEA surfactant fitted by model

The fittings for the other emulsions were similar to this and are presented in Appendix A. The results of fittings are listed in Table 5.1.

Table 5.1: Limiting diameter (D_{lim}) of emulsion droplets stabilised by different surfactants (8% wt. in the oil phase)

Surfactant type	D_0, μm	D_{lim}, μm	Θ, min
<i>Pibsa-MEA</i>	18.0	8.4	12.8
<i>Pibsa-IMIDE</i>	18.7	8.3	6.2
<i>Pibsa-UREA</i>	17.0	8.0	8.0
<i>Pibsa-MEA/SMO</i>	18.7	6.9	5.4
<i>SMO</i>	9.9	4.7	2.9

The results presented in Table 5.1 show the following trend for the limiting diameter and characteristic time in terms of surfactant type:

$$\text{Pibsa-MEA} > \text{Pibsa-IMIDE} > \text{Pibsa-UREA} > \text{Pibsa-MEA/SMO} > \text{SMO}$$

5.1.1.2 Viscoelastic and flow properties

The oscillation amplitude was selected as the variable and the frequency was kept constant in the amplitude sweep test. The frequency was 1 Hz and the strain was controlled between 0.1 and 200%. The corresponding storage modulus, relating to the elastic portion of the sample, and the loss modulus, the viscous portion of the sample, was measured as a function of strain. Figure 5.4 shows the evolution of the storage (G') modulus according to the increase of strain amplitude as a function of surfactant type for droplet size 12 micron.

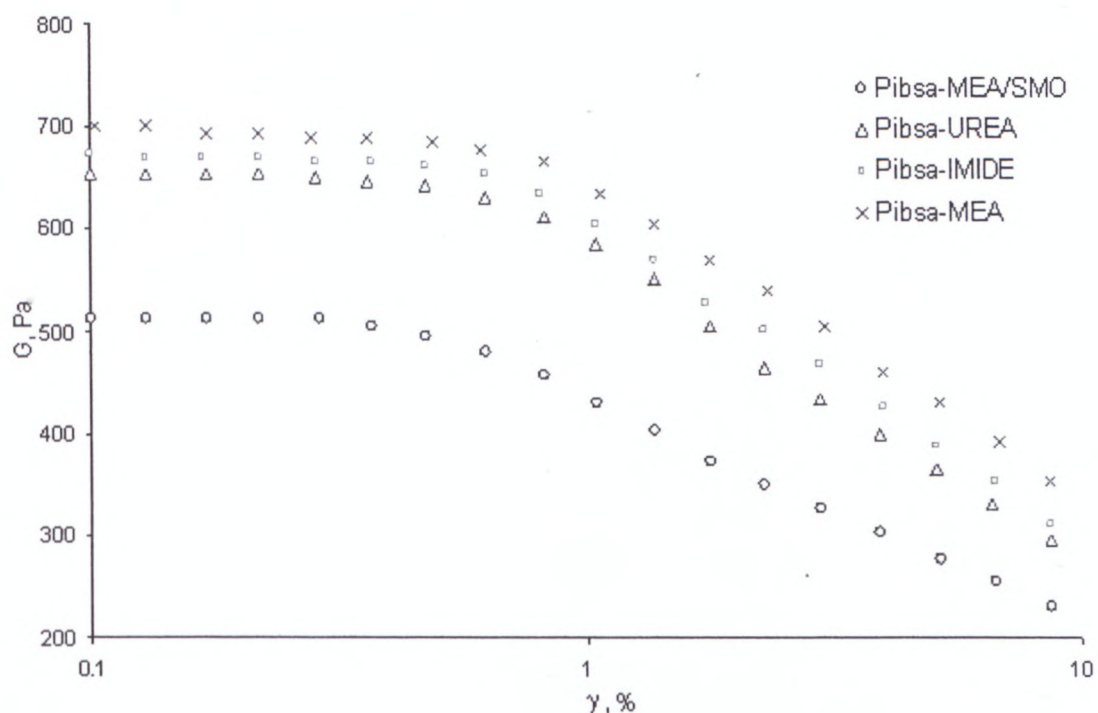


Figure 5.4: Storage Modulus as a function of surfactant type: DS[3.2] = 12 micron

For the material, the elastic modulus G' was greater than the viscous modulus G'' over the entire range of applied strain, indicating the predominantly elastic behaviour of the material with $G'/G'' \gg 10$ in all cases, at low test strains. As can be seen, the storage modulus was independent of strain amplitude up to some critical deformation, a zone of constant response (plateau region) indicating an unaltered structure not disturbed by shear. It was related only to the equilibrium microscopic structure, forces, and inherent dissipation of fluctuations (Bird, Armstrong & Hassager, 1987). In this linear region the particles were crowded and could not move freely past one another, which defined the elastic domain. At higher deformations, the values of the storage modulus decreased with a deformation increase, the applied strain being sufficient to allow the particles to move past one another and inducing a transition to the viscous domain. Above the critical shear stress value, emulsions lost their viscoelasticity

and became a fluid. This stress is known as yield stress. The length of the plateau of the elastic modulus is an indication of the structure's flexibility with regard to deformation and the drop of modulus is related to the break-down of the solid structure. The storage modulus was obtained from the linear region of the storage modulus by extrapolation of the curve to zero deformation.

There is no need to demonstrate all the results obtained for other droplet sizes (10 and 15 microns), since they are similar to this and can be found in Appendix A. All the data is summarised in Table 5.2.

Table 5.2: Storage modulus as a function of surfactant type for two surfactant concentrations (8% and 14%)

<i>d</i> , μm	<i>Pibsa</i> -MEA	<i>Pibsa</i> -IMIDE	<i>Pibsa</i> -UREA	<i>Pibsa</i> -MEA/SMO
<i>G'</i>, Pa; 8 % surfactant				
10	1012	948	911	661
12	696	669	656	511
15	439	433	428	401
<i>G'</i>, Pa; 14 % surfactant				
10	884	868	809	550
12	630	622	603	-

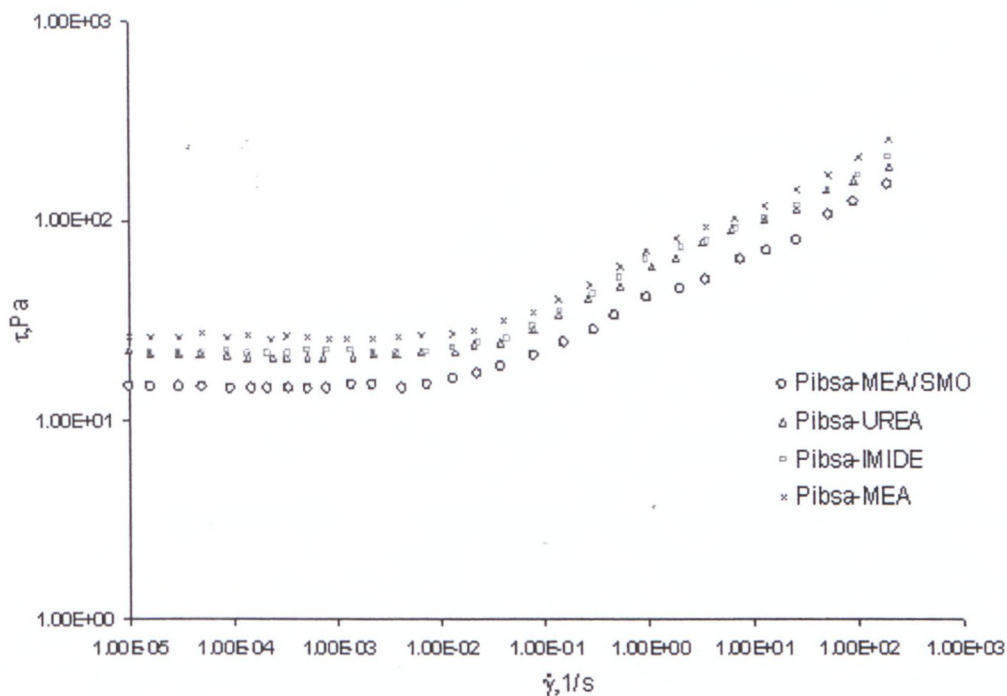


Figure 5.5: Yield Stress as a function of surfactant type: DS[3.2] = 12 micron

The flow curves show (Figure 5.5) an inflection point at some specific value of shear stress, as pointed out earlier (Masalova & Malkin 2005; 2007c; Malkin & Masalova 2007; Kharatiyan, 2005). According to these authors, two competing processes occur in the shearing of an explosive emulsion. One of them dominates at low shear rates and leads to an increase in viscosity, while the other prevails at high shear rates, resulting in typical shear thinning behaviour. According to the authors, drops maintain their shape in the low shear rate domain and flow proceeds as larger particles rolling over smaller ones until a critical shear stress (“second yield stress”) is reached.

The effect of surfactant type on the yield stress was essentially the same for all emulsion droplet sizes studied. Graphical views of the data can be found in Appendix A. The results are given in Table 5.3.

Table 5.3: Yield stress of emulsions stabilised by different surfactant types for two surfactant concentrations (8% and 14%)

$d, \mu\text{m}$	<i>Pibsa-MEA</i>	<i>Pibsa-IMIDE</i>	<i>Pibsa-UREA</i>	<i>Pibsa-MEA/SMO</i>
$\tau_y, \text{Pa}; 8\% \text{ surfactant}$				
10	42	37	35	23
12	25	22	22	15
15	16	16	15	12
$\tau_y, \text{Pa}; 14\% \text{ surfactant}$				
10	34	30	25	18
12	21	19	16	-

From analysing the results in Tables 5.2 and 5.3 it can be mentioned that:

- Surfactant nature has an effect on storage modulus and yield stress of highly concentrated emulsions. It is obvious that the viscoelastic and flow properties of the emulsion decreases in the following order *Pibsa-MEA* > *Pibsa-IMIDE* > *Pibsa-UREA* > *SMO/Pibsa-MEA* (the trend corresponds with the sequence which was found for the critical diameter values). The difference in G^0 and τ_y concerning the first three emulsions (stabilised by polymeric surfactants) can be associated only with the chemical structure of surfactant head groups which influenced the interfacial properties and interface structure.
- The bigger difference is observed between emulsions stabilised by a polymeric surfactant and an emulsion stabilised by a mixture of a polymeric and a low molecular weight (LMW) surfactant. It can be seen that a small addition of LMW surfactant (*Pibsa-MEA/SMO* = 10:1) lowered the G^0 and τ_y significantly.

A comparison between Table 4.1 and Table 5.3 reveals that, except for IMIDE-based emulsions, the bulk elasticity of *Pibsa*-based emulsions followed the same trend as the interfacial properties (interfacial tension or interfacial dilatational elasticity). This could be an indication of the high impact of interfacial elasticity on the bulk elasticity of emulsions prepared with MEA, UREA or the mixture MEA/SMO. For these surfactants the obtained results also suggest a link between the surfactant interactions with the matter of the drops and the rheological properties of fresh emulsions, since the interfacial elasticity is dependent on the surfactant interactions at the W/O interface.

It is more instructive to plot the data in the $G/(\gamma/R)$ - γ coordinates, γ being the interfacial tension, and R being the mean drop radius. This type of plot provides the possibility of

comparing the results, with exclusion of the effects of particle size and interfacial tension (Dimitrova & Leal-Caledron, 2004). By doing this, one can easily detect the presence of any additional source of elasticity in the system (see Figure 5.6).

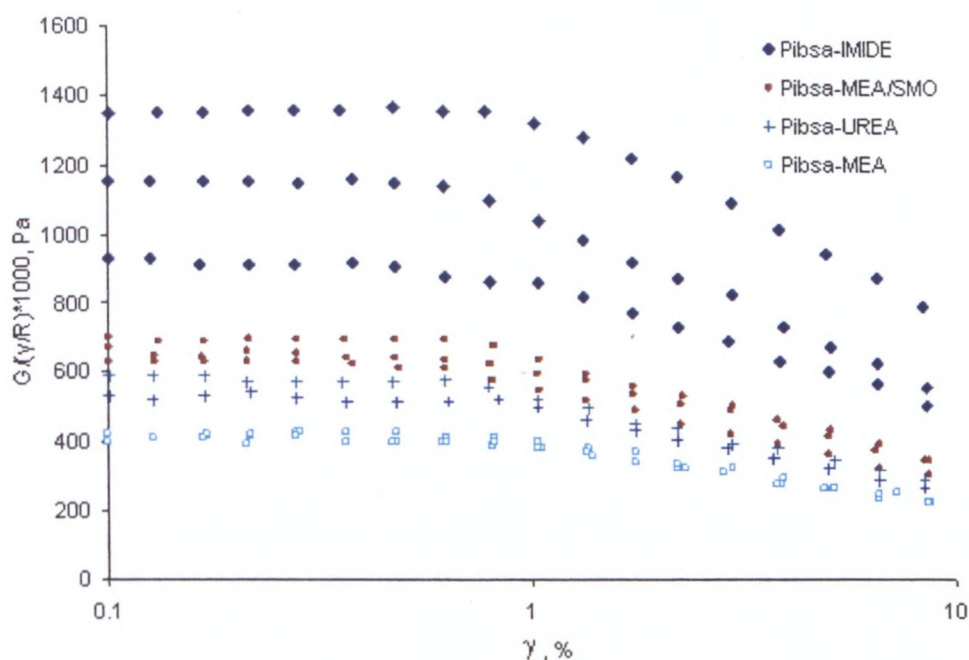


Figure 5.6: Effect of surfactant type on the dimensionless elastic modulus

The effect of surfactant type on the dimensionless elastic modulus of emulsion explosives is quite evident from Figure 5.6, above:

- This shows that the scaled elastic moduli $G/(\gamma/R)$ obtained for emulsions stabilised by different surfactant types do not collapse on a single master curve. Thus, additional sources of elasticity exist in the system.
- The dimensionless elastic moduli emphasise the considerable difference between W/O emulsions prepared with Pibsa-IMIDE and W/O emulsions stabilised with other Pibsa-based surfactants. Indeed, other factors such as electrolyte concentration, phase ratio, surfactant concentration and the nature of the external phase being kept constant, IMIDE-based emulsions show very high dimensionless elastic moduli compared to other Pibsa-based emulsions. Therefore the observed differences have to be attributed primarily to the different chemical structures of the surfactant head group and their influence on the surfactant-electrolyte interactions.

The effect of surfactant type on the dimensionless elastic modulus can be accounted for on the basis of the balance between Van der Waals attraction and repulsive forces (DLVO theory). The dominant interaction energy between droplets could be due to Van der Waals attraction (Alvarez *et al.*, 2006; Bibette, Leal-Calderon & Poulin, 1999; Baravian, Mougel &

Alvarez, 2006; Quintero *et al.*, 2008). The latter could act as a source of additional elasticity (Alvarez *et al.*, 2006; Baravian *et al.*, 2006; Quintero *et al.*, 2008). Moreover, because of the presence of ions (NH_4^+ , NO_3^-) within the aqueous droplets, an additional attractive potential energy could be generated in the thin film between droplets. Indeed, ion fluctuation gives rise to attraction between adjacent micro droplets, similar to the Van der Waals interaction between neutral atoms (Sheng & Tsao, 2004; Tsao, Sheng & Chen, 2002). On the other hand, the interactions between the surfactant head group and the matter of the droplets could increase the separation distance between the AN ions (Adya & Neilson, 1991; Ganguly *et al.*, 1992) and result in electrostatic repulsion between adjacent droplets due to the charge separation. The balance of repulsive forces-attractive forces could be one of the major factors which could determine the magnitude of the additional elasticity of explosive emulsions. The strong deviation of the IMIDE-scaled elastic modulus in comparison with other surfactants could be due to the increased surfactant concentration at the interface, which probably can result in enhanced repulsive forces due to the "brush" formation. The addition of SMO to Pibsa-MEA could probably reduce the repulsion between the layers. This could be due to the fact that the replacement of some MEA surfactant by SMO is expected to reduce the degree of charge separation inside the droplet, because the surfactant-electrolyte interaction is more intense in the case of MEA, compared to SMO (Ganguly *et al.*, 1992).

From the above analysis, it is possible to conclude that the differences in elasticity shown by different surfactant types used in this study could result from the combination of interfacial properties (interfacial tension and interfacial dilatational modulus which are governed by surfactant interactions at the W/O interface) and the Van der Waals attraction, and ion-fluctuation attraction as an additional source of elasticity. Due to their different influences on surfactant-electrolyte interactions, different surfactant types induce different interfacial properties and could induce a different balance of repulsive forces-attractive forces in the thin film between droplets; therefore, make different contributions of additional elasticity.

5.1.2 Effect of electrolyte concentration and composition on rheological properties of highly concentrated emulsions

This part of study presents the results of the investigation of the electrolyte concentration and composition on the rheological properties.

5.1.2.1 Effect of electrolyte concentration on rheological properties of highly concentrated emulsions.

The discussion of the effect of electrolyte concentration on the rheological properties of highly concentrated emulsions is provided in terms of surfactant-electrolyte interactions.

5.1.2.1.1 Droplet size distribution

The evolution of droplet burst during the emulsification process was followed by taking samples from the evolving emulsion at different processing times, and analysing their DSD.

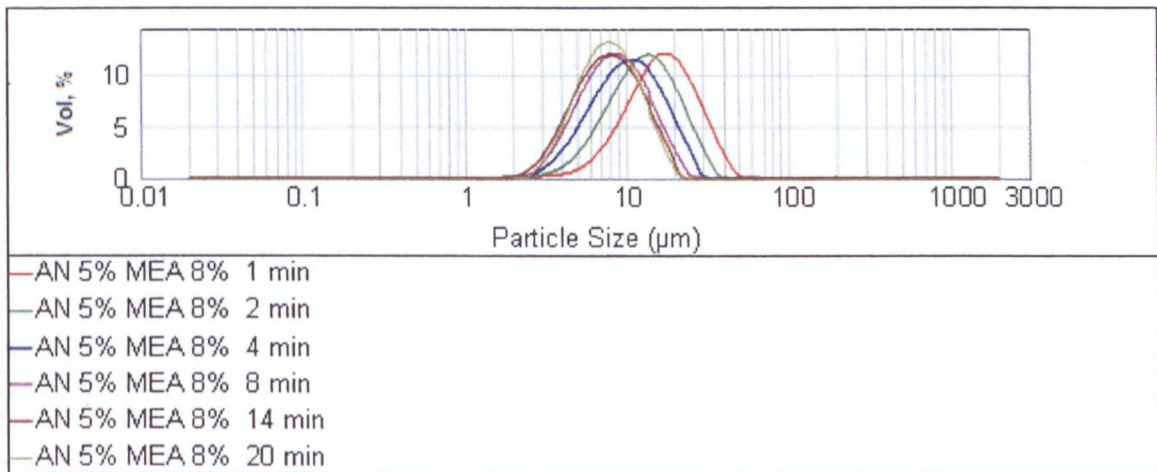


Figure 5.7: Histogram of drop size distribution of the emulsions containing 5% of AN at different mixing times

It can be seen from Figure 5.7 that droplet size distribution was unimodal and its width became narrower with longer mixing times. Histograms of DSD for emulsions with other concentrations of AN are very similar to this and can be found in Appendix B.

All the emulsions were mixed for a long time to reach the critical (limiting) diameter value (D_{lim}). Typical experimental results of droplet size evolution for emulsions with a different AN content in the aqueous phase are shown in Figure 5.8.

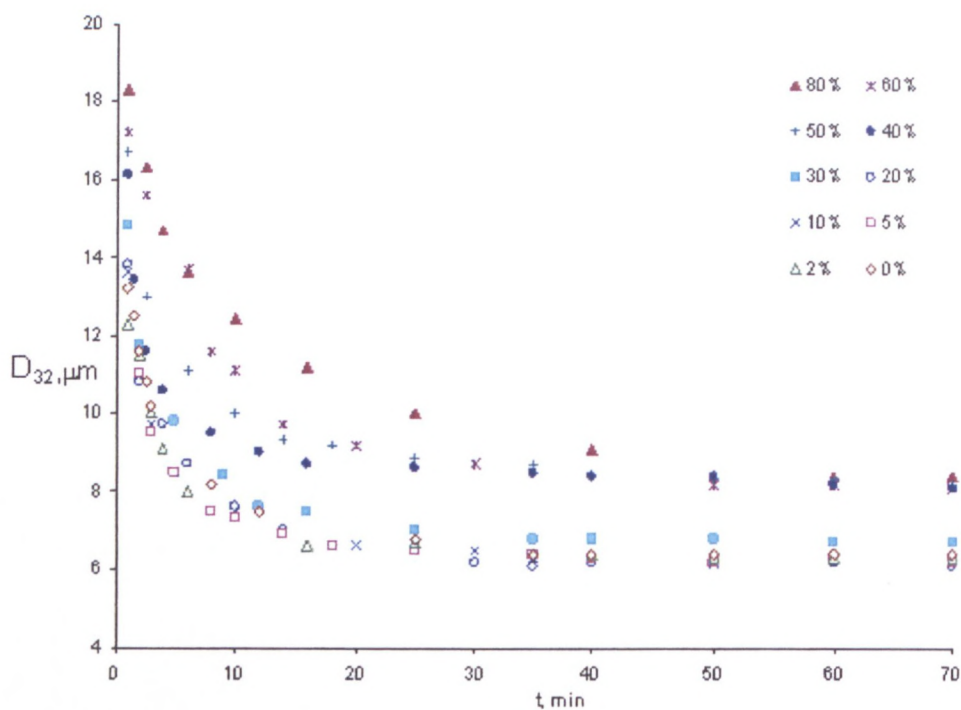


Figure 5.8: Droplet size as a function of mixing time for emulsions with 0, 2, 5, 10, 20, 30, 40, 50, 60 and 80% AN in the aqueous phase

As illustrated in Figure 5.8, droplet break-up is fast during the first 15 minutes, which results in droplet size diminution. The droplet size reaches an approximately constant value after 50 minutes of mixing. It is clearly seen that there is a gap between the curves which separates emulsions into two sets: emulsions with low ammonium nitrate concentration in the aqueous phase (0% to 30%) and emulsions with a high concentration of ammonium nitrate in the aqueous phase (40% to 80%). Equation 5.1 was used for the determination of D_{lim} .

The fit of data from the emulsion with 5% AN in the water phase is presented in Figure 5.9.

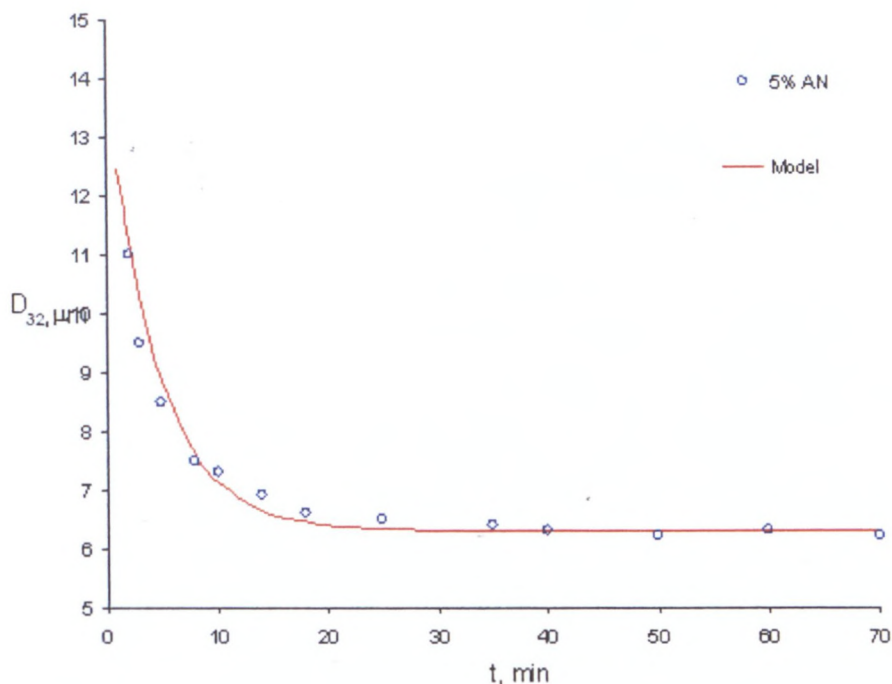


Figure 5.9: Droplet size as a function of mixing time for the 5% AN emulsion fitted by model

The fittings for the other emulsions are similar to this and are presented in Appendix B.

The results of fittings are listed in Table 5.4.

Table 5.4: Critical diameter of emulsion droplets containing different AN concentrations

[AN], %	D_0 , μm	D_{lim} , μm	Θ , min
0	14.8	6.4	4.2
2	14.0	6.3	4.3
5	14.0	6.3	4.5
10	14.5	6.3	4.5
20	14.5	6.3	5
30	15.5	6.8	5.1
40	15.7	8.2	5.1
50	16.0	8.2	7.5
60	17.8	8.2	8.5
80	18.0	8.4	12.8

It can be seen, from the above, that the increase in AN concentration in the aqueous phase led to higher D_{lim} values and characteristic times. It has to be mentioned here that a clearly pronounced distance between values of 30% and 40% AN in the aqueous phase of emulsions is observed and this can probably be attributed to the change in structure of the AN solution (see section 4.1.2.2.1). Samples with similar droplet sizes (8 micron) were chosen for the rheological investigation.

5.1.2.1.2 Viscoelastic and flow properties

The oscillation amplitude was selected as the variable and the frequency was kept constant in the amplitude sweep test. The frequency was 1 Hz and the strain was controlled between 0.1 and 200%. The corresponding storage modulus, relating to the elastic portion of the sample, and the loss modulus, the viscous portion of the sample, was measured as a function of strain. Figure 5.10 shows the evolution of the storage (G') modulus according to the increase of strain amplitude as a function of ammonium nitrate concentration for droplet size 8 micron.

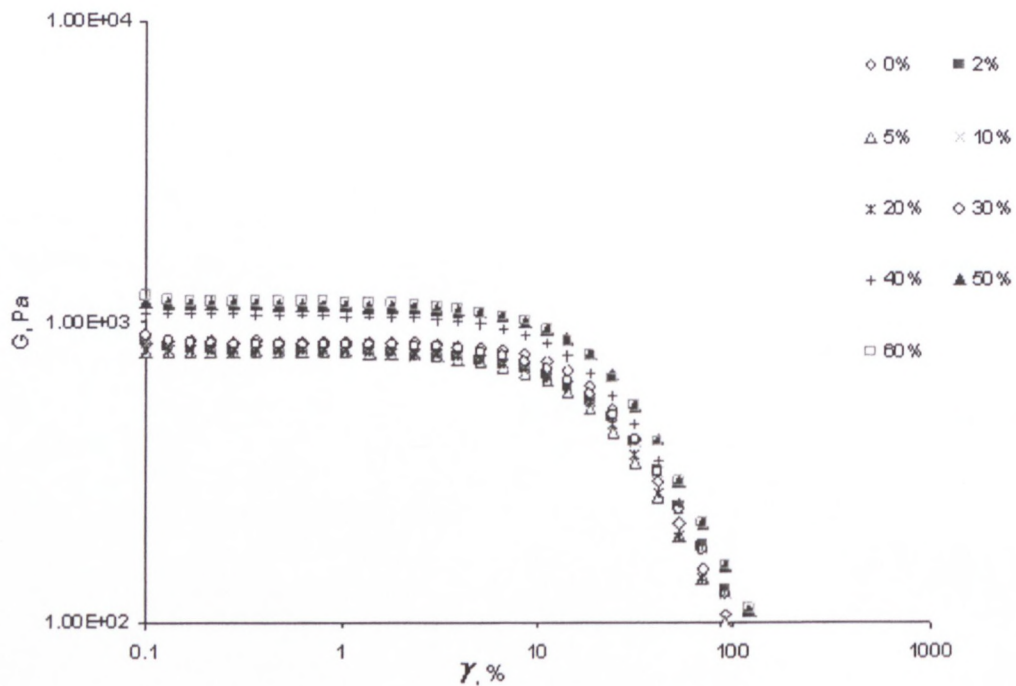


Figure 5.10: Storage Modulus as a function of ammonium nitrate concentration: DS[3,2] = 8 micron

The flow curves of the samples are shown in Figure 5.11.

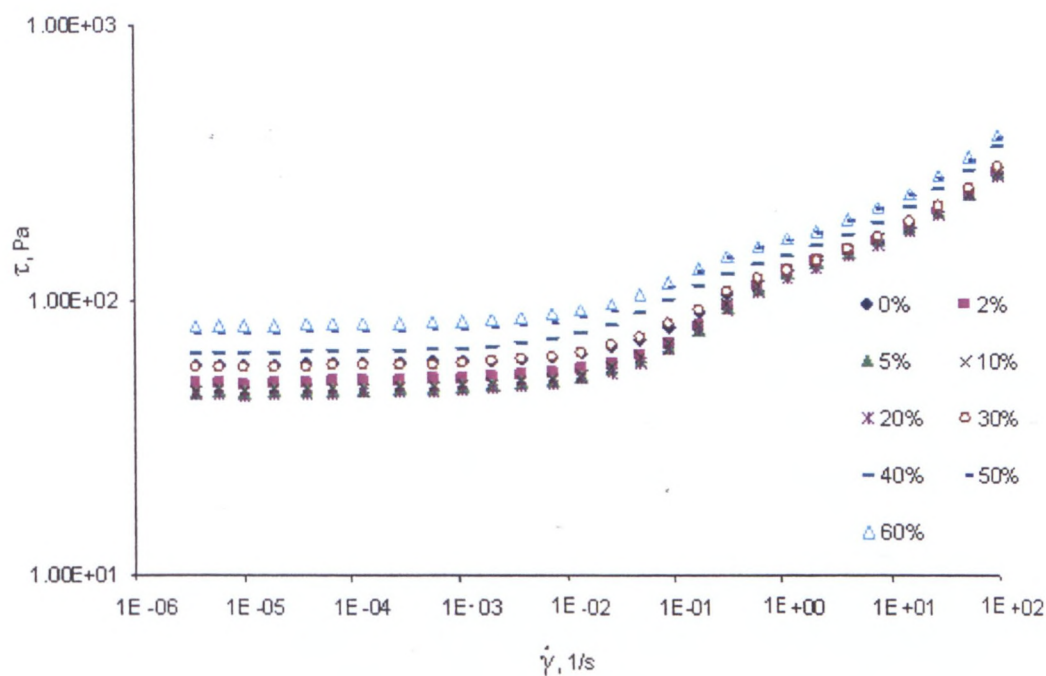


Figure 5.11: Yield Stress as a function of ammonium nitrate concentration:
DS[3,2] = 8 micron

The results are listed in Table 5.5.

Table 5.5: Storage Modulus and Yield Stress of emulsions with different concentrations of ammonium nitrate: DS[3,2] = 8 micron

[AN], %	G^0 , Pa	τ_y , Pa	G^0/τ_0	D_{32} , μm
0	804	50	15.6	8.0
2	801	50	16.0	7.9
5	788	47	16.8	8.2
10	791	48	16.5	8.0
20	786	46	17.0	8.2
30	842	54	15.6	8.0
40	1059	64	16.5	8.1
50	1140	75	15.2	8.1
60	1170	81	14.4	8.1

The results in Table 5.5 show the evolution of the Storage Modulus with salt concentrations for the emulsions studied:

- In the above it is clearly seen that the plateau modulus, as well as the yield stress, increases significantly with salt concentration, but more rapidly at the higher portion of AN in the aqueous phase. A more pronounced difference is observed in experimental

results for between 30% and 40% AN content. This behaviour can be attributed mostly to the structural changes in the AN solution.

- The elastic modulus and yield stress show an opposite trend, with the interfacial tension as a function of AN concentration. This implies that interfacial tension does not contribute to the rise of the storage modulus and yield stress and cannot explain this observation. In this case, the additional sources of elasticity have to be taken into account. It is reasonable to consider an electrolyte effect on the surfactant-electrolyte interactions and droplet-droplet interactions as additional source of elasticity.

Attendant to the discussion in section 4.1.2.2.2, it seems that the effect of AN concentration on the viscoelastic (flow) properties is related to the change in the molecular conformation of the surfactant at the interface and to the structure of the AN solution:

- Ion-ion interaction begins to dominate in the aqueous phase at a high AN concentration that results in a more shear-resistant microstructure of the solution and leads to the progressive increase in emulsion droplet size with increasing AN concentration. Besides this, it was shown that the droplet film becomes more stable and presumably more rigid (due to a change in the chain conformation of the surfactant at the interface (Chattopadhyay *et al.*, 1992; Ghaicha *et al.*, 1993) and increased lateral interactions of surfactant molecules due to dehydration of the hydrophilic portion of the surfactant (Solans *et al.*, 1993)) that makes the shearing process more difficult in the presence of salt (Solans *et al.*, 1993; Martinez *et al.*, 2007).
- On the other hand, increasing interdroplet repulsive interactions induced by the presence of salt in the aqueous phase may also affect the rheological properties due to increased droplet compression that will result in higher values of the linear viscoelastic functions associated with a relatively higher elastic response.

5.1.2.2 Effect of electrolyte type on rheological properties

Since the electrolyte concentration (ionic strength in solution) affects the rheological properties and emulsion stability, it is reasonable to investigate the effect of pH and different electrolytes on the emulsion properties. This part of the study presents the investigation of interfacial and rheological properties regarding the pH and different electrolyte type effects.

The evolution of the DSD of prepared samples is shown in Figure 5.12.

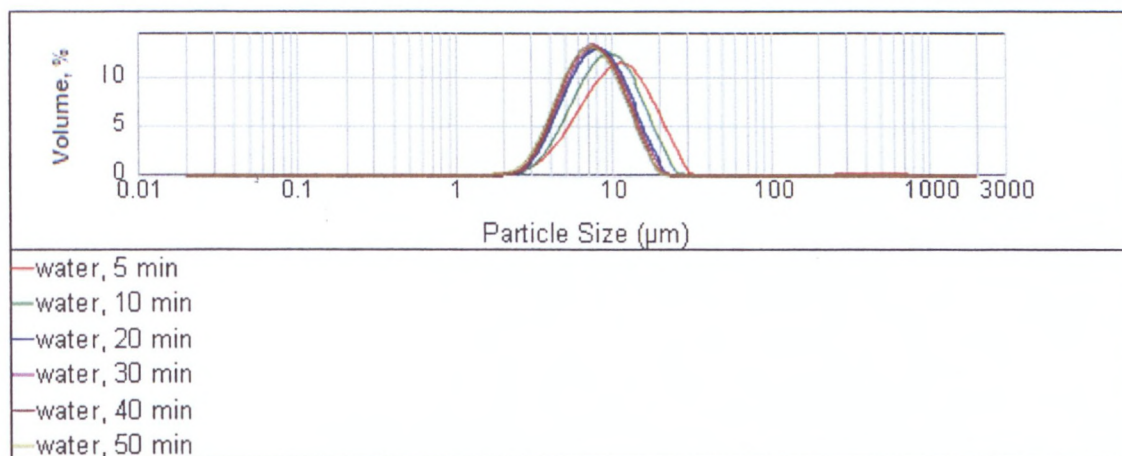


Figure 5.12: Histogram of drop size distribution of the water emulsion at different mixing times

The droplet size distribution of other studied samples is similar to this and all the graphs are presented in Appendix C.

All the emulsions were mixed for a long time to reach the critical diameter value (D_{lim}). Typical experimental results of droplet size evolution for emulsions with different salts in the aqueous phase are shown in Figure 5.13.

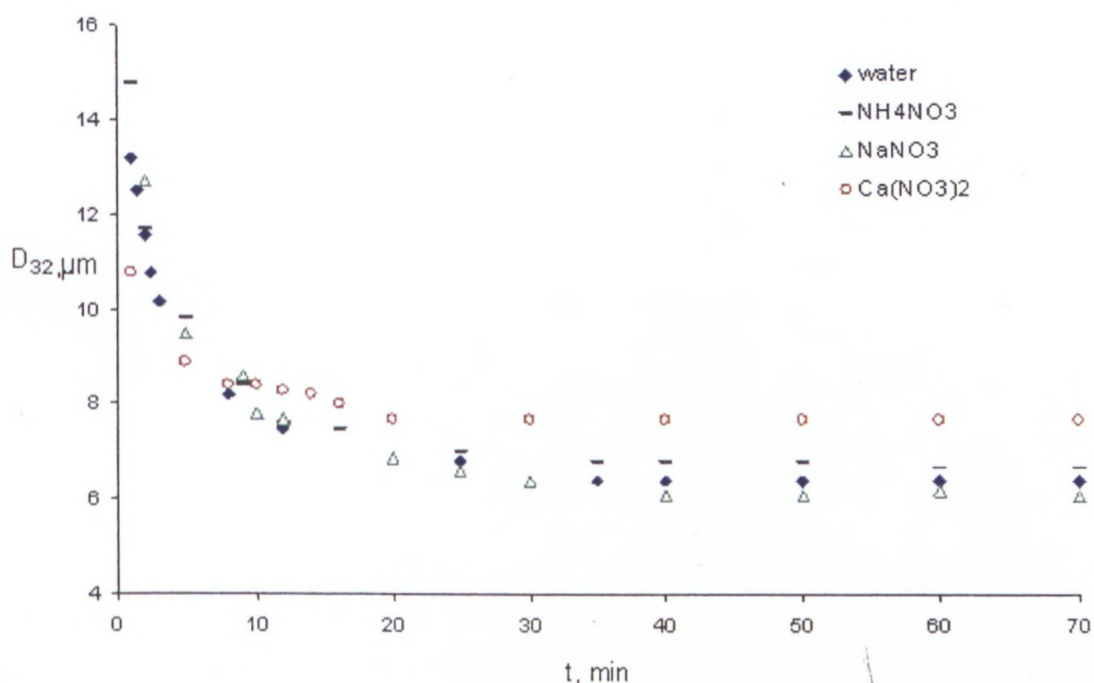


Figure 5.13: Droplet size as a function of mixing time for emulsions with water, AN, SN and CN solutions as an aqueous phase

Equation 5.1 was used for D_{lim} determination.

The fit of data for the water emulsion is presented in Figure 5.14.

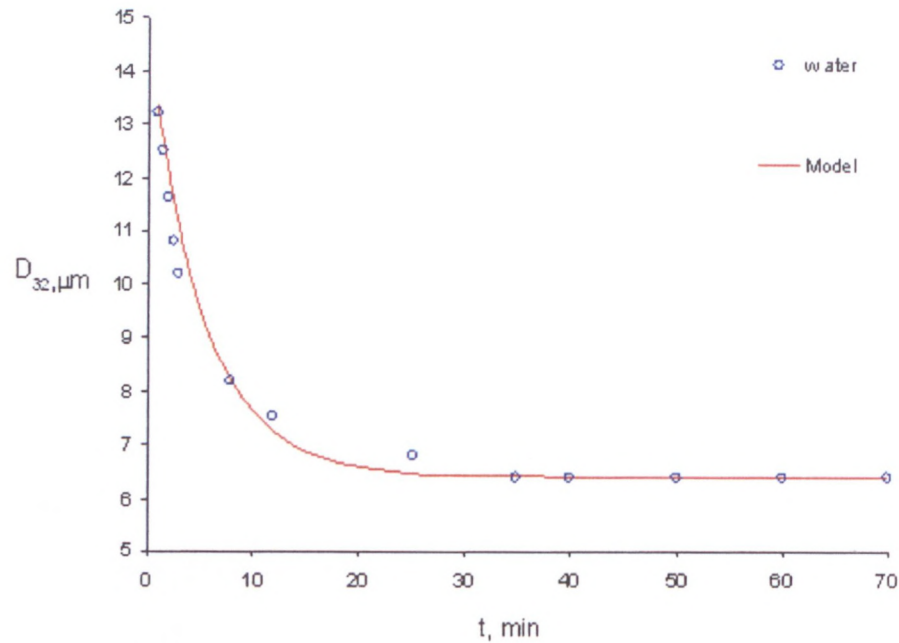


Figure 5.14: Droplet size as a function of mixing time for an emulsion with water as an aqueous phase

The values of D_{lim} obtained from fittings are summarised in Table 5.6.

Table 5.6: Critical diameter of emulsions with different salts in the aqueous phase

<i>Aqueous phase</i>	<i>$D_0, \mu m$</i>	<i>$D_{lim}, \mu m$</i>	<i>Θ, min</i>
<i>$NaNO_3$</i>	13.8	6.1	7.5
<i>Water</i>	14.8	6.4	5.2
<i>NH_4NO_3</i>	15.5	6.8	5.1
<i>$Ca(NO_3)_2$</i>	11.3	7.7	5.6

From the obtained results presented in Table 5.6, the following can be seen:

- The droplet refinement depends on the cation type present in the aqueous phase. The difference is especially evident between the single- and double-charge cations.
- The critical droplet size of the studied emulsions can be described by the following trend:

$$Na^+ < H_3O^+ < NH_4^+ < Ca^{2+}.$$

5.1.2.2.1 Viscoelastic and flow properties

The viscoelastic and flow properties were measured using the same settings as was described previously. The results obtained for the emulsions with the presence of different cations in the aqueous phase are given below, in Figures 5.15 and 5.16.

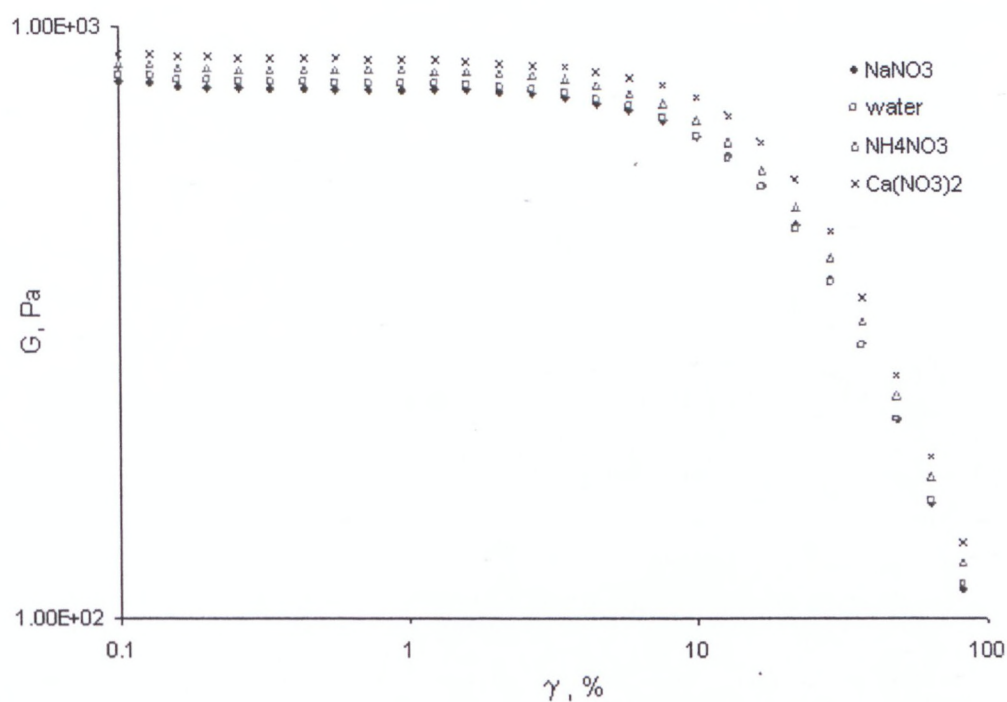


Figure 5.15: Storage modulus as a function of electrolyte type presence in the aqueous phase

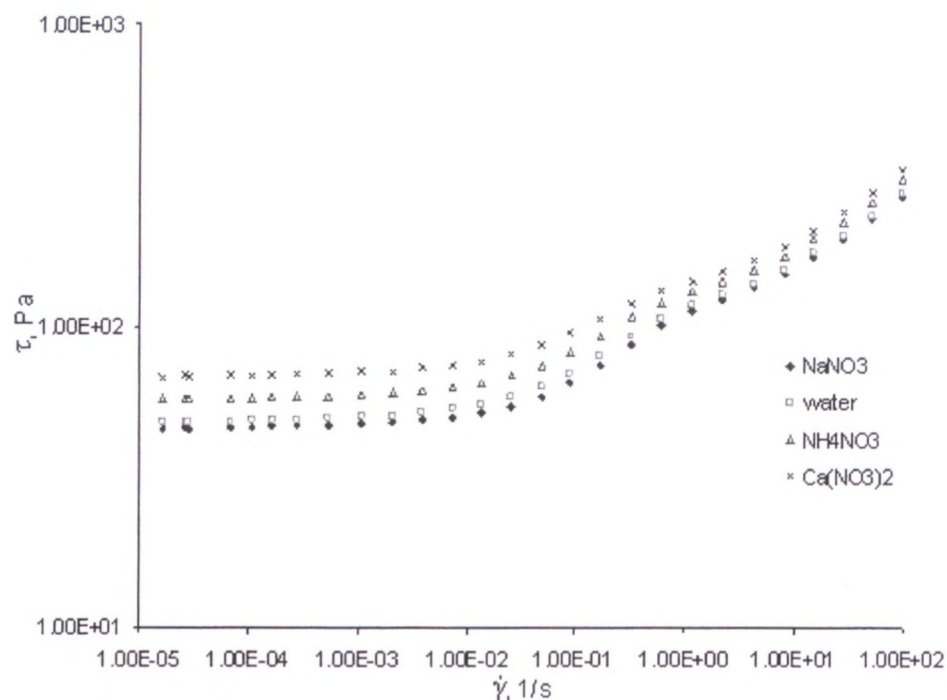


Figure 5.16: Yield Stress as a function of electrolyte type presence in the aqueous phase

The values for the above are listed in Table 5.7.

Table 5.7: Storage Modulus and Yield Stress dependence on the type of salt added to the aqueous phase

<i>Aqueous phase</i>	G_0, Pa	τ_y, Pa
$NaNO_3$	785	45
<i>Water</i>	804	50
NH_4NO_3	843	54
$Ca(NO_3)_2$	883	67

- The viscoelastic and flow properties (Storage Modulus and Yield Stress, respectively) of emulsions with different salt types in the aqueous phase show an apparent reduction as a function of cation type in the following order: $Ca^{2+} > NH_4^+ > H_3O^+ > Na^+$. These results corresponded well with the trend observed in the critical diameter values.
- Elastic modulus and yield stress do not follow the trend observed in interfacial tension measurements (see the following section). This reflects additional sources that govern the rheological properties.

5.1.2.2.1.1 Scaling by Laplace pressure

It is more instructive to plot the data in the $G/(\gamma/R)$ - γ coordinates, γ being the interfacial tension, and R being the mean drop radius. This type of plot provides the possibility of comparing the results with exclusion of the effects of particle size and interfacial tension (Dimitrova & Leal-Caledron, 2004).

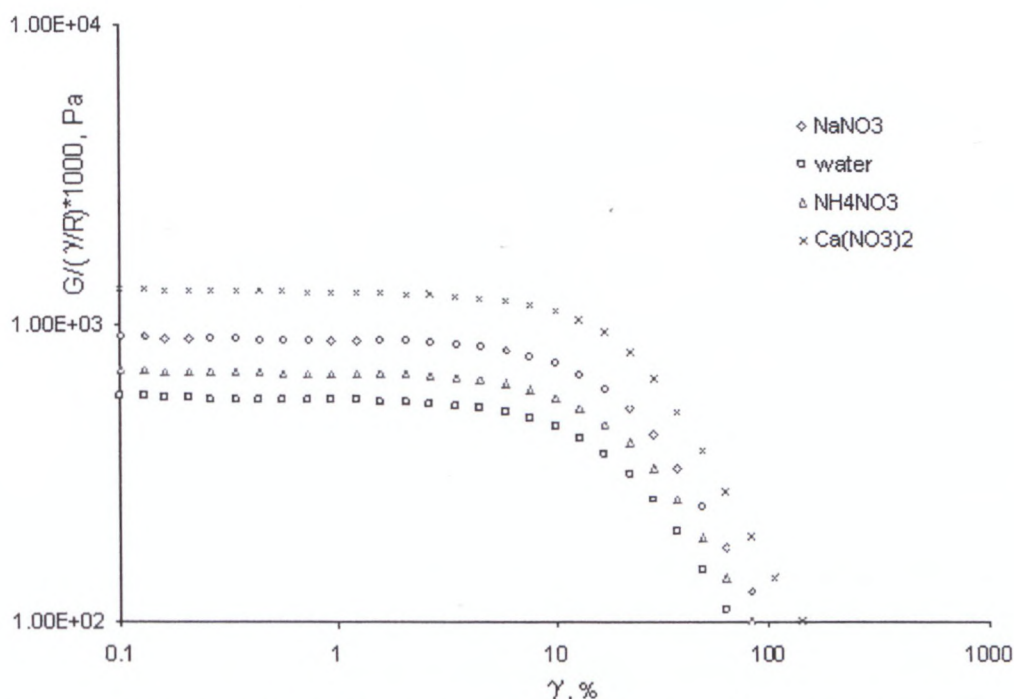


Figure 5.17: Storage modulus as a function of electrolyte type scaled by Laplace pressure

- It is clearly seen that the curves do not merge after the scaling procedure. This shows that an additional source of elasticity is present in the system. Moreover, the trend in the viscoelastic properties changed for $\text{Ca}^{2+} > \text{Na}^+ > \text{NH}_4^+ > \text{H}_3\text{O}^+$ after the effect of interfacial tension on the storage modulus was removed.

It is apparent that the storage modulus tends to increase with the increasing charge density of cations ($\text{NH}_4^+ > \text{Na}^+ > \text{Ca}^{2+}$). It is reasonable to assume that the charge of the droplets increases in the same way, therefore the observed differences can be attributed primarily to the increased repulsive interactions (steric and electrostatic) between the droplets. The steric repulsion in this case can be derived from surfactant-electrolyte interactions (hydrogen bonding network, attraction between ions and Pibsa-MEA head group) which affect the orientation of the surfactant head group/tail at the interface (see sections 4.1.1.2 and 4.1.2.1.2). These strong interactions can probably bring the head groups closer to each other (associate them) and result in higher lateral interactions between the surfactant tails and increase the steric repulsion between the droplets, and result in higher Storage Modulus and

Yield Stress. The ability of sodium and ammonium ions to interact with the head group seems to be lower in comparison with the calcium ion and this has possibly led to the weaker steric repulsion. The electrostatic repulsion between drops could possibly arise from the different droplet charges, due to the presence of differently charged ions (Ca^{++} , Na^+ , NH_4^+). In this case, repulsion increases in the same order as the charge density of cations ($\text{Ca}^{++} > \text{Na}^+ > \text{NH}_4^+$).

5.1.3 General conclusion regarding the effect of surfactant type and the AN concentration/composition of the aqueous phase on the rheological properties of highly concentrated emulsions

The type of surfactant influences the rheological properties of explosive emulsions. In fact, both the elastic modulus and the yield stress decrease in the following order: Pibsa-MEA > Pibsa-IMIDE > Pibsa-UREA > Pibsa-MEA/SMO. In the linear regime, the dimensionless elastic modulus was found to depend on the type of surfactant. This was an indication of the existence of additional sources of elasticity in the system. The differences in elasticity shown by different surfactant types used in this study could have resulted from the combination of interfacial properties (interfacial tension and interfacial dilatational modulus which are governed by surfactant interactions at the W/O interface) and the Van der Waals attraction, and ion-fluctuation attraction as an additional source of elasticity. Due to their different influences on surfactant-electrolyte interactions, different surfactant types induce different interfacial properties and could induce a different balance of repulsive forces-attractive forces in the thin film between droplets; therefore, different contributions of additional elasticity.

The effect of the AN concentration and salt composition in the aqueous phase has been investigated. From the experimental results it could be concluded that the rheological properties of the emulsions studied were significantly influenced by salt content and the composition of an aqueous phase.

In general, salt addition produces a progressive increase of viscoelastic and flow parameters (Aronson & Petko, 1993; Martinez *et al.*, 2006) and improves emulsion stability against freezing (Ganguly *et al.*, 1992). The effect of the salt (AN) concentration on the Storage Modulus and Yield Stress could be related to the following:

- Addition of the salt (AN) to the aqueous phase of the emulsion stabilises the interface due to the interaction with the surfactant. The hydrogen bonding and salt (complex)

formation between the salt ions and surfactant head group allow the surfactant molecule to anchor better at the interface and probably affect the tail conformation at the interface, leading to the more developed interactions between the chains that result in a more rigid and more shear-resistant structure at the interface.

- Increasing the AN concentration in the aqueous phase results in structural changes in the solution due to the domination of ion-ion interactions in comparison with ion-solvent interactions (Adya & Nielson, 1991). These changes result in a more shear-resistant microstructure of the solution.

CHAPTER 6

SUMMARY

The interfacial properties and interactions and emulsion stability to crystal initiation were investigated in the present study. The rheological investigation was undertaken as an application of the first two investigations. The effect of surfactant and electrolyte type/concentration on the interfacial properties and interactions, stability and rheological properties was studied experimentally.

The measurements included the following:

- Interfacial tension and interfacial elasticity
- IR spectra of the aqueous phases and emulsions
- Emulsion freezing temperature
- Viscoelastic and flow properties

It was confirmed that the surfactant and electrolyte type/concentration play an important role in emulsion stability and affect the interfacial and rheological properties of emulsions. The FT-IR data indicated that there are interactions between the surfactant head group and the electrolyte present in the aqueous phase (Ganguly *et al.*, 1992; Ghaicha *et al.*, 1993; Yubai *et al.*, 1996; Maheshwari & Dhathathreyan, 2004). Such interactions can appear in the form of hydrogen bonds and salt (complex) formation or dipole-dipole interactions. The results obtained for the Pibsa-based surfactants indicated that the strength and type of these possible interactions depend on the chemical structure of the surfactant head group, as well as on electrolyte concentration and nature, thus influencing the surface activity of the emulsifier; interfacial elasticity, and, as a consequence of these, the emulsion stability and rheological properties. The present research project found, for the first time, that the strength of interactions between the AN solution and surfactant followed the trend Pibsa-MEA > = Pibsa-UREA > Pibsa-IMIDE. Pibsa-MEA and Pibsa-UREA molecules contain more interactive functional groups (COOH, NH₂); this provides stronger binding and anchoring of the surfactant at the interface in comparison with Pibsa-IMIDE. The presence of COOH and NH₂ functional groups in the chemical structure of the head group increases the degree of attraction between surfactant and droplet. These are higher for Pibsa-MEA and Pibsa-UREA among the three polymeric surfactants studied.

The research indicated the extent of the factors influencing the attraction between Pibsa-based surfactants and emulsion droplets; they are following:

- The polarity of the head group which leads to the solubility in the aqueous phase (the polarity of the surfactant head group is one of the factors which affect the interfacial behaviour of a surfactant and greater polarity results in stronger attraction of the surfactant to the aqueous phase).
- The ability to form hydrogen bonds (the presence of COOH and OH groups seems to be necessary). Increasing the hydrogen bond network at the interface leads to stronger attraction of the surfactant to the aqueous phase.
- The ability to form salt with oxidizer ions (the presence of COOH and the NH group seems to be important).

It could be suggested that all these factors are important to consider in designing more efficient emulsifiers for emulsion stabilisation.

The interfacial properties (interfacial tension and interfacial elasticity) are governed by the interaction of the surfactant with the matter of droplets and by the chemical structure of molecules. The stronger interaction of Pibsa-MEA or Pibsa-UREA results in higher interfacial tension and interfacial elasticity (due to conformational rearrangement at the interface), while less interactive surfactants (Pibsa-IMIDE or SMO) lead to the lowering of interfacial tension and elasticity/strength of the interface (due to increased surfactant concentration at the interface). It has been shown that SMO molecules are present at the interface and compete with the Pibsa-MEA in the monolayer. An admixture of SMO to the Pibsa-MEA results in lower interfacial tension in comparison with pure Pibsa-MEA surfactant, due to the presence of SMO at the interface, and in reducing the interaction of Pibsa-MEA with the aqueous phase and between the surfactant tail groups.

The type of surfactant influences the rheological properties of explosive emulsions. In fact, both the elastic modulus and the yield stress decrease in the following order: Pibsa-MEA > Pibsa-IMIDE > Pibsa-UREA > Pibsa-MEA/SMO. In the linear regime, the dimensionless elastic modulus was found to depend on the type of surfactant. This was an indication of the existence of additional sources of elasticity in the system. The differences in elasticity shown by different surfactant types used in this study could have resulted from the combination of interfacial properties (interfacial tension and interfacial dilatational modulus, which are governed by surfactant interactions at the W/O interface) and the Van der Waals attraction, and ion-fluctuation attraction as an additional source of elasticity. Due to their different influences on

surfactant-electrolyte interactions, different surfactant types induce different interfacial properties and could induce a different balance of repulsive forces-attractive forces in the thin film between droplets; therefore, make different contributions of additional elasticity.

The effect of the content and nature of electrolytes on rheological properties was also observed. In general, salt addition produces an increase of viscoelastic and flow parameters (Aronson & Petko, 1993; Martinez *et al.*, 2006). The effect of salt (AN) concentration on the Storage Modulus and Yield Stress was attributed to the following:

- Addition of salt (AN) to the aqueous phase of an emulsion stabilises the interface, due to the interaction with the surfactant. The hydrogen bonding and salt (complex) formation between the salt ions and surfactant head group allow the surfactant molecule to anchor better at the interface and probably affect the tail conformation at the interface, thereby leading to more developed interactions between the chains, which result in a more rigid and more shear-resistant structure at the interface.
- Increasing the AN concentration in the aqueous phase results in structural changes in the solution due to the domination of ion-ion interactions in comparison with ion-solvent interactions (Adya & Nelson, 1991). These changes result in a more shear-resistant microstructure of the solution.

The influence of the nature of the salt on the rheological properties was related to the differences in strength of steric and electrostatic repulsion between the droplets, which followed the trend observed in the cation density charge for the studied salts ($\text{Ca}^{2+} > \text{Na}^+ > \text{NH}_4^+$). The steric repulsion in this case can be derived from surfactant-electrolyte interactions (hydrogen bonding network, attraction between ions and Pibsa-MEA head group) which influence the orientation of the surfactant head group/tail at the interface. The results suggested stronger interaction of the surfactant with the Ca^{2+} ions, followed by Na^+ and NH_4^+ leading to stronger steric repulsion between droplets. Electrostatic repulsion between drops probably could be stronger in the of the $\text{Ca}(\text{NO}_3)_2$ solution used as an aqueous phase due to the higher cation density charge of calcium ions, followed by sodium and ammonium.

It was shown that DSC analysis can be used as a quick method to determine the emulsion stability. The results obtained in this work are in good agreement with the aging study performed on these emulsions. On the basis of the results obtained in this work, it appears that the freezing behaviour of emulsified aqueous solutions is governed by several factors, the important ones being electrolyte concentration, surfactant concentration and the physico-chemical characteristics of the surfactant (Ganguly *et al.*, 1992). It was found that interfacial

properties (interfacial tension, interfacial elasticity), strength of interactions between the studied surfactant head groups and the matter of droplets follow the same trend as the stability of the emulsion to crystal initiation stabilised by these surfactants (Pibsa-MEA > =Pibsa-UREA > Pibsa-MEA/SMO > Pibsa-IMIDE > SMO). Such similarity in trends leads to the suggestion that there is considerable interdependence between molecular-level behaviour and the bulk properties. These observations might support the fact that the initiation of crystallisation could depend mostly on surfactant-electrolyte interaction and might play a major role in the overall process of crystallisation in the case of emulsions with dissolved electrolytes in the aqueous phase. The weaker interactions/reduction of interactions between surfactant and an aqueous phase lead to an unstable interface and thereby to an unstable emulsion. Moreover, molecular conformation and packing at the interface (governed by interactions of the surfactant head group with the electrolyte) could probably have an impact on the emulsion stability.

Besides this, stability of the AN melt is influenced by the incorporation of Ca^{2+} and Na^+ ions. The overall relaxation of the structure of the AN solution results in separating the NH_4^+ and NO_3^- ions from each other, which leads to the delay of crystallisation. Emulsion stability to coalescence furthermore is affected by the pH of the aqueous phase. Emulsion instability at pH equal to 7 was attributed to the low surfactant solubility in the aqueous phase leading to the lack of a hydrogen bond network and interaction resulting in weak surfactant adsorption at the interface.

The following aspects have not been covered in this thesis and should be investigated:

- Effect of surfactant blends (different ratios of conventional emulsifiers) on interfacial, rheological properties of emulsions and emulsion stability;
- Effect of surfactant molecular weight on the interfacial, rheological properties of emulsions and emulsion stability.

BIBLIOGRAPHY

- Adamson, A.W. 1997. *Physical chemistry of surfaces*. 6th ed. New York: Wiley-Interscience.
- Adya, A.K. & Neilson, G.W. 1991. Structure of a 50 mol kg⁻¹ aqueous solution of ammonium nitrate at 373 K by the isotopic difference method of neutron diffraction. *J Chem. Soc. Faraday Trans.*, 87:279–286.
- Adya, A.K. & Neilson, G.W. 1996. Neutron diffraction results from some nitrate melts. *Journal of Non-Crystalline Solids*, 205-207:168–171.
- Aivarez, O., Mougel, J., Baravian, C., Caton, F., Marchai, P., Stébé, J.M. & Choplin, L. 2006. Aging of an unstable water-in-oil gel emulsion with a nonionic surfactant. *Rheol. Acta*, 45:555–560.
- Aronson, M.P. & Petko, M.F. 1993. Highly concentrated Water-in-Oil Emulsions: Influence of Electrolyte on their properties and stability. *J Colloids and Interface Science*, 159: 134-149.
- Babak, V. G. & Stebe, M-J. 2002. Highly concentrated emulsions: Physicochemical Principles of Formulation. *J Dispersion Science and Technology*, 23: 1-22.
- Baker, R. 1971. *Organic chemistry of biological compounds*. Englewood Cliffs, NJ: Prentice-Hall.
- Bampffield, H.A. & Cooper, J. 1988. In Becher, *Encyclopedia of emulsion technology*. New York: Marcel Dekker. vol. 3.
- Barnes, H.A. 2000. *Handbook of elementary rheology*. Aberystwyth: University of Wales Institute of Non-Newtonian Fluid Mechanics.
- Becher, P. 1988. *Encyclopedia of Emulsion Technology*. New York: Marcel Dekker, and Basel, vol. 3.
- Bengtsson, L.A., Frostemark, F. & Holmberg, B. 1994. Speciation, structural characteristics and proton dynamics in the systems NH₄NO₃·1.5H₂O and NH₄NO₃·1.5H₂O –(HNO₃, NH₄F, NH₃)-H₂O at 50°C. *J Chem. Soc. Faraday Trans.*, 90:559–570.
- Bengoechea, C., Cordobés, F. & Guerrero, A. 2006. Rheology and microstructure of gluten and soya-based o/w emulsions. *Rheol. Acta*, 46:3–21.

- Binet, R., Cloutier, J.A.R., Edmonds, A.C.F., Holden, H.W. & McNicol, M.A. Explosive compositions based on time-stable colloidal dispersions. United States Patent. 4 357 184. 1982-11-02.
- Binks, B.P. 1998. *Modern aspects of emulsion science*. Cambridge: The Royal Society of Chemistry.
- Bluhm, H.F. Ammonium nitrate emulsion blasting agent and method of preparing same. United States Patent. 3 447 978, 1967-08-3.
- Boer, W.G. Composition and emulsifier. United States Patent. 6 630 596 B2. 2003-10-07.
- Buzza, D.M.A. & Cates, M.E, 1994. Uniaxial elastic modulus of concentrated emulsions. *Langmuir*, 10:4503–4508.
- Bressy, L., Hebraud, P., Schmitt, V. & Bibette, J. 2003. Rheology of emulsions stabilized by solid interface. *Langmuir*, 19:598–604.
- Chattopadhyay, A.K., Ghaicha, L., Oh, S.G. & Shah, D.O. 1992. Salt effects on monolayers and their contribution to surface viscosity. *J. Physical Chemistry*, 96:6509–6513.
- Chattopadhyay, A.K. Emulsion explosive. United States Patent. 5 500 062. 1996-03-19.
- Chen, C-M., Lu, C-H., Chang, C-H., Yang Y-M. & Maa, J-R. 2000. Influence of pH on the stability of oil-in-water emulsions stabilized by a splittable surfactant. *Colloids and Surfaces A*, 170:173–179.
- Clare, D.A., Lillard, S.J., Ramsey, S.R., Amato, P.M. & Daubert, C.R. 2007. Calcium effects on the functionality of a modified whey protein ingredient. *Journal of agricultural and food chemistry*, 55:10932–10940.
- Clausse, D., Gomez, F., Pezron, I., Komunjer, L. & Dalmazzone, C. 2005. Morphology characterization of emulsions by differential scanning calorimetry. *Advances in Colloid and Interface Science*, 117:59–74.
- Cooper, J. & Baker, A.S. Emulsion explosive composition. United States Patent. 4 822 433. 1989-04-18.

Coupland, J.N. 2002. Crystallization in emulsions. *Current opinion in Colloid and Interface Science*, 7:445–450.

Dickinson, E. 2001. Milk protein interfacial layers and the relationship to emulsion stability and rheology. *Colloids and Surfaces*, 20: 197-210.

Dimitrova, T.D. & Leal-Calderon, F. 2001. Bulk elasticity of concentrated protein-stabilized emulsions. *Langmuir*, 17(11):3235–3244.

Dimitrova, T.D. & Leal-Calderon, F. 2004. Rheological properties of highly concentrated protein-stabilized emulsions. *Advances in Colloid & Interface Science*, 108–109:49–61.

Dittrich, M. & Sibling, S. 2006. Influence of H and Calcium Ions on surface functional groups of *Synechococcus* PCC 7942 Cells. *Langmuir*, 22:5435–5442.

Domenicano, A. & Hargittai, I. 2002. *Strength from weakness: Structural consequences of weak interactions in molecules, supermolecules, and crystals*. Netherlands: Kluwer Academic Publishes.

Feuz, L. 2006. On the conformation of graft-copolymers with polyelectrolyte backbone in solution and adsorbed on surfaces. Doctor of Science thesis. Swiss Federal Institute of Technology, Zurich, Switzerland.

Forsberg, J.W. Salt compositions for explosives. United States Patent. 4 828 633. 1989-05-09.

Franco, J.M., Berjano, M. & Gallegos, C. 1997. Linear viscoelasticity of salad dressing emulsions. *J. Agric. Food Chem.*, 45:713–719.

Franco, J.M., Guerrero, A. & Gallegos, C. 1995. Rheology and processing of salad dressing emulsions. *Rheol. Acta*, 34:513–524.

Ganguly, S., Mohan, V.K., Bhasu, V.C.J., Mathews, E., Adisheshaiah, K.S. & Kumar, A.S. 1992. Surfactant-electrolyte interactions in concentrated water-in-oil emulsions: FT-IR spectroscopic and low-temperature differential scanning calorimetric studies. *Colloid and surfaces*, 65:243–256.

Guerrero, A., Partal, P. & Gallegos, C. 1998. Linear viscoelastic properties of sucrose ester-stabilized oil-in-water emulsions. *J. Rheol.*, 42:1375–1388.

- Garti, N. 2000. *Thermal behavior of dispersed systems*. New York: Marcel Dekker.
- Ghaicha, L., Leblanc, R.M., & Chattopadhyay, A.K. 1993. Influence of concentrated ammonium nitrate solution on monolayers of some dicarboxylic acid derivatives at the air/water interface. *Langmuir*, 9:288–293.
- Ghaicha, L., Leblanc, R.M., Villamagna, F. & Chattopadhyay, A.K. 1995. Monolayers of mixed surfactants at the oil-water interface, hydrophobic interactions, and stability of water-in-oil emulsions. *Langmuir*, 11:585–590.
- Goodwin, J.W. & Hughes, R.W. 2000. *Rheology for chemists*. Cambridge: The Royal Society of Chemistry.
- Grassi, M., Lapasin, R. & Prici, S. 1996. A study of the rheological behaviour of scleroglucan weak gel systems. *Carbohydrate Polymers*, 29:169–181.
- Hackley, V.A. & Ferraris, C.F. 2001. *Guide to Rheological Nomenclature: Measurements in Ceramic Particulate Systems*. National Institute of Standards and Technology, Special Publication 949.
- Hales, R.H., Cranney, D.H., Hurley, E.K. & Preston, S.B. Emulsion phase having improved stability. United States Patent. 6 808 573 B2. 2004-10-26.
- Hemar, Y., Hocquart, R. & Lequeux, F. 1995. Effect of interfacial rheology on foams viscoelasticity, an effective medium approach. *J. Phys. II France*, 5:1567–1576.
- Hemar, Y. & Horne, D.S. 2000. Dynamic rheological properties of highly concentrated protein-stabilized emulsions. *Langmuir*, 16:3050–3057.
- Hiemenz, P.C. 1986. *Principles of Colloids and Surface Chemistry*. 2nd ed. New York: Marcel Dekker.
- Hiemenz, P.C. & Rajagopalan, R. 1997. *Principles of colloid and surface chemistry*. New York: Marcel Dekker.
- Holmberg, K., Jönsson, B., Kronberg, B. & Lindman, B. 2002. *Surfactants and polymers in aqueous solution*. 2nd edition. Chichester: Wiley & Sons.
- Hunter, R.J. 1993. *Introduction to Modern Colloid Science*. Oxford: Oxford University Press.

- Israelachvili, J.N. 1992. *Intermolecular and Surface Forces*. London: Academic Press.
- Jager-Lézer, N., Tranchant, J.-F., Alard, V., Vu, C., Tchoreloff, P.C. & Grossiord, J.-L. 1998. Rheological analysis of highly concentrated w/o emulsions. *Rheol. Acta*, 37:129–138.
- Kent, P. & Saunders, B. R. 2001. The role of electrolyte in the stabilization of inverse emulsions. *J Colloid and Interface Science*, 242: 437-442.
- Khan, S.A. & Armstrong, R.G. 1986. Rheology of foam. I. Theory for dry foams. *J. non-Newt. Fluid Mech.*, 22:1–22.
- Kharatiyan, E. 2005. Time effects in evolution of structure and rheology of highly concentrated emulsions. Unpublished DTech thesis, Cape Peninsula University of Technology, Cape Town, South Africa.
- Khutoryanskiy, V.V., Mun, G.A., Nurkeeva, Z.S. & Dubolazov, A.V. 2004. pH and salt effects on interpolymer complexation via hydrogen bonding in aqueous solutions. *Polymer International*, 53:1382–1387.
- Kizling, J. & Kronberg, B. 2001. On the formation of concentrated stable w/o emulsions. *Advances in Colloid and Interface Science*, 89-90: 395–399.
- Lacasse, M.D., Grest, G.S. & Levine, D. 1996. Deformation of Small Compressed Droplets. *Phys. Rev. E*, 54:5436–5446.
- Lee, S.J. 2006. Emulsion rheology and properties of polymerized high internal phase emulsions. *Korea-Australia Rheol. J.* 18:183–189.
- Macosko, C.W. 1994. *Rheology: Principles, Measurements and Applications*, New York: VCH Publishers.
- Madiedo, J.M. & Gallegos, C. 1997. Rheological characterization of oil-in-water emulsions by means of relaxation and retardation spectra. *Recent Res. Dev. Oil Chem.*, 1:79–90.
- Maheshwari, R. & Dhathathayan, A. 2004. Influence of ammonium nitrate transitions of Langmuir and Langmuir-Blgett films at air/solution and solid/solution interfaces. *J Colloid and Interface Science*, 275: 270-276.
- Malkin, A. Ya. 1994. *Rheology Fundamentals*. Canada: ChemTac Publishing.

- Malkin, A. Ya. & Masalova, I. 2007. Shear and normal stresses in flow of highly concentrated emulsions. *J. Non-Newtonian Fluid Mech.*, 147:65–68.
- Malkin, A. Ya., Masalova, I., Slatter, P. & Wilson, K. 2004a. Effect of droplet size on the rheological properties of highly-concentrated w/o emulsions. *Rheol. Acta*, 43:584–591.
- Manca, S., Lapasin, R., Partal, P. & Gallegos, C. 2001. Influence of surfactant addition on the rheological properties of aqueous Welan matrices. *Rheol. Acta*, 40:128–134.
- Masalova, I. & Malkin, A.Ya. 2007a. Peculiarities of rheological properties and flow of highly concentrated emulsions: The role of concentration and droplet size. *Colloid Journal*, 69(2):185–197.
- Masalova, I. & Malkin, A.Ya. 2007b. A new mechanism of aging of highly concentrated emulsions: correlation between crystallization and plasticity. *Colloid Journal*, 69(2):198–202.
- Masalova, I. & Malkin, A.Ya. 2007c. Rheology of highly concentrated emulsions - Concentration and droplet size dependencies. *Appl. Rheol.*, 17(4):1–9.
- Masalova, I., Malkin, A. Ya, Ferg, E., Taylor, M., Kharatiyan, E. & Haldenwang, R. 2006. Evolution of rheological properties of highly concentrated emulsions with aging—Emulsion-to-suspension transition. *J. Rheol.*, 50(4):435–451.
- Masalova, I., Malkin, A.Ya., Slatter, P. & Wilson, K. 2003a. The rheological characterization and pipeline flow of high concentration water-in-oil emulsions. *J. Non-Newtonian Fluid Mech.*, 112:101–114.
- Masalova, I., Malkin, A.Ya. & Slatter, P. 2003b. Effect of droplet size on the rheological properties of super-concentrated emulsions. *Proc. First Annual Rheology Conference, date? Guimaraes (Portugal)*.
- Mason, T.G., Bibette, J. & Weitz, D.A. 1996. Yielding and flow of monodisperse emulsions. *J. Colloid Int. Sci.*, 179:439–448.
- Mason, T.G., Lacasse, M.-D., Grest, G.S., Levine, D., Bibette, J. & Weitz, D.A. 1997. Osmotic pressure and viscoelastic shear moduli of concentrated emulsions. *Phys. Rev. E*: 56(3):3150–3166.

- Martinez, I., Riscardo, M.A. & Franco, J.M. 2007. Effect of salt content on rheological properties of salad dressing-type emulsions stabilized by emulsifier blends. *Journal of Food Engineering*, 80:1272–1281.
- McClements, D.J. 1999. *Food Emulsion: Principles, Practice, and Techniques*. New York: CRC Press LLC.
- McClements, D.J. 2005. *Food Emulsion: Principles, Practice, and Techniques*. New York: CRC Press LLC.
- McKenzie, L.F. & Lawrence D.L. Emulsion explosives containing a polymeric emulsifier. United States Patent. 4 931 110. 1989-01-05.
- McKenzie, L.F. Stabilized emulsion explosive and method. United States Patent. 5 086 867. 1990-12-31.
- Mezger, T.G. 2002. *Handbook of rheology*. New York: Vincents.
- Moses, J.P., Inayathullah, N.M., Murugesan, M., Andrews M.E., Balasubramanian, M.P. & Jayakumar, R. 2003. Effect of Ca^{2+} on the self assembly of a nonionic peptide aggregate. *Letters in Peptide Science*, 10:25–32.
- Morrison, R.T. & Boyd, R.N. 1987. *Organic chemistry*. 5th ed. Massachusetts: Allyn & Bacon.
- Myers, D. 1992. *Surfactant science and technology*. 2nd ed. New York: VCH Publishers.
- Myers, D. 1999. *Surfaces, interfaces and colloids. Principles and applications*. 2nd ed. New York: Wiley VCH.
- Neilson, G.W. & Tromp, R.H. 1991. Neutron and X-ray diffraction on aqueous solutions. *Annu. Rep. Prog. Chem. Sect. C: Phys. Chem.*, 88:45–75.
- Nguyen, A.D. Chemically gassed emulsion explosive. United States Patent. 4 997 494. 1991-03-5.
- Opawale, F. O. & Burgess, D. J. 1997. Influence of interfacial properties of lipophilic surfactants on water-in-oil emulsion stability. *J of Colloid and Interface Science*, 197: 142-150.

- Oxley, J.C., Kaushik, S.M. & Gilson, N.S. 1992. Thermal stability and compatibility of ammonium nitrate explosives on a small and large scale. *Thermochimica Acta*, 212:77–85.
- Pal, R. 1997. Scaling of relative viscosity of emulsions, *J. Rheol.*, 41:141–150.
- Pal, R. 2000a. Slippage during the flow of emulsions in rheometers. *Colloids Surf.*, 162:55–66.
- Pal, R. 2000b. Linear viscoelastic behaviour of multiphase dispersions. *J. Colloid Interface Sci.*, 232:50–63.
- Pal, R. 2001. Novel viscosity equations for emulsions of two immiscible liquids. *J. Rheol.*, 45:509–520.
- Palierne, J.P. 1990. Linear rheology of viscoelastic emulsions with interfacial tension. *Rheol. Acta*, 29:204–214.
- Papke, B.L. & Robinson, L.M. 1994. Factors affecting Poly(isobutenyl)succinimide dispersant adsorption onto surfactant-coated colloidal particles in nonaqueous media. *Langmuir*, 10:1741–1748.
- Para, G., Jarek, E. & Warszynski, P. 2006. The Hofmeister series effect in adsorption of cationic surfactants – theoretical description and experimental results. *Advances in Colloid and Interface Science*, 122:39–55.
- Park, C.I., Cho, W.-G. & Lee, S.G. 2003. Emulsion stability of cosmetic creams based on water-in-oil high internal phase emulsions. *Rheology Journal*, 15:125–130.
- Pedraza, E.P. & Soucek, M.D. 2008. Influence of acid-base pairs on film formation and catalysis for acidic acrylic latexes. *Progress in Organic Coatings*, 62:417–424.
- Petersen, P.B. & Saykally, R.J. 2006. On the nature of ions at the liquid water surface. *Annual Review in Physical Chemistry*, 57:333–364.
- Perrin, P. 2000. Droplet-droplet interactions in both direct and inverse emulsions stabilized by a balanced amphiphilic polyelectrolyte. *Langmuir*, 16(3):881–884.
- Pons, R., Solans, C. & Tadros, T.F. 1995. Rheological behaviour of highly concentrated oil-in-water (o/w) emulsions. *Langmuir*, 11:1966–1971.

- Princen, H.M. 1983. Rheology of foams and highly concentrated emulsions. I. Elastic properties and yield stress of a cylindrical modes system. *J. Colloid & Interface Sci.*, 91:160–175.
- Princen, H.M. & Kiss, A.D. 1986. Rheology of foams and highly concentrated emulsions. IV. An experimental study of the shear viscosity and yield stress of concentrated emulsions. *J. Colloid & Interface Sci.*, 128:176–187.
- Princen, H.M. & Kiss, A.D. 1989. Rheology of foams and highly concentrated emulsions. IV. An experimental study of the shear viscosity and yield stress of concentrated emulsions. *J. Colloid & Interface Sci.*, 128:176–187.
- Radeva, T. 2001. *Physical chemistry of polyelectrolytes*. New York: Marcel Dekker.
- Reinelt, D.A. & Kraynik, A.M. 1989. Viscous effects in the rheology of foams and concentrated emulsions. *J. Colloid Int. Sci.*, 132:491–503.
- Reinelt, D.A. & Kraynik, A.M. 1990. On the shearing flow of foams and concentrated emulsions. *J. Fluid Mech.*, 215:431–455.
- Reynolds, P.A., Gilbert, E.P & White, J.W. 2000. High internal phase water-in-oil emulsions studied by small angle neutron scattering. *J Physical Chemistry B*, 104:7012–7022.
- Reynolds, P.A., Gilbert, E.P. & White, J.W. 2001. High internal phase water-in-oil emulsions and related microemulsions studied by small angle neutron scattering. 2. The distribution of surfactant. *J. Physical Chemistry B*, 105:6925–6932.
- Rosen, M.J. 2004. *Surfactants and interfacial phenomena*. 3d ed. New Jersey: Wiley-Interscience.
- Rudnick, L.R. 2003. *Lubricant additives. Chemistry and applications*. New York: Marcel Dekker.
- Sánchez, M.C., Berjano, M., Brito, E., Guerrero, A. & Gallegos, C. 1998. Evolution of the microstructure and rheology of o/w emulsions during the emulsification process. *Can. J. Chem. Eng.*, 76:479–485.
- Senapati, S. 2007. How strongly can calcium ion influence the hydrogen-bond dynamics at complex aqueous interfaces? *The journal of chemical physics*, 126:204710.

- Shen, Y. & Duhamel, J. 2008. Micellization and adsorption of a series of succinimide dispersants. *Langmuir*, 24(19):10665–10673.
- Sheng, Y-J. & Tsao, H-K. 2004. Electrostatic attraction between neutral microdroplets by ion fluctuations. *Physical review*, 69: 060401.
- Sherman, P. (ed.). 1968. *Emulsion Science*. London: Academic Press.
- Singh, P.K., Singh, V.K. & Singh M. 2007. Zwitterionic polyelectrolytes: A Review. *E-Polymers*, No. 030.
- Sjöblom, J. 2006. *Emulsion and emulsion stability*. 2nd.ed. Boca Raton: Taylor & Francis.
- Solans, C., Pons, R., Zhu, S., Davis, H.T., Evans, D.F., Nakamura, K. & Kunieda, H. 1993. Studies on macro- and microstructure of highly concentrated water-in-oil emulsions (gel emulsions). *Langmuir*, 9:1479–1482.
- Sudweeks, W.B. & Harvey, A.J. Emulsion blasting agent. United States Patent. 4 141 767. 1979-02-27.
- Tadros, T.F. 1994. Fundamental principles of emulsion rheology and their applications. *Colloids and Surface A, Physical and Engineering aspects*, 91:39–55.
- Tadros, T.F. 2005. *Applied surfactants. Principles and applications*. Weinheim: WILEY – VCH.
- Tikhonov, A.M., Patel, H., Garde, S. & Schlossman, M.L. 2006. Tail ordering due to Headgroup hydrogen bonding interactions in surfactant monolayers at the water-oil interface. *The journal of physical chemistry B*, 110:19093–19096.
- Tomlinson, A., Danks, T.N., Heyes, D.M., Taylor, S.E. & Moreton, D.J. 1997. Interfacial characterization of succinimide surfactants. *Langmuir*, 13:5881–5893.
- Tsao, H-K., Sheng, Y-J. & Chen, S-B. 2002. Electrostatic interaction between two aqueous microdroplets in an apolar medium. *Physical review*, 65: 061403.
- Venter, P.N. & Kruger, F. Emulsifier. European Patent. 0 718 033 A2. 1996-06-26.

- Villamagna, F., Whitehead, M.A. & Chattopadhyay, A.K. 1995. Mobility of surfactants at the water-in-oil emulsion interface. *J. Dispersion science and Technology*, 16:105–114.
- Walker, P.A.M., Lawrence, D.G., Neilson, G.W. & Cooper, J. 1989. The structure of concentrated aqueous ammonium nitrate solutions. *J. Chem. Soc. Faraday Trans.*, 85:1365–1372.
- Webber, R.M. 1999. Relation between Laplace pressure and the rheology of high internal phase emulsions. *AIChE*:226–232.
- White, W.J., Henderson, J.M. & Perriman, A. 2004. The crystallization of supersaturated emulsions. *Isis experimental report*. 14591.
- White, W.J., Reynolds, P.A., Hawley, A. & Perriman, A. 2005. Interfacial structure of block copolymers at the oil/water interface. *Isis experimental report*. 15255.
- Xuguang, W. 1994. *Emulsion explosives*. Beijing: Metallurgical industry press.
- Yates, D.E. & Dack, S.W. Emulsion explosive composition. United States Patent. 4 710 248. 1987-12-01. *J Chem. Soc. Faraday Trans.*, 85:1365–1372.
- Yoshimura, T., Nyuta, K. & Esumi, K. 2005. Zwitterionic heterogemini surfactants containing ammonium and carboxylate headgroups. 1. Adsorption and micellization. *Langmuir*, 21:2682–2688.
- Yubai, B., Munger, G., Leblanc, R.M., Ghaicha, L. & Chattopadhyay, A.K. 1996. Crystallization of ammonium nitrate under organized monolayers of various amphiphiles. *J. Dispersion science and Technology*, 17(4):391–405.
- Zhang, Y. & Cremer, P.S. 2006. Interactions between macromolecules and ions: the Hofmeister series. *Current Opinion in Chemical Biology*, 10:658–663.

APPENDICES

APPENDIX A

EFFECT OF SURFACTANT TYPE/CONCENTRATION ON RHEOLOGICAL PROPERTIES
AND PHYSICAL STABILITY OF EMULSIONS

1A. Rheological properties

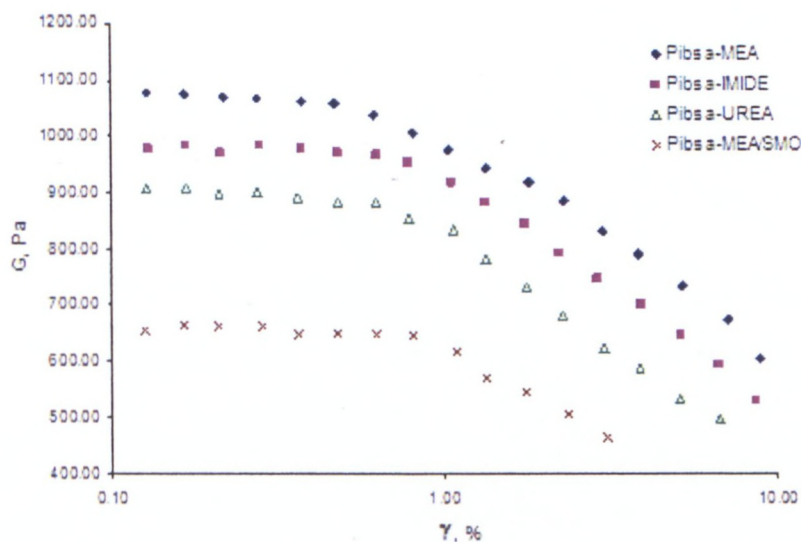


Figure 1. Storage Modulus as a function of surfactant type. DS[3.2] =10 micron

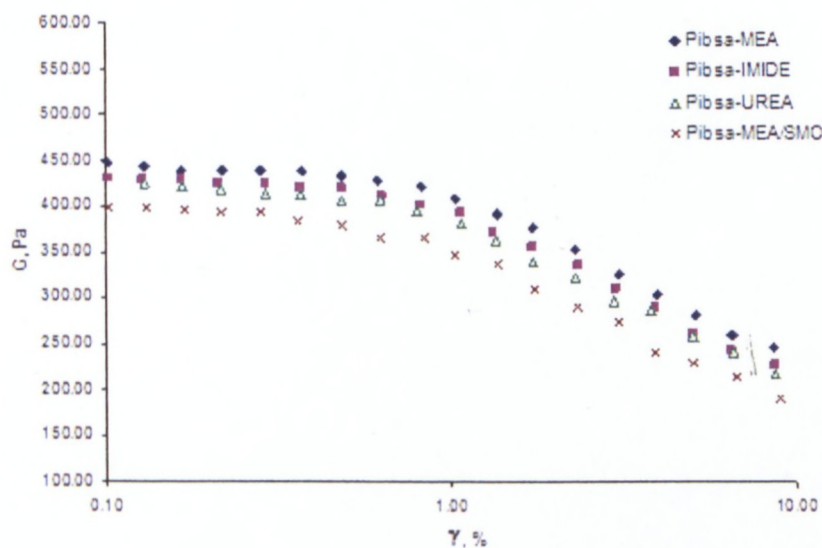


Figure 2. Storage Modulus as a function of surfactant type. DS[3.2] =15 micron

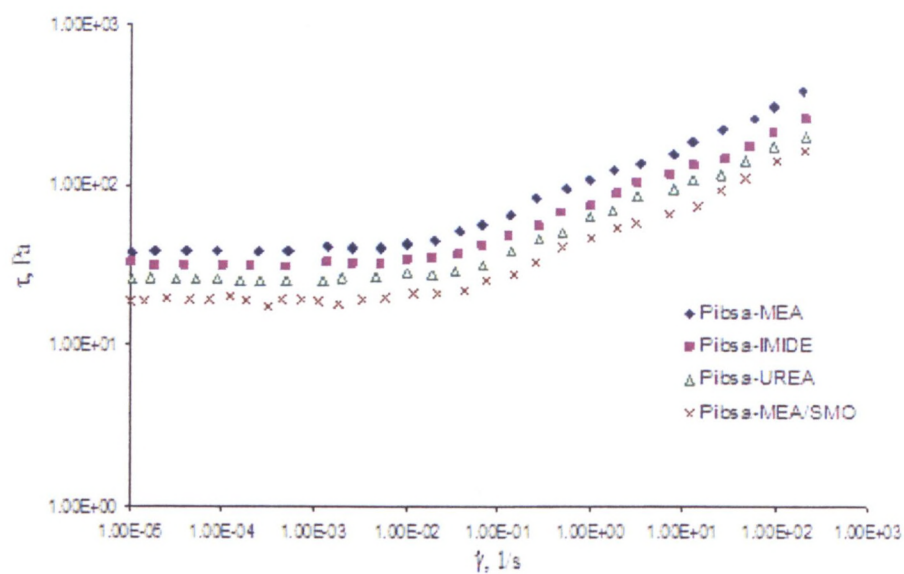


Figure 3. Yield stress as a function of surfactant type. DS[3.2] =10 micron

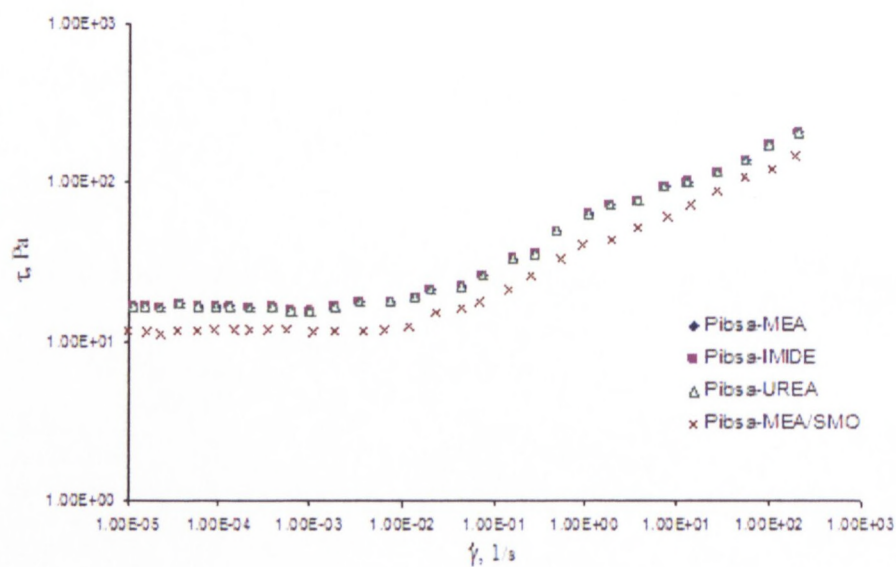


Figure 4. Yield stress as a function of surfactant type. DS[3.2] =15 micron

2A. Interfacial properties

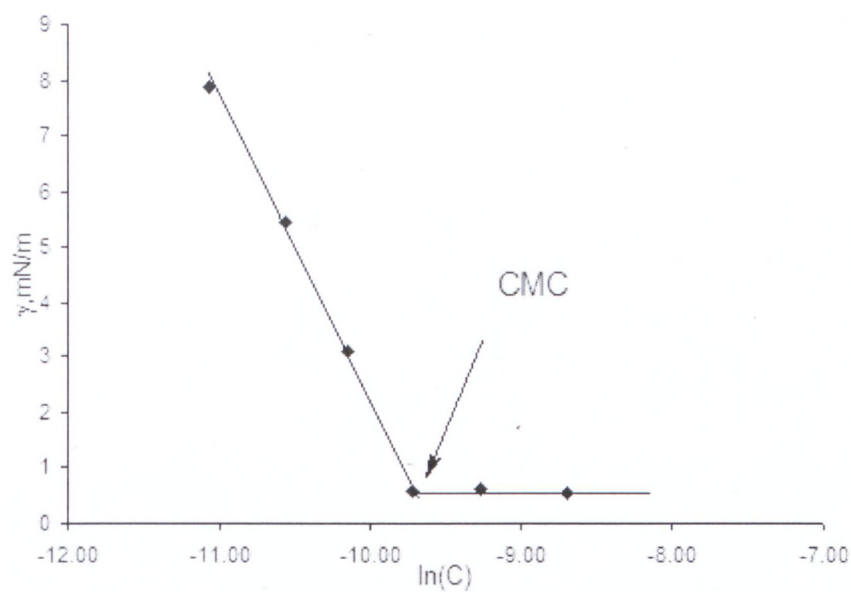


Figure 5. Determination of CMC value of SMO surfactant

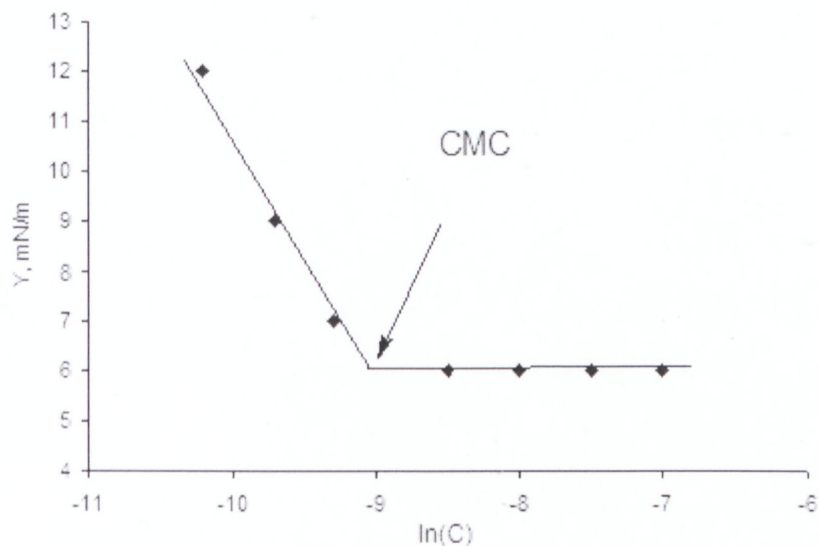


Figure 6. Determination of CMC value of Pibsa-UREA surfactant

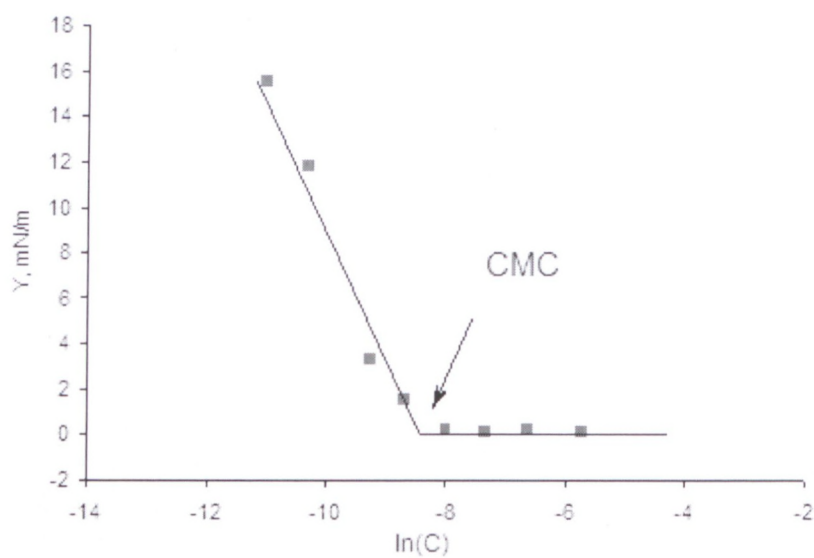


Figure 7. Determination of CMC value of Pibsa-IMIDE surfactant

3A. FT-IR spectra

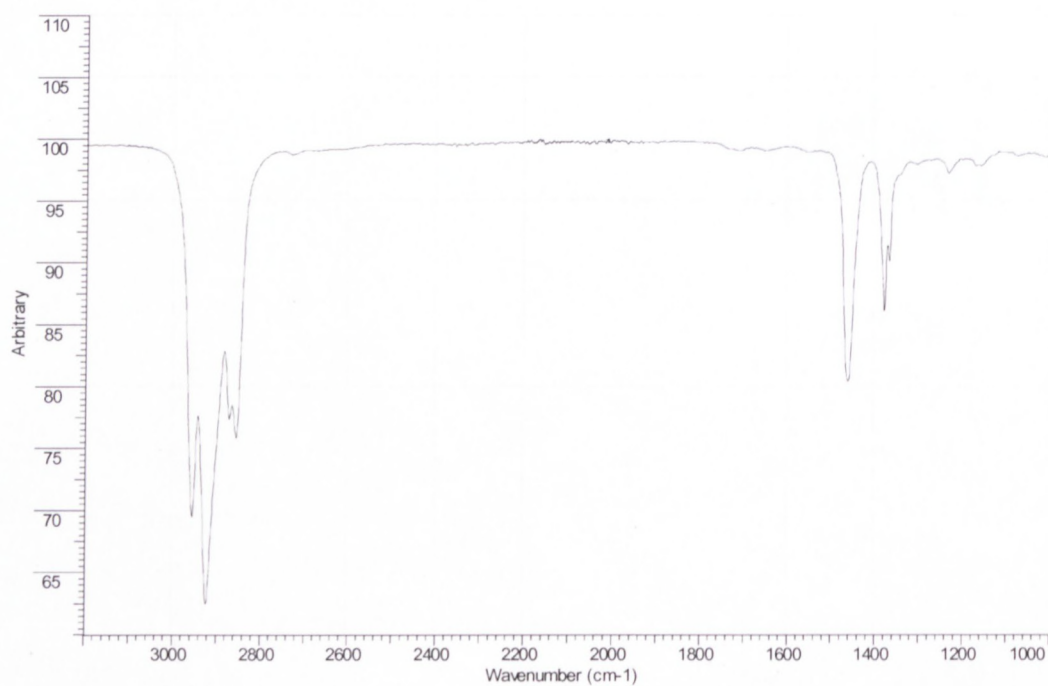


Figure 8. FT-IR spectrum of Pibsa MEA solution in Mosspar oil

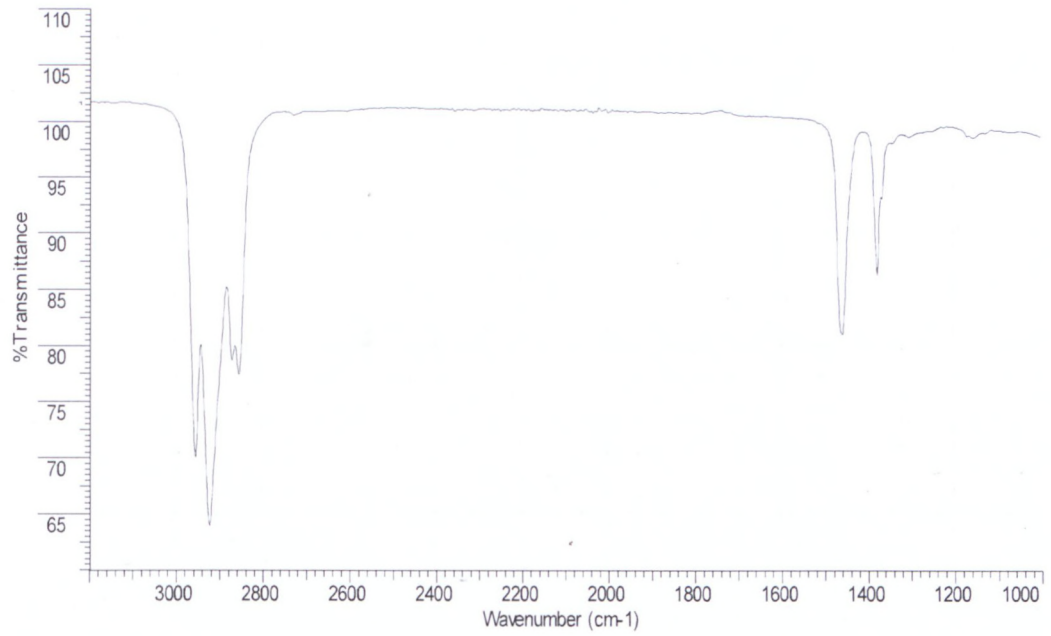


Figure 9. FT-IR spectrum of Mosspar oil

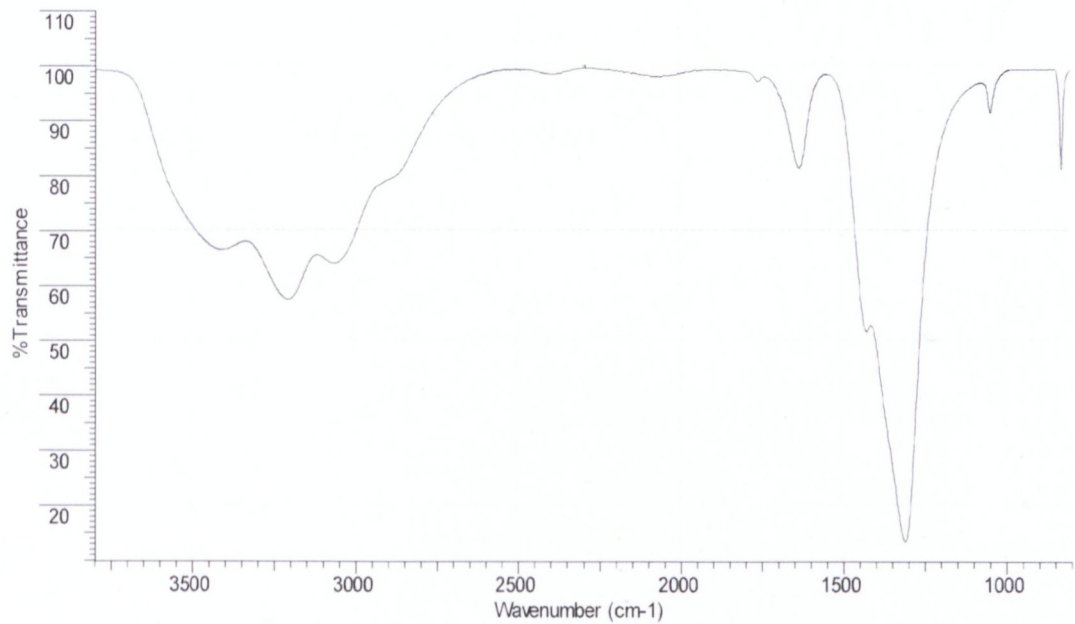


Figure 10. FT-IR spectrum of AN solution (60%)

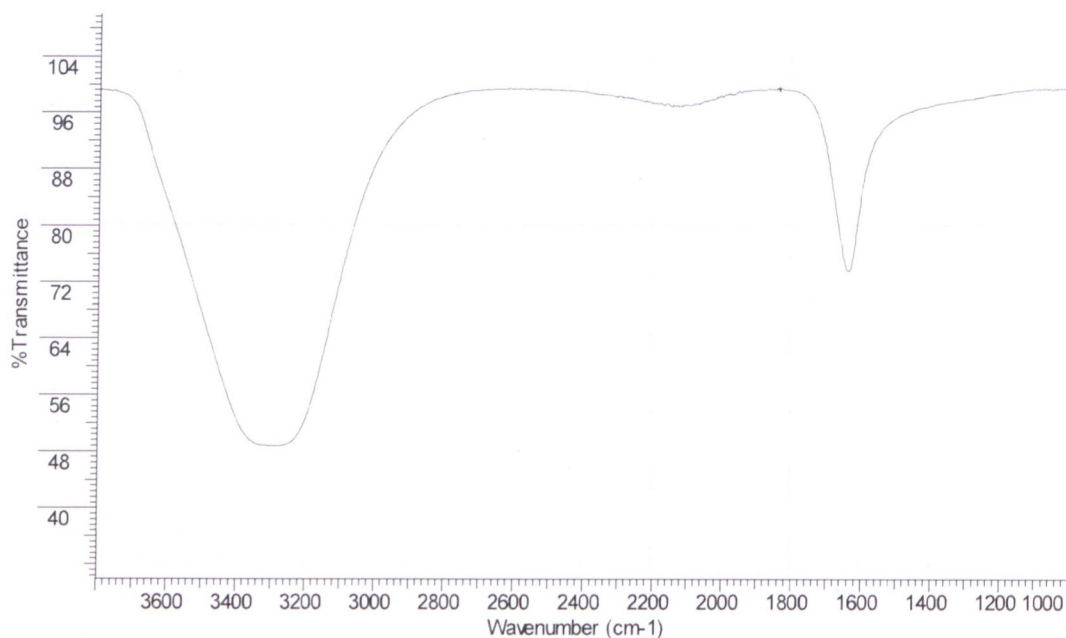


Figure 11. FT-IR spectrum of pure water

4A. DSC diagrams

Emulsions with 80% AN as an aqueous phase stabilized by Pibsa MEA, Pibsa UREA, Pibsa IMIDE, Pibsa MEA/SMO

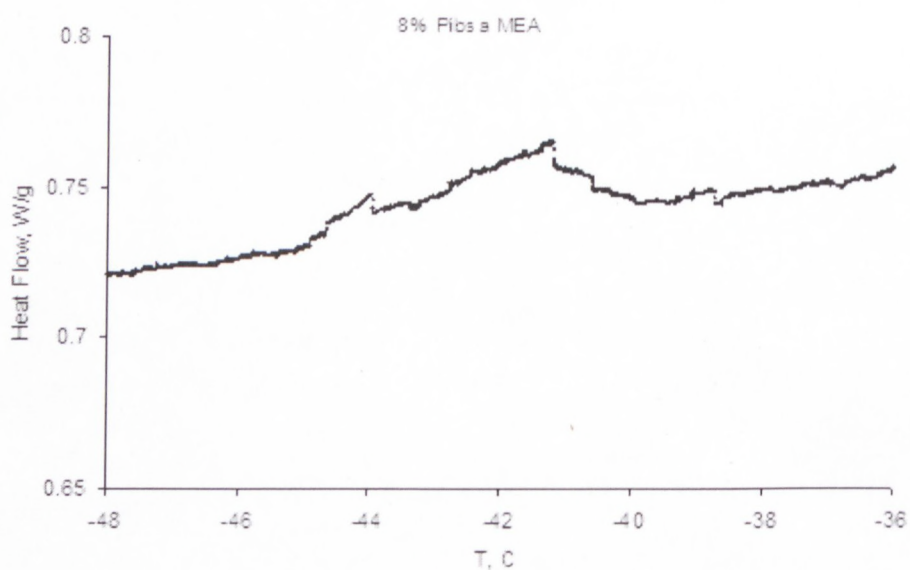


Figure 12. Heat Flow of emulsion stabilized by Pibsa MEA (8%) as a function of temperature

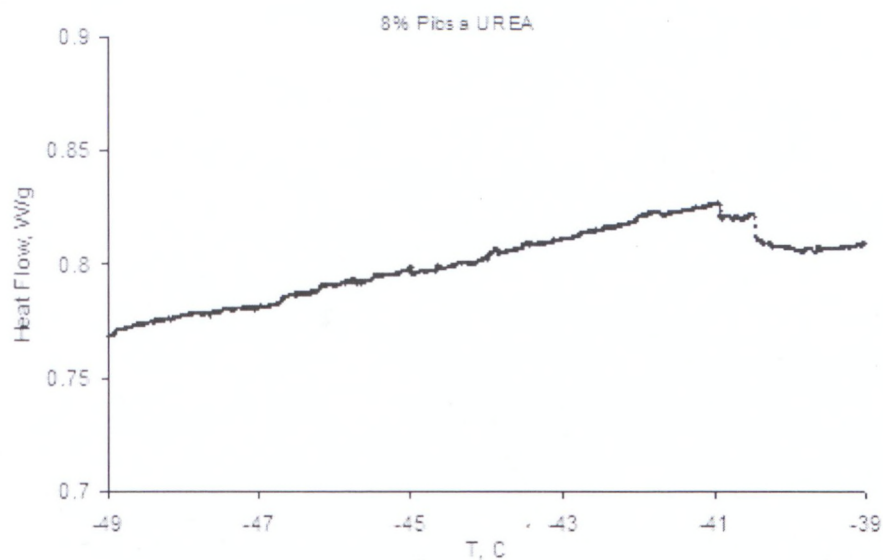


Figure 13. Heat Flow of emulsion stabilized by Pibsa UREA (8%) as a function of temperature

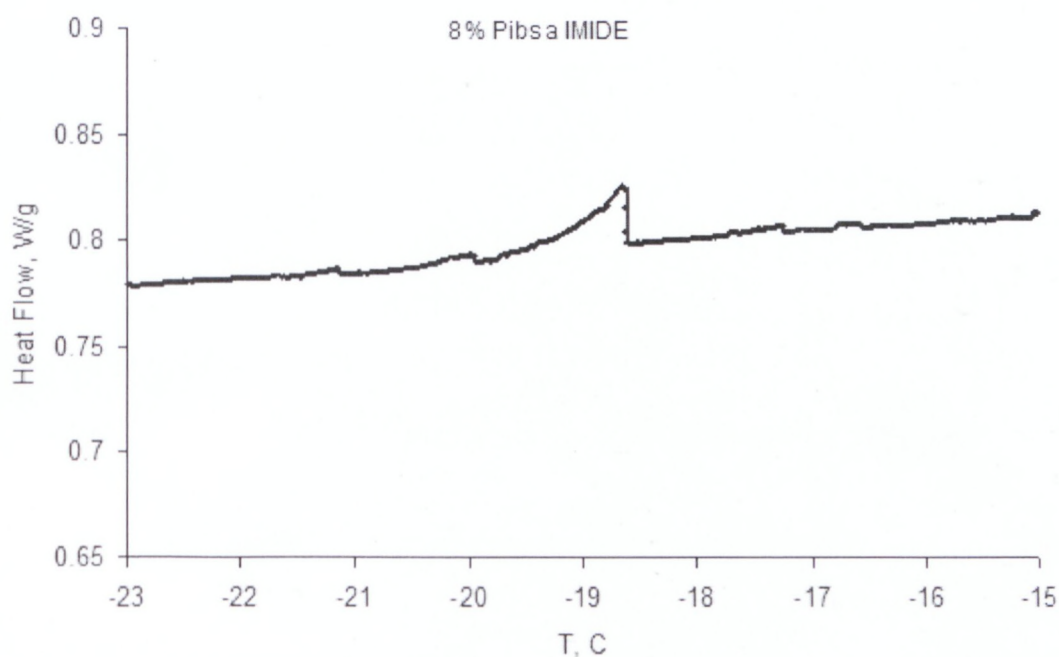


Figure 14. Heat Flow of emulsion stabilized by Pibsa IMIDE (8%) as a function of temperature

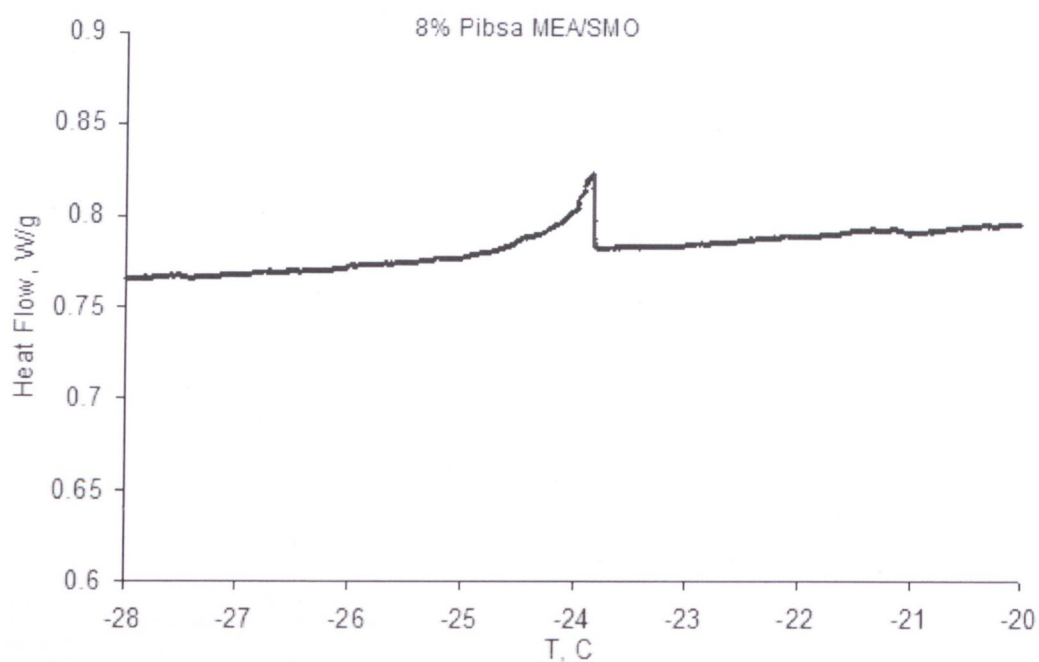


Figure 15. Heat Flow of emulsion stabilized by Pibsa MEA/SMO (8%) as a function of temperature

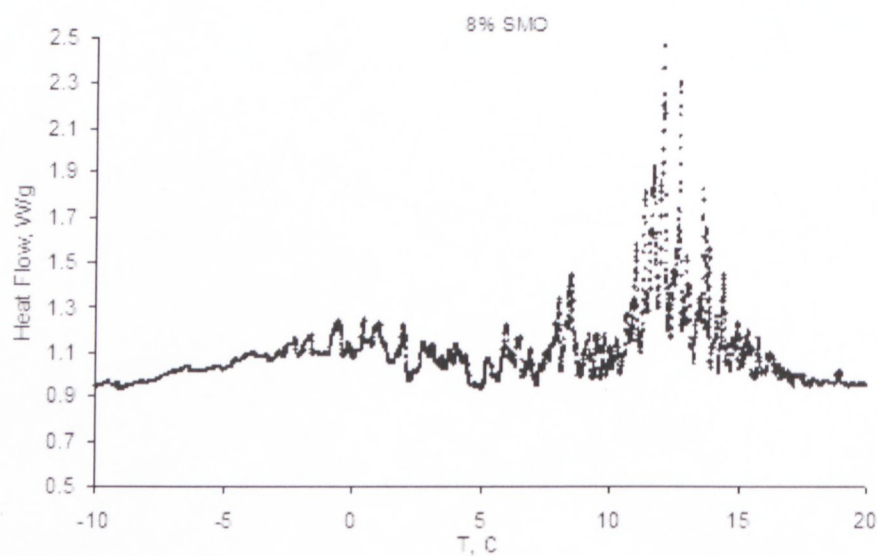


Figure 16. Heat Flow of emulsion stabilized by SMO (8%) as a function of temperature

APPENDIX B

EFFECT OF ELECTROLYTE TYPE/CONCENTRATION ON RHEOLOGICAL PROPERTIES
AND PHYSICAL STABILITY OF EMULSIONS

1B. Droplet size distribution

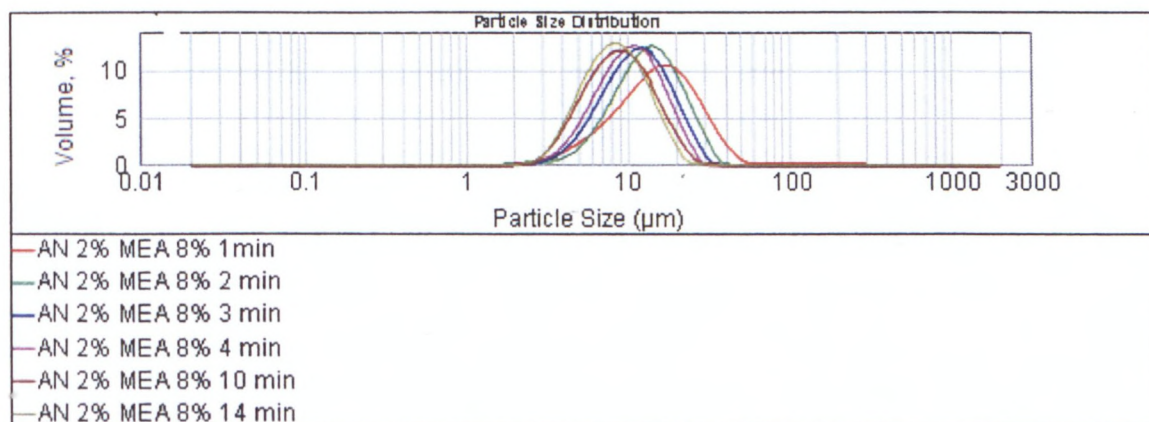


Figure 17. Droplet size distributions of emulsions with 2% of AN in aqueous phase

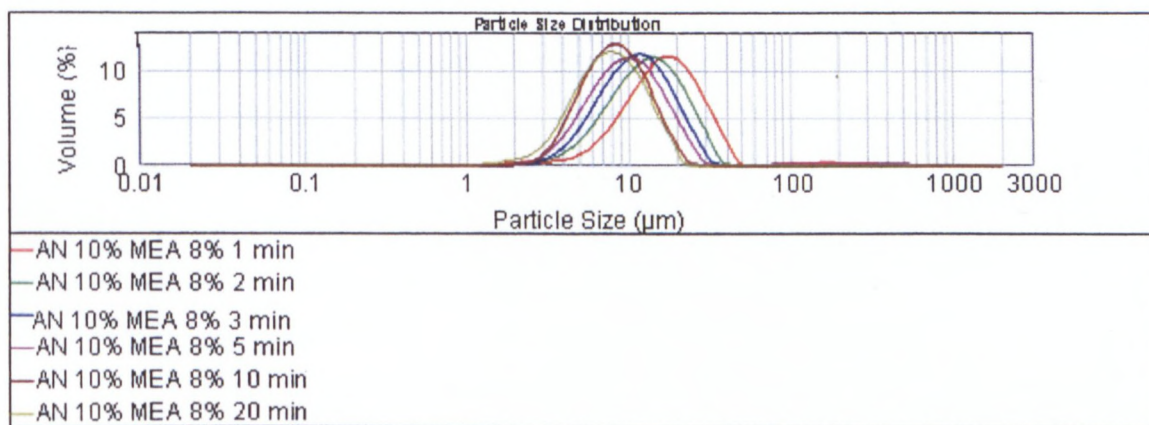


Figure 18. Droplet size distributions of emulsions with 10% of AN in aqueous phase

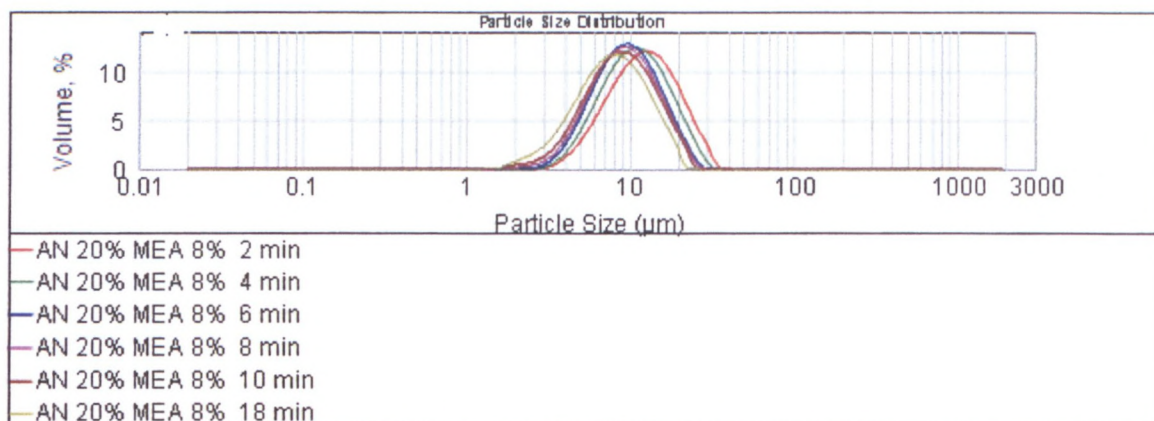


Figure 19. Droplet size distributions of emulsions with 20% of AN in aqueous phase

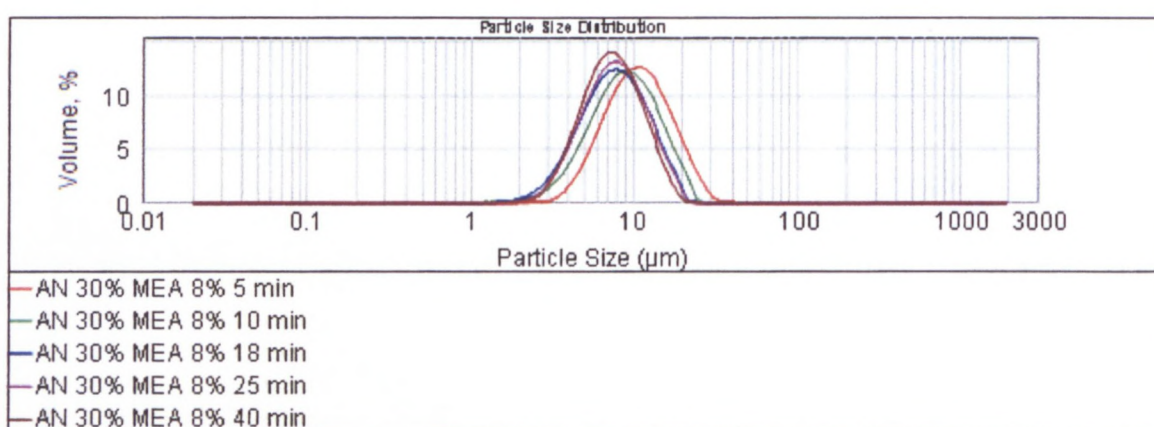


Figure 20. Droplet size distributions of emulsions with 30% of AN in aqueous phase

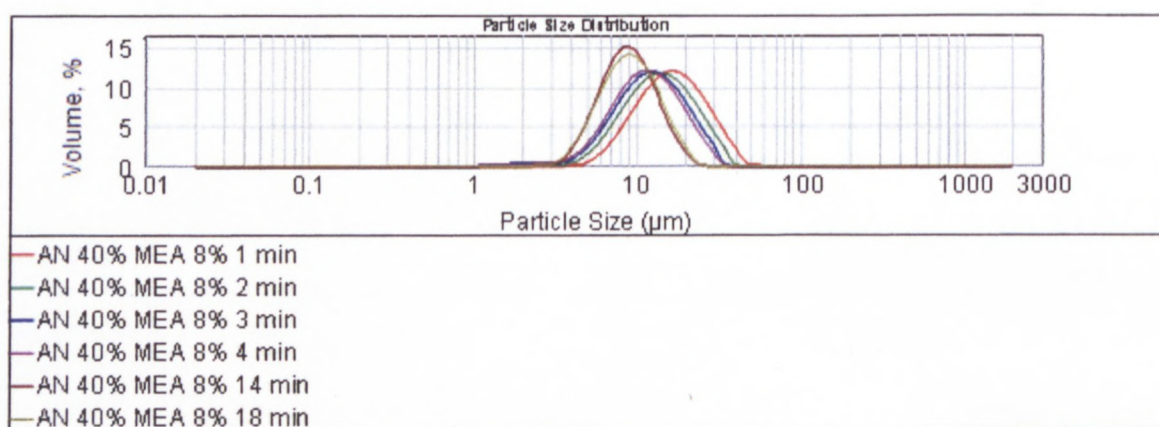


Figure 21. Droplet size distributions of emulsions with 40% of AN in aqueous phase

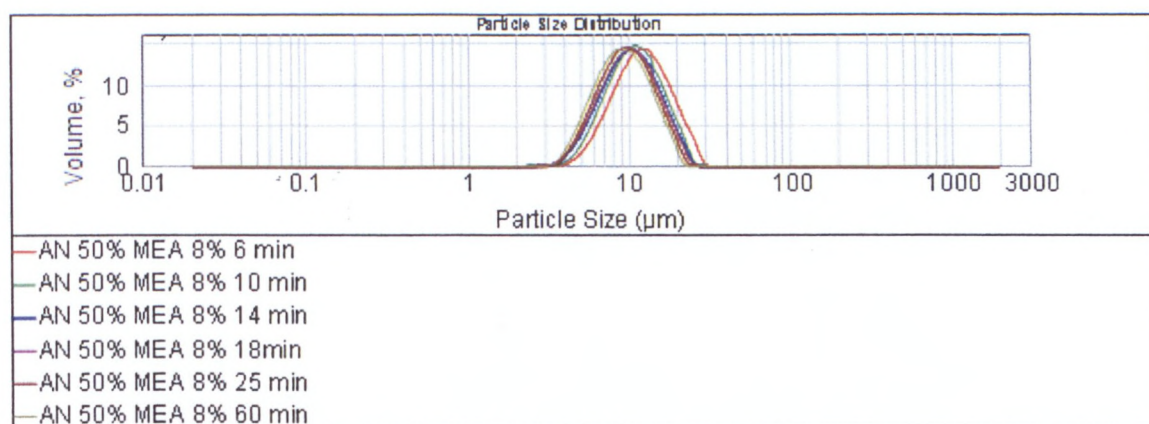


Figure 22. Droplet size distributions of emulsions with 50% of AN in aqueous phase

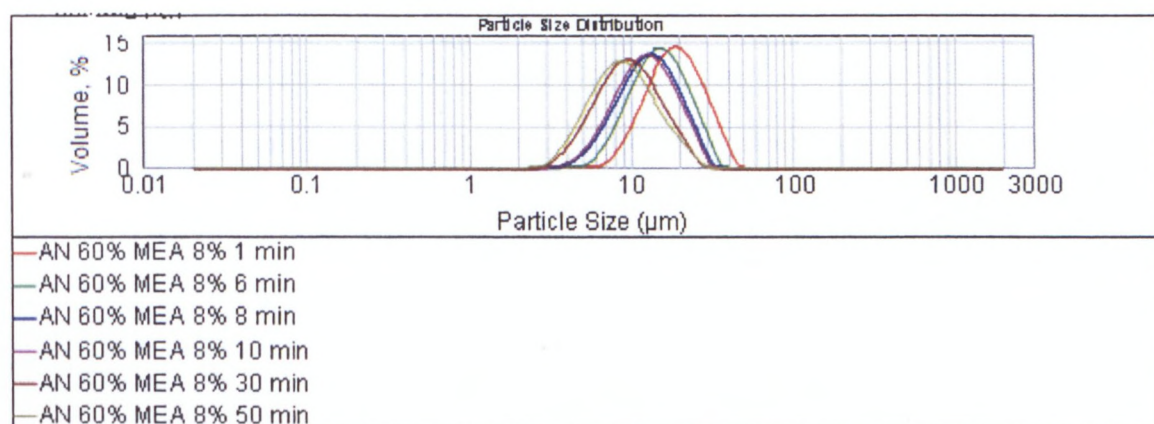


Figure 23. Droplet size distributions of emulsions with 60% of AN in aqueous phase

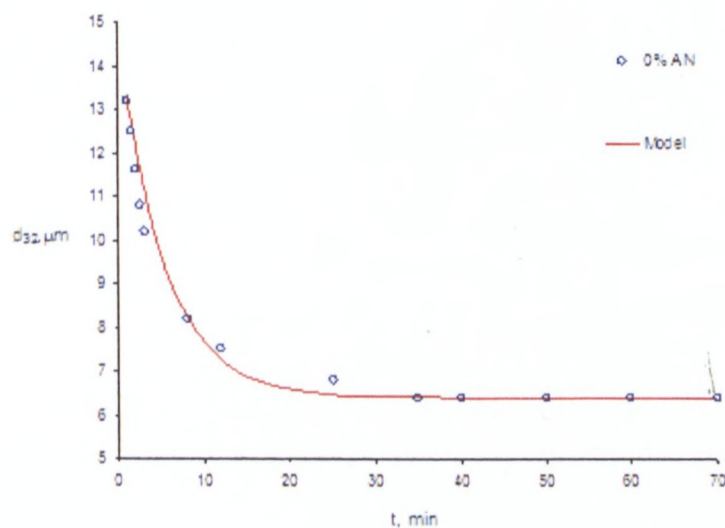


Figure 24. Droplet size as a function of mixing time for emulsion with 0% AN in aqueous phase

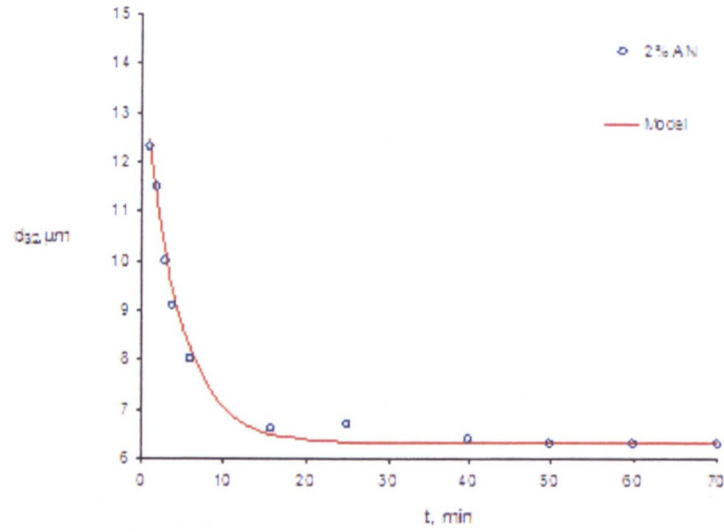


Figure 25. Droplet size as a function of mixing time for emulsion with 2% AN in aqueous phase

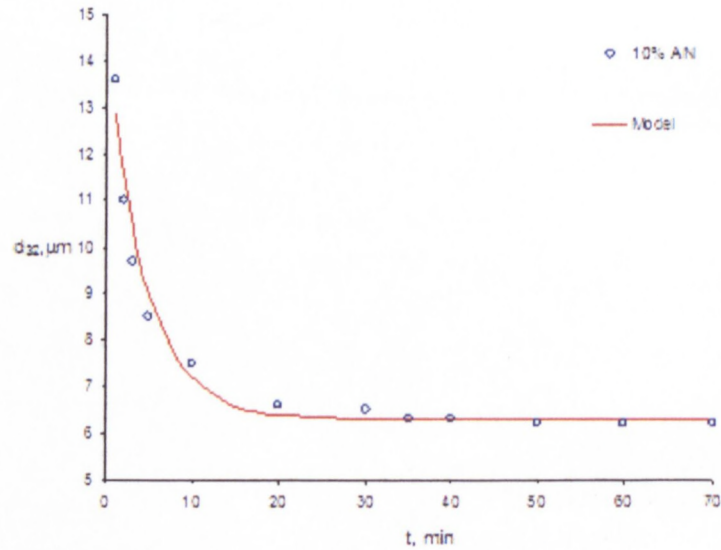


Figure 26. Droplet size as a function of mixing time for emulsion with 10% AN in aqueous phase

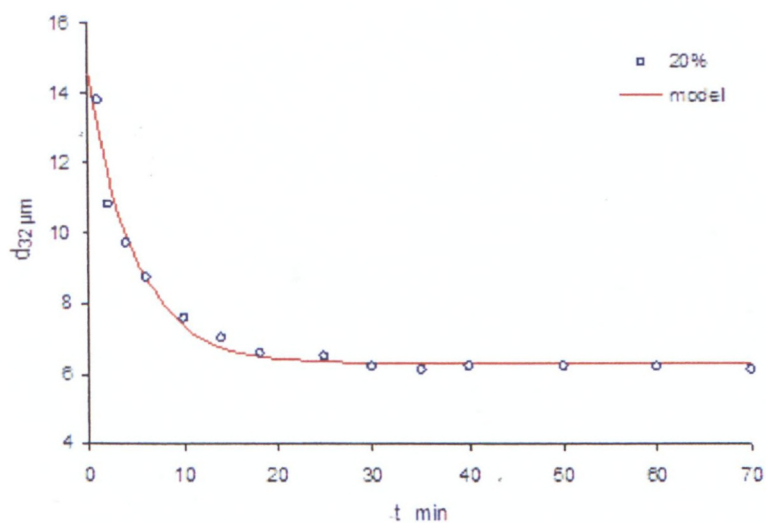


Figure 27. Droplet size as a function of mixing time for emulsion with 20% AN in aqueous phase

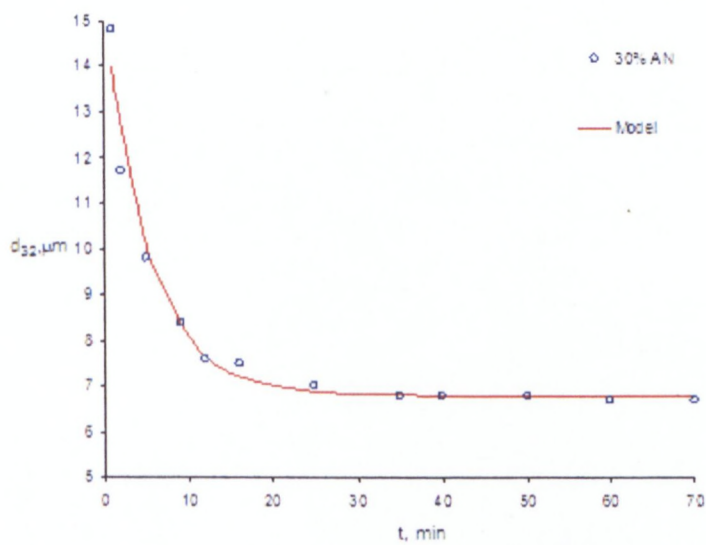


Figure 28. Droplet size as a function of mixing time for emulsion with 30% AN in aqueous phase

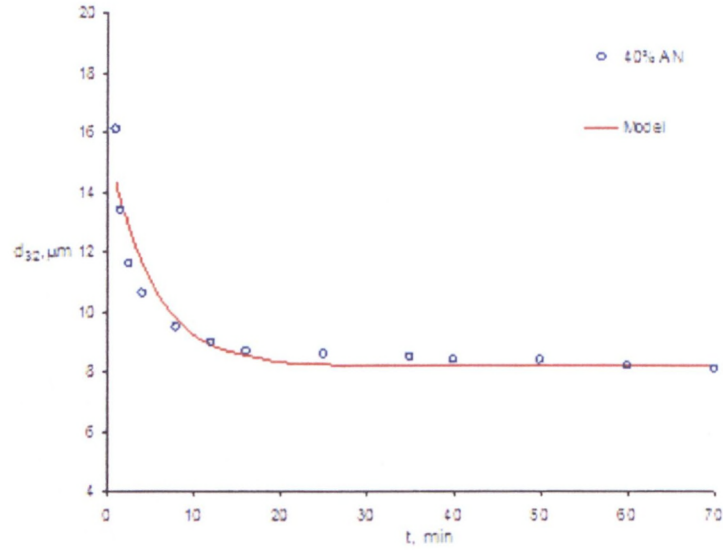


Figure 29. Droplet size as a function of mixing time for emulsion with 40% AN in aqueous phase

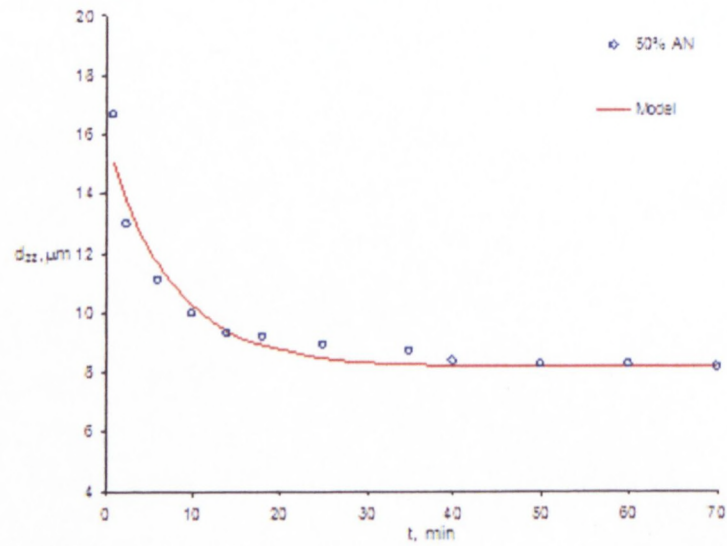


Figure 30. Droplet size as a function of mixing time for emulsion with 50% AN in aqueous phase

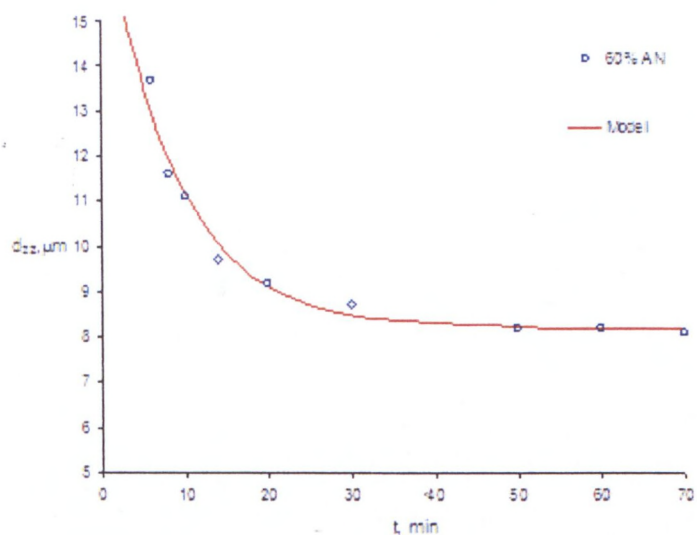


Figure 31. Droplet size as a function of mixing time for emulsion with 60% AN in aqueous phase

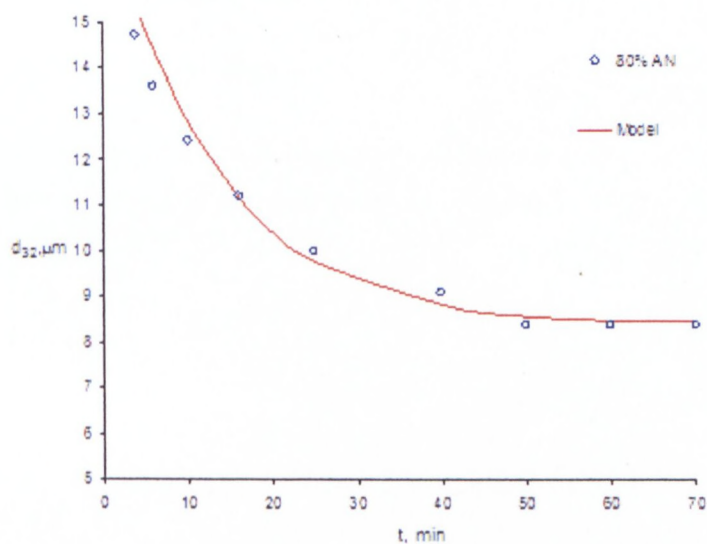


Figure 32. Droplet size as a function of mixing time for emulsion with 80% AN in aqueous phase

2B. Interfacial properties

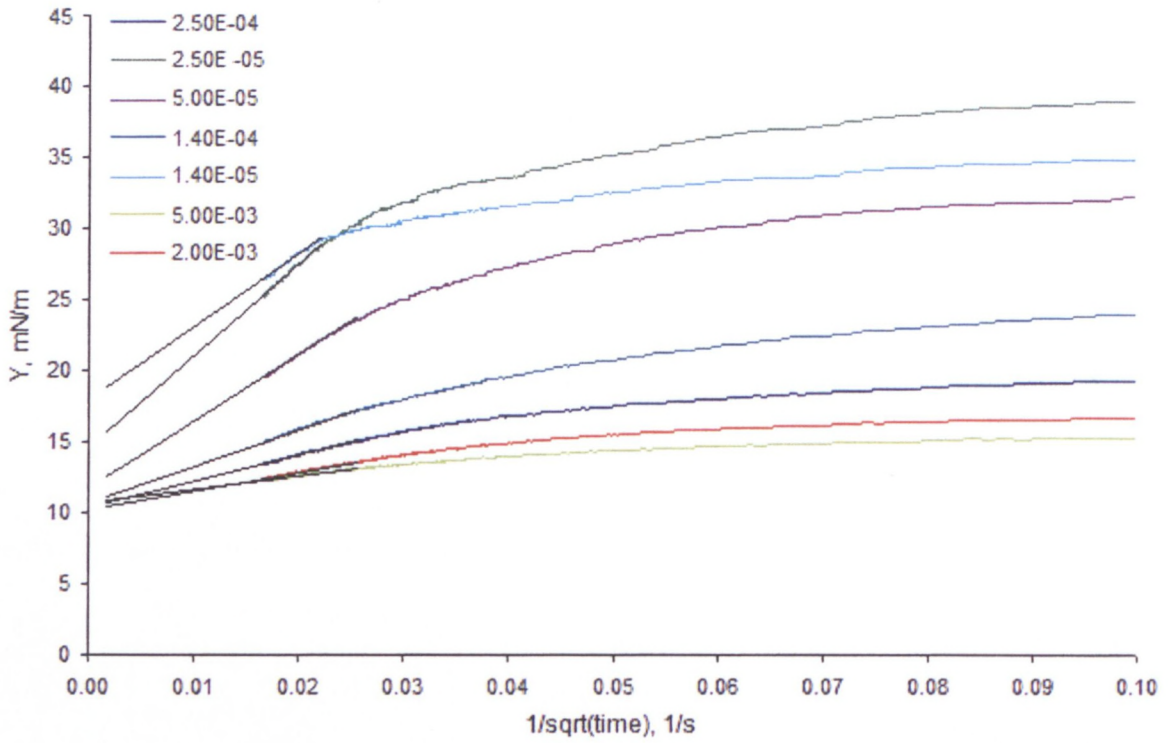


Figure 33. Determination of the interfacial tension by extrapolation to the infinity of time for the 10% of AN in aqueous phase (Pibsa-MEA)

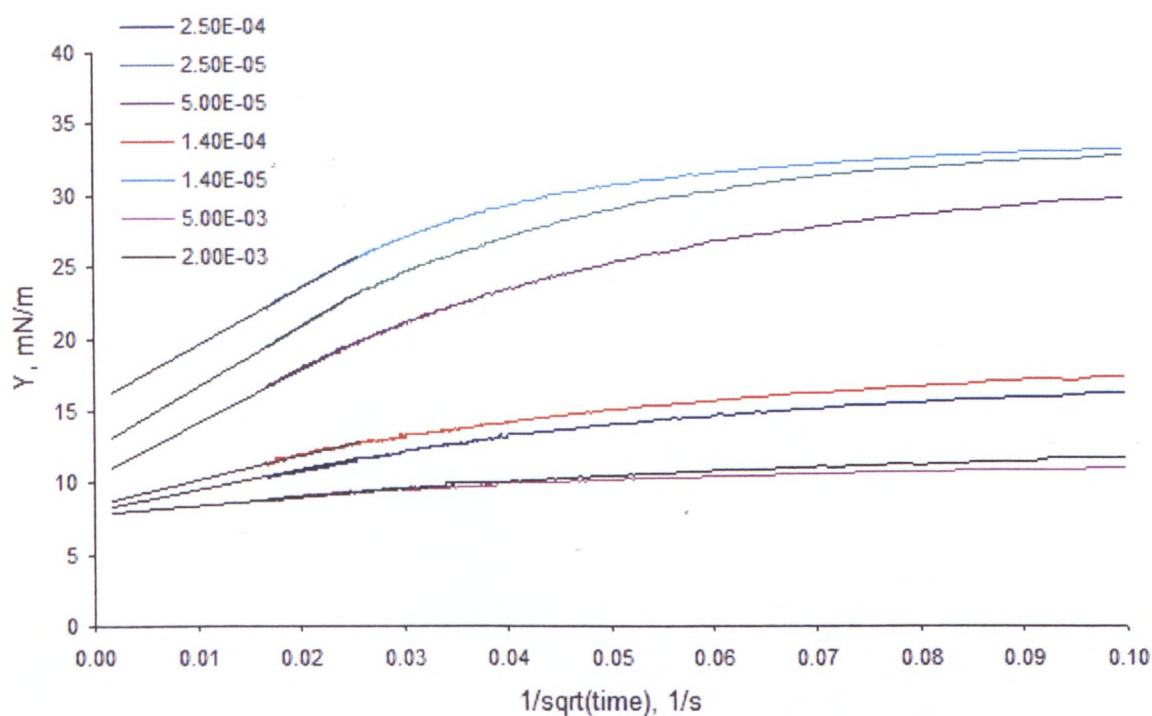


Figure 34. Determination of the interfacial tension by extrapolation to the infinity of time for the 60% of AN in aqueous phase (Pibsa-MEA)

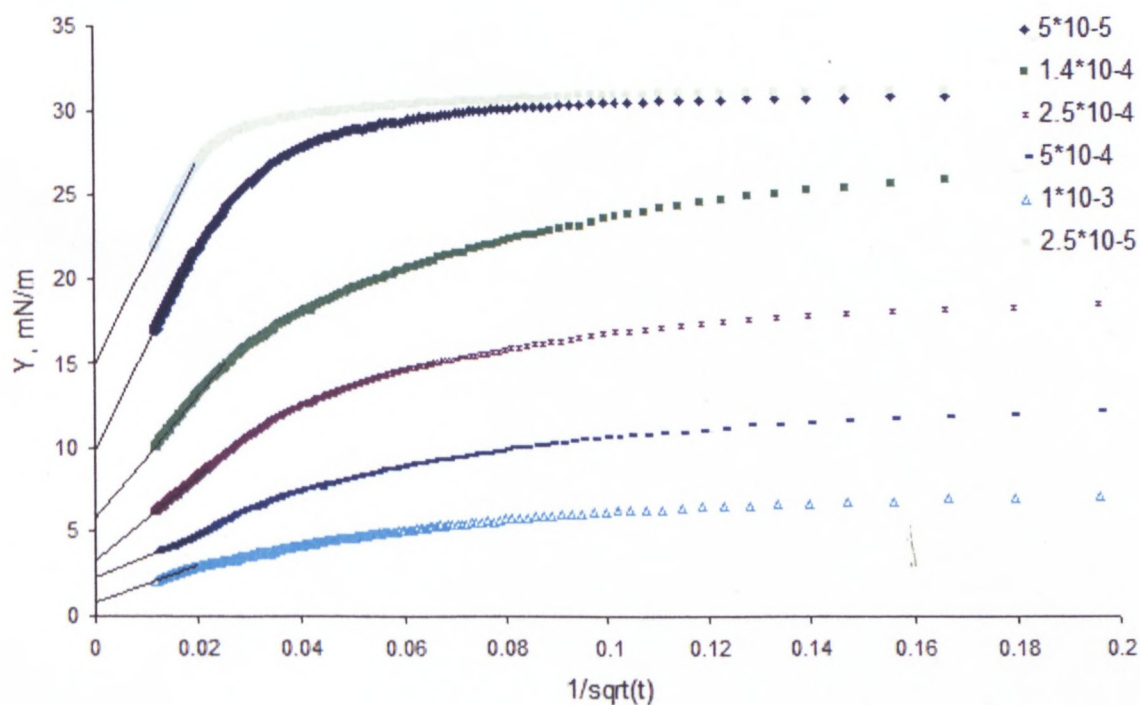


Figure 35. Determination of the interfacial tension by extrapolation to the infinity of time for the 10% of AN in aqueous phase (Pibsa-IMIDE)

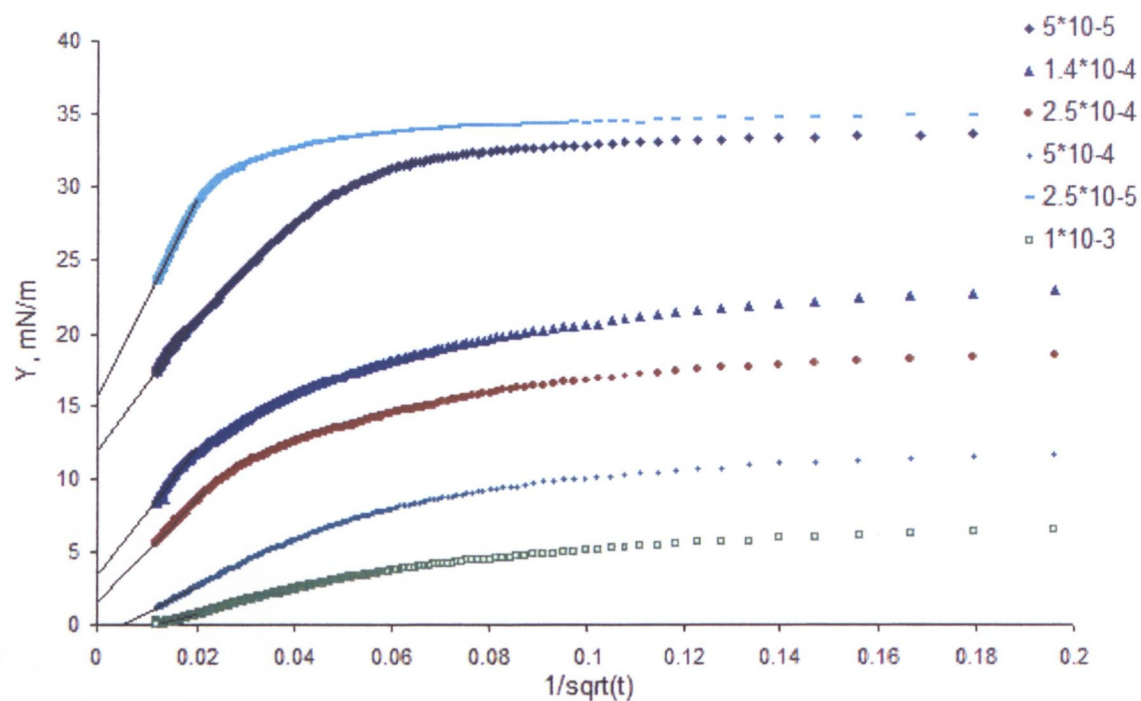


Figure 36. Determination of the interfacial tension by extrapolation to the infinity of time for the 60% of AN in aqueous phase (Pibsa-IMIDE)

